New Economic Windows

Ji-Ping Huang

Experimental Econophysics

Properties and Mechanisms of Laboratory Markets

Springer

Experimental Econophysics

New Economic Windows

Ji-Ping Huang

Experimental Econophysics

Properties and Mechanisms of Laboratory Markets

Springer

Ji-Ping Huang
Department of Physics
Fudan University
Shanghai
China

ISSN 2039-411X ISSN 2039-4128 (electronic)
New Economic Windows
ISBN 978-3-662-44233-3 ISBN 978-3-662-44234-0 (eBook)
DOI 10.1007/978-3-662-44234-0

Library of Congress Control Number: 2014944720

Springer Heidelberg New York Dordrecht London

Printed on acid-free paper

Springer is part of Springer Science+Business Media (www.springer.com)

Preface

I feel obliged to say something in the preface, in an attempt to help the reader love the book, regardless of whether he/she chooses to read the book fortunately or unfortunately. This preface contains five parts. Let me start in the first part about my beloved physics.

Physical Methods Make Physics Mature

From Aristotle (384–322 B.C.) to the time before G. Galilei (February 15, 1564–January 8, 1642), physics was developed mainly on the basis of empirical analysis (observations), which offered correlations (namely relationships involving dependence). Owing to G. Galileo, the situation was significantly changed because he brought controlled experiments into the research of physics. This approach directly reveals cause and effect, which represents a deeper understanding than the correlation brought by empirical analysis. Next, it was I. Newton (December 25, 1642–March 20, 1726) who realized the necessity of introducing the tool of theoretical analysis (based on mathematics) to generalize the results obtained from both empirical analysis and controlled experiments. As a result, physics developed much faster than before, and currently physics has already become a mature discipline.

Physical Methods Might Help Econophysics to Grow Up

The historical route of developing physics sheds light on how to develop econophysics (even though econophysics is only a branch of physics, at least to physicists like me). In fact, if we compare physics with econophysics, we can find a similar route. In the mid-1990s, econophysics got its own name and started to board the stage of history as a new research direction (certainly, I also agree that researches within the scope of econophysics appeared much earlier than the

mid-1990s, but at that time, the word "econophysics" was not yet coined). Since then, studies on econophysics have been mainly based on empirical analysis (as well as agent-based simulations, especially after the birth of the minority game in 1997 [1]; these simulations are used to understand empirical observations). Since the last decade, the situation has been updated by introducing controlled experiments into econophysics, say, the study of the minority game [2–4], political exchange for election outcome prediction [5, 6], the market-directed resource-allocation game [7–10], and a laboratory stock market [11]. In the early stage of introducing controlled experiments [2–4], controlled human experiments (which will be simply called "controlled experiments" throughout this book) were purely performed to yield new results. However, such human experiments often have unavoidable limitations such as specific subjects with specific identities in specific avenues at specific time. Thus, it becomes somehow difficult to generalize the results obtained from controlled experiments. To overcome these limitations and also to achieve more results (that cannot even be obtained from pure human experiments due to the lack of resources like time, money, and/or human subjects), since 2009 [7], my group has introduced a combination method of empirical analysis, controlled experiments, and theoretical analysis (based on agent-based simulations and/or analytical theory) [7–10] into the research of econophysics. Owing to the big success of the combination approach in physics, we expect more from the combination method in the field of econophysics. Because controlled experiments play the most important role in the combination approach, I call the econophysics related to the controlled experiments as *Experimental Econophysics*, which is the topic of this book.

To benefit the reader, a few well-known scholars have published several elegant English monographs on econophysics:

- R.N. Mantegna and H.E. Stanley, An Introduction to Econophysics, Cambridge University Press (2000);
- N.F. Johnson, P. Jefferies, and P.M. Hui, Financial Market Complexity, Oxford University Press (2003);
- J. Voit, The Statistical Mechanics of Financial Markets (3rd edition), Springer (2005);
- D. Challet, M. Marsili, and Y.-C. Zhang, Minority Games: Interacting Agents in Financial Markets, Oxford University Press (2005).

However, these monographs have not touched the field of experimental econophysics. So, the present book in your hand would be the first English monograph on *Experimental Econophysics*. I hope it will help to foster the development of econophysics, at least to some extent.

Peer Responses to Experimental Econophysics

What is experimental econophysics in the eyes of econophysicists? I prefer to answer this question as below.

From May 31 to June 2, 2014, I attended the International Conference on Econophysics (ICE2014) in Shanghai, China. During the ICE2014, I presented an invited talk, entitled "Experimental Econophysics: A laboratory market for modeling real stock markets." The talk presented both my key thoughts on experimental econophysics and the content of Chap. 3 of this book. Surprisingly, the audience appreciated this talk very much, and evoked much stronger repercussions than what I had expected. As a result, during or after my talk, many scholars (including Prof. R.N. Mantegna of the University of Palermo in Italy) had great interest to discuss with me the controlled experiments conducted by my group. In particular, on June 4, 2014, Prof. D. Sornette of ETH Zurich in Switzerland, who is both a chairman of ICE2014 and a leading worldwide expert in the field of econophysics, also emailed me:

> "I like very much your presentation at ICE2014. I would be glad if you could send me your presentation in pdf format. I would also appreciate receiving your papers that you listed, especially the ones on your lab experiments."

Such peer appreciation implies that experimental econophysics, coined by me, has had a good start. Nevertheless, a good start does not mean a good ending; to achieve the latter, we must do much better.

Who Should Read This Book?

One of my dreams, which are genuine dreams beyond reality, is to let this book attract a huge number of readers. So, the dream is as follows.

On one hand, everyone who has an interest in physics should read this book because it guides him/her to know how to develop statistical physics into the field of economics or finance.

On the other hand, everyone who has an interest in economics or finance should read this book because it helps him/her know of economic or financial problems from a different perspective.

The word "everyone" appearing in the above two paragraphs should include undergraduate students, graduate students, teachers in universities, and researchers in universities, institutes or industries, who are working in the field related to physics, economics/finance, complexity science, artificial intelligence, management science, sociology, ecology, or evolutionary biology.

Acknowledgments

First, I take this opportunity to express my gratitude to some of my group members for their great help in preparing some parts of the book. The details are as follows.

- Chapter 2: Mr. K.N. An, Mr. X.H. Li, Mr. C. Xin, and Mr. G. Yang;
- Chapter 4: Mr. C.G. Zhu, Mr. K.N. An, and Mr. G. Yang;
- Chapter 7: Dr. Y. Liang and Mr. K.N. An;
- Chapter 9: Mr. X.H. Li, Mr. G. Yang, and Mr. K.N. An;
- Chapter 12: Ms. L. Liu;
- Bibliography: Mr. G. Yang.

Besides, I have completed the other chapters according to the articles published by my group. So, I must also thank all the other group members who coauthored these articles. In addition, all my current group members have also helped to look over the whole book and relay to me many constructive comments and suggestions, which are appreciated very much. Below is the name list of my current group members: Dr. X.W. Meng, Miss T. Qiu, Mr. G. Yang, Mr. X.H. Li, Miss L. Liu, Mr. C.G. Zhu, Mr. X.Y. Shen, Mr. G.X. Nie, Mr. H.S. Zhang, Mr. K.N. An, Miss Y.X. Chen, Mr. C. Xin, Miss F.F. Gu, and Mr. Q. Ji.

Second, for completing the book I have profited from valuable and stimulating collaborations and discussions with Prof. H.E. Stanley of Boston University, Prof. Y.-C. Zhang of Fribourg University, Prof. B.H. Wang of The University of Science and Technology of China, Prof. P.M. Hui of The Chinese University of Hong Kong, and Dr. Yu Chen of Tokyo University.

Third, I am so grateful to Prof. R.B. Tao and Prof. B.L. Hao of Fudan University for encouraging me to conduct econophysics in the Department of Physics at Fudan University. As the two professors are senior and experienced, their encouragement means a lot to me.

Fourth, I am indebted to my family members, especially two daughters (Ji-Yan Huang with the nickname of Qian-Qian and Ji-Yang Huang with the nickname of Yue-Yue), for their support when I spent many nights preparing the book, rather than accompanying them.

Last but not least, I acknowledge the financial support by the National Natural Science Foundation of China under Grant Nos. 11075035 and 11222544, by the Fok Ying Tung Education Foundation under Grant No. 131008, by the Program for New Century Excellent Talents in University (NCET-12-0121), by the Shanghai Rising-Star Program (No. 12QA1400200), and by Shanghai Key Laboratory of Financial Information Technology (Shanghai University of Finance and Economics).

Shanghai, China, June 2014 Ji-Ping Huang

Contents

Abstract

Experimental Econophysics describes the method of controlled human experiments, which is developed by physicists to study problems in economics or finance, namely stylized facts, fluctuation phenomena, herd behavior, contrarian behavior, hedge behavior, cooperation, business cycles, partial information, risk management, and stock prediction. Experimental econophysics along with empirical econophysics are two branches in the field of econophysics. The latter has been extensively discussed in the existing literature, while the former has been seldom touched. In this book, the author focuses on the branch of experimental econophysics. Empirical econophysics is based on the analysis of data in real markets using statistical tools borrowed from traditional statistical physics. Differently, inspired by the role of controlled experiments and system modeling (for computer simulations and/or analytical theory) in developing modern physics, experimental econophysics specifically relies on controlled human experiments in the laboratory (producing data for analysis) together with agent-based modeling (for computer simulations and/or analytical theory), with an aim to reveal the general cause–effect relationship between specific parameters and emergent properties of real economic/financial markets. This book covers the basic concepts, experimental methods, modeling approaches, and latest progress in the field of experimental econophysics.

Chapter 1
Introduction

Abstract In this chapter, I attempt to offer a general background of experimental econophysics, the theme of the book. For this purpose, I start by answering some fundamental questions. That is, why does physics need economics or finance, and vice versa? What are physical ideas or methods? Then, I introduce both the birth of econophysics and the two branches of econophysics (namely, empirical econophysics and experimental econophysics). Finally, I present the methodology of experimental econophysics.

Keywords Experimental econophysics · Physical idea · Physical method · Controlled experiment

It might be a kind of human inability that a single scientist cannot research on *all* the aspects of the nature and society. Owing to the human inability, science has been divided into many disciplines, e.g., mathematics, physics, chemistry, biology, economics/finance, and so on. As a result, specific researchers always work in the field of a specific discipline. For example, the researchers, under the name of physicists, work in the specific field of physics. After a longtime separation between physics and economics/finance, now the time is ripe for their combination, so that they could help each other to develop, at least to some extent.

1.1 Why Physics Needs Economics or Finance?

If one counts from G. Galilei (February 15, 1564–January 8, 1642), physics, the study of nature, has been developing for 400 years or so. This duration is not very long compared to the millions of years for which humans have lived on earth. However, everyone has witnessed the significant changes in human life brought about by physics, such as electricity, computers, mobile phones, artificial satellites, utilization of nuclear energy, and so on. All of these changes are an outcome of the physical knowledge of the natural world. According to this fact, it is no doubt that the ideas and methods of physics are useful to handle the natural world. Here, the natural world means it contains non-intelligent units that have no adaptability due to the lack of learning ability. For example, such non-intelligent units are electrons, atoms,

J.-P. Huang, *Experimental Econophysics*, New Economic Windows,
DOI 10.1007/978-3-662-44234-0_1

molecules, colloidal particles, and so on. In sharp contrast to the natural world, the social world is full of intelligent units, which have adaptability due to the existence of learning ability; such intelligent units involve humans, companies (containing many humans), countries, and so on.

Science is always driven by curiosity, and physics is no exception. Inspired by the success of physics in handling the natural world, one might curiously ask whether the ideas and methods originally developed from physics for treating the natural world are also useful for the social world. The answer is definitely in the affirmative. But, the reader might proceed to ask: "what do you mean by saying the ideas and methods originally developed from physics for treating the natural world?" or "what are physical ideas and methods?"

1.1.1 What Are Physical Ideas?

1.1.1.1 Extracting Reasons Should be Coarse-Grained

Let me take the freely falling object as an example. The number of reasons determining falling height could be based on N: time, air resistance, atmospheric pressure, humidity, etc. However, G. Galilei (February 15, 1564–January 8, 1642) neglected the $N-1$ reasons and considered only the relation between falling height (h) and time (t), yielding $h = (1/2)gt^2$. Here, g is acceleration (a constant). As a result, he established the law of free fall, which helped I. Newton (December 25, 1642–March 20, 1726) to successfully establish classical mechanics in the discipline of physics. Based on this law, the first idea of physics comes to appear: one should extract crucial reasons, or equivalently *extracting reasons should be coarse-grained*.

1.1.1.2 Results Obtained Should Be Universal

After Galilei's $h = (1/2)gt^2$, I. Newton (December 25, 1642–March 20, 1726) revealed his second law, $F = ma$, where F is force, m is mass, and a is acceleration. This second law helps to explain not only the freely falling object on the earth (by setting $a = g$ and seeing F as gravity), but also the planetary motion in the sky (that had been empirically summarized in the laws of planetary motion by J. Kepler (December 27, 1571–November 15, 1630)). Besides, Newton's second law can even be used to predict new phenomena. For example, on August 31, 1846, U. Le Verrier (March 11, 1811–September 23, 1877) first predicted the existence and position of Neptune using Newton's second law plus Newton's law of gravity; Neptune was subsequently observed on September 23, 1846, by J. G. Galle (June 9, 1812–July 10, 1910) and H. L. d'Arrest (August 13, 1822–June 14, 1875). The success of Newton's second law indicates the second idea of physics, which is "results obtained should be universal." Here, "universal" means that the results should not only help to explain the existing phenomena, but also help to predict the future or unknowns.

1.1.2 What Are Physical Methods?

1.1.2.1 Empirical Analysis

From Aristotle (384–322 BC) to J. Kepler (December 27, 1571–November 15, 1630), physicists first observed the natural world and then analyzed the observations, yielding many empirical results, such as Kepler's laws of planetary motion. Such analysis is simply empirical analysis, which is based on existing data in nature.

Advantages of empirical analysis: reliability and huge data. Here, "reliability" means that according to the data collected from nature itself, any results obtained from the data should be reliable; "huge data" means that the number of data in nature is huge, which is definitely helpful for understanding the natural world.

Disadvantages of empirical analysis: uncontrollability (correlation) and non-formatting. Since the data are collected from nature, they are always uncontrollable. Then, what empirical analysis can produce is correlation but not causality. Clearly, causality represents a deeper understanding than correlation. Regarding "non-formatting," it is easy to understand that: the format of data existing in nature is not fixed but dependent on how people collect them. The non-formatting of data causes trouble for people to investigate.

1.1.2.2 Controlled Experiments

Since empirical analysis helps to reveal correlation rather than causality, G. Galilei (February 15, 1564–January 8, 1642) started to perform experiments in the laboratory by purposefully tuning one or a few parameters/conditions (all the other parameters/conditions are fixed) in order to reveal cause–effect relationships (causality). His method was that of controlled experiments.

Advantages of controlled experiments: controllability (causality) and formatting. These are the inverse of the above-mentioned disadvantages of empirical analysis. Such experiments are controllable because one can tune a variable and see its effect (causality). As regards "formatting," it means the format of data could be conveniently organized during the experiment.

Disadvantages of controlled experiments: deviations and few data. Since such experiments are conducted in the laboratory, the experimental data may be different from their counterparts in nature. This difference is what we term as "deviations." On the other hand, the experimental data produced in the laboratory cannot be huge, as one can easily imagine. Thus, I indicate "few data" herein.

1.1.2.3 The Combination of Empirical Analysis, Controlled Experiments, and Theoretical Analysis

Due to the above-mentioned advantages and disadvantages of either empirical analysis or controlled experiments, I. Newton (December 25, 1642–March 20, 1726) combined both empirical analysis and controlled experiments; for instance, when he explained Kepler's laws of planetary motion (outcome of empirical analysis), he also explained Galilei's law of free fall (outcome of controlled experiments). The combination of empirical analysis and controlled experiments reserves their advantages, but removes their disadvantages. More importantly, Newton also realized that the combination of empirical analysis and controlled experiments can produce results only for specific areas: empirical analysis corresponds to the specific objects producing empirical data (e.g., Kepler's laws of planetary motion are only valid for planets); controlled experiments are related to specific laboratory samples/devices producing experimental data (e.g., Galilei's law of free fall specifically holds for the freely falling object in the laboratory). As a result, Newton utilized theoretical analysis (based on mathematics like calculus) to generalize the results (obtained from the combination of empirical analysis and controlled experiments) from specific areas to broad areas. For example, his second law ($F = ma$) helps to explain not only the motion of either planets (described by Kepler's laws of planetary motion) or freely falling objects (described by Galilei's law of free fall), but also the motion of many other objects, including a single molecule. Owing to the unprecedent success of this generalization (which is proved by the fact that physics has significantly improved human life), the method of combining empirical analysis, controlled experiments, and theoretical analysis has become the fundamental method for developing physics. Certainly, in reality, it is already enough for achieving some excellent results by using only one or two of empirical analysis, controlled experiments, and theoretical analysis. This fact depends on specific topics, for e.g., in modern condensed matter physics, where empirical analysis is hardly used. However, in modern astrophysics, controlled experiments are rare. It is not necessary for me to go into details here. In principle, the above-mentioned combination is an ideal, complete method.

So far, I have answered the question "what are physical ideas and methods?"

Last but not least, even though physics has helped to significantly improve human life due to the deep understanding of the natural world using the above-mentioned physical ideas and methods, it might be not suitable for people to immediately expect too much when physical ideas and methods are used to understand the social world. Why? Please note many of the above-listed applications brought about by physics are not a direct purpose of original research. For example, when M. Faraday (September 22, 1791–August 25, 1867) discovered the law that magnetism is able to produce electricity, he did not know whether it would be genuinely useful to humans. The reason he conducted the research was due only to curiosity. In fact, in history, the large-scale application of electricity only started at the end of the nineteenth century when Faraday had passed away for many years. This means people must be patient to wait for the application of a physical discovery as physicists need time to study.

In other words, the reason that physics needs economics/finance lies in the curiosity of physicists, which may broaden the realm of physics, especially statistical physics.

1.2 Why Economics or Finance Needs Physics?

Briefly speaking, economics is a discipline on how to allocate scarce resources efficiently. Since the time of A. Smith (June 5, 1723–July 17, 1790), economics has developed for more than 200 years. In the duration, mathematics was introduced into economics, thus causing economics to be a quantitative discipline. Because the subject discussed in the field of economics is human-activities-related phenomena in the social world, which is too complex, economics is still far from perfect. For example, existing economic theories fail to envisage even the possibility of a financial crisis like the recent one [12]. Thus, economics needs different ideas or methods in an attempt to perfect itself. Physics may be a candidate discipline for economics to absorb such ideas and methods. In this sense, economics needs physics so that people might scrutinize economic problems from a different perspective, thus yielding different insights. Certainly, economics can also resort to ideas or methods that are beyond physics, e.g., evolutionary biology.

The above conclusion also holds for finance. As regards finance, its relation to economics is similar to the relation between applied physics and basic physics. That is, finance focuses on application research, but economics focuses on basic research. For example, if a seller sells a pen at a price of 1 Chinese Yuan, the exchange behavior between me and the seller belongs to finance, but the reason that the pen costs 1 Chinese Yuan rather than 100 Chinese Yuan belongs to economics. Nevertheless, throughout this book, I do not sperate economics and finance distinctly because both are closely related to the trading behavior of humans.

1.3 Physics + Economics or Finance → Econophysics

Physics meets economics or finance, yielding econophysics (the wording "econophysics" first appeared in the literature as early as 1996 [13]). According to the above, econophysics is a branch of physics (at least in the eye of physicists like me), which uses physical ideas and methods (listed in Sect. 1.1) to analyze problems related to economics and finance. Loosely speaking, econophysics is what physicists do in the field of economics or finance since these physicists are naturally armed with physical ideas and methods. To briefly summarize the above, the aim of econophysicists could be at least twofold: first, to broaden the realm of traditional physics (throughout this book, the phrase "traditional physics" means the physics that is used to study nature with non-intelligent units like atoms, rather than the society with intelligent units like humans), especially statistical physics, second, to scrutinize economic or financial problems from a physical perspective.

1.4 Dividing Econophysics into Two Branches: Empirical Econophysics and Experimental Econophysics

In general, econophysics contains three methods: empirical analysis (starting from the articles by H. E. Stanley and coworkers in the mid-1990s, see for example Ref. [14]), controlled experiments (starting as early as 2003 by T. Platkowski and M. Ramsza [2]), and theoretical analysis (starting from the establishment of minority game in 1997 by Challet and Zhang [1]). Here, empirical analysis in the field of econophysics is based on existing data in real markets, and controlled experiments mean experiments conducted in the laboratory which produce data by tuning one (or few) variable(s)/condition(s). The theoretical analysis in the field of econophysics is based on agent-based modeling (or system modeling), which has two approaches: agent-based simulations (also called computer simulations) and analytical theory. Agent-based simulations have helped to develop econophysics significantly, which are an analog of molecular dynamics simulations [15], Monte Carlo simulations [16], or finite element simulations [17, 18] in traditional physics. According to traditional physics, for analytical theory, one needs to start from some common laws or principles that are often lacking in social human systems (the research object of econophysics). Thus, compared with agent-based simulations, analytical theory has not played a very important role in econophysics.

Since the birth of econophysics in the mid-1990s [13], empirical analysis has dominated the research community of econophysics till now, which forms a branch of econophysics called empirical econophysics. However, as a discipline, econophysics is still too young, with vast development space. As one knows, the maturity of traditional physics is mainly due to the role of controlled experiments in the laboratory. Accordingly, it seems unbelievable that in the future, econophysics without controlled experiments could be as mature as traditional physics. Thus, I believe that for developing econophysics in a healthy manner, econophysicists must resort to controlled experiments. In this sense, for the time being, to emphasize the importance of controlled experiments, I suggest a different branch in econophysics, i.e., experimental econophysics, which mainly focuses on controlled experiments in the laboratory. Accordingly, in this book, econophysics is divided into two branches: empirical econophysics and experimental econophysics.

Clearly, the above two branches are divided according to the two different methods. It is worth noting that in the above paragraph, I did not mention theoretical analysis. But, for physicists like me, these simulations must be used to understand either empirical data (in real markets) or experimental data (in laboratories). So, for understanding empirical data, theoretical analysis is only a supplementary tool in empirical econophysics. On the other hand, for mainly understanding experimental data, theoretical analysis serves as an additional tool in experimental econophysics.

The focus of this book is experimental econophysics [19]. Regarding empirical econophysics, I refer the reader to some excellent monographs [14, 20–22] and reviews [23, 24]. If the reader can read Chinese, I would also recommend him/her to read two relevant monographs in Chinese [25, 26].

1.5 Methodology of Experimental Econophysics

Section 1.1 describes the combination of empirical analysis, controlled experiments, and theoretical analysis, which are fundamental in traditional physics. Owing to the great success of this combination method in traditional physics, I believe experimental econophysics should also follow this combination method (which actually starts from the article by my group in 2009 [7]). For this purpose, one should follow three steps:

- Step 1: He/she should either perform empirical analysis or survey the literature on empirical data in real markets. Obtain or find empirical results.
- Step 2: Then, he/she should consider how to design a controlled experiment in the laboratory. In the mean time, he/she should keep the above-mentioned physical idea ("Extracting reasons should be coarse-grained") in mind and extract the key factor(s) that affects the empirical results. Perform controlled experiments, revealing cause–effect relationships between the factor(s) and the above empirical results.
- Step 3: Perform theoretical analysis (agent-based simulations and/or analytical theory) to extend the cause–effect relationships obtained in Step 2 beyond the specific experimental limitations (namely specific subjects, specific avenue, and specific time). Use the relationships to explain existing phenomena (empirical results) and predict the future or unknowns. In other words, until the end of Step 3, the final results (relationships) should be universal enough, which echoes the above-mentioned second physical idea ("Results obtained should be universal").

The above three steps serve as the complete, ideal methodology for experimental econophysics. But, here I should remark that some projects in econophysics cannot strictly follow the three steps (at least for the time being) due to the complexity of real human systems like stock markets; see for example Chap. 3 or Chap. 12.

Chapter 2
Fundamentals

Abstract In this chapter, I introduce some fundamental knowledge in the field. My main focus is on how to design both controlled experiments and agent-based models. For showing the validity of the former, I present the Hayek hypothesis in advance; for clarifying the latter, I first present the El Farol bar problem and minority game. In addition, I also present both the information theory (with an emphasis on the Shannon entropy) and a nonparametric regression analysis (Hodrick-Prescott filter), which will be used in some other chapters.

Keywords Controlled experiments · Agent-based model · Hayek hypothesis · Minority game · Shannon entropy · Regression analysis

This chapter presents some fundamental knowledge or background that may help to understand the forthcoming chapters.

2.1 Hayek Hypothesis

Even nowadays, the typical method to study economic problems is the hypothetical–deductive method. Economists often derive an optimal situation of a system from certain assumptions, such as the complete knowledge of a preference system or information. F. A. Hayek (May 8, 1899–March 23, 1992; 1974 Nobel Prize winner in Economic Sciences) pointed out in his famous thesis "The Use of Knowledge in Society" published in 1945 [27] that this was totally a misunderstanding of social problems because no one could simply acquire the entire data of such assumptions. So despite the allocation problem under certain assumptions, a more important problem was how to obtain and use the decentralized resources and information.

Another thing economists always neglect is the specific knowledge of the individual. Other than scientific knowledge, this specific knowledge only gives its owner a unique benefit due to his/her own understanding of people, environment, and other special circumstances. That is, the exact part of knowledge economists put into the assumptions is equally important as scientific knowledge. As the comparative

J.-P. Huang, *Experimental Econophysics*, New Economic Windows,
DOI 10.1007/978-3-662-44234-0_2

stability of the aggregates cannot be accounted for by the "law of large numbers" or the mutual compensation of random changes and the fact that knowledge of this kind by its nature cannot enter into statistics, all plans should be made by the "man on the spot" rather than by any central authorities.

Since central authorities are limited, will the plans made by individuals reach a so-called equilibrium state? Hayek's answer was "yes." If all individuals follow the simple regulation of "equivalence of marginal rates of substitution," which is the basic of microeconomics, the market will indeed be in an equilibrium state finally, without the necessity of the knowledge of the entire market. Under the "magical" market mechanism of price, once someone finds an arbitrage opportunity of a commodity, the price of this commodity will change. Thus the marginal rates of substitution of this commodity to other commodities change, causing another round of price change. This effect spreads to more and more kinds of commodities and gradually covers the whole market, though maybe no one knows why such changes happen. The whole acts as one market, not because any of its members survey the whole field, but because their limited individual fields of vision sufficiently overlap so that through many intermediaries the relevant information is communicated to all.

Actually, the price system is just what A. Smith (June 5, 1723–July 17, 1790) called "the invisible hand" [28], a mechanism for communicating information, and the most significant fact about this system is the economy of knowledge with which it operates, or how little the individual participants need to know to be able to take the right action. Even if people know about all the factors of a commodity, the actual price is not available unless obtained from a market with price system.

The above content is known as the Hayek hypothesis [27], which asserts that markets can work correctly even though the participants have very limited knowledge of their environment or other participants. Certainly, traders have different talents, interests, and abilities, and they may interpret data differently or be swayed by fads. However, there is still room for markets to operate efficiently.

In 1982, "the father of experimental economics" V. L. Smith (2002 Nobel Prize winner in Economic Sciences) [29] tried proving the Hayek hypothesis using 150–200 experiments under different circumstances which he thought the correct method to select a reliable theory. The trading behavior of the market participants led the market to a competitive equilibrium under a double auction regulation without any extra information (the participants, i.e., subjects, only knew their own value of the commodity and the market price), the result of which was contrary to the classical theory of price taking hypothesis and complete knowledge hypothesis.

A key characteristic of controlled experiments was its specific convertible supply and demand condition and the reward system to stimulate the subjects. Once the supply and demand are determined, the equilibrium market price is also determined and whether the market was operated well could be easily observed. Although all the experiments [29] had different subjects and supply and demand conditions, they all ended with the equilibrium state, whether in a stationary or dynamic environment. Although the experiments [29] were still not perfect, a reliable result related to the Hayek hypothesis was that the attainment of competitive equilibrium outcomes is possible under less stringent conditions.

To sum, the Hayek hypothesis helps to account for the reliability of controlled experiments that contain finite subjects. Thus, this Hayek hypothesis may serve as a theoretical foundation for experimental economics [30] and experimental econophysics (introduced in this book), both of which are based on controlled human experiments in the laboratory. Besides, in the field of experimental econophysics, theoretical analysis also helps to validate and generalize results obtained from controlled experiments; details can be found in Sects. 1.1 and 1.5.

2.2 How to Design Computer-Aided Controlled Experiments

In the following chapters, I shall introduce the research progress on controlled experiments in the field of experimental econophysics. As a source of econophysics research ideas, the method of controlled experiments has become increasingly important in relative studies. Controlled experiments can be conducted in various ways. For example, in a simple experiment based on the minority game [1], the organizer may require subjects to close their eyes and raise hands to signal their choices between the two rooms in the game. Here, closing eyes prevents communications among the subjects so that it can be guaranteed that they make decisions independently. However, when regulations of an experiment become more complicated, or when the number of subjects becomes larger, computer-aided controlled experiments begin to show their efficiency as they can implement any experimental design easily and also collect experimental data and reveal real-time statistical results quickly.

A computer-aided controlled experiment needs programming of both the server and the client (Fig. 2.1). Two primary missions of the client are to distribute related information to users and also to provide users a channel to upload their own personalized choices. The server's main tasks are to store users' information, process users' uploaded data, and generate new information based on feedback from the behaviors of users. Generally, the client may be designed in the form of web pages to reduce costs and increase scalability. Any computer with a network connection can be easily set as a client. The servers of all the experiments in Chaps. 3–12 were constructed on the architecture of Linux + Apache + MySQL + PHP/Python (Readers can download a source code example from the link: http://t.cn/zOlkLEk).

Figure 2.1 shows a general schematic flowchart abstracted from the various experimental systems which will be introduced in Chaps. 3–12. Actually, the detailed designs of various systems are different in many aspects. For example, in the experiment of controlled laboratory stock market (Chap. 3), the server has to process every new order immediately since the time in the experiment is continuous. The herd experiment in Chap. 5 needs to add some robot agents (produced by a computer program) when computing the final outcome. The experiment of risk and return in Chap. 12 requires every subject to set their initial investment ratio, and the final outcome is not simply the "win" or "lose" but the final returns. Hence, we need to make minor revisions of the server and the web page accordingly for each specific system.

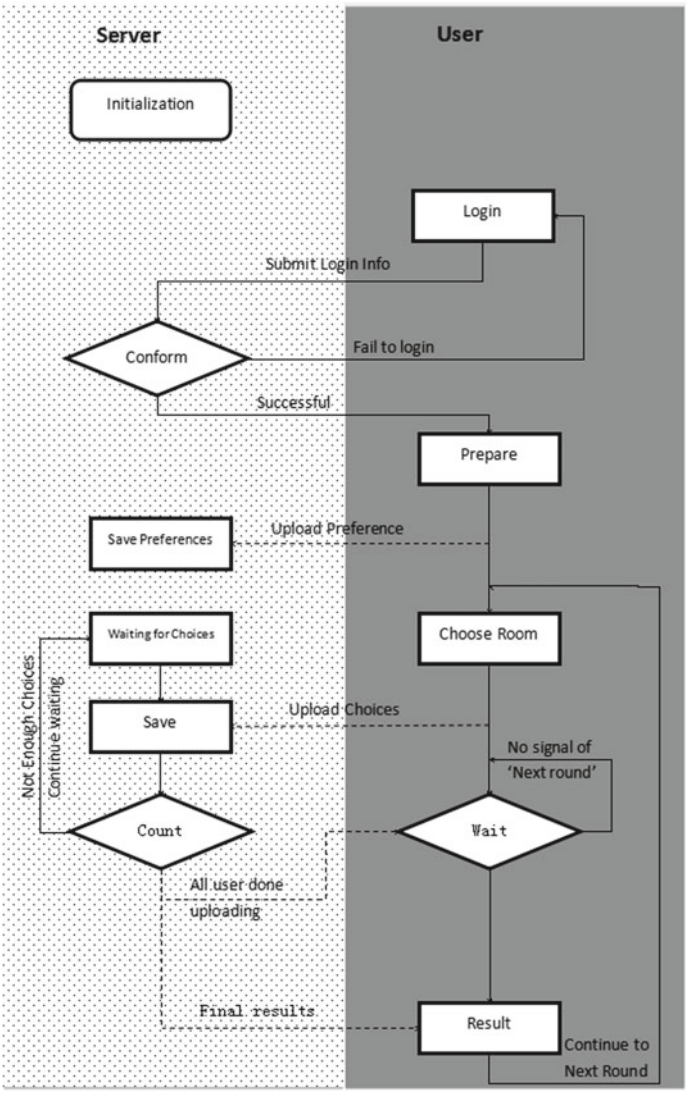

Fig. 2.1 A schematic flowchart showing how to compile the computer program for conducting controlled experiments. Adapted from Ref. [26]

Figure 2.2 depicts some screenshots of web pages in a certain controlled experiment. Figure 2.3 shows a site photograph in a controlled experiment.

Fig. 2.2 Web pages of a controlled experiment. **a** Background management interface, **b** login, **c** login successful, **d** choose a room, **e** waiting for the result, and **f** result. Adapted from Ref. [26]

Fig. 2.3 A site photograph in a controlled experiment organized by my group on September 28, 2013

2.3 El Farol Bar Problem and Minority Game

Here, we first present the real El Farol bar problem [31], which gave birth to the minority game [1] discussed in Chaps. 5–8. An early summary of minority games can be found in the book by Challet et al. [21].

2.3.1 El Farol Bar Problem

The essence of formation of human social activities lies in the acquisitiveness for resources. In many social and biological systems, the agents always spontaneously adaptively compete for limited resources, and thus change their environments. In order to effectively describe the system with the complexity, scientists have made a series of attempts. Such a resource competition system is just a kind of complex adaptive system.

For economic systems, the basic issue appears as well. Generally, in an economic market, if the resources are rationally allocated the market is full of vitality. Otherwise, the development will be impeded at least to some extent. Thus, the allocation of resources is the most fundamental economic problem. As is known, most popular economic theories are related to deductive reasoning. According to these economic theories, as long as all individuals are almost smart, everyone will choose the best action, and then each individual can reason his/her best action.

However, people gradually find that in real life, individuals often have no complete rationality and superb deductive reasoning ability when making decisions. Instead,

it is common for them to simply use a feasible method of trial and error. Therefore, it looks like inductive generalization and continuous learning when real individuals make decisions (namely, inductive reasoning).

In the game theory, researchers often use evolutionary games to study the similar dynamic process. However, when using evolutionary game models, economists usually do not take into account the character of limited rationality. Therefore, they cannot convincingly yield interesting phenomena and critical phase transition behaviors. A social human system contains a large number of agents who have the limited ability for inductive reasoning. Even so, the microscopic simplicity can still lead to the complexity of the macroscopic system. Obviously, from a physical point of view, this system has a variety of statistical physical phenomena.

In the past, there were studies on the allocation of resources. For example, in 1994, economist W. B. Arthur put forward a very representative resource allocation problem, the El Farol Bar problem, when he studied the inductive reasoning and bounded rationality. [31] It can be described as follows.

There is the El Farol bar in Santa Fe (a city in New Mexico of United States) which offers Irish music every Thursday night. Each Thursday, 100 persons (here 100 is only set for concreteness) need to decide independently whether to go to this bar for fun or stay at home because there are only 60 seats in the bar. If more than 60 persons are present, the bar is so crowded that the customers get a worse experience than staying at home. If most people choose to stay at home on that day, then the people who go to the bar enjoy the elegant environment and make a wise choice.

In this problem, Arthur assumed no communication in advance among the 100 persons. They only know the historical numbers from the past weeks and have to make decisions independently. In order to make a wise choice, each person needs to possess his own strategies which are used to predict the attendance in the bar this week. People cannot obtain the perfect equilibrium solutions at initial time when making decisions. They must consider others' decisions, and keep learning according to the limited historical experience in their mind. The elements of inductive reasoning and limited rationality in the El Farol bar problem lay the foundation for the further development of modeling in econophysics, as shown in Sect. 2.3.2.

2.3.2 Minority Game

Inspired by the above El Farol bar problem, physicists D. Challet and Y. C. Zhang in 1997 proposed a minority game to quantitatively describe this problem and statistically analyzed the emerging collective phenomena in complex adaptive systems [1]. In the following years, scientists did extensive research on the minority game and its applications in different fields, which have significantly promoted the development of econophysics. [20, 21] We introduce the minority game model as follows.

There are two rooms (indicated as Room A and Room B) and N agents, where N is an odd number. Each agent chooses independently to enter one of the two rooms. If one room contains fewer agents than the other, then the agents in this

Table 2.1 A model strategy table in the minority game with memory length $m = 2$

Information	Choice
00	1
01	0
10	1
11	0

room win. That is to say, the minority wins. The two rooms in the minority game actually correspond to the case of unbiased distribution of two resources. This game is repeated. Each agent can only make a decision next time according to the historical information. As a matter of fact, in daily life, people often face similar choices. Examples include choosing which road to avoid traffic jam during rush hours and choosing a less crowded emergency exit to escape. Although each of us can keep learning from limited historical experiences, it does not guarantee that we will make a correct choice every time.

In the minority game, the decision-making process which is based on historical information is modeled to form strategy tables. For the minority game, one assumes that agents' memory length of the historical information is limited. Each agent can only remember the latest m rounds. If $m = 2$, it can form a strategy as shown in Table 2.1. The historical information in the left column records the attendance in the past two rounds, which is filled with a string of bits of 0 and 1. For example, a string of "10" represents the past two winning rooms, Room A and Room B. The right column is the prediction which is filled with bits of 0 or 1. Bit 1 is linked to the choice of Room A for entrance, while bit 0 to that of Room B. So one can obtain a strategy pool with a size of 2^{2^m}. As m increases, the total number of strategy tables increases rapidly. In the original minority game model, the designers let each agent randomly select strategy tables. That is, the right column of each strategy table is randomly filled with 0 or 1. These agents are likely to repeat the same selected strategy (namely, the right columns of the strategy tables are the same). However, appropriately increasing the memory length can significantly reduce the repetition probability. Here, it is worth noting a special case: if the right column of a strategy table is all 1 (or 0), this strategy means that the agents are always locked into Room A (or B) no matter what happens.

According to these results, it is not hard to find that the minority game model with such a strategy structure is closely related to memory length m. And the historical information can only increase with 2^m.

In econophysics, minority game models have been widely used to simulate a special kind of complex adaptive systems, the stock markets [20, 32, 33]. Researchers always hope to generate similar stock market data through the minority game model. The stand or fall of this similarity often needs to be tested to see whether model data have the same stylized facts as the real market data. Besides, the minority game can also be used to study competition problems about an unbiased distribution of resources [3, 34–36].

2.4 How to Design Agent-Based Models

Agent-based modeling [37] plays an important role in the progress of complex systems researches. Differing from stochastic equations, agent-based models try to regenerate the evolution of a complex system via a bottom-up approach by means of simulating the behaviors of plentiful homogeneous or heterogeneous agents at the micro scale. There are two general ideas that can guide the design of a particular agent-based model. I shall discuss the two ideas in the following two subsections.

2.4.1 Modeling by Abstracting Real-World Systems

The minority game is a famous agent-based model in the field of econophysics. As one can see from Sect. 2.3, it originates from the El Farol bar problem. There have been many modifications on the minority game. A particular one is to model on the stock market [20]. It can be seen that the minority game on stock market has many simplifications compared to the real market, such as the adoption of linear relation between excess demand and price change, the neglect of transaction costs, etc. Even under such simplifications, the minority game can still reproduce many statistical characteristics of the stock market successfully [20], which gives a clear illustration of the capabilities of agent-based models to reveal the endogenous mechanisms under financial markets. Hence, one important idea when trying to build an agent-based model is to abstract real-world systems. First, regulations in the associated real-world system should be written down one by one. Second, the importance of each regulation should be evaluated; key regulations should be introduced into the model, while trivial ones can be eliminated to make the model simple and clear. Third, decision-making process for the virtual agents should be carefully designed to mimic the behaviors of real-world humans. Finally, one can complete the designs of an agent-based model by combining the simplified structure and a large number of interacting virtual agents. It can be seen that this idea guides our designs of all the models appearing in Chaps. 5–11.

One more thing I wish to discuss is the simplifications made in the agent-based modeling method. In real financial markets, it can be seen that the price of an asset is the reflection of every market participant's information-collecting and decision-making abilities. Moreover, there also exist communications among participants that may lead to the herding phenomenon. Clearly, if we want to include all these factors into our agent-based model, the model can become much more complicated. So we have to compromise by simplifying the model accordingly. But does our model lose its generality and reasonability? One may refer to the famous Ising model in statistical physics. In the Ising model, the time is discrete, which is clearly an unreal assumption in our real world. However, the model can regenerate many ferromagnetic phenomena very successfully. Hence, we can conclude that a proper simplification can wipe off trivial factors in the real-world system and make the model more

powerful in explanations of the real-world phenomena. But as we know, making a good simplification is not always a simple task.

Next, we discuss the second approach for building agent-based models, that is, building models through physical models.

2.4.2 Modeling Through Borrowing from Physical Models

Since many physical models have already been proven proper to explain related natural phenomena, it is worth academic research to extend them to economic or social systems. Here, the Ising model is taken as an example for illustrating this idea.

The Ising model aims at studying the temperature dependence of magnetic susceptibility during the ferromagnetic phase transition. The model contains a large number of interacting spins which form a certain topological structure. It is usually assumed that (1) each spin only has two states, i.e., $\sigma_j = +\frac{1}{2}$ for the up direction and $\sigma_j = -\frac{1}{2}$ for the down direction; (2) the range of spin interactions is limited to the first neighborhood [38].

The fundamental physical picture of the ferromagnetic phase transition is that when increasing temperature, the dominant state (up or down) shown in the overall lattice changes through spin interactions. On one hand, the principle of least action requests that all spins are aligned in the same direction so that the spin interactions are at the lowest level. On the other hand, thermal motions tend to drive the directions of the spins to a random arrangement at which the system's entropy is the largest. The probabilities of spin states obey the Boltzmann distribution. As long as the system's temperature gets higher than the Curie temperature, the thermal motions among the spins become dominant so that a phase transition occurs from ferromagnetic to paramagnetic. For a spin, suppose its energy is E_+ for the up state (i.e., $\sigma_j = \left|+\frac{1}{2}\right\rangle$), and E_- for the down state ($\sigma_j = \left|-\frac{1}{2}\right\rangle$). When $E_- > E_+$, the probability for the spin to be in the up state $\left|+\frac{1}{2}\right\rangle$ in the next time step is denoted as p_+, and in the opposite state $\left|-\frac{1}{2}\right\rangle$ with a probability of p_-. Then we can write,

$$p_+ = \frac{e^{-\frac{E_+}{kT}}}{e^{-\frac{E_+}{kT}} + e^{-\frac{E_-}{kT}}},\ p_- = \frac{e^{-\frac{E_-}{kT}}}{e^{-\frac{E_+}{kT}} + e^{-\frac{E_-}{kT}}}.$$

It can be seen that when the temperature T gets closer to 0, $p_+ \to \frac{E_+}{E_+ + E_-}$, $p_- \to \frac{E_-}{E_+ + E_-}$, now all the spins tend to be arranged in the same direction. If T becomes much large, $p_+ \to p_- \to \frac{1}{2}$, which means that the directions of spins become totally random. That is, the system transfer from ferromagnetic to paramagnetic as T increases.

To have a further discussion of the Ising model, here we take the two-dimensional orthogonal cubic lattice for example. The Hamiltonian can be composed of two parts:

$$H(\sigma_j) = -\sum_i J_{i,j}\sigma_i\sigma_j - h_j\sigma_j.$$

Here, the first part $J_{i,j}\sigma_i\sigma_j$ represents interactions between spins (near-field or local effect), where spin i belongs to the first neighborhood of spin j. The second part $h_j\sigma_j$ is the Hamiltonian of σ_j in the external magnetic field h_j (global effect). According to the principle of least action, every spin tends to choose states that obey the Boltzmann distribution. Under this distribution, the probability of being the least energy state for $H(\sigma_j)$ is the largest. The state probability is

$$P(\sigma_j) = \frac{e^{-\beta H}}{\sum_{\sigma_j} e^{-\beta H}},$$

where $\beta = k_B T$.

In the simulations, a spin in the lattice is selected randomly and the state of the spin is adjusted on the basis of thermodynamical laws. By repeating this procedure, the system can finally reach equilibrium. At equilibrium, one macroscopic property of the system simply equals the ensemble average of the associated microscopic property among all the spins. Note that $P(\sigma_j)$ is not independent of T, thus we can obtain the relation between one observation of the value of E and the temperature T or other parameters:

$$E(f) = \sum_j f(\sigma_j)P(\sigma_j).$$

A logical framework of the Ising model is shown in Fig. 2.4.

By comparing the similarities between ferromagnetic lattice and financial markets, one can establish an agent-based model for financial markets based on the logical framework of the Ising model (Fig. 2.5). The analogy between financial markets and ferromagnetic lattice is obvious.

First, from the point of interactions, in the Ising model, the spin states depend on the combined result of both global effect from the macro-external magnetic field and local effect from the micro-neighboring spin states. And in the financial markets, investing strategies made by market participants also depend on the combined result of global information such as the price and trading volume of an asset, fundamental market information (like GDP or CPI), and local information from the "neighboring" traders (here "neighboring" means the first neighborhood in the social network appearing in financial markets for a trader). Hence, we may write the associated "Hamiltonian" at one lattice grid for traders as $H(\sigma_j) = -\sum_i J_{i,j}\sigma_i\sigma_j - h_j\sigma_j$.

Second, from the point of "strategies," in the Ising model, spins always tend to change their states to find the best one that confirms the least action and the maximum entropy principles; similarly, in the financial market model, agents should also be able to modify their investing strategies to find the best one that brings in maximum

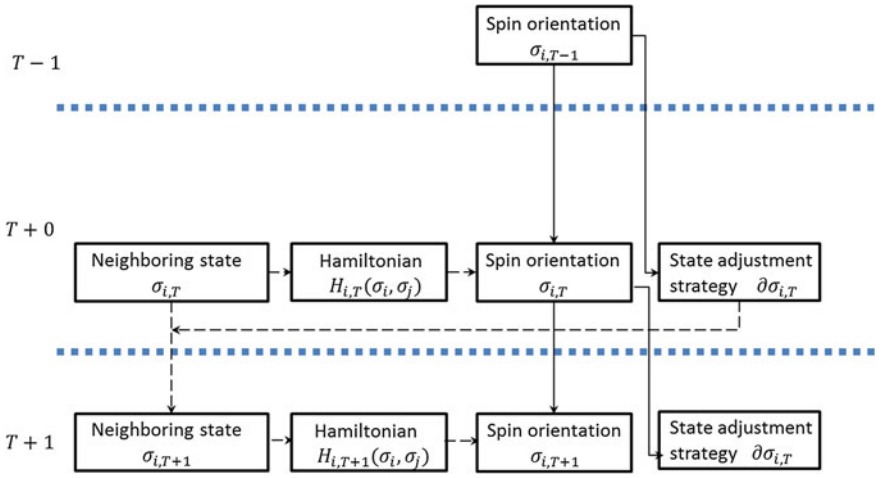

Fig. 2.4 Two-dimensional ferromagnetic phase transition in the Ising Model. Adapted from Ref. [26]

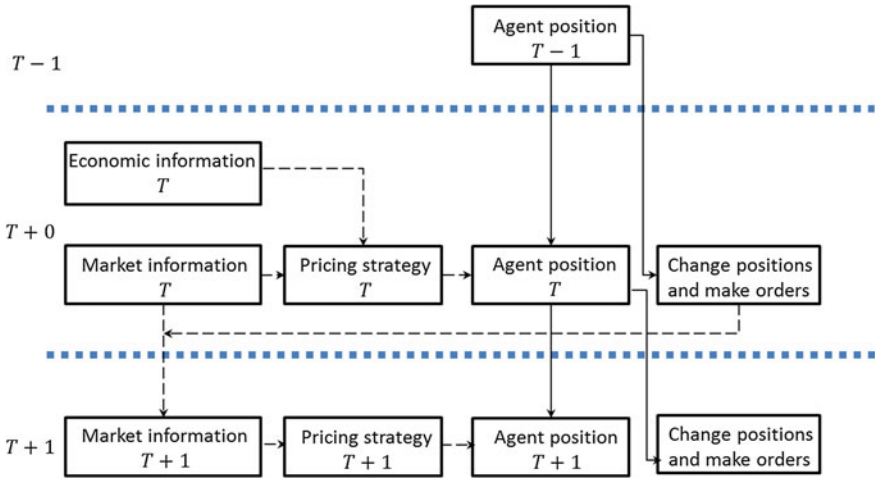

Fig. 2.5 Agent-based financial market model borrowing from the framework of the Ising Model in Fig. 2.4. Adapted from Ref. [26]

returns with minimum risks. Third, from the point of feedback process, in the Ising model, the macromagnetic susceptibility can be obtained by summing up all the microspin states; accordingly, in the financial market model, through the match of orders executed by market makers, price at each time is generated.

Thus, we can see that there exists a deep analogy between physical and economic models.

The financial market models based on the Ising model's framework have received preliminary success [39, 40]. But what strategies should be adopted by agents so that the real-world phenomena in financial markets can be regenerated? What kind of payoff function is able to reflect the investment demands properly? Do the time scales at which agents make decisions impact on global information? All these questions are still waiting to be answered in the future.

2.4.3 How to Test the Reliability of Agent-Based Models

Whether the agent-based model is successful or not depends on whether it can stand empirical and experimental tests. Despite that it seems reasonable for the two ideas of building an agent-based model introduced in Sects. 2.4.1 and 2.4.2, yet the process does not equal results. The logicality and rationality of the course of establishing a model cannot prove that the final model is perfectly correct and dependable.

Compared with experimental observations, it is the only way to test whether an agent-based model is reliable. The experimental observation mentioned here can be the induction and analysis of not only the existing economical or financial data but also the controlled experiment data. The former corresponds to empirical econophysics [14], however, the latter corresponds to experimental econophysics (topic of this book). From this, it can be seen that agent-based modeling is a fundamental method and it may have stronger development in the future.

2.5 Information Theory

2.5.1 Initial Remarks

In books on statistical mechanics, information theory is a chapter that cannot be ignored. At first look, you may wonder how information theory is linked to statistical physics. They seem like two totally different scientific fields. In this section, I give a brief introduction to the theory. Through it, you can see how information theory borrowed the concept of entropy from physics and then how physicists used information theory to reinterpret their statistical researches and further developed information theory. What is more, inspired by information theory, physicists also gave new explanations to the long-hunted Maxwell's demon. Needless to say, in econophysics, information theory can have applications as well; see Chap. 9.

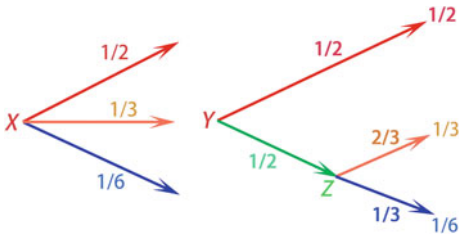

Fig. 2.6 Illustration of the composition law of H. Adapted from Ref. [19]

2.5.2 Shannon Entropy: Historical Beginning and the Unit of Information

2.5.2.1 Historical Beginning

In 1948, C. E. Shannon (April 30, 1916–February 24, 2001) published his classic article "A mathematical theory of communication" [41] in the *Bell System Technical Journal* which established the discipline of information theory. Obviously, the article title showed no relation to the physical world. In this article, Shannon discussed how to quantitatively analyze the amount of uncertainty in a discrete source of information.

Suppose for an experiment, there are n possible outcomes each of which happens at a rate of p_1, p_2, …, and p_n, respectively. Under different probability distributions of the outcomes, the experiment contains various amounts of uncertainty. To compare the uncertainty quantitatively, a measure, denoted as $H(p_1, p_2, \ldots, p_n)$, should be found. Shannon suggested the expression of H having the following three properties:

1. H should be a continuous function of the p_i's.
2. If all the p_i's are equal, i.e., $p_i = 1/n$, H should increase monotonically with n. This is easy to understand, because with equally likely outcomes, there is more uncertainty when there are more possible outcomes.
3. The composition law: if an experiment is broken into two successive experiments, the original H should be the weighted sum of the two individual values of H. Figure 2.6 shows an illustration of the composition law. The single experiment X on the left has three outcomes with probabilities of $p_1 = 1/2$, $p_2 = 1/3$, and $p_3 = 1/6$. For the two successive experiments on the right, the experiment Y has two outcomes, each with a probability of 1/2, and if the second occurs, the other experiment Z takes place with two outcomes under probabilities 2/3 and 1/3. It can be seen that the final outcomes of the two successive experiments Y and Z have the same probabilities as the ones in the single experiment X. Then, the composition law requires, in this special case, that $H(\frac{1}{2}, \frac{1}{3}, \frac{1}{6}) = H(\frac{1}{2}, \frac{1}{2}) + \frac{1}{2}H(\frac{2}{3}, \frac{1}{3})$. Here, the coefficient $\frac{1}{2}$ in the equation is because the experiment Z only takes place half the time.

To satisfy the three properties above, Shannon showed that the simplest form for H is

$$H(p_1, p_2, \ldots, p_n) = \sum_{i=1}^{n} f(p_i), \tag{2.1}$$

where $f(p_i)$ is a continuous function due to the first property. Considering that the expression of H is universal for any set of probability distributions $\{p_1, p_2, \ldots, p_n\}$, we can deduce H under the special case of equal probabilities, namely, $p_i = 1/n, \forall i$. Then, Eq. (2.1) gives

$$H\left(\frac{1}{n}, \frac{1}{n}, \ldots, \frac{1}{n}\right) = nf\left(\frac{1}{n}\right). \tag{2.2}$$

Suppose a single experiment has n outcomes with equal probabilities of $1/n$. It breaks into two successive experiments: the first one has r evenly happened outcomes and for each of its outcomes, the second occurs sequentially with s evenly happened outcomes. And there is $n = rs$. Then, the composition law requires

$$H\left(\frac{1}{n}, \frac{1}{n}, \ldots, \frac{1}{n}\right) = H\left(\frac{1}{rs}, \frac{1}{rs}, \ldots, \frac{1}{rs}\right) = H\left(\frac{1}{r}, \frac{1}{r}, \ldots, \frac{1}{r}\right) + H\left(\frac{1}{s}, \frac{1}{s}, \ldots, \frac{1}{s}\right). \tag{2.3}$$

Plugging Eq. (2.3) into Eq. (2.2) yields

$$rsf\left(\frac{1}{rs}\right) = rf\left(\frac{1}{r}\right) + sf\left(\frac{1}{s}\right). \tag{2.4}$$

Let

$$g(M) = \frac{1}{M} f(M), \tag{2.5}$$

then Eq. (2.4) becomes

$$g(RS) = g(R) + g(S), \tag{2.6}$$

where $R = 1/r$, $S = 1/s$. Differentiating Eq. (2.6) with respect to R or S yields the following two equations accordingly:

$$Sg'(RS) = g'(R), \tag{2.7}$$

$$Rg'(RS) = g'(S), \tag{2.8}$$

where $g'(M)$ means differentiating $g(M)$ with respect to M. So we obtain

$$Rg'(R) = Sg'(S). \tag{2.9}$$

Because R and S are two independent variables, Eq. (2.9) gives

$$Mg'(M) = Rg'(R) = Sg'(S) = A, \tag{2.10}$$

where A is a constant. Integrating Eq. (2.10) for the unspecified variable M, we can get the general expression of function $g(M)$

$$g(M) = A\ln(M) + C, \tag{2.11}$$

where C is also a constant and $\ln(M)$ gives the natural logarithm of M. Plugging Eq. (2.11) into Eq. (2.5) and letting $M = \frac{1}{n}$, we obtain

$$f\left(\frac{1}{n}\right) = -\frac{A}{n}\ln(n) + \frac{C}{n}. \tag{2.12}$$

Now we should try to find the values of the two constants, A and C. On the boundary condition $n = 1$, the experiment only has one sure outcome. Therefore, now the uncertainty should be zero. From Eqs. (2.2) and (2.12), we have $H(1) = f(1) = C = 0$. Hence, for equal probabilities, there is

$$H\left(\frac{1}{n}, \frac{1}{n}, \ldots, \frac{1}{n}\right) = -A\ln(n). \tag{2.13}$$

Now, let us turn to the second property of H. It is said that H should increase with n monotonically, hence $\frac{dH}{dn} = -\frac{A}{n} \geq 0$, which means $A \leq 0$. It is obvious that $A \neq 0$. So, we let $K = -A$ with K being a positive constant. Then we obtain the general expression of function $f(p_i)$, namely

$$f(p_i) = -Kp_i\ln(p_i). \tag{2.14}$$

Back to Eq. (2.1), now we can write the final form of H that satisfies the three properties,

$$H(p_1, p_2, \ldots, p_n) = -K\sum_{i=1}^{n} p_i\ln(p_i), \tag{2.15}$$

where K is a positive constant.

Now let us take a break from information theory and turn our attention to the physical world. Consider a system that contains N distinguishable particles obeying Boltzmann statistics. Assume there are n nondegenerate quantum states, then we can obtain the entropy of the system expressed as [42],

$$S = -kN\sum_{j=1}^{n}\left(\frac{N_j}{N}\right)\ln\left(\frac{N_j}{N}\right), \tag{2.16}$$

where k is the Boltzmann's constant and N_j stands for the number of particles at the jth state. If we link $\frac{N_j}{N}$ to the probability p_j which means that in average N_j particles are in the jth state, Eq. (2.16) becomes

$$S = -kN \sum_{j=1}^{n} p_j \ln(p_j). \tag{2.17}$$

Compared with Eq. (2.15), we can see the relation between H and S is

$$S = \frac{kN}{K} H. \tag{2.18}$$

In Shannon's 1948 article [41], he wrote "The form of H will be recognized as that of entropy as defined in certain formulations of statistical mechanics…We shall call $H = -\sum p_i \log p_i$ the entropy of the set of probabilities $p_1, \ldots, p_n$." This is where the information theory and Shannon entropy all began.

2.5.2.2 The Unit of Information

In the expression of Shannon entropy, i.e., Eq. (2.15), K is still left as a constant with no specific value. In information theory, a common unit for Shannon entropy is *bit*, which is a contraction of *binary digit*. One bit is typically defined as the uncertainty in one time of coin toss that has equally likely outcomes (i.e., heads or tails). Hence, in this case, there is $H(\frac{1}{2}, \frac{1}{2}) = K\ln(2) = 1$, which yields $K = 1/\ln(2)$. Then the expression of Shannon entropy becomes

$$H(p_1, p_2, \ldots, p_n) = -\sum_{i=1}^{n} p_i \log_2(p_i). \tag{2.19}$$

Now we can calculate the Shannon entropy for some specific cases. Here is one example. For a decimal digit, suppose it can choose a value from 0 to 9 with equal probabilities, i.e., $p = \frac{1}{10}$. Then, using Eq. (2.19), it can be calculated that $H = \sum_{i=1}^{10} \frac{1}{10} \log_2(10) = \log_2(10) = 3.32$. Therefore, the decimal digit contains 3.32 bits of uncertainty.

2.5.3 When Information Meets Physics: The Principle of Maximum Entropy and the Fight with Maxwell's Demon

2.5.3.1 The Principle of Maximum Entropy

Now we have seen that Shannon entropy and the entropy of statistical mechanics have similar forms. Is this a coincidence? The answer is no. In physics, entropy is a measure of system's disorder. The word "disorder" means there is a lack of "information" for us to know the exact physical state of the system. Hence, in other words, we can say entropy is the amount of additional information needed to specify

the exact state of a system. This shows a kind of qualitative relationship between the two concepts of entropy. In 1957, E. T. Jaynes [43] further developed information theory by expounding the principle of maximum entropy, and then reinterpreted statistical mechanics through the viewpoints of information theory. Reading this article, we can see a deeper connection between the two fields.

The principle of maximum entropy states that given only partial information of a system, the probability distribution with the largest entropy is the least biased estimate possible for its current state. Suppose for a particular variable x, it can have n discrete values $x_i, i = 1, 2, \ldots, n$. If one knows that the mean value of x is $\bar{x}$, the restrictions on the unknown probability distribution $\{p_1, p_2, \ldots, p_n\}$ of x now are

$$\bar{x} = \sum_{i=1}^{n} p_i x_i, \tag{2.20}$$

$$\sum_{i=1}^{n} p_i = 1. \tag{2.21}$$

So, now the principle of maximum entropy tells us that the most proper values of $\{p_1, p_2, \ldots, p_n\}$ are those that maximize the Shannon entropy H in Eq. (2.15). Using the method of Lagrange multipliers [42], we can finally get the expression for $\{p_1, p_2, \ldots, p_n\}$, i.e.,

$$p_i = \frac{e^{-\mu x_i}}{Z}, \tag{2.22}$$

where Z is the partition function,

$$Z \equiv \sum_{i=1}^{n} e^{-\mu x_i}, \tag{2.23}$$

and μ can be derived from the expression

$$\bar{x} = -\frac{\partial}{\partial \mu} \ln(Z). \tag{2.24}$$

Inserting Eq. (2.22) into Eq. (2.15) leads to the maximal Shannon entropy

$$H_{\max} = K\mu\bar{x} + K\ln(Z). \tag{2.25}$$

Now let us turn to statistical mechanics. For the physical system containing N distinguishable particles described in Sect. 2.5.2, the expression of entropy is given in Eq. (2.16). Here, assume the associated energy level for each state is ε_j, $j = 1, 2, \ldots, n$, and the average energy of the system is U. Then, we can follow the same steps above to obtain the most proper particle distribution using the principle of maximum entropy, which is

$$\frac{N_j}{N} = \frac{e^{-\beta\varepsilon_j}}{Z}, \tag{2.26}$$

where the partition function Z is

$$Z = \sum_{j=1}^{n} e^{-\beta\varepsilon_j}. \tag{2.27}$$

It is obvious that Eqs. (2.26) and (2.27) fit the Boltzmann distribution for nondegenerate energy states. And $\beta = 1/kT$ where k is the Boltzmann constant. Now the entropy of the physical system is maximal, which is

$$S_{\max} = \frac{U}{T} + Nk\ln(Z). \tag{2.28}$$

Note that Eq. (2.28) also has a similar form with Eq. (2.25).

Hence, in Ref. [43], E. T. Jaynes stated that "If one considers statistical mechanics as a form of statistical inference rather than as a physical theory, it is found that the usual computational rules, starting with the determination of the partition function, are an immediate consequence of the maximum-entropy principle."

Now we have seen that the principle of maximum entropy can be used in both statistical mechanics and information theory, which means the methodologies in both fields can be connected together. But can we further integrate the two concepts of entropy as a uniform one? The Maxwell's demon may help to give an answer.

2.5.3.2 The Fight with Maxwell's Demon

There are various descriptions of the second law of thermodynamics. One is called the principle of increasing entropy, i.e., the entropy of an isolated system increases in any irreversible process and is unaltered in any reversible process. Another is the Clausius statement, namely heat can never pass from a colder to a warmer body without external work being performed on the system.

In 1867, J. C. Maxwell (June 13, 1831–November 5, 1879) first proposed a thought experiment that challenged the second law of thermodynamics. This is when the Maxwell's demon was born. An illustration of the thought experiment is shown in Fig. 2.7. The detailed process is described in the following:

1. Suppose there is a container which is divided by an adiabatic diaphragm into two parts, denoted as part A and part B, respectively, as shown in Fig. 2.7. The container is filled with a sort of gas and the gas in part A is assumed to be hotter than the gas in part B.
2. Imagine there is a demon. He can know the paths and velocities of every gas molecule by simple inspection. He can do nothing but to open or close a hole in the diaphragm with a zero-mass frictionless slide.

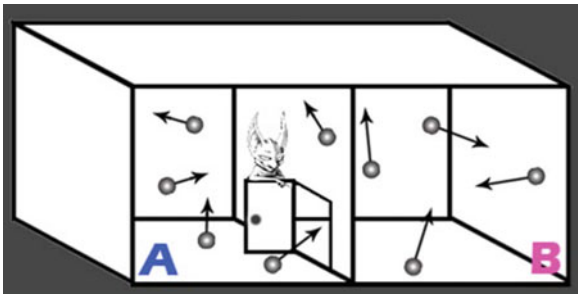

Fig. 2.7 Illustration of Maxwell's demon who apparently violates the second law of thermodynamics

3. His mission is to open the hole to let a gas molecule in part A to enter part B when that molecule has a velocity less than the *rms* velocity (*rms* is short for *root mean square*; and the *rms* velocity is expressed by $v_{\text{rms}} \equiv \sqrt{\overline{v^2}}$) in B; meanwhile, a gas molecule from B is allowed to pass into A through the hole if its velocity exceeds the *rms* velocity in A. The two procedures are conducted in such a way that the total number of gas molecules in A or B is unchanged.

We know that a higher temperature shown in a gas system's macrostate means a higher average kinetic energy of the gas molecules in the microstate, and vice versa. Hence, through the demon's operation, the hotter part A gets hotter and the colder part B gets colder, and no external work is done. This violates the second law of thermodynamics obviously.

Since the demon was born, it has attracted a huge amount of discussion. Different explanations have been proposed. After Ref. [41], a new explanation framework emerged which combines the demon with information theory and computer science. In 1961, R. Landauer (February 4, 1927–April 28, 1999) proposed a physical principle which was later called Landauer's principle [44]. It states that any logically irreversible manipulation of information, such as the erasure of a bit or the merging of two computation paths, must be accompanied by a corresponding entropy increase in noninformation-bearing degrees of freedom of the information processing apparatus or its environment [45]. In 1982, C. H. Bennett argued that to determine whether to let a molecule pass the hole, the demon must acquire information about the molecule's state and then store it; but no matter how well the demon prepares in advance, he will eventually run out of his information storage space and must begin to erase the previous information he has collected; since erasing information is a thermodynamically irreversible process according to Landauer's principle, an additional part of entropy will be created [46]. Hence, this means no matter how hard the demon works, he still cannot violate the second law of thermodynamics.

Nowadays, the subject of Maxwell's demon with information theory and computer science draws a lot of attention. For example, in Ref. [47], an inanimate device that

mimics the intelligent Maxwell's demon is designed. The device only requires a memory register to store information, which is quite interesting.

2.5.4 Discussion

So far, we have seen how information theory and statistical mechanics are connected and influence each other. This may give us many inspirations when we deal with econophysics. First, in econophysics, we also need to deal with situations where a lot of uncertainty exists, such as the different kinds of human behavior in some game models or the movement of a stock price. In these situations, the Shannon entropy may have application; see Chap. 9. Second, econophysics has already adopted many physical concepts or methods (such as fractals, chaos, or even quantum mechanics) to tackle economic problems. But now it is still far from mature, lacking fundamental theories or principles. So comparing with the development history of information theory, we can be confident that maybe one day, in textbooks of physics such as statistical mechanics, there will be a chapter on econophysics that cannot be neglected.

2.6 Nonparametric Regression Analysis: Hodrick-Prescott Filter

When talking about the analysis of data (e.g., obtained from controlled experiments or collected from real markets) in econophysics, we often focus on statistical distribution analysis and time correlation analysis for the time series. Commonly, we transform the initial raw time series into the dimension of return. On one hand, we always neglect the time attribute of a series when analyzing the statistical distribution problem. On the other hand, the statistical attribute is also ignored when arguing about the time correlation. So, the critical point is that we need not face the time series directly and primordially but in a side way. It becomes a reduced problem about the linear or other obvious relationship between two physical quantities, which is what econophysicists like to do. Compared with the situation where the relationship is known with an equation, sometimes there is no specific relationship between two quantities. Therefore, except linear regression or other parametric regression, nonparametric regression may be preferred occasionally. For example, for a price time series about one stock, if we want to know its cyclical volatility, one method is to directly consider the relationship between price and time. However, the price curve is possibly without regularity. At this time, for perfect effectiveness when solving real economic problems, economists begin to pay more and more attention to nonparametric regression analysis. For e.g., here I introduce a kind of nonparametric regression analysis method.

As is known, a filter generally refers to a physical tool widely used in signal processing. We can also regard the economic time series as one kind of signal. Since the signal contains too much information and behaves too randomly, naturally we

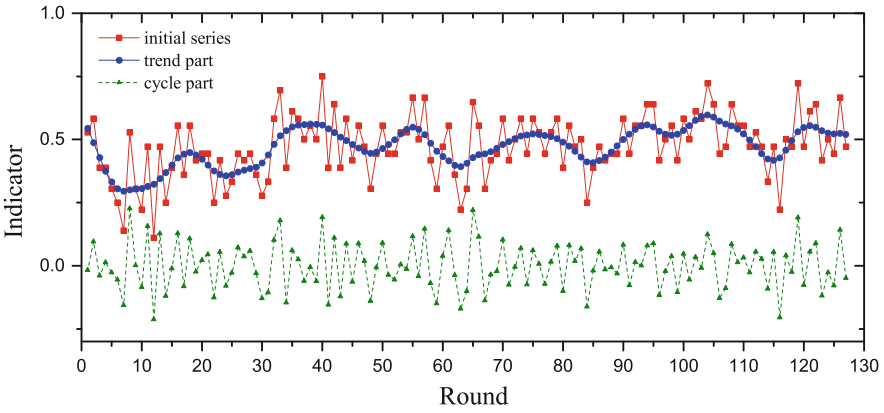

Fig. 2.8 An example showing the Hodrick-Prescott filter method

can use filters to decompose it and extract useful information from it. To separate the behavior of a time series into regular and irregular components, several filters have been developed and are already commonly used in studies of macroeconomic and financial phenomena. Such filters are Hodrick-Prescott filter [48, 49], Baxter King filter [50, 51], Christiano-Fitzgerald random walk filter [52, 53], and Butterworth square wave filter [54, 55]. The Hodrick-Prescott filter is one of the most commonly used and known methods. It was first proposed in 1980 by R. J. Hodrick and E. C. Prescott when they tried to analyze postwar United States business cycles [48]. Since economic quantities are changing tardily rather than invariably, they think that economic performance can be reckoned as the combination of two parts, long-term potential growth, and short-term fluctuation. The core thought in this method is to decompose the time series X_t into trend component G_t and cyclical component C_t, that is, $X_t = G_t + C_t$. However, economists are more interested in cyclical component, which refers to business cycles. That is why the Hodrick-Prescott filter is called as a detrending method and a high-pass filter. If we denote L as a linear lag operator, $L \cdot G_t = G_{t-1}$ and the second difference will be like

$$\Delta^2 G = (1 - L)^2 \cdot G_t = (G_t - G_{t-1}) - (G_{t-1} - G_{t-2}).$$

Suppose that both the cyclical part and the second difference in growth part have a zero mean value and a normally distributed variance. Then, through solving the minimization problem below

$$\min \sum_{t=1}^{T} \left\{ C_t^2 + \lambda \left[(G_{t+1} - G_t) - (G_t - G_{t-1}) \right]^2 \right\},$$

the optimal trend and cyclical components can be obtained from the original series. Actually, this optimal result refers to the minimized sum of both variance of cyclical

part and squares of growth part's second difference. The only parameter λ is given as the ratio of the two variances

$$\lambda = \frac{\sigma_C^2}{\sigma_{\Delta^2 G}^2},$$

which determines the smoothness for the trend part. As long as λ gets larger, the trend part G_t will get smoother. So it becomes an important problem to select an appropriate λ when applying the Hodrick-Prescott filter to economic data of different frequencies. We should have known that the trend component, which represents the potential growth in an area, is always steady and mainly affected by long-term economic policies or others. Economists adopt several distinct λ to fit for different economic cycles. Empirically, most economists use 6.25 for annual data [56], $\lambda = 1600$ for quarterly economic data, and 1,29,600 for monthly data [56].

Figure 2.8 schematically shows an example of a time series applied with the Hodrick-Prescott filter. The original data come from one human experiment conducted by my group (for clarity, experimental details are neglected herein; relevant experiments can be found in Chap. 9), which aims to study a kind of business cycle. The horizonal axis stands for experimental rounds, and the vertical axis represents one economic indicator, shown in red, which may present cyclical property. After we apply the Hodrick-Prescott filter, the separated trend part and cyclical part are shown above in blue and green, respectively.

Chapter 3
Stylized Facts: Scaling Law and Clustering Behavior

Abstract To our knowledge, the existing laboratory experiments have not convincingly reappeared the stylized facts (say, scaling law and clustering behavior) that have been revealed for real economic/financial markets by econophysicists. An important reason is that in these experiments, discrete trading time makes these laboratory markets deviated from real markets where trading time is naturally continuous. Here we attempt to overcome this problem by designing a continuous double-auction stock-trading market and conducting several human experiments in the laboratory. As a result, the present artificial financial market can indeed reproduce some stylized facts related to scaling laws and clustering behavior. Also, it predicts some other scaling laws in human behavior dynamics that are hard to achieve in real markets due to the difficulty in getting the data. Thus, it becomes possible to study real stock markets by conducting controlled experiments on such laboratory stock markets producing high frequency data.

Keywords Artificial stock market · Scaling law · Clustering behavior · Human dynamics

3.1 Opening Remarks

Inspired by H. E. Stanley and his coauthors' pioneering work [14, 57], physicists began studying the statistical properties of financial markets using methods widely used in statistical physics. As a result, many universal rules, e.g., scaling laws (namely power-law distributions in the eyes of econophysicists) and clustering behaviors, were empirically observed from stock markets of different countries [14, 57–63] (and even in the field of music [64]). Clearly, because it is illegal or immoral to control real markets, these researches lack controllability which, however, is very important to know the impact of a specific condition on such universal rules. In this direction, S. P. Li and coworkers [5] conducted an experiment on political exchange for election outcome prediction, with a focus on the Taiwan general election in 2004.

J.-P. Huang, *Experimental Econophysics*, New Economic Windows,
DOI 10.1007/978-3-662-44234-0_3

Future contracts for election outcome were created and traded among participants in a web-based market. The liquidation value was determined by the percentage of votes a candidate would receive on the day of election. It is a good prediction because participants predict the vote percentage rather than simply buying future contracts of the candidate they support. Finally, the result was compared to that of the polls. Interestingly, when investigating the network topology of such an experimental futures exchange, researchers [6] showed that the network topology is hierarchical, disassortative, and small-world with a power-law exponent, 1.02 ± 0.09, in the degree distribution. They also showed power-law distributions of the net incomes and inter-transaction time intervals [6]. After identifying communities in the network as groups of the like-minded, they showed that the distribution of the community size is also distributed in the power law with an exponent, 1.19 ± 0.16 [6].

Inspired by their work [5, 6], we believe that it is also possible to design stock markets in the laboratory, so that we can reveal the underlying mechanism of the universal rules.

In fact, economists have already done a lot of great work in laboratory human stock markets [30, 65]. In the 1990s, Freidman wrote an article to show his series of experiments; these experiments gave laboratory evidence of the efficiency of two different trading institutions [66]. Later, Porter and Smith designed a laboratory market with dividends, and also with several other extensions including short sells, limited price changing rules, associated future markets, etc.; they confirmed the existence of price bubbles in this market and examined the influence of each extension on the bubbles [67]. Hirota et al. published an article based on a similar market structure; studying the trading horizons, they suggested that the investors' short horizons and consequent difficulties of backward inductions are important contributors to the emergence of price bubbles [68]. These experiments offered good insights into the associated research problems. However, to our knowledge, all the experiments mentioned above have not convincingly reproduced the stylized facts (say, scaling laws) that have been revealed for real economic/financial markets by econophysicists. An important reason may be that in these experiments, time is divided into trading cycles, e.g., 5 min. Hence, the participators have to make decisions on the cycles [30, 65–68]. In other words, discrete time steps deviate these laboratory markets from real markets where trading time is naturally continuous. In this chapter, we attempt to overcome this problem by designing a continuous double-auction stock-trading market and then carrying out several human experiments in the laboratory. As an initial work, the present artificial financial market can produce some stylized facts (clustering effects and scaling behaviors) that are in qualitative agreement with those of real markets. Also, it predicts some other scaling laws in human behavior dynamics that are difficult to achieve in real markets due to the difficulty in getting data.

3.2 Market Structure

3.2.1 Basic Framework

Consider a market with N traders, indexed by i. Trading time is indicated by t. To simplify the problem, traders only decide how to manage their portfolios consisting of one stock and risk-free asset. The risk-free asset in our market is simply bank savings (cash). There are Q shares of stocks issued in the market. The price of the stock is determined by the traders' trading activities and it is updated every time a deal is made.

3.2.2 Double-Auction Order Book

Double auction has been the most widely used system in equity markets for more than 140 years [69]. In our market, a computer-aided double-auction order book is introduced to help deal with the traders' orders. Traders can have limit orders. Compared to a market order that only contains a desired amount of stock to be bought or sold and is executed on the current price, a limit order in addition has a request of specific limit of price. For example, a limit sell order with a bid price p and amount q means that this trader is willing to sell q shares of the stock in any price no less than p. A limit buy order with an ask price p and amount q means that this trader is willing to buy q shares of stock in any price no more than p. Traders could have unlimited numbers of orders, but neither borrowing nor short selling is allowed. Our order book works in the following ways:

1. At first the order book is empty;
2. When an order, for example, a buy order, is posted, the maximum amount of cash that may be needed is frozen;
3. The system will check if there are sell orders with lower prices. If there is no such order, storing the buy order in the order book and the process is done; if there exist such orders, the system will pick out the ones with the lowest prices and sort them by time to find the oldest one;
4. The system will exchange cash and stock between the traders of this buy order and the chosen orders in step 3; these cash and stock will be unfrozen and delivered to the account of the traders. If the buy order is fully digested, the process is done; if not, the rest will be treated as a new order and again steps 2 and 3 will be repeated;
5. When an order is aborted, the frozen cash or stock is released to the trader's account. An example of our double-auction order system can be found in Fig. 3.1.

Fig. 3.1 An example of how our order book updates. Adapted from Ref. [11]

3.2.3 Exogenous Rewards

It is known that real stock markets are always full of various kinds of information, but such information has only two roles: tending to increase or decrease the stock price. Because the stock in our laboratory market has no underlying value, our solution is to add exogenous rewards to the system. For this purpose, we resort to dividends (that are used to potentially increase the stock price) and interests (that are utilized to potentially decrease the stock price) to give traders information about the macroenvironment and the stock. In detail, there will be stochastic rewards for holding stock or cash every few minutes. The rewards for stock are a random amount of cash d directly added to traders' account; they are like the dividends in real markets. As a result, this may increase the stock price. The rewards for cash mean increasing the traders' cash by a random percent f, which represent the interests. So, this may decrease the stock price. The rewards also cover the stock and cash frozen in the order book. To let the traders have time to evaluate their strategies, all the rewards are forecast with partial information from the coordinator 2 min before they are distributed. For example, if the coordinator is going to pay a dividend of "2 cash per share" at 10:00 a.m., he broadcasts to the traders that there will be a dividend of "1–3 cash per share" at 9:58 a.m.

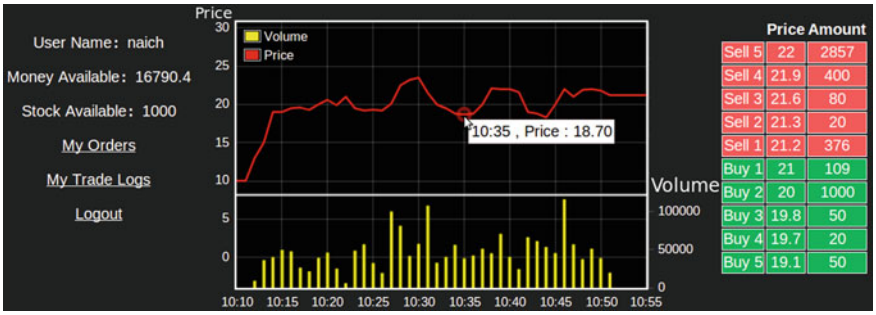

Fig. 3.2 A screenshot of the trading platform: the *left* part shows the trader's nickname, usable cash, and stock (the number of shares); the *middle chart* demonstrates the stock price and trading volume as a function of time; the right table gives the five highest bid prices and the five lowest ask prices. The middle chart refreshes per minute; when the mouse pointer (denoted by the *white arrow*) hovers above the stock price, it shows detailed information about the time and the price of that time, say, "10:35, Price: 18.70" as shown in the chart. Adapted from Ref. [11]

3.3 Controlled Experiments

3.3.1 Platform and Subjects

We designed and conducted a series of computer-aided human experiments. The experiments were held in a big computer laboratory of Fudan University; each subject had a computer to work with. All the computers were linked to an internal local area network and we deployed a web server to handle all the requests. We recruited 63 subjects to act as traders, all of whom were students of Fudan University. Our trading platform provided the following information to the traders: 1 min close prices, 1 min trading volumes, five highest buy orders' prices and amounts, five lowest sell orders' prices and amounts, the trader's own cash and stock available, the trader's trading/ordering history and the trader's rewards-getting history. Details are shown in Fig. 3.2. According to our server's performance, the close price and volume were shown in a chart which was automatically updated after every 1 min, the order book information was updated every 15 s, and the traders could look at their histories at any time during the experiments.

3.3.2 Experimental Settings

Before the experiments, 10 min for trade training was arranged to help the subjects to get used to the trading interface and market rules. Then, we had two rounds of experiments. Every round of experiment lasted for 30–40 min, but the traders did not know when the experiment would end, thus there would be less ending boundary

effect. At the beginning of a new round, the stock price would be set to 10. In the first round of experiment, all the traders started with 10,000 cash and 1,000 shares of stock, while in the second round of experiment, the traders started with a random amount of cash and stock. In the second round, the traders' initial stock was randomly distributed between 200 and 1,800, and to make the total amount of stock and cash comparable with the first round, every trader's initial cash was 10 times his/her stock in number. In the first round of experiment, we initiated 63,000 shares of stock and 630,000 cash; in the second round of experiment, we initiated 63,478 shares of stock and 634,780 cash.

3.3.3 Payoffs

Our experiments were carried out during the Econophysics course taught in Fudan University. The subjects were students enrolled in this course. 47 of the 63 subjects selected the course and 16 students were auditors. The performance of the students who selected the course took 10 % of their final score of this course. They were required to trade at least 20 times to get a base score of 3.3 %. And based on their final wealth ranking, they could get another 3.3–6.7 % score: based on their scores, top 10 % students would get all of the 6.7 % score, top 10–30 % would get 6.0 % of the final score, $\cdots$, and the last 10 % would only get 3.3 % score. Their final total scores were the calculated score rounded to the nearest whole number.

It is worth noting that the crucial role of markets is to let participants have the chance to pursue profits. In different situations, "profits" could have different forms. For example, in real stock markets, investors pursue money ("profits") by exchanging stocks and money. In our laboratory market, 47 students who selected the course pursued scores ("profits"), and the other 16 auditors voluntarily participated in the experiments with an aim to learn how laboratory experiments are conducted for econophysics ("profits"). In this sense, our laboratory market can be equivalent to real stock markets, at least to some extent.

3.4 Results and Discussion

3.4.1 Price, Volume, and Return Series

In this section, we will show the data we get from the human experiments (Fig. 3.3). First, the 1 min close price series, *p(t)*. Here, a 1 min close price is the last transaction price that occurs at the end of a certain minute: if there is no order execution in this minute, the close price will stay the same as the price of the last minute. The (log) return *r(t)* is defined as follows:

$$r(t) = \ln p(t) - \ln p(t-1), \tag{3.1}$$

where trading time t is denoted by the count seconds from the start of the experiment. Figure 3.3a, b gives the price series of our experiments: during the first round of experiment, there are 2 interests (rewards for cash) and 2 dividends (rewards for stock), and during the second round of experiment, there are 1 dividend (rewards for stock) and 4 interests (rewards for cash). Because our rewards are forecast 2 min in advance, there are notable price changes before the distribution of rewards. Specifically, before a reward for stock, the price goes up; before a reward for cash, the price goes down. This could be explained: when a signal of holding stock is sent to the traders, they tend to hold more units of stock. As a result, more buy orders will come to the order book and pull up the price. However, if one buys the stock for a price much higher than the present price, he will gain less profit in this turn of reward. Thus, the price will not go up infinitely. The same theory works for the case of rewards for cash. Because traders have different strategies and predictions of future events and our forecast is not accurate, different traders have different responses to the news. This mechanism provides liquidity to our markets. Figure 3.3c, d shows the trading volume series. It is observed that trade activities occur constantly all the time.

Figure 3.3e, f shows the return series of the two rounds of experiments. It is easy to recognize that there are clusters in the return series; this is distinctly different from Gaussian random series. So we analyze the return series' statistical properties. In order to compare the data from the two rounds clearly, the normalized return, $g(t)$, is used

$$g(t) = \frac{r(t) - \langle r \rangle}{\sigma(r)}. \tag{3.2}$$

Here, $\langle \cdots \rangle$ denotes the average of time series $\cdots$, and $\sigma(\cdots)$ means the standard deviation of $\cdots$. We calculate the cumulative distribution function (CDF) of the first and second round, respectively. Since the returns distribute symmetrically around zero, we respectively calculate the positive returns and negative returns and put them in Fig. 3.4 for comparison. For the two rounds (Fig. 3.4), the negative and positive tails share almost the same CDF. Further, in the log–log plot, all the four tails have a particular region that is approximated by a straight line. Clearly, this behavior is the evidence of scaling, which meets the statistical analysis of many real stock markets [50].

The autocorrelation function is another important feature of the return series [60]. If $x(t)$ is a time series, the autocorrelation function, $C(\Delta T)$, is defined as

$$C(\Delta T) = \frac{\langle (X_{-\Delta T} - \langle X_{-\Delta T} \rangle)(X_{\Delta T} - \langle X_{\Delta T} \rangle) \rangle}{\sqrt{\sigma(X_{-\Delta T})\sigma(X_{\Delta T})}}, \tag{3.3}$$

where $X_{-\Delta T}$ is the series with the last ΔT elements removed and $X_{\Delta T}$ with the first ΔT elements removed. $\langle X \rangle$ denotes the average of X and $\sigma(X)$ the standard deviation. Our calculations of $g(t)$ confirm the existence of short negative correlation (less than 20 s or so) on both rounds of experiments (as indicated by the green dashed

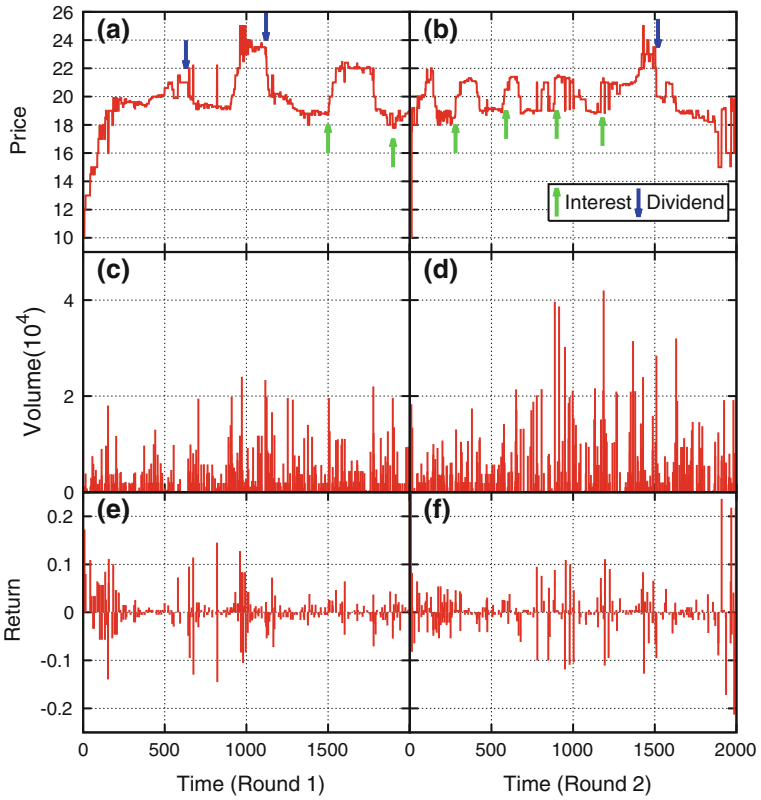

Fig. 3.3 Time series of **a**, **b** 1 min closing prices, **c**, **d** volumes and **e**, **f** returns for the **a**, **c**, **e** first and **b**, **d**, **f** second round of the laboratory human experiment. In **a** and **b**, *up arrows* demonstrate the time when there is an interest (reward for cash), and *down arrows* demonstrate the time when there is a dividend (reward for stock). In **a**, from *left* to *right*, the *four arrows* denote rewarding "2 cash per share," "2.4 cash per share," "10 % of the cash," and "6 % of the cash," respectively. In **b**, from *left* to *right*, the arrows means rewarding "3, 5, 7, and 9 % of the cash" for the four *up arrows*, and "3.2 cash per share" for the *down arrow*. **c** and **d** show the trading activities lasting through the experiments. In **e** and **f**, clustering behavior occurs. Adapted from Ref. [11]

line in Fig. 3.5a), which shows our laboratory market is similar to the real developed stock markets [70]. The short-time correlation also fits our order book information refreshing time (15 s). We also calculate the autocorrelation of absolute normalized return, $|g(t)|$, and find that the correlation lasts longer than 20 s (see Fig. 3.5b). This result confirms the volatility clustering behavior in our market, and echoes many other articles, for example, see Refs. [62, 70]. In addition, if we compare the two rounds we can conclude that in the present market, the initial wealth distribution has little influence on the statistical properties of return.

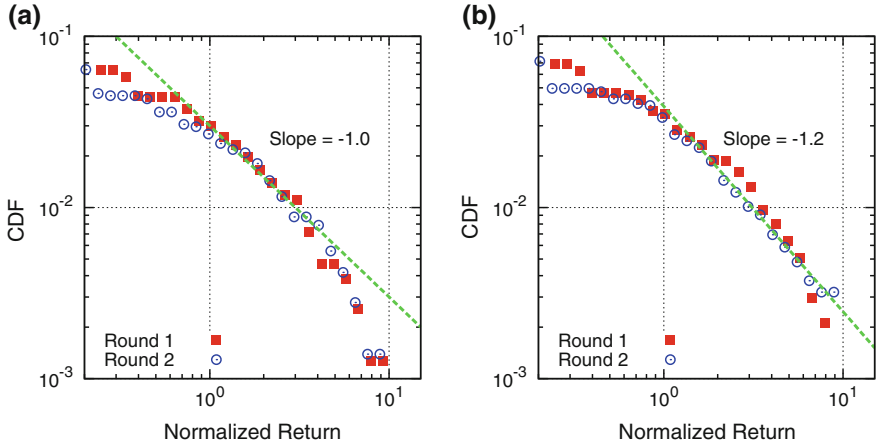

Fig. 3.4 Cumulative distribution functions (CDFs) of the normalized return: **a** the negative tails of the experiments and **b** the positive tails of the experiments. Symbols of *squares* and *circles* denote the results obtained from the first and second round of experiments, respectively. Here, the negative tails in **a** denote the CDF (<0.064) of the absolute value of negative normalized returns, and the positive tails in **b** denote the CDF (<0.071) of the value of positive normalized returns. In **a** or **b**, "Slope" denotes the slope of the corresponding *green dashed line*. Adapted from Ref. [11]

3.4.2 Human Behavior Dynamics

Our market experiments also give us an opportunity to study human behavior dynamics. In 2005, Barabasi et al. analyzed the letters of Darwin and Einstein; they found that both Darwin's/Einstein's patterns of correspondence and today's electronic exchanges follow the same scaling laws [71]. They used an agent-based model to explain the origin of this scaling [72]. Here, we turn our eyes to the waiting time of traders' actions. We define two kinds of waiting time, stock waiting time and trader waiting time. Stock waiting time describes the gaps between which two different orders are posted, see Fig. 3.6. We put all the orders from all the traders together, sort them by time and calculate the time gaps between two successive orders. While the stock waiting time focuses on the collective behavior of a group, by defining the trader waiting time we try to focus on the decision-making processes of individuals. For trader waiting time, we put orders from different traders in different piles, sort them respectively, and then calculate the gaps. This is because for any particular trader she/he only has tens of orders, which are insufficient for statistical analysis. Instead, if we are looking into the rules that work across the crowds, we could put all the gaps together and thus get thousands of data. This method has been used in the literature on human behavior dynamics [73, 74].

The probability density function (PDF) is calculated; see Fig. 3.7. Figure. 3.7a demonstrates the PDF of stock waiting time in a log plot graph. The data points obviously locate in a straight line, which means the stock waiting time obeys an

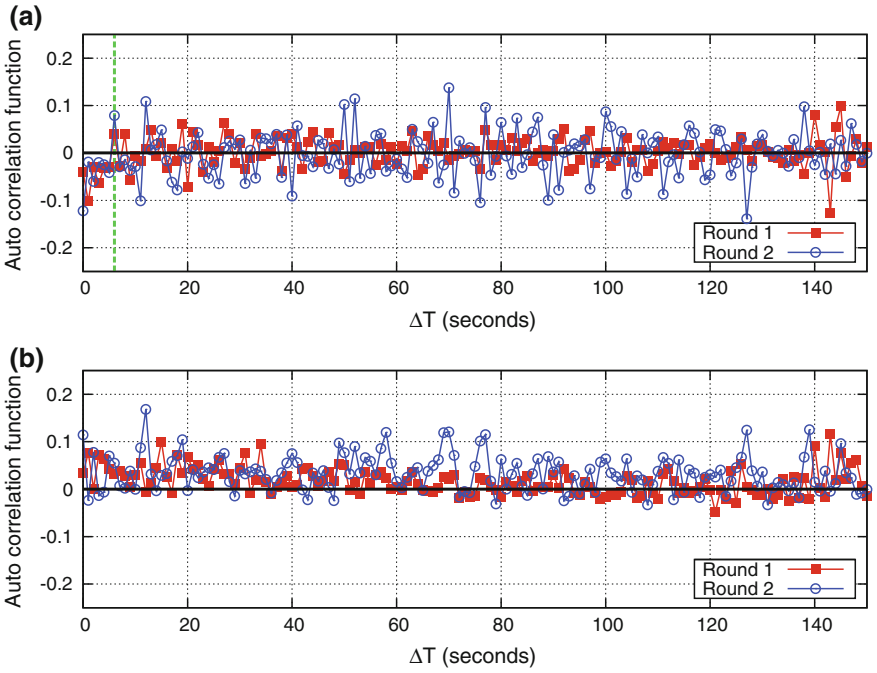

Fig. 3.5 Autocorrelation function of **a** normalized return series, $g(t)$, and **b** absolute normalized return series, $|g(t)|$, for Round 1 and Round 2. In **a**, the *green dashed line* indicates the transition point. Details can be found in the text. Adapted from Ref. [11]

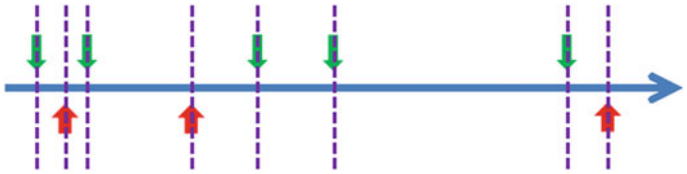

Fig. 3.6 Demonstration of the definition of waiting time. The axis represents the time. Assume our market has only two traders, the first trader's orders are marked with *down arrows* and the second trader's orders are marked with *up arrows*. The stock waiting time is shown by the gaps between each pair of nearby *slash lines*, and the trader waiting time is indicated by the gaps between each pair of nearby *down arrows* and the gaps between each pair of nearby *up arrows*. Adapted from Ref. [11]

exponential distribution [72]. This is because the traders have little interactions when submitting orders, their actions can be seen as independent decisions and overall exhibit a random-like behavior. However, in Fig. 3.7b, we could find the trader waiting time is quite different. The PDF in a log–log plot forms a straight line for gaps shorter than 100 s, and the tail of the PDF drops below the line when the gap is longer than 100 s. In the previous literature, Barabási showed that the power-law distribution of

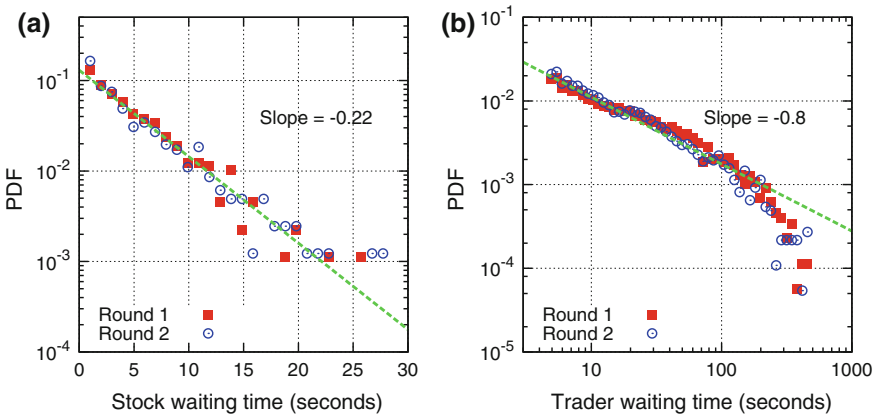

Fig. 3.7 Probability density functions (PDFs) of waiting times: **a** the stock waiting time and **b** the trader waiting time. Symbols of *squares* and *circles* denote the first and second round of experiments, respectively. In **a** or **b**, "Slope" denotes the slope of the corresponding *green dashed line*. Adapted from Ref. [11]

waiting time may come from a priority queuing system [72]. In our market, when traders make decisions on whether he/she should submit an order, there is no obvious use of a task queue. So the origin of power law in trader waiting time may contain some other mechanism. The turning point from which the PDF's tail drops from the straight line fits our rewarding time gaps in magnitude. We suspect that the tail of PDF may present the effect of our exogenous rewards. Such news breaks the traders' original decision-making processes. For example, if there is no news in the market, a trader might trade every 20 min; however, if there is periodic news every few minutes, he/she is likely to respond according to the news. Therefore, the gap of 20 min will no longer exist. In a word, we believe that the lack of long waiting time causes the fall of the tail in Fig. 3.7b.

3.5 Conclusions

In contrast to existing laboratory markets where trading time is set to be discrete [7–9, 65–69], we have designed a double-auction stock-trading market where trading time is continuous. We have run two experiments in the laboratory with human subjects and found that the initial outputs of the market fit some existing stylized facts (clustering effects and scaling behaviors). In addition, we have analyzed the orders and discovered some scaling laws in human behavior dynamics. Our laboratory market still has some weak points. For example, the traders of our experiments are university students and there might be differences if we choose different groups of traders other than university students. However, as a model market, it is easy for us

to change different control parameters or add more extensions. Thus, this market is expected to produce more results in future researches, such as, on either the effect of leverage (Chap. 4) or the birth of bubbles. The market and its output might also help modelers to mimic human behaviors in a more precise and realistic way. This chapter shows a way to study real stock markets by conducting controlled experiments on laboratory stock markets producing high frequency data.

Chapter 4
Fluctuation Phenomena: Leverage Could Be Positive and Negative

Abstract Real stock markets are always full of fluctuations in prices. Overall fluctuations (i.e., volatility), which can be calculated by the variance of log returns of a time series of prices, can represent investment risks; extremely big fluctuations, which are indicated by fat tails in the probability distribution of these log returns, can incur financial crises. Therefore, it is particularly important to understand such fluctuations, especially in case of the introduction of new financial instruments like the leverage of borrowing money. Here we include this leverage into a kind of one-stock market in the laboratory, whose original version was experimentally shown to produce some stylized facts like scaling laws and clustering behavior in Chap. 3. When the leverage becomes higher (which means borrowing more money), our human experiments and computer simulations show that the value of overall fluctuations (or extremely big fluctuations) increases (or decreases), which is a negative (or positive) effect. The negative effect means that the investment risk of the whole market increases; the positive effect indicates that fat tails are shrunk, thus lowering the probability of the outbreak of financial crises in the market. We reveal that the underlying mechanism lies in the effect of margin calls. In addition, since wealth distribution affects the harmony and stabilization of a society, we also study the leverage effect on wealth distribution in the laboratory market, and report some interesting findings and mechanisms. This work not only helps to understand the leverage appropriately, but also helps to enrich fluctuation theory in statistical mechanics.

Keywords Leveraged trading · Fluctuation · Investment risk · Financial crisis · Wealth distribution

4.1 Opening Remarks

The preceding chapter successfully shows some stylized facts (scaling and clustering) of laboratory stock markets that do not have derivative financial instruments; the

J.-P. Huang, *Experimental Econophysics*, New Economic Windows,
DOI 10.1007/978-3-662-44234-0_4

initial success encourages us to proceed further by adding some derivative financial instruments like leverage.

In the recent years, leverage has played an increasingly important role in both the developed and emerging markets. With its growing usage in many financial derivatives, it has provided investors with innovative tools to manage their wealth. However, with its popularity growing, it has also attracted many arguments around its effects on financial markets. While some believe it is a positive tool for gaining without abundant resources, and a powerful financing source for investors especially qualified companies to compete [75–78], others reckon that the overused leverage will lead to more fluctuations (namely "volatilities" according to the wording of economics or finance) and worse instability in the financial markets, and consider it as a main cause for the recent financial crisis [79–82].

For example, on one hand, leverage is treated as an effective tool for controlling financial crises. In the work of Feldman [75], he recognized the merits of leverage in the regime with shared restriction by using an agent-based model to simulate the effects of regulations of financial leverage in a stock market containing one stock only (a one-stock market), and the result suggested that leverage in the regime with share restriction would lead to less financial crises per century. That is to say, leverage has helped in controlling fat tails (corresponding to extremely large fluctuations) in the markets so that the possibility of extreme cases like financial crises is lowered. Besides, leverage is also treated as a useful strategy for competition. In the article by Hamel [76], they used empirical analysis on the performance of different firms and found leverage an effective tool for successful companies to get a bigger bang for their buck in the markets, and to allocate the resources more wisely and efficiently. This competition advantage is deeply combined with the risk control of the companies, since only those who are able to avoid big falls in asset prices can compete in a stable and continuous way.

On the other hand, leverage has been criticized, especially for causing the extremely large fluctuations in the markets. For instance, Thurner and Farmer [79] claimed that it was leverage that caused fat tails in the markets. They designed a model where leveraged assets can be purchased with margin calls, and investments funds are able to use the strategy of value investing, i.e., systematically attempting to buy underpriced assets. The results showed that leveraged funds could sometimes lead to higher profits in good times, but in more cases could also cause the downward price to go worse and suffer substantial losses due to margin calls, making the extremely large fluctuations even worse. What is more, the leverage also caused the return of the price to change from normal distribution to fat tails. This result indicates that leverage is the reason for the increasing probability of extremely large fluctuations in the financial markets. In Carmassi's work [80], they reviewed the related articles and used the method of empirical analysis on the economic data to identify excessive leverage as one main cause of the recent subprime crisis. To avoid similar events, they believed that regulations on leverage must be hard. Similarly, in the above-mentioned work by Feldman [75], he also pointed out the demerits of leverage in the regime with either margin calls or bubble puncture. All of these works

show that the growing usage of leverage has come along with the breakout of the crisis, which corresponds to the extremely large fluctuations (or fat tails).

According to extremely large fluctuations, which can lead to financial crises, the existing literature on leverage in financial markets is either supportive or critical within the framework of a model market or regime. This controversy attracts us. To our knowledge, so far, controlled (human) experiments have not been utilized to study the impact of leverage. In view of the laboratory stock market recently established by us [11] (Chap. 3), which can produce some stylized facts (like scaling) as real stock markets, we feel obliged to raise a question: what is the impact of leverage in this laboratory stock market (which is also a one-stock market)? The answer could be useful to understand the pure impact of tuning the strength of leverage [denoted by "leverage ratio (LR)"] because the market is strictly controlled: except for LRs, others including trading regulations are fixed. To this end, we reveal that the impact of leverage of borrowing money in the stock market decreases extremely large fluctuations (or shrinks fat tails), which reduces the probability of occurrence of financial crises (a positive effect). Meanwhile, this leverage increases overall fluctuations, which improves risks of investment in the stock market (a negative effect).

4.2 The Design of Controlled Experiments and Agent-Based Modeling

4.2.1 Key Ideas of Leverage

Since financial leverage in real markets has detailed and complicated rules which vary in different countries and markets, here we pick up the most general and essential ideas of leverage: leverage qualifications, LRs (leverage ratios, which describe the strength of leverage), and margin calls. The details are as follows.

- Leverage qualifications: In real markets, leverage needs strict qualifications for candidates, including wealth, experiences in the field, credit level, etc. Only qualified investors can have access to leverage. In both our human experiments and agent-based simulations, we set the amount of wealth as the trigger of financial leverage. That is, if a subject or an agent has earned enough money to meet a demand line, he/she will get extra funds to buy stocks. This should be a reasonable simplification since those subjects/agents whose wealth exceeds the demanded level of money are those who have better trading skills and larger profits.
- LRs: The LR is a key element not only in this chapter, but also in real markets. It is defined as the ratio of one's total assets to his/her own wealth. In the regulations of leverage, this ratio is decided by another important concept: margin rate. Here margin rate means the least proportion of the earnest money (also known as margin) an agent should hold in his/her total assets (including the borrowed funds), and it

controls the size of the leverage ratio. For e.g., if the margin rate is 50 % and the earnest money that the borrower must offer is W, then the funds he/she can borrow is $W/50\,\% = 2W$. For consideration of risk control, most countries regulate the margin rate by setting the least proportion, so that investors can use a higher margin rate to reduce the total amount of borrowed money to lower the risk of default. The least margin rate varies in different countries. For example, in the United States, the margin rate has been adjusted many times by the Federal Reserve, and 50 % has been adopted since 1974. In Japan, it has been changed many times and has been set as 30 % since 1991. In China, it has been 50 % since the mechanics of leverage was introduced. So, when the margin rate is decided, the initially allowed LR in the market is decided at the same time. Here is the case when the margin rate is 50 %: $\mathrm{LR} = (W + W/50\,\%)/W = 3$. In this chapter, we take the LR as a key variable in the market.

- Margin calls: Investors might perform poorly and suffer losses to some extent. But, under the threat of failing to get back the funds, financial agencies will demand borrowers to add their margin to bring the LR back to a safe level to keep the borrowed funds. If they fail to do so, financial agencies will force borrowers to return the funds immediately by selling the stocks they hold. This process is a margin call. The lowest standard by which the financial agency will still maintain lending can be interpreted as the maintenance requirement, which is also differently ruled in different countries: in the United States, it is required that the margin should compose at least 25 % of the net asset value; in China, whether to trigger a margin call is decided by the maintenance guaranty ratio (MGR):

$$\mathrm{MGR} = \frac{\text{Own Assets} + \text{Borrowed Assets}}{\text{Borrowed Assets}}. \tag{4.1}$$

Since the least margin rate in China is 50 %, the initial MGR is 1.5. With the borrowed assets unchanged, MGR is only affected by the change of one's own assets. However, the official lowest requirement of MGR is 1.3. That is to say, the Chinese financial lending agencies will allow borrowers to lose at most 40 % of their own wealth when they are using the highest allowed leverage (Own Assets have suffered a loss from 0.5 to 0.3 times Borrowed Assets). Here we take this method as our margin call rule. Besides, in order to focus on the effect of leverage, we set the subjects/agents to use their whole own wealth as the initial margin to borrow money. So, without extra assets as reserved margin, they will be forced to return the debts immediately when they meet the margin call.

Next, for both experiments and simulations, we design a mutual structure by adopting these key ideas and defining some other important rules.

4.2.2 Mutual Structure for Experiments and Simulations

First, each subject/agent in the market will have the same portfolio at the beginning: 10,000 Yuan cash and 1,000 shares of the stock with an initial price of 10 Yuan. Setting W, M and E to respectively stand for Wealth, Money, and Equity, we express his/her total wealth at time t as

$$W(t) = M(t) + P(t)E(t), \tag{4.2}$$

where $P(t)$ is the stock price at time t. So, the initial wealth of a subject or an agent, $W(0)$, is 20,000.

Then, the price movement of the stock is decided by the excess supply or demand: more demand leads to higher price while more supply makes it lower. To rule the price definition, we resort to Refs. [83, 84]. Then, when $P(t)$ is available, we determine the new price $P(t+1)$ according to the supply and demand at time t,

$$\ln P(t+1) - \ln P(t) = \lambda(\ln \text{Call} - \ln \text{Put}). \tag{4.3}$$

Namely

$$P(t+1) = P(t)(\text{Call}/\text{Put})^{\lambda}. \tag{4.4}$$

Here "Call" (or "Put") is the total value of call/buy (or put/sell) orders, and λ represents a market depth. The market depth shows the sensitivity of price to supply and demand. Reasons: when λ is high, the market would fluctuate heavily in case of huge buy or sell orders; however, a deep market with a low λ can still be stable when facing the same situation. For example, for the initial price $P(0) = 10$, in the first round of transaction, if the total call order is 100,000 and the total put order is 50,000, then according to Eq. (4.4), the new price $P(1)$ equals $10 \times 2^{\lambda}$. Due to the different number of subjects/agents and length of time in experiments and simulations, we set λ differently: $\lambda = 0.005$ for simulations and $\lambda = 0.16$ for experiments.

However, in real markets, when an investor sees a stock price and gives orders, he/she may not actually have the strike price on the expected value. This is because all the deals are cleared one by one. During the process, the strike price will change from $P(t)$ to $P(t+1)$. Here we assume the strike price is identical for all the subjects/agents at each time step. So we define the strike price for time t as [85],

$$P(t)_{\text{strike}} = (1-\beta)P(t) + \beta P(t+1), \tag{4.5}$$

where β is a market impact factor and it reflects the group effect of subjects/agents' participation: a larger β would make the majority at time t in the market has bigger power to decide the strike price, since the strike price would be closer to the new price $P(t+1)$, which is decided by the buy and sell orders at t. In the extreme cases, subjects/agents would trade just with the new price $P(t+1)$ when $\beta = 1$, and trade with the immediate price $P(t)$ when $\beta = 0$ [85]. After tests, since in the relatively short time length of experiments (which will be notified later) , we want the human

subjects to take the highest impact and motivation level of participation, we set $\beta = 1$ for experiments; and for simulations, we set β as 0.5, in order to moderately represent the group effect in the longer time length of the agent-based simulation market.

Having defined the trading and pricing dynamics, let us move to the trigger of financial leverage. As mentioned before, only well-performing subjects and agents can get access to leverage. Assuming the initial wealth of subjects/agents is $W(0)$, we set a wealth standard W_s for them to trigger the extra funds: a return of 25 %, means they should at least accumulate their wealth to $1.25W(0)$ to get qualified for the further leveraged trading. When a subject or an agent meets this requirement, say at time t, he/she could borrow money according to the margin rate. If the margin rate is p, then the amount of borrowed funds is $W(t)/p$. So, the LR is determined according to LR$= (W(t) + W(t)/p) / W(t)$. In the human experiment, we use the four LRs: 1, 2, 3, and 5; in the simulations, we vary the LR from 1 to 9 by an interval of 0.2.

With the funds, the subjects/agents now have the ability to operate in the markets with larger orders. In real markets, all the borrowed funds would be immediately used to buy stocks. But since our qualification standard for subjects/agents is set as the same, we cannot just simply copy the mechanics in the real markets, which would make all the amplified orders in almost the same scale and weaken the unpredictability of both experiments and simulations. So to lower the predictability and improve the diversity of subjects/agents' behavior, we provide a more reasonable order size strategy separately for human subjects and computer agents, which will be discussed later.

Now we are in a position to talk about the margin calls. In case of leveraging, if a subject or an agent suffers a great loss, the margin call will happen and he/she will be forced to sell stocks and return funds at once. For all LRs of experiments and simulations, the margin call will appear when a subject or an agent with borrowed funds has lost 40 % of his/her own wealth (which is set to be the same as the official rule in China).

Lastly, to simplify the process of transactions, we assume that all the orders on each trading step will be executed. That is, the market is not a closed one and there exists a market maker whose job is to balance the stock supply and demand. So, the trading volume at each time step is

$$\text{Volume} = \text{Max}(\text{Call}, \text{Put}). \tag{4.6}$$

4.2.3 Controlled Experiments

Now we specifically introduce the artificial stock market in the laboratory. The subjects in the experiments could choose to buy or sell stock by their own strategies to gain profits. As mentioned above, the initial conditions are as below:

The starting price $P(0) = 10$, the initial wealth of a subject $W(0) = 20{,}000$ (10,000 in cash and 10,000 in stock), the demanded wealth to trigger leverage $W_s =$

25,000 (which is a 25 % raise of the initial wealth), and a 40 % loss of subjects' own assets triggering the margin call.

When margin calls happen, the system would help subjects to make sell orders automatically to return funds. To make the market more robust and diversified, we also introduce noise traders by randomly giving call or put orders, which both consist of a small proportion (within the range from 10 to 30 %) of the total orders in the market at each time step.

In order to make our experimental results more general, we conducted two experiments at different times and recruited different groups of subjects. Since the stock price in the experiments is defined by the proportion of buyers and sellers, and thanks to the random traders' mechanics, the extreme cases of price fluctuations (all buy or all sell) for any number of subjects would be confined in the same scale, so the absolute number of subjects will not affect the results. This is convenient for the related experiments to be conducted in the future. Our first experiment was conducted on July 8, 2013, for which we recruited 22 subjects and studied LR = 1 and 5. Similarly, the second experiment was conducted on September 27, 2013, for which we recruited 46 subjects and investigated LR = 2 and 3.
Besides, there is some other detailed information about the experiments:

- The subjects were students from Department of Physics and School of Economics of Fudan University, who had the necessary knowledge of financial markets and could make their trading decisions independently.
- The experiments were done in the computer laboratory of Fudan University, each subject had a computer to work with. All the computers were linked to an internal local network and a web server was set up to handle all the transactions.
- For each LR, we conducted 60 time steps.
- We gave the subjects rights to decide their order sizes based on their total wealth. For each time step, subjects could decide both their investment direction (buy or sell) and proportion (choose from 1, 20, 40, 60, 80, 100 %). See Fig. 4.1.
- When leveraged, subjects were encouraged to operate in big orders, and when short of a certain kind of asset, they could not operate with this kind of asset. So with the last two items mentioned above, we make the order size strategy for the subjects diversified, reflecting the size effect when they are leveraged.
- The web page on which the subjects operated in the experiment is shown in Fig. 4.1: With all these information that would be updated each time step during the experiments, the subjects could have an overall understanding of the current situation and their historical performance, and then they could make their own strategies and decisions.

Next we introduce the incentive mechanism and scoring rules in the experiments. In order to build an economic environment where the experimental results are reasonable and reliable, we have related the performance of subjects with profits. The first experiment is rewarded with cash (Chinese Yuan), and the second experiment is rewarded with course scores to make sure that all the members have a strong incentive to perform well and strive for the best return.

In the first experiment with cash reward, we set the total cash pool for reward as the number of subjects multiplied by 100 Chinese Yuan, namely $22 \times 100 = 2{,}200$ Chinese Yuan. Then we distribute this amount of reward by the scores of subjects. We assign 70 points as the total full score for each subject in the two rounds of experiment, each round corresponding to one LR: 30 points for each round and 10 points for their participating. At the end of each round, we have a wealth list of all the subjects. We set the highest wealth amount in the list as 30 points, and all the other wealth amounts would take a proportion from the highest and then multiply 30 as its score in this round. For example, for a certain LR, if the amount of the highest wealth is 50,000 and a subject achieves 30,000, then his/her score for this single round is $(30{,}000/50{,}000) \times 30 = 18$. So, we can have the final score of each subject as the sum of the 10 participating points and the two scores from the two rounds of experiment. Finally, we sum these scores of all the 22 subjects and calculate the percentage of each subject's score to decide his/her final reward from the total cash pool. Assume this percentage is 10 %, then his/her final reward would be $10\,\% \times 2{,}200 = 220$ Yuan. Besides, the top three subjects would have extra bonus: 150 Yuan for the champion, 100 Yuan for the second place, and 50 Yuan for the third place. So the well-performing subjects would have good opportunity to gain a reward which is higher than the average level.

In the second experiment with score reward, all the subjects are the students of the course, Econophysics, and the experiment is part of the course to let the

Fig. 4.1 A screenshot of the operating platform for conducting the human experiments (in both English and Chinese). The *left* part is the information wall, which shows the current status of the subject (subject) and stock: subject ID, his/her cash, number of his/her stock shares, total assets as the sum of cash and stocks, and the present stock price. The *right* part is the operating panel, which allows subjects to buy (or sell) the stock with the amount of cash (or the number of stock shares) determined by six investing proportions, each corresponding to a percentage of his/her cash (or stock shares). Adapted from Ref. [86]

students understand how human experiments help in the study of econophysics. This experiment takes 15 % of the full score (100) in the course. Here we use a different mechanics of rewarding by ranking the total wealth of each subject after the experiment, and then give the top six students full marks of 15, leaving 40 students to mark. Then we give them marks with 4 score levels: 13, 11, 9, and 7. This system is designed from the courses grading system of Fudan University (score levels of A, B, C, D, F, etc.). Since this experiment is part of the course, this mechanics of scoring is the most suitable way to encourage students to perform well by elevating their final course scores.

We know that one vital role of financial markets is to let participants have the opportunity to pursue profits. Besides economic rewards like money in both real markets and our first experiment, profits can take different forms as well. Such as a better course score in our second experiment, which is also quite attractive to students. In this sense, we have built a profit-oriented environment in the experiments, which is equivalent to real stock markets (at least to some extent). As a result, both incentive mechanics have triggered strong motivations of good performance for the subjects, and played an active role in improving the morale and atmosphere during the experiments.

4.2.4 Agent-Based Modeling

Agent-based simulations are based on a revised version of minority game (MG) [1, 31, 85, 87]. To comply with the experiments, the simulation model also contains two kinds of agents: noise traders and speculators. The former gives orders randomly in the scale of 10–30 % of the total orders, just like the design in the experiments; the latter uses the strategy books to amplify their profits. The mechanics of agents' strategy books in the traditional MG model were introduced by Challet and Zhang in 1997 [1], here we revise the classic methods using the following approach to form the speculators' strategy books in our model.

The strategy book in our model is a choice table that consists of two columns, as shown in Table 4.1. A traditional MG strategy book also consists of two columns: the left column is for the m history length, and the right column is for choices, which are the same as in our table. But in the MG model, the history bit "1" or "0" stands for Room 1 or 2 being the winning side, while in our history series, "1" represents stock price rising or staying the same, "0" for price falling; and we also modified the choices to "1" for buying, "−1" for selling and "0" for holding, rather than choosing rooms in the MG model. So with a length of memory as m, there are totally $P = 2^m$ historical situations and 3^P possible strategies. Before the game starts, each agent will choose s strategies to help him/her make a decision at each time step.

The stock positions of each strategy will also vary with time: adding one when buying, subtracting one when selling, and stay unchanged when holding. We rate the strategies with virtual wealth: the wealth that the agent would get if he/she uses it all the time. And the strategies with higher virtual wealth are preferred by agents: at

each time step, based on the historical price change sequence, each agent operates on his/her stock or cash account with the help of his/her best-scored strategy. In our model, we set $m = 3$ and $s = 4$.

Then we come to the order size of agents. To diversify the behavior of agents and to make the model simulations consistent with the experiments, we define a parameter r as the risk controller to let each agent in the model decide his/her size of orders. It works as

$$r = 1 - \exp[-cW(t)], \tag{4.7}$$

where $W(t)$ is the wealth of an agent at time t (total wealth, including borrowed funds) and c is a constant. We can easily tell that r has a positive correlation with $W(t)$ in the scale of (0, 1), and it reaches the limit of 1 when $W(t)$ goes to positive infinity. So this risk controller will make the richer agents give bigger orders. The buy or sell orders for agents are

$$\text{Buy order} = rM(t)/P(t), \tag{4.8}$$

$$\text{Sell order} = rE(t). \tag{4.9}$$

By adjusting c, we can get the ideal r that makes the agents in this model behave reasonably, neither too aggressively nor conservatively. So this method provides us with a reasonable resemblance of the diversity and unpredictability of the real markets (at least to some extent).

Here are some other simulation conditions: the price-determining mechanics are also based on supply and demand, and margin calls trigger at a 40 % loss of one's own wealth, the same as the experiments. Compared to the experiments, in the simulations we have built a much more complete database with 1,000 agents and 100 rounds for each LR. Each round has run 10,000 time steps. The other parameters adopted in the simulations are $P(0) = 10$, $M(0) = 10000$, $E(0) = 1000$, $W_s = 25000$, $\lambda = 0.005$, $\beta = 0.5$, $c = 0.00005$, $m = 3$, and $s = 4$.

Table 4.1 The strategy table of agents in the simulation (when $m = 3$). Adapted from Ref. [86]

History	Choices
000	1
001	−1
011	0
...	...
110	1
111	−1

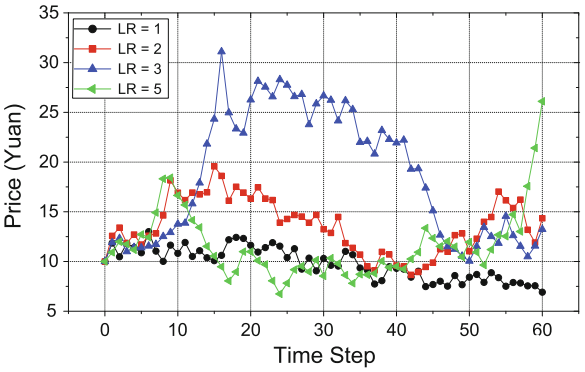

Fig. 4.2 Time series of prices produced by human experiments with four different LRs (leverage ratios). The time steps are fixed at 60. Adapted from Ref. [86]

4.3 Results: Experiments and Simulations

4.3.1 Overall Fluctuations

Here we first present our results about the effect of leverage on the overall fluctuations of the market.

Figure 4.2 demonstrates a direct impression of price movements in the experiment. We can tell a clear tendency that the situation with larger LRs would have more fluctuations. Besides, the price series moves in a relatively random way while there is no leverage (LR = 1); however, with leverage included as LR changes from 2 to 5, the price movement has become more reasonable, forming several stable trends which are somehow similar to real markets. This is mainly because there is no instructive information for the subjects to choose investment direction, and in the zero leverage (LR = 1) case, subjects could only operate with their own assets, which are relatively in small scale. However, in the leveraged cases (LR = 2, 3, and 5), when borrowing money is triggered, a group of subjects may have excessive amounts of money to invest in the stock market and this buying power could lead to the upward trends in the price. And when they decide to sell a lot, or when margin calls are met, they would make big sell orders to bring down the price, which may cause others to suffer a loss and trigger more margin calls. So when the leverage causes more overall fluctuations, it also offers a reasonable mechanism of how borrowing and returning funds may affect the change in prices.

However, the experiment alone has limitations in the size of dataset, due to the limited time and manpower we could have. The simulations have a more complete dataset with longer time series and more LRs. So let us combine the results of both experiments and simulations to see the effects of leverage on fluctuations clearly.

Figure 4.3a displays a clear tendency in the ascending variance along with LRs, both in experiments and simulations. This echoes the results we get in Fig. 4.2. That is

to say, with more leverage allowed in the market, more overall fluctuations appear as well. This is a negative feature of the leverage, since overall fluctuations (volatility) is a measure of investing risk in the market.

Why does leverage have this effect on price fluctuations? We think that both the extent of allowed leverage scale and its regulation are the reasons behind; while a larger LR leads to bigger orders of investment, it also brings larger possibility of meeting margin calls at the same time. See Fig. 4.3b and c. From Fig. 4.3b, we can tell both in experiments and simulations that as the LR rises, margin calls happen more frequently, which is consistent with the trend in volatility. Since we have different number of subjects in the two experiments, and the number of agents in simulations is also quite different from the numbers in the experiments, we show the margin calls met by each participant here to make the results more comparable. We can see that the human subjects are more likely to meet margin calls, which is mostly because their strategies are more aggressive than computer agents. While the per capita times of margin calls rise (Fig. 4.3b), the relative possibility of margin calls also increases in a similar pattern; see Fig. 4.3c. Figure 4.3c shows that the probability of meeting margin calls after using leverage gets bigger when LR is higher. This is because a bigger LR amplifies the orders of participants, which makes it easier for them to suffer a relatively bigger loss and meet the margin calls. And when margin calls happen, the subjects and the agents will all be forced to sell stock shares to return the funds immediately. These increase unwilling sales, which mostly violate agents' original trading strategies and cause the price to fluctuate at an unnatural pace leading to more fluctuations (i.e., greater volatility). Yet, human subjects have confronted with margin calls with higher possibility.

Now we can say that our model simulations have provided us with a reasonable approach to study leverage because of its well-fitted results with our experiments and other related articles [79, 88, 89]. Also, it helps us to obtain a much more complete dataset in a more controllable way. So we use the simulation to study more features of leverage, which must be based on the statistical results of large datasets such as fat tails.

4.3.2 Fat Tails or Extremely Large Fluctuations

Besides the overall fluctuations discussed above, we also need to study the leverage effects on fat tails of the price return, where the extremely large fluctuations happen. This is because all the extreme cases like financial crises take place in the part of tails, with low probability but high severity. For this purpose, we resort to the kurtosis. It is known that a higher kurtosis corresponds to fatter tails (and sharper peaks).

Figure 4.4a shows that the kurtosis falls down with the increasing LR, while we have already shown in Fig. 4.3 that there are actually more fluctuations brought in at the same time. This seems to be a little surprising, since if leverage is an absolutely good or bad thing, these two values should follow the same trend. Ideally, we want both fewer overall fluctuations and fewer extremely large fluctuations in order to

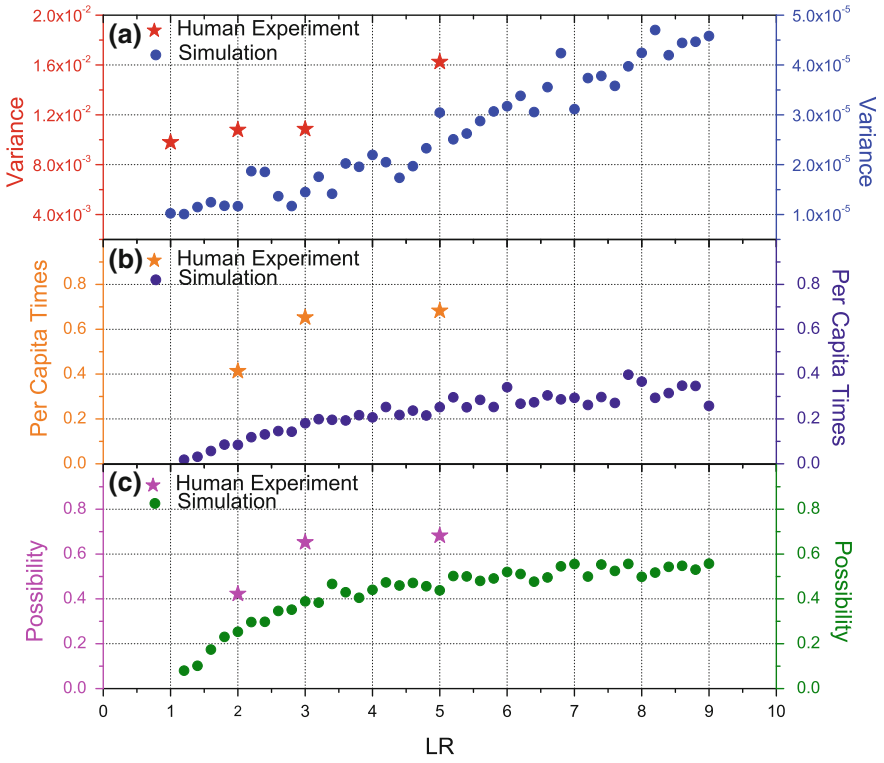

Fig. 4.3 Results obtained from human experiments (*left vertical axis*) and agent-based simulations (*right vertical axis*) as a function of LRs: **a** the variance in log returns of a time series of prices, which corresponds to the overall fluctuations or volatility of the system; **b** per capita times of margin calls, namely the total number of margin calls divided by the number of subjects or agents; and **c** the possibility of margin calls, which is defined as the ratio between the times margin calls occur and the times the leverage is triggered. All the stars stand for experimental results of a single round of human experiment with 60 time steps, and all the solid circles represent simulation results, which are the average of 100 simulation rounds, each having 10,000 time steps. Adapted from Ref. [86]

have a more stable market. But after we bring higher leverage into the market, more overall fluctuations have come along with the thinner tails, cutting the possibility of extreme fluctuations, which is a positive sign for the control over crises in the markets.

In order to see what exactly happened to form the statistical feature as shown in Fig. 4.4a, we draw the probability distribution function (PDF) of price returns for different LRs; see Fig. 4.4b where the PDF is a function of the normalized log return. To make the curves comparable, especially on the tails, we standardize the returns for each LR so that they all have the mean of zero and the standard deviation of one. The standard Gaussian distribution is also added in Fig. 4.4b. Figure 4.4 displays both a clear pattern of the kurtosis trend (Fig. 4.4a) and a direct view of the change in fat tails (Fig. 4.4b). It is obvious that higher LRs lead to lower kurtosis, where the tails

get thinner and move toward the standard Gaussian distribution. So it is clear that the leverage can be used to control the fat tails.

To explain this behavior of cutting fat tails, we go back to Fig. 4.3b and c where the change in margin calls is shown as a function of LRs. While the increased unwillingly sales originating from the leverage cause the price to fluctuate in an unnatural pace, leading to more fluctuations as we have shown in Fig. 4.3a, the accompanying margin calls could also confine the scale of losses by poorly performed participants, control the risk of lending agencies, and lead to a lower possibility of extreme fluctuations in the price. In other words, to lower the risk of defaults by borrowers, the relatively generous lending policy is combined with a more strict returning policy, demanding the borrowers to have a high standard of financial performance.

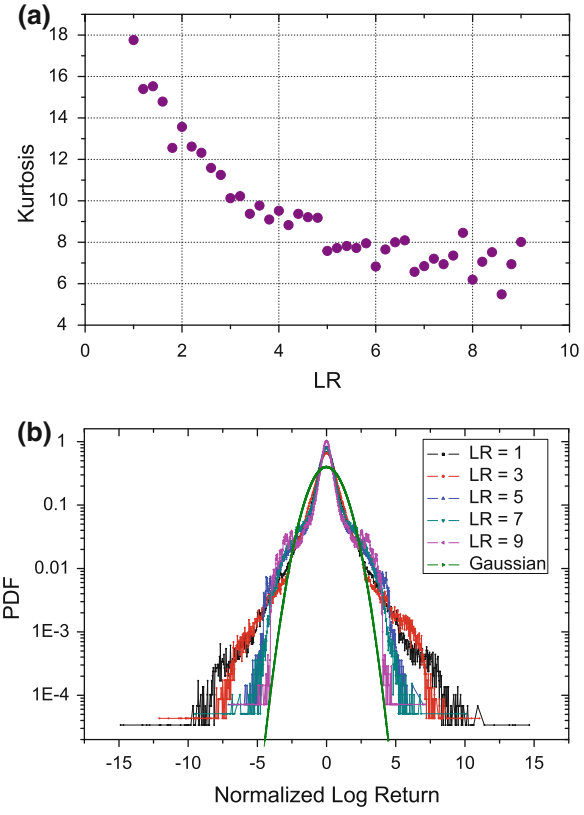

Fig. 4.4 Simulation results for leverage effects on fat tails: **a** shows the kurtosis as a function of LRs. **b** displays the PDF of normalized log returns for different LRs, which is compared with the standard Gaussian distribution (denoted as "Gaussian" in the figure). Here the "normalized log return" is defined as "(log return - μ)/σ, where μ (or σ) is the average value (or standard deviation) of log returns of a time series of prices. Both **a** and **b** are the averaged results of 100 simulation rounds, each having 10,000 time steps. Adapted from Ref. [86]

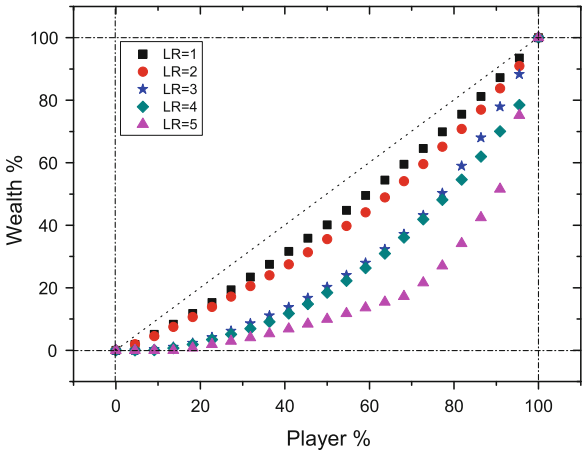

Fig. 4.5 The cumulative percentage of wealth (*Y axis*) as a function of the cumulative percentage of subjects (*X axis*). Compared with Figs. 4.2 and 4.3, $LR = 4$ is also added herein. Adapted from Ref. [90]

4.3.3 Wealth Distribution

In Sects. 4.3.1 and 4.3.2, we discussed the overall and extreme fluctuations in the laboratory market. Since the aim of investors in markets is to pursue profits, we are now in a position to ask a question: what is the wealth distribution of the subjects in our laboratory market with leveraged trading? Nowadays, wealth distribution has always been a heated and vital issue in economics, since it greatly concerns the happiness and stabilization of populations in different countries. If the wealth or income gap in a country or region between the rich and the poor is too wide, it may cause many economic and social troubles. So it has drawn great attention from not only the academia, but also from governments in various countries. Definitely, wealth distribution is a very general topic which is determined by many factors. However, against the background of the recent financial crisis, in which innovative financial tools have been used frequently to raise leverage, the present laboratory market allow us to specifically study how wealth distribution is affected by using leverage for borrowing money.

According to Fig. 4.5, as the LR goes up, wealth distribution becomes more uneven. In other words, with more leverage allowed in the market, the performance of different subjects has become more diversified. Why does this feature happen? More volatility in the price fluctuations has raised risk in the market and helped in creating more and bigger gaining and losing opportunities for the subjects. So the subjects with better trading skills could use higher leverage as a weapon for them to gain more wealth than others while the relatively weaker performers would suffer bigger losses in a more leveraged environment. As a result, wealth distribution becomes more uneven.

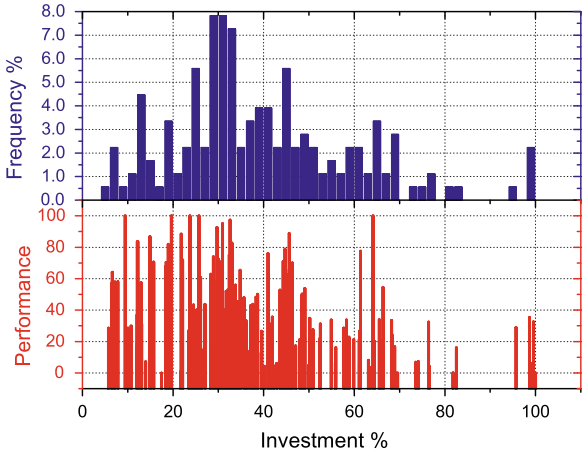

Fig. 4.6 The effect of risk preference on the subjects' wealth in all the experiments. The *blue bar* (*upper panel*) displays the frequency counting numbers of the investment proportion which lies in the certain range on the *X axis*. The *red line* (*lower panel*) shows the performance score of a certain subject in a certain experiment, in the scale of 0–100; for each experiment, the highest wealth amount W_h is treated as 100, and another score of a certain wealth amount W_n is calculated as $100W_n/W_h$. Adapted from Ref. [90]

In fact, besides the reason of higher risk with leverage and different trading skills of subjects, the subjects' preference of risk also plays an important role in wealth distribution. Since in our experiments subjects could choose the investment proportion within 1, 20, 40, 60, 80, and 100 %, it is obvious that when choosing to invest in a larger percentage, subjects would carry more risk. So subjects who like to invest in a higher percentage have higher preference for risk. Does this preference show its effect on wealth distribution? We have calculated the average investment proportion of each subject in all the five experiments and tried to find the relation between their risk preference and the final wealth distribution. The results are shown in Figs. 4.6 and 4.7.

From Fig. 4.6, we get an overall view of the relation between risk preference and wealth distribution in the market. Most choices of investment proportion were between the range of 20–50 %, which means that most of the subjects were relatively conservative when making decisions; as a result, most of the high performance scores also fell in this range. However, the more aggressive subjects who chose a higher proportion mostly did not get a higher score. So we can tell that generally the difference in risk preference also leads to different wealth performance.

To study this phenomenon clearly, we separately show the subjects' risk preference and wealth performance in each round of experiments, as shown in Fig. 4.7. Black dots are the average investment proportion of each subject in a certain round of experiments; colorful dots represent the final wealth of each subject in the same round. We can see that basically two patterns have been formed in the five cases: for LR = 1 and 3 (Fig. 4.7a and c), the black dots lie in a relatively smaller scale

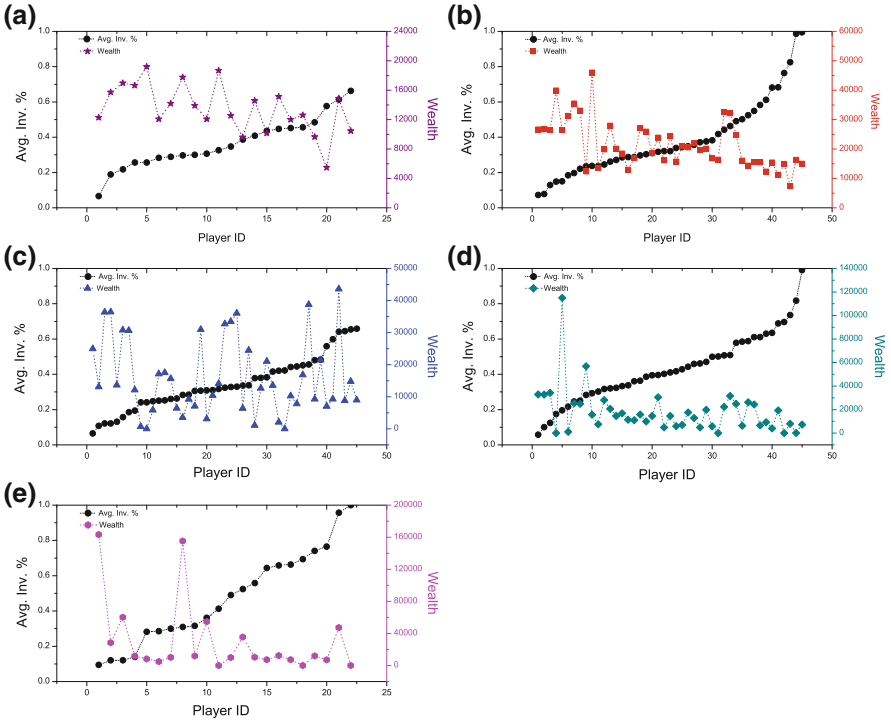

Fig. 4.7 The subjects' risk preference and wealth amount in each experiment: **a** $LR = 1$, **b** $LR = 2$, **c** $LR = 3$, **d** $LR = 4$, and **e** $LR = 5$. The *left vertical axis* denotes the average investment proportion of each subject in a certain experiment; the *right vertical axis* corresponds to the final wealth amount of the subject. In order to see the relation between risk preferences and final wealth amounts, subject ID in each experiment is put in the order of growing average investment proportions. Adapted from Ref. [90]

(from 0 to 0.7), which means no extremely risk-chasing subjects occur in the two experiments. As a result, the wealth distribution has less relation with risk preference sequence, distributed more randomly; for LR = 2, 4 and 5 (Fig. 4.7b, d and e), the risk preference rates have covered the range from 0 to 1, indicating that certain subjects have operated with the highest risk preference in the experiments (namely always used the biggest orders they can bid). Meanwhile, the wealth of subjects has basically declined with the growing investment proportion, leaving very few subjects owning much wealth while most of the others have poor wealth performance. This is because the existence of extremely aggressive subjects has helped in increasing the volatility and unpredictability of the market. So, the diversified risk preference of subjects has also contributed to the risk in the market. Especially in the environment of leverage where the population is exposed to higher risk, this effect of diversity is amplified, including both different trading skills and risk preference of individuals, and then eventually showing in the form of a more diversified wealth distribution.

4.4 Conclusions

We have utilized the combination approach of both controlled experiments and agent-based simulations to study the impact of leverage in a laboratory stock market. Our results indicate that the leverage of borrowing money has both merits and demerits. On one hand, this leverage shrinks the fat tails and reduces the value of extremely large fluctuations in prices, thus decreasing the probability of outbreak of financial crises. On the other hand, it also leads to higher value of overall fluctuations in the market, thus increasing the risk of investment in the market. The two-sided effect originates from the strict regulation of margin calls.

In addition, we have also shown that the leverage could make wealth distribution more uneven. This result comes from higher risk with leverage, different trading skills of subjects, and the subjects' preference of risk.

The content reported in this chapter is of value for people to understand and utilize the leverage appropriately, and it also sheds light on how to study real stock markets by conducting controlled laboratory experiments.

Chapter 5
Herd Behavior: Beyond the Known Ruinous Role

Abstract In order to survive, self-serving agents in various kinds of complex adaptive systems (CASs) must compete against others for sharing limited resources with biased or unbiased distribution by conducting strategic behaviors. This competition can globally result in the balance of resource allocation. As a result, most of the agents (say, species) can survive well. However, it is a common belief that the formation of a herd in a CAS will cause excess volatility, which can ruin the balance of resource allocation in the CAS. Here this belief is challenged with the results obtained from a modeled resource-allocation system. Based on this system, we design and conduct a series of computer-aided controlled human experiments, including herd behavior. We also perform agent-based simulations and theoretical analyses, in order to confirm the experimental observations and reveal the underlying mechanism. We report that, as long as the ratio of the two resources for allocation is biased enough, the formation of a typically sized herd can help the system to reach the balanced state. This resource ratio also serves as the critical point for a class of phase transition identified herein, which can be used to discover the role change of herd behavior, from a ruinous one to a helpful one. This chapter is also of value to some fields, ranging from management and social science, to ecology and evolution, and to physics.

Keywords Resource-allocation system · Herd behavior · Helpful role · Phase transition

5.1 Opening Remarks

The preceding chapter discussed some fluctuation phenomena in laboratory stock markets, namely overall fluctuations and extremely large fluctuations. In reality, the latter may lead to crises. It is common knowledge that crises always originate from herd behavior of human beings (see for example Ref. [83]). Clearly, this common knowledge displays the ruinous role of herd behavior. The aim of the present chapter is to investigate the different roles of herd behavior.

J.-P. Huang, *Experimental Econophysics*, New Economic Windows,
DOI 10.1007/978-3-662-44234-0_5

Most of the social, ecological, and biological systems that involve a large number of interacting agents can be seen as complex adaptive systems (CASs), as they are characterized by a high degree of adaptive capacities to the changing environment. Their dynamics and collective behaviors have attracted much attention among physical scientists [91–93]. In order to survive, self-serving agents in these CASs must compete against others for limited resources with biased or unbiased distribution by conducting strategic behaviors. This can globally result in balanced or unbalanced resource allocation. Examples of such phenomena evolve many species like humans. For instance, drivers select different traffic routes, people bet on horse racing with odds, and so on. In general, the allocation of the resources in a CAS could reach a balanced state due to the preferences and decision-making ability of agents, as revealed by investigating a biasedly distributed resource allocation problem [7]. In practice, however, it will sometimes fail to reach the balanced state. For this, one important reason is due to the formation of a herd. In fact, herding extensively exists in collective behaviors of many species in CASs, including humans. Though human decisions are basically made according to individual thinking, people tend to pay heed to what others are doing, emulate successful persons, or those of higher status, and thus follow the current trend. For example, young girls often copy the clothing style of famous stars who are named as trendsetters in the fashion world. Similarly, researchers would rather choose to work on a topic that is currently hot in the scientific society. As a result, large numbers of people may act in concert, and this unplanned formation of crowds is called herd behavior [94]. Locally, for an individual agent, herd behavior may suggest either irrationality [95, 96] or rationality [97–99] with an implication that herding can ruin the balance of the whole resource-allocation system by causing excess volatility. Accordingly, herd behavior is commonly seen as a tailor-made cause for explaining bubbles and crashes in a CAS with the existence of extremely high volatility. But is this "common sense" always right? Based on results of this study, we argue that herd behavior should not be labeled as the killer all the time. Here, we focus on the effect of herding on the whole CAS for resource allocation, because it is most important for as many agents (involving humans) as possible to survive in various kinds of CASs like social, ecological, or biological systems. As a result, we do not study or consider the details of how to reach a herd through contagion and/or imitating because our results are not dependent on the process of herding formation.

5.2 Controlled Experiments

To model realistic huge systems of resource allocation including the effects of herding, we designed and conducted a series of computer-aided human experiments, on the basis of the resource-allocation system [1, 4, 7], to study the necessary conditions for a CAS to reach the ideal balanced state. Using such experimental settings will allow us to investigate the herd behavior in a well-regulated abstract system for resource allocation, which reflects the fundamental characteristics of many CASs [35, 87, 100]. Human subjects of the resource-allocation experiment were

students recruited from several departments of Fudan University. Before the start of experiments, a leaflet (as shown in Part I of Supplementary Materials at the end of this chapter) was provided which explained the configurations of the experiment and actions of the subjects. There are two rooms (Room 1 and Room 2) and the amount of resources in these two rooms are M_1 and M_2 ($\leqslant M_1$), respectively. As the experiment evolves, M_1 and M_2 are kept fixed and unknown to all the subjects. For each experiment round, each subject has to choose one of the two rooms to enter. Those who go into the same room should share alike the virtual resource (M_1 or M_2) in it. Apart from human subjects, there are also imitating agents joining the experiment. All the imitating agents are generated by a computer program, since their decisions are made by mimicking human subjects' behaviors. In particular, each imitating agent will randomly select a new group (of size 5) of human subjects at every experiment round, and then follow the choice of the best subject (who has the highest score) in the group for the next round. In each round of the experiment, the number of human subjects and imitating agents in Room 1 is denoted as N_1 and the number in Room 2 as N_2. Therefore, the total number of human subjects and imitating agents can be counted as $N = N_1 + N_2$. The human subjects or imitating agents who earned more than the global average $(M_1 + M_2)/N$ are regarded as winners of the round, and the room which the winners had entered as the winning room. The total number of human subjects or imitating agents can also be expressed as $N = N_n + N_m$. Here, N_n is the total number of human subjects who make decisions by their own, and N_m is the total number of imitating agents who do not have their own ideas. The ratio between imitating agents and human subjects is defined as $\beta = N_m/N_n$. More details about the experiment can be found in Part II of Supplementary Materials.

The resource-allocation experiments are conducted repeatedly with different values of M_1/M_2 and β. The modeled system is designed as an open system in which the number of human subjects N_n is fixed while the number of imitating agents N_m is increased in an implicit manner. As shown in the previous study [7], the heterogeneity of preferences is an indispensable factor for the whole system to reach a balanced state. Hence the preferences of human subjects need to be checked under the influence of imitating agents. For a human subject in the experiment, his/her preference is evaluated as the average rate that he/she chooses to enter Room 1. Preferences of the 44 subjects are plotted in Fig. 5.1 with different M_1/M_2 s and/or β s. Figure 5.1a shows the preferences of human subjects when $M_1/M_2 = 1$ and the imitating agents are absent. Distinctions among the preferences of human subjects can be easily identified. For example, the 4th subject is strongly partial to entering Room 2 while the 6th subject prefers Room 1 much more. It can be found in Fig. 5.1b, c, that the human subjects still have diverse preferences even when M_1 becomes much larger than M_2. In addition, the heterogeneity of preferences remains even for the cases in which $N_m(= N_n/2)$ imitating agents are involved; see Fig. 5.1g–i. Despite this heterogeneity, the average of subjects' preferences changes along with M_1/M_2. In other words, human subjects have the ability to adapt themselves to fit the environment.

Comparisons of the distributions of human subjects' preferences, as the resource distribution M_1/M_2 is varied and/or the imitating agents are involved, are shown in

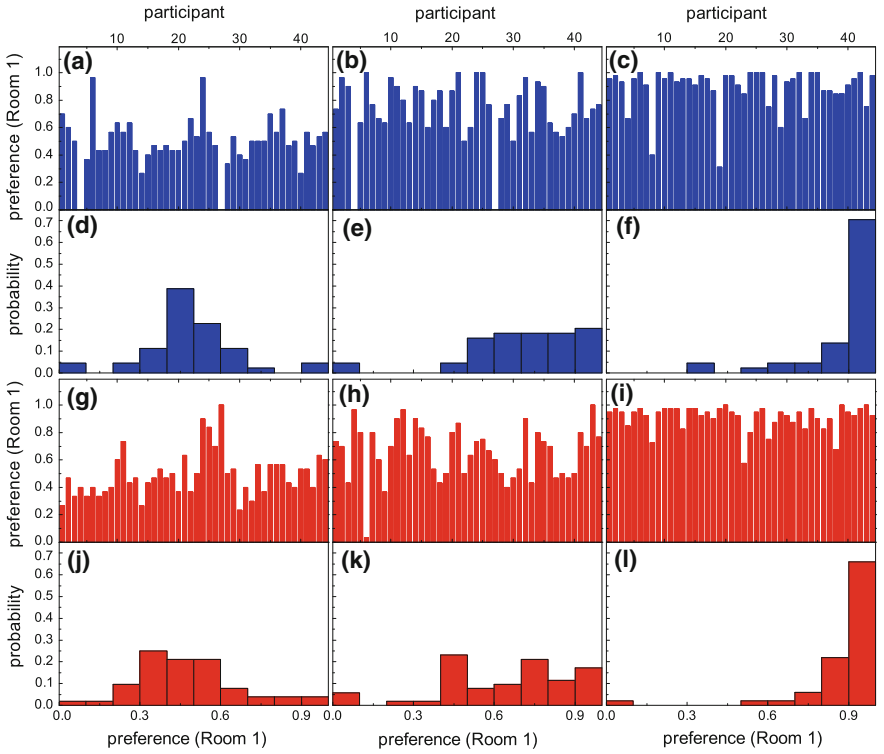

Fig. 5.1 Data obtained from the human experiment. **a–c, g–i** Preferences of the 44 subjects in sequence to Room 1 for the cases **a–c** without and **g–i** with imitating agents, β= (**a–c**) 0 and (**g–i**) 0.5, for the resource distributions $M_1/M_2 =$ (**a, g**) 1, (**b, h**) 3, and (**c, i**) 20. Here, "Mean" denotes the average value of the preferences of the 44 subjects. **d–f, j–l** Distribution of the 44 subjects' preferences. Adapted from Ref. [8]

Fig. 5.1d–f, j–l. From Fig. 5.1d, e, one can find that when M_1/M_2 is not so biased, human subjects alone can do the analysis of the system so well that they can make the whole system reach the balanced state. Note that the preference distribution has a peak at 0.5 in Fig. 5.1d and the subjects' preferences are mainly distributed around 0.75 in Fig. 5.1e. Both the observations can be deduced from the resource distribution, $M_1/M_2 = 1$ and $M_1/M_2 = 3$. When the imitating agents are involved, however, the two preference distributions have some changes in Fig. 5.1j, k. In particular, the peak almost disappears in Fig. 5.1j and the mean value of subjects' preference deviates from the resource distribution bias in Fig. 5.1k. A possible reason for these changes can be inferred as that human subjects may get confused by the behavior of imitating agents. Hence in this case, the herd (which is formed by imitating agents) indeed disturbs the system and weakens the analyzing ability of human subjects. Things are different if M_1/M_2 gets even larger, as shown in Fig. 5.1f, l. Here, the involvement of imitating agents does not bring much change to the preference distribution of human

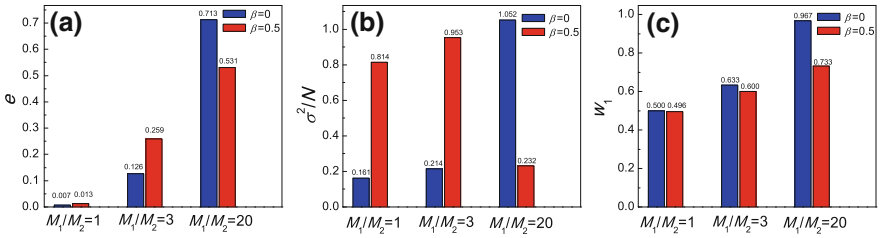

Fig. 5.2 Experimental results for **a** efficiency e, **b** stability σ^2/N, and **c** predictability w_1 of the modeled resource-allocation system, with human subjects $N_n = 50$. $\beta = 0$ and 0.5 correspond to imitating agents $N_m = 0$ and 25, respectively. Each experiment lasts for 30 rounds. Adapted from Ref. [8]

subjects. One may say that, in this case, herd behavior has no harmful effect on the analyzing ability of the human subjects. Finally, it is interesting to note from the same figure that a minority of human subjects with preference to Room 2 can stay alive even in a highly biased system ($M_1/M_2 \gg 1$) when the imitating agents exist.

To evaluate the performance of the whole system, we have calculated efficiency (which, herein, only describes the degree of balance of resource allocation), stability, and predictability of the resource-allocation system. The efficiency of the whole system can be defined as $e = |\langle N_1\rangle/\langle N_2\rangle - M_1/M_2|/(M_1/M_2)$. A smaller e means a higher efficiency in the allocation of resources. The stability of the resource-allocation system can be described as $\sigma^2/N \equiv \frac{1}{2N}\sum_{i=1}^{2}\langle(N_i - \tilde{N}_i)^2\rangle$, where $\langle A\rangle$ denotes the average of time series A. This definition describes the fluctuation (volatility) in the room population away from the balanced state, where the optimal room populations $\tilde{N}_i = M_i N/\sum M_i$ can be realized. The predictability of the system is measured by the "uniformity" of the winning rates in different rooms. The winning rate in Room 1 is denoted as w_1. It is obvious that if w_1 is close to 0.5, choices of the two rooms are symmetrical and the system is unpredictable. If the winning rate were too biased, smart subjects should be able to predict the next winning room in the experiment. As shown in Fig. 5.2, when M_1/M_2 is small ($M_1/M_2 = 1$ or 3), adding some imitating agents will lower the efficiency and cause large fluctuations. On the other hand, when M_1/M_2 gets even larger ($M_1/M_2 = 20$), the formation of herd can improve the efficiency, the stability, and the unpredictability of the resource-allocation system.

5.3 Agent-Based Modeling

An agent-based model is developed to fully understand the preceding experimental results. Consider a situation where N agents repeatedly join a resource-allocation system. Among these agents, there are N_n normal agents (which correspond to human subjects in the preceding experiments) and N_m imitating agents, so that the total number of agents can be calculated as $N = N_n + N_m$. To play in the resource-

allocation system, each normal agent will take S strategies from the full strategy space and compose a strategy book. A strategy for the resource-allocation experiment is typically a choice table which consists of two columns. The left column is for the P possible situations, and the right column is filled with bits of 0 or 1. Bit 1 is linked to the choice for the entrance of Room 1, while bit 0 to that of Room 2. In the strategy book of a normal agent, strategies differ from each other in preference, which is defined as an integer L ($0 \leq L \leq P$). To model the heterogeneity of preference, let the normal agent pick up a preference number L first. Then each element of the strategy's right column is filled in by 1 with the probability L/P, and by 0 with the probability $(P - L)/P$ (more detailed explanations can be found in Part III of Supplementary Materials). The process will be repeated S times, each time with a randomly chosen L for each normal agent to complete the construction of its strategy book. From the start of the resource-allocation experiment, each normal agent will score all the strategies in its strategy book so as to evaluate how successful they are to predict the winning room. Following the hitherto best performing strategy in their strategy books, normal agents are enabled to make decision to enter one of the two rooms, once the current situation is randomly given.[1] Imitating agents in the model behave in a different way during the process of decision-making. Before each round of the play starts, each imitating agent will randomly select a group of k ($1 \leq k \leq N_n$) normal agents.[2] Within this group, the imitating agent will find the normal agent who has the best performance so far and imitate its behavior in the following experiment round. It is assumed that the imitating agents know neither the historical record of the winning room nor the details of strategy books of other group members. The only information for them to access is the performance of the normal agents, that is, the virtual money that these normal agents have earned from the beginning of the experiment. If the number of imitating agents N_m kept increasing, there would be more and more positive correlations among agents' decisions, which would trigger the formation of a herd in the system.

5.4 Simulation Results

Agent-based simulations are carried out in an open system condition, in reference to the experiments. (Please refer to Part IV of Supplementary Materials to see the results for a closed system.) Following the analysis of experimental results, we first investigate the simulation results for the preferences of normal agents. Clearly, Fig. 5.3 shows distributions of the preferences similar to those shown in Fig. 5.1. The qualitative agreement indicates that our agent-based modeling has taken into account

[1] Here the situation is not the history of winning rooms. Broadly speaking, it can be explained as a mixture of endogenous and exogenous system information. Results obtained with the real history bit strings have no essential difference with the current study, though the use of random information makes the theoretical analysis easier.

[2] This corresponds to the case of primary imitators. In fact, in the real system, there might exist multilevel imitations where some imitators can copy other imitators' behavior. Similar conclusions could be achieved.

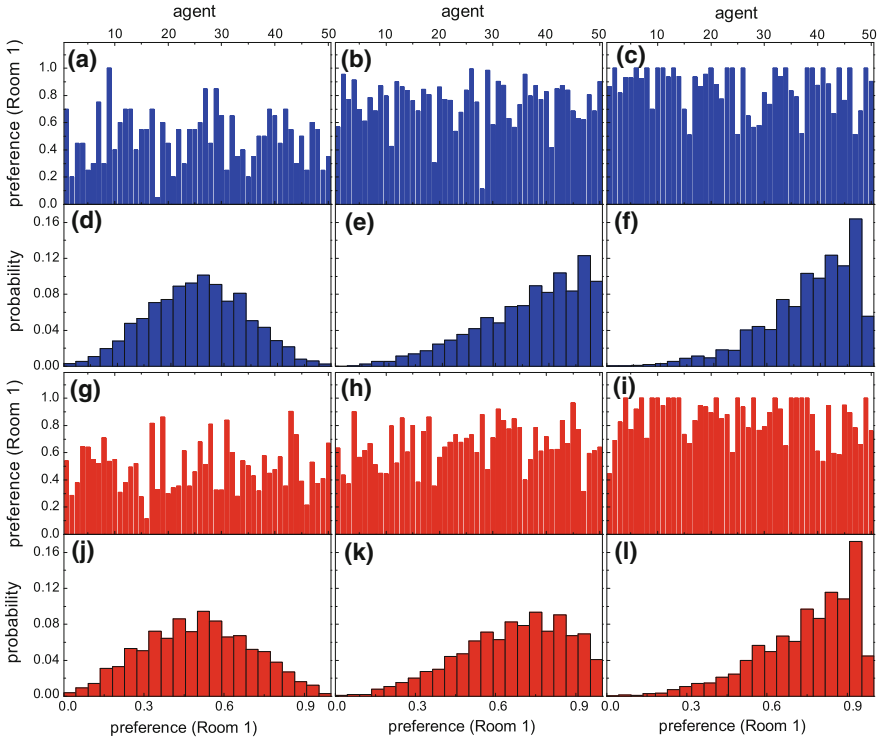

Fig. 5.3 Simulation results obtained from the agent-based simulations. **a–c, g–i** Preferences of the 50 normal agents to Room 1 for the cases **a–c** without ($\beta = 0$) and **g–i** with ($\beta = 0.5$) imitating agents, and for the resource distributions M_1/M_2 =(**a, g**) 1, (**b, h**) 3, and (**c, i**) 20. We have run the simulations for 200 times, each over 400 time steps (first half for equilibration, the remaining half for statistics). **a–c, g–i** are typical results of one of the 200 runs. In **a–c, g–i**, "Mean" denotes the mean value of the preferences of the 50 normal agents. **d–f, j–l** Distribution of the 50 normal agents' preferences. Note that **d–f, j–l** are obtained from the average over the 200 runs, and also the "Mean" in **d–f, j–l** denotes this average. Simulation parameters: $S = 4$, $P = 16$, and $N_n = 50$. Adapted from Ref. [8]

the heterogeneity of preferences with reasonable modeling of the decision-making process for the human subjects. (We had also investigated the preferences of normal agents in an alternative way by analyzing the Shannon information entropy; see Part V of Supplementary Materials.) Next, efficiency, stability, and predictability of the whole modeled system are calculated according to the definitions made in the experimental study. The change in system behavior along with the variation of the resource ratio M_1/M_2 is shown in Fig. 5.4. Differently colored symbols in the figure represent results obtained under different values of β. As shown in Fig. 5.4a, when the resource distribution is comparable ($M_1/M_2 \approx 1$), the averaged population ratio $\langle N_1 \rangle / \langle N_2 \rangle$ can always be in concert with M_1/M_2 no matter imitating agents are involved or not. On the other hand, as the resource distribution gets more and

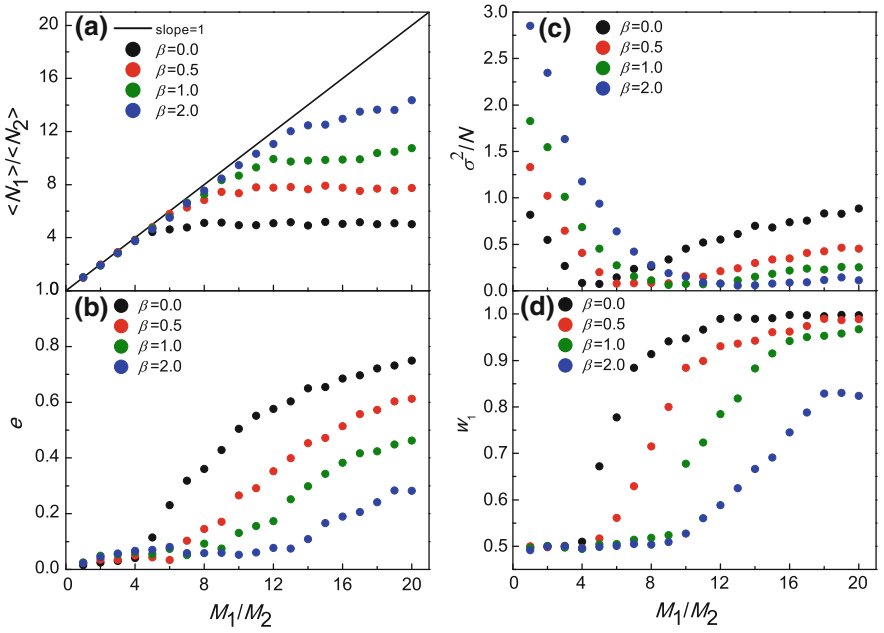

Fig. 5.4 **a** $\langle N_1\rangle/\langle N_2\rangle$, **b** e, **c** σ^2/N, and **d** w_1 as a function of M_1/M_2, for an open system in the agent-based simulations. Parameters: $N_n = 50$, $S = 4$, $P = 16$, $k = 5$, and $\beta = 0$, 0.5, 1.0, and 2.0. For each parameter set, simulations are run 200 times, each over 400 time steps (first half for equilibration, the remaining half for statistics). In **a**, "slope = 1" denotes the straight line with slope being 1. Adapted from Ref. [8]

more biased (M_1/M_2 increases), surprisingly the whole system tends to reach the balanced state only if more imitating agents (larger β) join the system. Figure 5.4b shows the change in efficiency of the resource-allocation system. The tendency is that when the resource ratio gets more biased, a larger size of herd is needed to realize a higher efficiency of the resource distribution. From both the subfigures, the so-called "M_1/M_2 phase transition" [7], where M_1/M_2 plays the role of control parameter, can also be identified. As shown in Fig. 5.4c, the increase of the number of imitating agents will cause larger fluctuations in the low M_1/M_2 region. However, as M_1/M_2 increases, more imitating agents can yield higher stability of the resource-allocation systems. Comparing system behaviors for the cases of $\beta = 0$ and $\beta \neq 0$, the M_1/M_2 phase transition also indicates the change of role for the herd behavior, namely from a ruinous herd into a helpful herd. It is clear that the critical point of the M_1/M_2 phase transitions get larger when the number of imitating agents increases. Denoted as $(M_1/M_2)_c$ hereafter, the critical point refers to the M_1/M_2 value where the minimum is achieved. This definition together with the mechanism for the increase of $(M_1/M_2)_c$ will be further discussed in the theoretical analysis of the model. Finally, the effect of herd behavior on the predictability of the resource-allocation system is shown in Fig. 5.4d. When more imitating agents are introduced to the system for

large M_1/M_2, the prediction of the next winning room becomes more difficult as winning rates for the two rooms are more symmetric. Notice that the system behavior under various conditions found herein by the agent-based simulations echoes with the observations in the experiment.

We summarize the simulation results here and make some more comments to emphasize the significance of findings in our study. The performance of the resource-allocation system consisting of normal agents or human subjects with the full decision-making ability is, in some cases, inferior to those including imitating agents (who form the herd). This might seem questionable at first sight. In particular, it may be argued that the failure to reach the balanced resource allocation for large M_1/M_2 when $\beta = 0$ is only due to the relatively small population of the normal agents. However, it has been proved in the theoretical analysis (see the equation for the population in the next section or Eq. (5.5) in Part III of Supplementary Materials) and the agent-based simulation of resource-allocation systems [7] that the total number of agents is indeed not a key factor. When the resource distribution is not biased so much, the normal agents can play pretty well so that the resource-allocation system behaves in a healthy manner (efficient or balanced, stable, and unpredictable). In such situations, adding imitating agents will only bring about a "crowded system" in which larger fluctuations (volatility) turn up. In this respect, our study shares some common features with the Binary-Agent-Resource model [101, 102]. In particular, the "crowd effect" has been observed in these models and the inclusion of imitating agents in our model can be explained as a special kind of networking effects. Only if the resource distribution becomes so biased that most normal agents cannot completely solve the decision-making problem by referencing their strategy books, adding the imitating agents could become a helpful factor in consuming the remained arbitrage opportunities in the system. This explains the reason why the herd behavior in the resource-allocation system can effectively help the system to realize the balanced state and reduce instability and predictability in the mean time.

5.5 Theoretical Analysis

To further understand the underlying mechanism for these phenomena, we also conduct theoretical analysis by deriving the critical points $(M_1/M_2)_c$ for the M_1/M_2 phase transition identified in the agent-based simulations. (For details of derivation, refer to Part III of Supplementary Materials.) As a result of the theoretical analysis, the maximum of population ratio in Room 1 $\langle R_1 (= N_1/N)\rangle_{\max}$ can be obtained under the condition $M_1 \geq M_2$. It reads as the following (the meaning of the symbols can also be found in Part III of Supplementary Materials),

$$\langle R_1\rangle_{\max} = 1 - \frac{1}{(\beta+1)P}\sum_{\tilde{L}=1}^{P}\left[\left(\frac{\tilde{L}}{P+1}\right)^{s} + \beta\left(\frac{\tilde{L}}{P+1}\right)^{ks}\right],$$

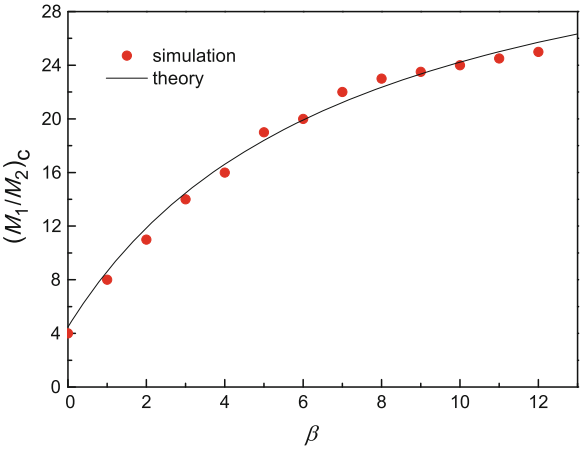

Fig. 5.5 Critical points of the M_1/M_2 phase transition, $(M_1/M_2)_c$, varying with different population ratios β: simulation results (*symbols*) versus theoretical results (*line*). The simulation results are obtained from the data in Fig. 5.4a, c. Adapted from Ref. [8]

where $\tilde{L}$ stands for the preference of a normal agent's strategy. If $\langle R_1 \rangle_{\max} = M_1/(M_1 + M_2)$, the system can fluctuate around the balanced state. Otherwise, the system can never reach the balanced state. Then some insightful comments can be added:

- The state of the resource-allocation system depends only on M_1/M_2, β, k, P, and S. It has no concern with N_n or N_m.
- An optimized value of β may be calculated by setting $\langle R_1 \rangle_{\max} = M_1/(M_1 + M_2)$, which could make the system more stable. After substituting this expression into the equation for $\langle R_1 \rangle_{max}$, we can obtain numerical solutions for the critical points $(M_1/M_2)_c$ of the phase transitions. Figure 5.5 shows a good agreement between the simulation results and those of theoretical derivation for the critical points.
- It is easy to prove that $\partial \langle R_1 \rangle_{\max}/\partial \beta > 0$, which means that β and $\langle R_1 \rangle_{\max}$ are positively related. When $\beta \to \infty$, the population ratio will converge to $\langle R_1 \rangle_{\max} \to 1 - \frac{1}{P} \sum_{\tilde{L}=1}^{P} (\frac{\tilde{L}}{P+1})^{ks}$. At this limit, the model suggested here will be equivalent to the original resource-allocation model without the imitating agents [102], except that in this case, each agent would occupy kS (instead of S) strategies.

5.6 Discussion and Conclusions

We have revealed that, if the bias between the two resources M_1/M_2 was large and is unknown to the subjects/agents, a herd of a typical size could help the overall system to reach the optimal state, namely the state with minimal fluctuation, high

efficiency, and relatively low predictability. The corresponding ratio between the two resources also works as the critical point of a class of M_1/M_2 phase transition. The phase transition can be used to discover the role change of herd behavior, namely from a ruinous herd to a helpful herd as the resources distribution gets more and more biased. The main reason for this generalization could be understood as follows. When a large bias exists in the distribution of resource, the richer room will offer more arbitrage opportunities so that it deserves to be chosen without too much deliberation. Since imitating agents learn from the local best human subject or normal agent, the herd formed by these agents will certainly be more oriented to the richer room. To balance a highly biased resource distribution, in fact, it correspondingly needs a suitable number of participants who have a highly biased orientation in their choices. But every coin has two sides. Normal agents will be confused if too many imitating agents are involved. Because in that case, they have to estimate not only the unknown system but also the behavior of the herd. The effect of herd behavior would become negative again under these situations. We emphasize that these arguments are quite general. In particular they are independent of the process of herding. In Part VI of Supplementary Materials, results of a different agent-based model, in which imitating agents follow the majority of the linked group, rather than the best normal agent, are shown. Similar results are achieved indeed.

This chapter is also expected to be important to some fields, ranging from management and social science, to ecology and evolution, and to physics. In management and social science, administrators should not only conduct risk management after the formation of herd, but also need to consider system environment and timing to see whether the herd is globally helpful or not. In ecology and evolution, it is not only necessary to study the mechanism of herd formation as usual, but also to pay more attention to the effect of herding on the whole ecological system and/or evolution groups. For physics, this chapter not only presents the existence of phase transition in such a CAS, but also proposes a new equilibrium theory. Namely, in the presence of symmetry breaking, a CAS is likely to reach the equilibrium state only through cluster performance after the elements that construct the system form typically sized clusters.

5.7 Supplementary Materials

5.7.1 Part I: Leaflet to the Human Experiments

There are totally 50 subjects doing the experiments together. The experiment situation is the same for everyone. Once the experiments begin, any kind of communication is not allowed.

Together with other subjects, you shall engage in a resource-allocation experiment. For the experiment, there are two virtual rooms (Room 1 and Room 2), and the amounts of virtual money in the two rooms are M_1 and M_2, respectively. The value

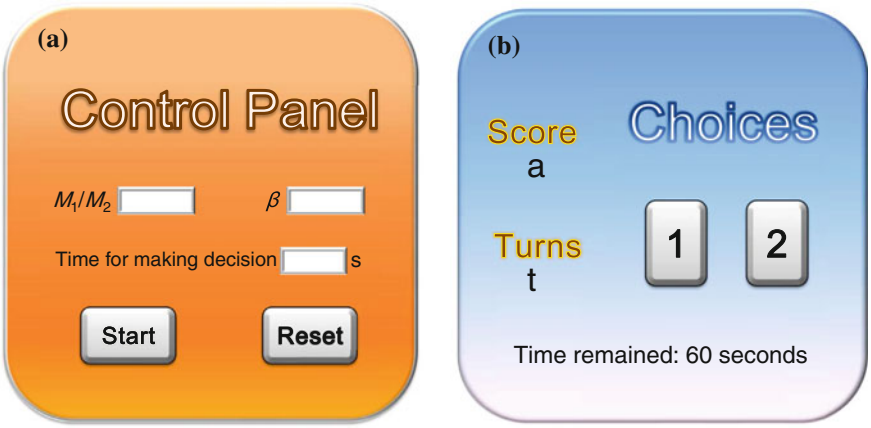

Fig. 5.6 The desktops of the experiment-control computer program used in the computer-aided human experiments: The control panel **a** for the coordinator and **b** for the human subjects. Adapted from the Supplementary Materials of Ref. [8]

of M_1/M_2 is fixed in one experiment, but is not announced. In each round, you have to choose to enter one of the two rooms, to share alike the virtual money inside the room. After everyone has made a decision, those who earned more than the global average are regarded as winners of the round, and the room which the winners had entered as the winning room.

After you log in, you will see the choosing panel on the computer screen (as shown in Fig. 5.6b), buttons with numbers of 1 and 2 are used to choose Room 1 and Room 2. The left of the panel displays your current score (a) and the current experiment round (t). During the experiment, 60 s were given for making choice. If you could not decide your choice within 60 s, the experiment-control computer program would assign you a random choice with probability 50 %. Nevertheless, the subject who borrowed the computer's choice twice would be automatically kicked out of the experiment. In each round of the experiment, the experiment-control computer program will update the score for each subject after all the subjects have made their choices. If your score is added 1 point, it means that the room you have chosen happened to be the winning room. If the score keeps unchanged, it may have two possible interpretations: either the other room won or neither of the rooms won (i.e., the experiment ended in a draw).

The initial capital of each subject is 0 point and the total payoff of a subject is the accumulated scores (points) of all the experiment rounds. At the end of the experiments, as a premium, this payoff (points) will be converted to the monetary payoff in Chinese Yuan with a fixed exchange rate 1:1 (namely, one point equals to one Chinese Yuan). Try to win more points, and then you can get more premium.

5.7.2 Part II: About the Computer-Aided Human Experiment

All the experiments are carried out in an online manner. Human subjects can get the necessary information only from their computer terminals. The desktop designs of the experiment-control computer program are shown in Fig. 5.6. The control panel for the experiment coordinator is configurated as panel (a), and that for human subjects as panel (b). At the beginning of the experiment, the coordinator input the value of M_1/M_2 and β, and set the time length (60) for the human subjects to make their decisions. When all the human subjects have logged in, the coordinator can click the "start" button to start the experiment. After all the subjects have made their choices, the coordinator clicks the "reset" button to end the current round and set anew. On panel (b), buttons with numbers of 1 and 2 are used to choose Room 1 and Room 2. The left of the panel displays the current score (a) of the subject and the current experiment round (t). To keep every subject conducting the experiment independently, procedures and rules of the experiment are designed carefully so that possible direct or indirect communications can be shut off. For example, subjects can only make their own choices by clicking the button instead of raising their hands. This could make sure that subjects cannot get information from sounds, expressions, or gestures of the others. There is also no need for the experiment coordinator to announce the result of winning room. Participants can only deduce the winning room from the change of their scores on the desktop panels. In addition, no human subjects had been kicked off during the experiments. For all the experiments with $M_1/M_2 = 1, 3$, and 20, the total number of human subjects was kept to be 50. Among those, 44 human subjects played through all the three experiment sessions. On the other hand, we had member changes for the remaining six subjects.

5.7.3 Part III: The CAS—Theoretical Analysis of the Agent-Based Modeling

Besides the simulations performed in the main text for the agent-based modeling, here we present some theoretical analysis for the same open system. It is reasonable to assume that, if P is not too small, the right column of a strategy filled in by 1 with probability L/P is equal to the one filled in by 1 with the number of L. Hence strategies with the same preference number L can be regarded as the same. It is worth noting that if the situations vary in a random manner, the probability is L/P for a normal agent to choose Room 1 using a strategy with preference number L. Next, we assume that the preference number of the best strategy held by normal agent i at time T, is L_i. Denote the choice of room as x_i so that $x_i = 1$ if Room 1 is chosen and $x_i = 0$ otherwise. At the same time, let imitating agent j choose to follow the normal agent μ, the best agent (who has the highest score) in the group of size k ($1 \leq k \leq N_n$). For the imitating agent, its choice of room is $y_j = x_\mu$, and its preference number becomes $L_j = L_\mu$. With these definitions, the total number

of agents in Room 1 at time T can be written as

$$N_1 = \sum_{i=1}^{N_n} x_i + \sum_{i=1}^{N_m} y_j, \tag{5.1}$$

It is obvious that $\langle x_i \rangle = L_i/P$, which can be used to respectively derive the expectation and the variance of the population in Room 1 as

$$\langle N_1 \rangle = \frac{1}{P}\left(\sum_{i=1}^{N_n} L_i + \sum_{i=1}^{N_m} L_j\right), \tag{5.2}$$

$$\begin{aligned}\sigma_{N_1}^2 = &\sum_{i=1}^{N_n} \sigma_{x_i}^2 + \sum_{j=1}^{N_m} \sigma_{y_j}^2 + \sum_{i=1}^{N_n}\sum_{j=1}^{N_m}(\langle x_i y_j \rangle - \langle x_i \rangle \langle y_j \rangle) \\ &+ \sum_{p,q=1, p\neq q}^{N_m} (\langle y_p y_q \rangle - \langle y_p \rangle \langle y_q \rangle).\end{aligned} \tag{5.3}$$

Owing to the specific method for the construction of strategies in the resource-allocation model, the covariance between the choices of different normal agents can be neglected. On the right-hand side of Eq. (5.3), the third item is the correlation between choices of the normal agents and those of the imitating agents who followed them. The fourth item is the correlation between the choices of different imitating agents who followed the same normal agent. Both terms should always be positive, which means that adding the imitating agents could cause large fluctuations (volatility) in the resource-allocation system. It should be emphasized here that the stability defined in the main text is different from the traditional definition of variance. The former characterizes both the deviation and the fluctuation to the idealized room population in the balanced state, while the latter only represents the fluctuation to the mean value of the time series. When the resource distribution is comparable ($M_1/M_2 \approx 1$), since normal agents are able to produce the idealized population or $\langle N_1 \rangle / \langle N_2 \rangle \approx M_1/M_2$, these two kinds of definitions are approximately equal. This explains why the stability can be destroyed when imitating agents are involved in situations with a nearly unbiased resource distribution. However, when the system environment becomes difficult for the normal agents to adapt to, the difference between the "variance" and the "stability" cannot be neglected. If no imitating agents are involved, the normal agents alone cannot make the system reach the balanced state. In that case, even if the fluctuation of N_1/N_2 to its average value could be made small, the deviation to the idealized population ratio can still be very large. This would make the system suffer from higher dissipation. If an appropriate portion of imitating agents is added, the deviation of N_1/N_2 to the idealized room population

diminishes, leaving only some fluctuations around M_1/M_2, which could result in a reduction of waste in the resource allocation.

Then, we study the performance of different strategies (namely, strategies with different preference numbers). We also consider the condition of $M_1/M_2 \geq 1$, as used in the main text. Assume that at time T, the winning rate of Room 1 is $\alpha(T)$. The expectation of the increment of score for the strategy with the preference number L should be $1 - \frac{L}{P} + (\frac{2L}{P} - 1)\alpha(T)$. Then the expectation of the cumulative score for this strategy from $t = 1$ to $t = T$ can be expressed as

$$f(L, T) = \left(1 - \frac{L}{P}\right) T + \left(\frac{2L}{P} - 1\right) \sum_{t=1}^{T} \alpha(t),$$

From this expression, we can calculate the dependence of the cumulative score on the preference number as

$$\frac{\Delta f}{\Delta L} = \frac{2}{P} \sum_{t=1}^{T} [\alpha(t) - 0.5]. \tag{5.4}$$

It is easy to derive from Eq. (5.3) that if $\sum_{t=1}^{T}[\alpha(t) - 0.5] > 0$, f should be a monotonically increasing function with L. Now we assume that $[\alpha(T) - 0.5]$ is always positive, which is not a too stringent condition as long as M_1 is large enough. As the experiment evolves under this assumption, the gap among different strategies of different preference numbers will become larger and larger. Eventually, the best performed strategy owned by a normal agent would be the one with the largest L in its strategy book. As a consequence, imitating agents will choose to follow those who own the strategy with the largest preference number $L_{\max}$. From Eq. (5.1), it is obvious that $\langle N_1 \rangle$ will also reach its maximum value $\langle N_1 \rangle_{\max}$, when both L_i and L_j reach their maximum values. With this maximum value of the expected population in Room 1, we can propose the following two conditions:

- If $\langle N_1 \rangle_{\max} < \frac{M_1}{M_1+M_2} N$, the system can never reach the balanced state.
- If $\langle N_1 \rangle_{\max} > \frac{M_1}{M_1+M_2} N$, the system can fluctuate around the balanced state.

Denoting the population ratio $\langle R_1 \rangle = \langle N_1 \rangle / N$, we need to calculate $\langle R_1 \rangle_{\max} = \langle N_1 \rangle_{\max} / N$, to evaluate the conditions above. As the normal agents construct their strategies in a random way, a strategy with an arbitrary preference number may be picked up with a uniform probability $1/(P + 1)$. Thus, among the S strategies of a normal agent, the probability to have $L_{\max} = \tilde{L}$ is $p(\tilde{L}) = (\frac{\tilde{L}+1}{P+1})^S - (\frac{\tilde{L}}{P+1})^S$. Since an imitating agent would choose the best normal agent among the k group members, the probability to have $(L_{\max})_{ks} = \tilde{L}$ should be $p'(\tilde{L}) = (\frac{\tilde{L}+1}{P+1})^{kS} - (\frac{\tilde{L}}{P+1})^{kS}$. With these probabilities, we obtain the population ratio as

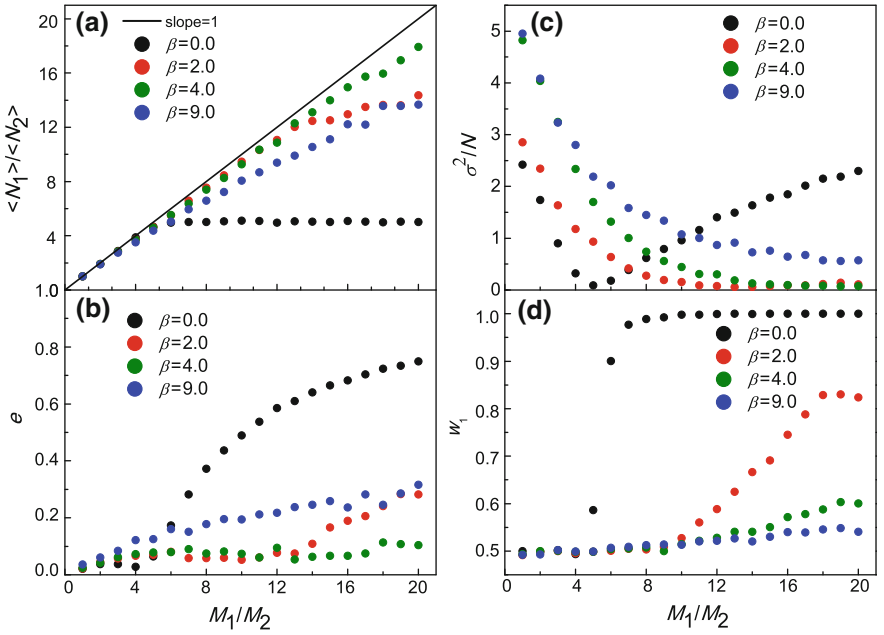

Fig. 5.7 **a** $\langle N_1\rangle/\langle N_2\rangle$, **b** e, **c** σ^2/N, and **d** w_1 as a function of M_1/M_2, for a closed system. Parameters: $N = 150$, $S = 4$, $P = 16$, $k = 5$, and $\beta = 0, 2.0, 4.0$, and 9.0. Simulations are run 200 times, each over 400 time steps (first half for equilibration, the remaining half for statistics). In **a**, "slope = 1" denotes the straight line with slope being 1. Adapted from the supplementary materials of Ref. [8]

$$\begin{aligned}\langle R_1\rangle &= \frac{1}{NP}\left(\sum_{i=1}^{N_n} L_i + \sum_{j=1}^{N_m} L_j\right)\\ &= \frac{1}{NP}\left[N_n \sum_{\tilde{L}=1}^{P} \tilde{L}\, p(\tilde{L}) + N_m \sum_{\tilde{L}=1}^{P} \tilde{L}\, p'(\tilde{L})\right]\\ &= 1 - \frac{1}{(\beta+1)P}\sum_{\tilde{L}=1}^{P}\left[\left(\frac{\tilde{L}}{P+1}\right)^{s} + \beta\left(\frac{\tilde{L}}{P+1}\right)^{ks}\right].\end{aligned} \tag{5.5}$$

5.7.4 Part IV: A Closed CAS—Simulations Based on Agent-Based Modeling

For the opensystem discussed in the main text, if there are too many imitating agents in the resource-allocation system, it may still become a disturbing factor to the

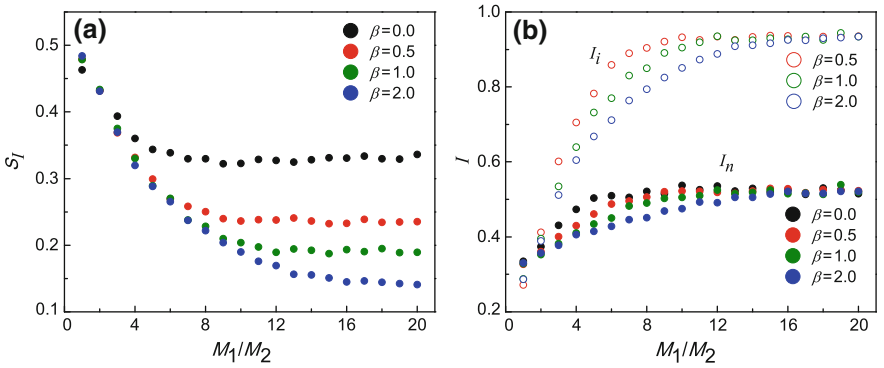

Fig. 5.8 The change in **a** the averaged information entropy (S_I) for all the agents including the normal agents and imitating agents and **b** the averaged information content for the normal agents (I_n) and imitating agents (I_m), respectively. Simulations are run 200 times, each over 400 time steps (first half for equilibration, the remaining half for statistics). Parameters: $N_n = 50$, $S = 4$, $P = 16$, and $k = 5$. Adapted from the supplementary materials of Ref. [8]

system. For completeness of the study, here we consider a closed system in which the number of normal and imitating agents is fixed at $N = 150$ with the parameter β being varied. As shown in Fig. 5.7, in the larger M_1/M_2 region, situations with the imitating agents ($\beta = 2.0$ and 4.0) are generally better than those without imitating agents ($\beta = 0$), similar to cases of the open system. Meanwhile, there clearly exists an optimized $\beta(= 4.0$ in the current case) with which the best state of the closed system can be realized in the aspects of the efficiency (which, herein, only describes the degree of balance of resource allocation in the model system) and the stability. When $\beta = 9.0$, the system seems to be disturbed by the imitating agents and the performance (except the system unpredictability) becomes even worse than the case of $\beta = 2.0$. The reason for this phenomenon may be explained as follows. If too many imitating agents join the system, even the best normal agents may be confused. Typically, they might have wrong estimations about the system situation and then make incorrect decisions. When their decisions are learnt by the imitating agents, the herd will over-consume the arbitraging opportunities in the system as a result of the distribution of biased resources, thus yielding a less efficient (or equivalently balanced) and less stable but still unpredictable state.

5.7.5 *Part V: An Alternative Approach to Analyzing Preferences of Normal Agents and Imitating Agents in the Agent-Based Modeling: Analysis of the Shannon Information Entropy*

To study the agents' preferences and their estimation of the system, the Shannon information entropy [41, 103] may be introduced to our agent-based modeling. The information entropy S_I of a discrete random variable X with possible values $\{x_1, ..., x_n\}$ is

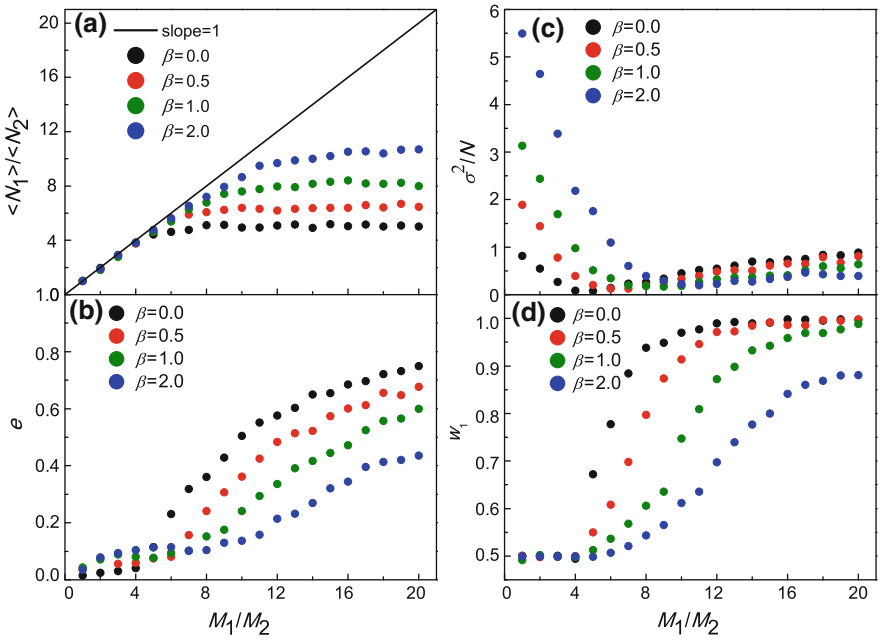

Fig. 5.9 **a** $\langle N_1\rangle/\langle N_2\rangle$, **b** e, **c** σ^2/N, and **d** w_1 as a function of M_1/M_2, for an open system. Parameters: $N_n = 50$, $P = 16$, $S = 4$, $k = 5$, and $\beta = 0, 0.5, 1.0$, and 2.0. The imitating agents follow the majority of their local groups. Simulations are run 200 times, each over 400 time steps (first half for equilibration, the remaining half for statistics). In **a**, "slope = 1" denotes the straight line with slope being 1. Adapted from the supplementary materials of Ref. [8]

defined as $S_I(X) = -\sum_{i=1}^{n} P(x_i) \ln P(x_i)$, in which $P(x_i)$ denotes the probability mass function of x_i. In the agent-based model, the information entropy for a normal agent is $S_{Ii} = -\frac{L_i}{P} \ln \frac{L_i}{P} - \frac{P-L_i}{p} \ln \frac{P-L_i}{P}$, where L_i stands for the preference of the current strategy. If the normal agent chooses two rooms with equal probability, this information entropy would reach the maximum value of $\ln 2$. On the other hand, the information entropy S_{Ij} for imitating agent j will be the same as that of the normal agent he/she follows in the local group. Thus the average information entropy of all the agents (i.e., normal agents and imitating agents) can be calculated as

$$S_I = \frac{1}{N}\left(\sum_{i=1}^{N_n} S_{Ii} + \sum_{j=1}^{N_m} S_{Ij}\right),$$

and the results are shown in Fig. 5.8a. As the average information entropy decreases as M_1/M_2 becomes larger, a clear-cut average preference of agents emerges as the distribution of resources gets more biased. This agrees with the analysis of subjects' preferences in the human experiments; see Fig. 5.1. Furthermore, the information content of agent i can be defined as $I_i = (\ln 2 - S_{Ii})/\ln 2$. Note that a larger I_i

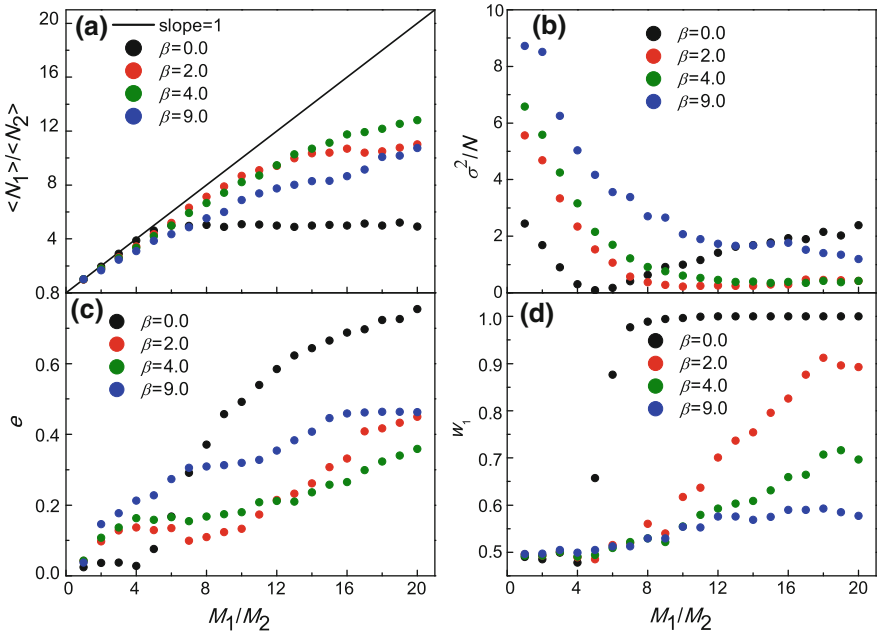

Fig. 5.10 **a** $\langle N_1\rangle/\langle N_2\rangle$, **b** e, **c** σ^2/N, and **d** w_1 as a function of M_1/M_2, for a closed system. Parameters: $N = 150$, $P = 16$, $S = 4$, $k = 5$, and $\beta = 0$, 2.0, 4.0, and 9.0. Others are the same as those in Fig. 5.8. Adapted from the supplementary materials of Ref. [8]

indicates that the agent has more confidence in a certain room. The average information content for all the normal agents (I_n) and imitating agents (I_m) are shown in Fig. 5.8b. In this figure, I_n decreases with the increase of the population of imitating agents when M_1/M_2 is small. This means that normal agents can be confused by the actions of imitating agents in a rather uniform distribution of the resource. When M_1/M_2 gets larger, $I_n$is nearly a constant implying that imitating agents will no longer affect the estimation of the normal agents. All these go well with the analysis of the experimental results in Fig. 5.1. The averaged information content of imitating agents has a rather drastic change as the environment varies. When $M_1/M_2 = 1$, I_m is pretty low, even lower than that of the normal agents, a fact indicating that imitating agents have almost unbiased preferences when the resource distribution is uniform. As M_1/M_2 increases, imitating agents are apt to flood into a specific room and thus form the herd in the modeled system.

5.7.6 *Part VI: A Different Agent-Based Modeling in Which Imitating Agents Follow the Majority, Rather than the Best Agent: An Open CAS Versus a Closed One*

To make our result more general, a different modeling is studied. Following the most successful person is often seen in daily life, and there is another common case following the majority. For example, people often decide which store or restaurant to patronize on the basis of how popular they are. In this sense, we make some changes to our agent-based modeling adopted in the main text. Their main structures are similar, but the difference between them is that the "imitating agent" now follows the majority decision of his/her group (namely the current imitating agents act as local majority followers). This means if more than half of the group members choose Room 1, he/she will enter Room 1 accordingly.

As shown in Figs. 5.9 and 5.10, the system behaviors are similar as those of "imitating the best." The main difference between Figs. 5.4 and 5.9 lies in Fig. 5.9c. When M_1/M_2 is small, adding imitating agents (local majority followers) will cause relatively larger fluctuations. From Fig. 5.10, we can find that in the closed system of "following the majority", there also exists a proper β for one certain system environment M_1/M_2. Compared with Figs. 5.7 and 5.10 shows that "following the majority" works not that well as "following the best" and this is easy to understand. The best normal agent owns the best strategy and is usually much more sensitive than common ones, while the majority reflects the average level of all the normal agents in the group. Although quantitatively different, the main conclusions arising from the two kinds of "following" are similar. Thus, the mechanism on how to form the herd is not an essential problem, and both "imitating the best" and "following the majority" can lead to similar conclusions.

Chapter 6
Contrarian Behavior: Beyond the Known Helpful Role

Abstract Similar to herd behavior discussed in Chap. 5, contrarian behavior is also a kind of self-organization in complex adaptive systems (CASs). Here we report the existence of a transition point in a model resource-allocation CAS with contrarian behavior by using human experiments, computer simulations, and theoretical analysis. The resource ratio and system predictability serve as the tuning parameter and order parameter, respectively. The transition point helps to reveal the positive or negative role of contrarian behavior. This finding is in contrast to the common belief that contrarian behavior always has a positive role in resource allocation, say, stabilizing resource allocation by shrinking the redundancy or the lack of resources. It is further shown that resource allocation can be optimized at the transition point by adding an appropriate size of contrarians. This chapter is also expected to be of value to some other fields ranging from management and social science to ecology and evolution.

Keywords Resource-allocation system · Contrarian behavior · Ruinous role · Phase transition

6.1 Opening Remarks

In the preceding chapter, we studied the role of herd behavior. Here "herd behavior" means following the majority. In this chapter, we want to raise and answer a connected question: what if one follows the minority, instead of the majority? Following the minority actually corresponds to contrarian behavior, an inverse behavior of herd.

For engaging in competitions for sharing resources, agents in complex adaptive systems (CASs) often utilize various kinds of strategic behaviors, one of which is contrarian behavior. Contrarian behavior means figuring out what the herd is doing, and doing the opposite [104]. Contrarian behavior can be regarded as a kind of self-organization, which is one of the characteristics that distinguish CASs [105] from other types of complex systems. To dig out the nature of contrarian behavior is also of practical importance when one faces relevant problems of resource allocation,

J.-P. Huang, *Experimental Econophysics*, New Economic Windows,
DOI 10.1007/978-3-662-44234-0_6

such as risk evaluation and crisis management. Thus, contrarian behavior has been an active subject of study in various fields like finance/economics [106], complexity science [107], and social science [108–111]. In the social field, previous contrarian studies using Galam model of two state opinion dynamics [108–110] aimed at the effect of contrarian choices on the dynamics of opinion forming, which shed significant light on hung elections. In this chapter, we designed to study the effect of contrarian behavior on social resource allocation. It is a common belief that contrarian behavior always stabilizes resource allocation by shrinking the redundancy or the lack of resources (positive role). However, is this common belief true? Here we specially raise this question because unbiased or biased distributions of resources are everywhere in Nature where contrarians are often needed. In other words, to comply with the real world, we need to investigate the role of contrarian behavior as the environment (which here is defined by the ratio between two resources, namely resource ratio) varies.

The above-mentioned CASs involving competitions of agents for various kinds of resources can be modeled as a typical class of artificial Well-Regulated Market-Directed resource-allocation systems (simply denoted as "resource-allocation systems" in the following) [7, 8], as an extension of the original minority game [1]. Such resource-allocation systems can reflect some fundamental characteristics of the above CASs in the real world [1, 7, 8, 20, 31], such as a resource-allocation balance emerged as a result of system efficiency [7, 8]. Thus, without loss of generality, we shall investigate the role of microscopic agents' contrarian behavior in the macroscopic properties of the resource-allocation system. In the process, we identify a class of transition points which help to distinguish the positive role (stabilizing, etc.) and the negative role (unstabilizing, etc.) of contrarian behavior for an unbiased/a weakly biased and a strongly biased distribution of resources, respectively. Comparing with the contrarian study of Galam [108], which also shows the transition point at a critical value of the contrarian proportion to identify opinion group forming, here the transition points in this chapter helps to reveal that the allocation of resources can be optimized at the transition point by adding an appropriate size of contrarians which is observed in human experiments. To proceed, based on the Extensively-Adopted approaches of both statistical analysis [14, 112–114] and Agent-Based modelling [1, 7, 8, 12, 20, 115], we resort to three complementary tools: human experiments (producing data for statistical analysis), Heterogeneous-Agent-Based computer simulations (of Agent-Based modeling), and Statistical-Mechanics-Based theoretical analysis (of Agent-Based modeling).

6.2 Controlled Experiments

We designed and conducted a series of computer-aided human experiments on the basis of the resource-allocation system [1, 7, 8, 20, 31]. As revealed in [7, 8] the system can reach macroscopic dynamic balance that corresponds to the most stable state where the resources are allocated most efficiently and the total utilities of the system

are maximal due to the absence of macroscopic arbitrage opportunities. Here we add a proportion of contrarians to observe how contrarian behavior affects the macroscopic properties of the resource-allocation system. For the experiments we recruited 171 subjects, all of which are students and teachers from several departments of Fudan University. The experiments were conducted in a big computer laboratory and each subject had a computer to work with. All the subjects were given a leaflet interpreting how the experiment would be performed before the experiment started. In the computer-aided online experiment, there are two virtual rooms: Room 1 and Room 2. Each room owns a certain amount of resources marked as M_1 or M_2 accordingly. The subjects do not know the exact resource ratio, M_1/M_2, at every experimental round. In the experiment, no kind of communication is allowed, and every subject chooses to enter Room 1 or Room 2 independently to share the resources in it. Meanwhile, the computer program secretly adds contrarians into the system whose behaviors are controlled by the following settings. In every round of the experiment, each contrarian randomly chooses five subjects as his/her group. Then the contrarian will choose to enter the less-entered room according to the group. For example, if most of the subjects in a contrarian's group choose to enter Room 1, the contrarian will choose to enter Room 2. The total number of subjects and contrarians entering Room 1 and Room 2 are denoted as N_1 and N_2, respectively. After every experimental round, if $M_1/N_1 > M_2/N_2$, we say Room 1 (or Room 2) is the winning (or losing) room, because the subjects and contrarians entering Room 1 obtain more resources per capita, and vice versa. The subjects in the winning room are granted 10 scores, and those in the losing room are given zero score. The final rewards are based on the scores each subject obtains in all the experimental rounds according to the exchange rate: 10 scores = 1 Chinese Renminbi. Besides, we pay every subject 30 Chinese Renminbi as attendance fee, and reward the top 10 subjects (having the highest scores) each with extra 100 Chinese Renminbi. The details are explained in Supplementary Materials at the end of this chapter.

In the experiment, we adjusted two parameters: one, resource ratio M_1/M_2 and, next, the ratio between the number of contrarians and subjects, β_c. 30 experimental rounds were repeated under each parameter set: M_1/M_2 and β_c. Let us denote the number of subjects as N_n and the number of contrarians as N_c , thus yielding $\beta_c = N_c/N_n$. In addition, the total number of all the subjects and contrarians is $N = N_n + N_c = N_1 + N_2$.

The experiment was conducted in two successive days: 88 subjects on the first day and 83 on the second day. The different numbers or different subjects show no influence on the results of the experiment. The experimental results are shown in Fig. 6.1 where $\langle N_1\rangle/\langle N_2\rangle$ is plotted as a function of M_1/M_2. When the distribution of resources is weakly biased up to $M_1/M_2 = 3$, the experimental results of $\langle N_1\rangle/\langle N_2\rangle$ are approximately located on the line with slope = 1 for the three values of β_c. In such cases, the system reaches dynamic balance at which the total utilities of the system are maximal due to the elimination of the macroscopic arbitrage opportunities. Nevertheless, for the strongly biased resource ratio, say $M_1/M_2 = 10$, the balance is broken as shown by the three experimental values that deviate far from the "slope = 1" line. In other words, as the resource ratio is unbiased or weakly biased, adding a

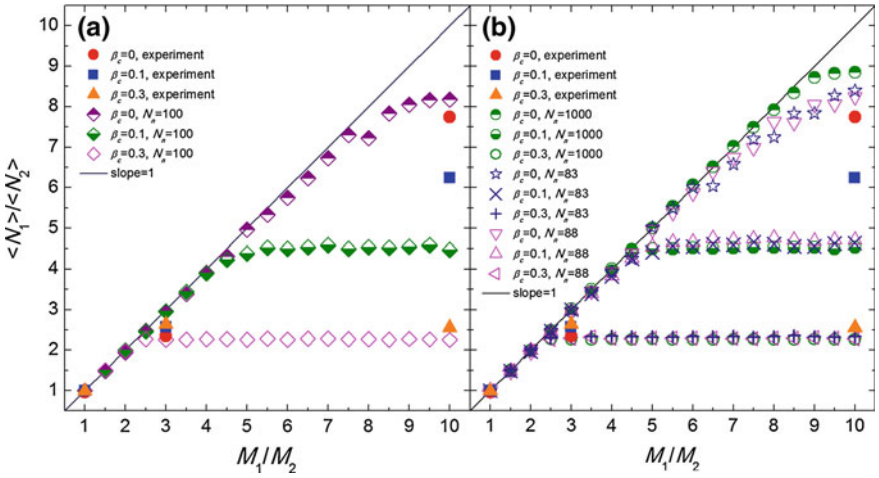

Fig. 6.1 Population ratio, $\langle N_1\rangle/\langle N_2\rangle$, as a function of resource ratio, M_1/M_2. The line with "slope = 1" indicates the balance state where $\langle N_1\rangle/\langle N_2\rangle = M_1/M_2$. Each experiment lasts for 30 rounds (the first six rounds for equilibration and the last 24 rounds for statistics). Simulations are run for 400 time steps (the last 200 time steps for statistics and the first 200 time steps for equilibration). In **a**, the number of normal agents in simulations is 100. In **b**, the numbers of normal agents are respectively 1,000, 83, and 88. $\langle\cdots\rangle$ denotes the average over the last 24 rounds for the experiment or the last 200 time steps for the simulations. The three experimental data at $M_1/M_2 = 1$ are overlapped. Parameters for the simulations: $S = 8$ and $P = 64$. Adapted from Ref. [9]

small proportion of contrarians does not hurt the system balance. In contrast, as the resource ratio is biased enough, the contrarians of the same proportion break the balance instead.

Then, we analyze the experimental results from both individual and overall aspects of preference. As we know, different individuals have different preferences to a resource, which reflects the heterogeneity of preferences. The heterogeneity has remarkable influence on achieving balance in the system. Here, the preference of each subject is defined as his/her average rate of entering Room 1 in the 30 rounds of experiments. The statistical results are shown in Fig. 6.2. Figure 6.2a shows the result for $M_1/M_2 = 1$ and $\beta_c = 0$. The preferences of the subjects are different in spite of the unbiased distribution of the two resources, $M_1/M_2 = 1$. We see that the third subject preferred Room 1 while the second subject preferred Room 2. Such heterogeneity of preferences remains after introducing contrarians in Fig. 6.2b–c. As for the larger resource ratios in Fig. 6.2d–f and g–i, the subjects still have different preferences. However, the average preference of all the subjects varies with M_1/M_2, which illustrates the environmental adaptability of the subjects.

Next, in order to clearly observe the influence of contrarians on the macroscopic system, we calculated the stability of the system, $f = \frac{1}{2N}\sum_{i=1}^{2}\langle(N_i - \tilde{N}_i)^2\rangle$ [7], where $\langle\cdots\rangle$ denotes the average of time series $\cdots$. This definition describes the fluctuation in the room population away from the balance state at which the optimal

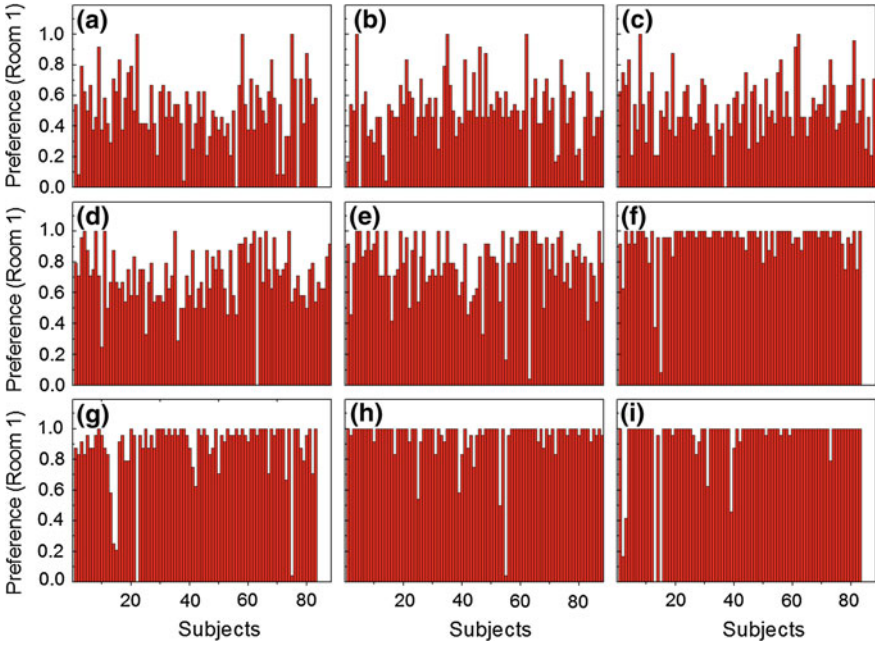

Fig. 6.2 Experimental data of the preference of each subject to Room 1 for the nine parameter sets with M_1/M_2 =1(**a**–**c**), 3(**d**–**e**), and 10(**g**–**i**) and $\beta_c = 0$(**a**, **d**, **g**), 0.1(**b**, **e**, **h**), and 0.3(**c**, **f**, **i**). For each parameter set, the experiment lasts for 30 rounds (the first six rounds for equilibration and the last 24 rounds for statistics). In the figure, "Mean" denotes the average preference of all the subjects. Adapted from Ref. [9]

room population, $\tilde{N}_i = M_i N/(M_1 + M_2)$, can be realized. Clearly, the smaller the value of f is, the closer the system approaches to dynamic stability. Figure 6.3a displays that, for small M_1/M_2, the fluctuations of the system decrease after introducing contrarians. Namely, the system becomes more stable. However, for large M_1/M_2, adding contrarians makes the system more unstable. Thus, we generally conclude that M_1/M_2 has a threshold, which distinguishes the different role of contrarians in the stability of the system. This experimental phenomenon will be further interpreted in the following part on computer simulations and theoretical analysis about transition points.

To further evaluate the performance of the overall system, we have also calculated the efficiency and predictability of the resource-allocation system. Here, efficiency is defined as $e = \left|\frac{\langle N_1\rangle}{\langle N_2\rangle} - M_1/M_2\right| /(M_1/M_2)$ [7]. Evidently, a larger value of e means a lower efficiency of resource allocation, and vice versa. Figure 6.3b shows the change of e when adding contrarians into the experiment. When M_1/M_2 is 1 or 3, the adding of contrarians makes the resource-allocation system more efficient. However, for $M_1/M_2 = 10$, the presence of contrarians reduces efficiency. Figure 6.3c shows the predictability of the system which is represented by the winning rate of Room 1,

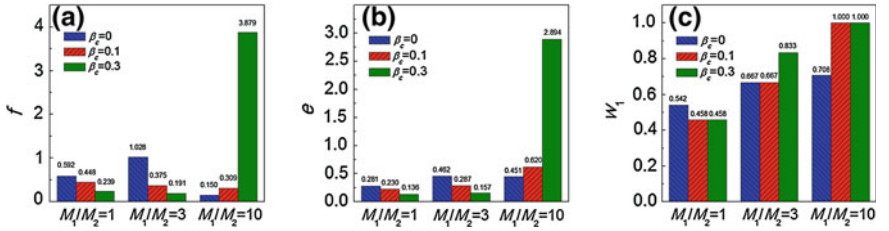

Fig. 6.3 Experimental data for **a** stability f, **b** efficiency e, and **c** predictability w_1 at $M_1/M_2 = 1$, 3, and 10. Each experiment lasts for 30 rounds (the first six rounds for equilibration and the last 24 rounds for statistics). Adapted from Ref. [9]

w_1 [8]. Note $w_1 = 0.5$ means the winning rate is the same for both Room 1 and Room 2, which is hard for the subjects to predict. If w_1 deviates from 0.5, the winning rate of one room is higher than the other, so the subjects can predict the results easily. According to Fig. 6.3c, when $M_1/M_2 = 1$, the winning rate w_1 fluctuates around 0.5 which means it is hard to carry out the prediction. But if M_1/M_2 becomes larger, the subjects are easy to predict the winning room for the next round especially when enough contrarians are added.

6.3 Agent-Based Modeling

Clearly the above experiment has some unavoidable limitations: specific time, specific experiment avenue (a computer room in Fudan University), specific subjects (students and teachers of Fudan University), and the limited number of subjects. Now we are obliged to extend the experimental results (Figs. 6.1, 6.2 and 6.3) beyond such limitations. For this purpose, we establish an Agent-Based model on the basis of the resource-allocation system. In this model, we denote N_n as normal agents and N_c as contrarians. Normal agents correspond to the subjects in the experiment and each of them decides to enter one of the two rooms using their strategy table which is the same as that designed in the Agent-Based model of market-directed resource-allocation game [7, 8]. Particularly, the table of a strategy is constructed by two columns. The left column represents P potential situations and the right column is filled with 0 and 1 according to the integer, L, which characterizes the heterogeneity in the decision-making of normal agents. For a certain value of L, ($L \in [0, P]$), there is a probability of L/P to be 1 in the right column of the table and a probability of $(P-L)/P$ to be 0. Here 0 and 1 represent entering Room 2 and Room 1, respectively. At each time step, normal agents choose to enter a room according to the right column of the strategy tables directed by the given situation P_i, ($P_i \in [1, P]$). Before the simulation starts, every normal agent will randomly choose S strategy tables, each determined by an L. At the end of every time step, each normal agent will score the S strategy tables by adding 1 (or 0) score if the strategy table predicts correctly (or incorrectly). Then, the

strategy table with the highest score will be used for the next time step. In addition, because contrarians have no strategy tables, their behavior is set to be the same as that already adopted in the experiment.

6.4 Simulation Results

For computer simulations, we use 100 normal agents and set $S = 8$ and $P = 64$. The result of $\langle N_1 \rangle / \langle N_2 \rangle$ versus M_1/M_2 is shown in Fig. 6.1a. Clearly, qualitative agreement between experiments and simulations is displayed. In order to confirm this result, we conduct more simulations with different number of normal agents to compare with experimental results, which is shown in Fig. 6.1b. We choose to use 83 and 88 normal agents which is consistent with experiments, and 1,000 normal agents which represents the case of a remarkably different size. Comparing the different simulations in Fig. 6.1a, b, their results show no qualitative differences though the number of normal agents varies. Therefore, we can say that the number of agents has no influence on our simulation results. This means that the experimental results reported in Fig. 6.1 are general (at least to some extent), being beyond the above-mentioned experimental limitations. Thus, we are confident to carry out more simulations in the following. For convenience, we use 100 normal agents in the remainder of this chapter.

In order to compare with the experiment, the preferences of 100 normal agents are also calculated; see Fig. 6.4. The simulation results are similar to the experimental results in Fig. 6.2. That is, normal agents also show the heterogeneity of preferences and the environmental adaptability.

Then we are in a position to scrutinize the role of contrarians. To compare with the experimental results in Fig. 6.3, we also calculate stability f, efficiency (e) and predictability (w_1); see Fig. 6.5.

From Fig. 6.5, we find that the resource-allocation system clearly exhibits a transition point when taking M_1/M_2 and w_1 as the tuning parameter and order parameter, respectively. This echoes what we have reported in [8]. In the mean time, at the transition point, $(M_1/M_2)_t$, f reaches the lowest value which means the system becomes the most stable. In detail, for a small β_c, increasing M_1/M_2 will increase the system stability until f has the minimum value at $(M_1/M_2)_t$, which corresponds to the most stable state of the system. Once the minimum value is passed, the stability of the system will worsen for larger M_1/M_2. The former (or the latter) is the positive (or negative) role of contrarians. As for large β_c, increasing M_1/M_2 will always make the system more unstable (negative role). Besides, as β_c increases, $(M_1/M_2)_t$ moves toward the direction of decreasing M_1/M_2. We discuss the movement of $(M_1/M_2)_t$ in the following theoretical analysis.

Figure 6.5b shows the simulation results for the change in system efficiency, e. When M_1/M_2 is small, increasing contrarians can make the system more efficient at a certain range. In contrast, for large M_1/M_2, adding contrarians always reduces the efficiency. Such simulation results echo the experimental results shown in Fig. 6.3b.

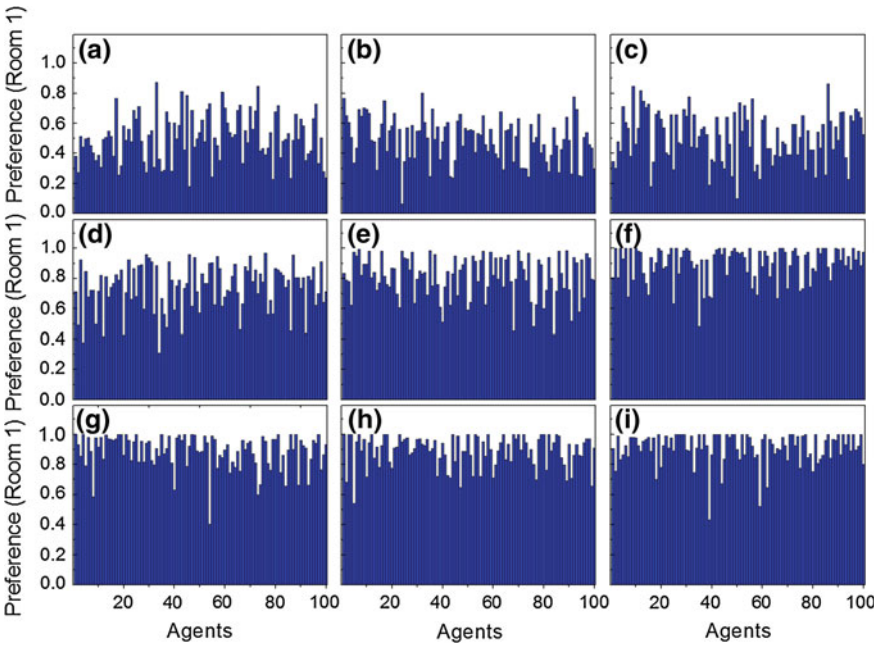

Fig. 6.4 Simulation data of the preference of each normal agent to Room 1 for the nine parameter sets with $M_1/M_2 = 1$(**a**–**c**), 3(**d**–**e**), and 10(**f**–**i**) and $\beta_c = 0$(**a**, **d**, **g**), 0.1(**b**, **e**, **h**), and 0.3(**c**, **f**, **i**). For each parameter set, simulations are run for 400 time steps (the last 200 time steps for statistics and the first 200 time steps for equilibration). In the figure, "Mean" denotes the average preference of the 100 normal agents. Adapted from Ref. [9]

Figure 6.5c displays the predictability of Room 1. Similarly, we can see from Fig. 6.5c that when M_1/M_2 is very small (close to 1), the winning rate of two rooms remains almost unchanged at 0.5 or so, even though β_c varies. That is, in this case, the system is unpredictable. When M_1/M_2 is gradually increasing, adding more contrarians will cause w_1 to increase from the value for $\beta_c = 0$; namely it becomes more easy for agents to predict the winning room. Again, these simulation results agree with the experimental results in Fig. 6.3c.

Now, we understand the role of contrarians in the resource-allocation system. On one hand, contrarians have positive roles as M_1/M_2 is small. Namely, adding contrarians help to not only improve the system stability, but also increase the system efficiency while keeping the system unpredictable. On the other hand, contrarians have negative roles as M_1/M_2 becomes large enough. That is, adding contrarians can hurt the system stability and efficiency while making the system more predictable. Both positive and negative roles have been well distinguished by identifying a transition point, $(M_1/M_2)_t$. Further, it is clear that the transition points identified herein also help to reveal that the allocation of resources can be optimal (i.e., stable, efficient, and unpredictable) at $(M_1/M_2)_t$ by adding an appropriate size of contrarians.

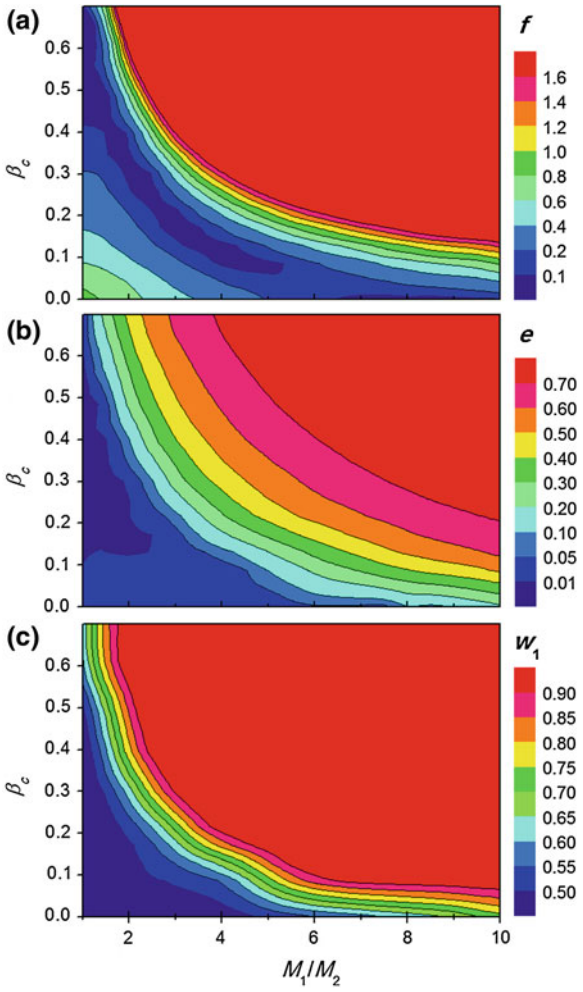

Fig. 6.5 $\beta_c - M_1/M_2$ contour plots for **a** stability f , **b** efficiency e, and **c** predictability w_1. For each parameter set, simulations are run for 400 time steps (the last 200 time steps for statistics and the first 200 time steps for equilibration). Adapted from Ref. [9]

6.5 Theoretical Analysis

In order to get a better understanding of the underlying mechanics of the Agent-Based model, we conduct theoretical analysis. When S and P are fixed, the system of our interest could reach the most stable state only at the transition point, i.e., a particular ratio between the two resources, $\left(\frac{M_1}{M_2}\right)_t$. If we adjust the values of β_c, the transition point, $\left(\frac{M_1}{M_2}\right)_t$, will change accordingly.

6.5.1 The properties of the transition point, $\left(\frac{M_1}{M_2}\right)_t$

6.5.1.1 Without contrarians

It can be proved that for the Agent-Based model, the transition point has two properties: (1) every normal agent uses the strategy with the largest preference, $(L_i)_{\max}$, in his/her hand; (2) the system is in the balance state, which means the ratio between the numbers of agents in the two rooms is equal to the ratio between the two resources [7]. We first define

$$N_1 = \sum x_i \ ,$$

where the choice of agent i is denoted as $x_i = 1$ (Room 1) or 0 (Room 2). Then, at the transition point, the expected ratio of normal agents who choose to enter Room 1 is

$$\frac{\langle N_1 \rangle}{N_n} = \frac{\sum \langle x_i \rangle}{N_n} = \frac{\sum_i^{N_n} (L_i)_{\max}}{P N_n} = \left(\frac{M_1}{M_1 + M_2}\right)_t , \tag{6.1}$$

where $\langle \cdots \rangle$ denotes the averaged value of $\cdots$. Equation (6.1) shows that when $\frac{M_1}{M_1+M_2} > \left(\frac{M_1}{M_1+M_2}\right)_t$, Room 1 will become unsaturated. This means the system does not stay at the balance state.

6.5.1.2 With contrarians

From the properties of the transition point and the behavior of the contrarians, it can be shown that, all the normal agents still use the largest-preference strategy $(L_i)_{\max}$ at the transition point when contrarians are added. Every contrarian follows the minority in his/her group to make a choice denoted as x_c. Then the expected ratio of agents (both normal agents and contrarians) who choose to enter Room 1 at the transition point becomes

$$\frac{\langle N_1 \rangle}{N} = \frac{\sum_i^{N_n} (L_i)_{\max} + P \sum_c^{N_c} \langle x_c \rangle}{(1 + \beta_c) P N_n} = \left(\frac{M_1}{M_1 + M_2}\right)_{t'} , \tag{6.2}$$

where $\beta_c = \frac{N_c}{N_n}$ and $\left(\frac{M_1}{M_1+M_2}\right)_{t'}$ stands for the new transition point with contrarians added.

6.5.2 Finding the expressions of $\sum_i^{N_n}(L_i)_{\max}$ and $\sum_c^{N_c}\langle x_c\rangle$

6.5.2.1 Without contrarians

The probability that L_i takes a certain integer from the range 0 to P is $\frac{1}{P+1}$. Then, the probability of $(L_i)_{\max}$ being a certain value of L is

$$p(L) = \left(\frac{L+1}{P+1}\right)^S - \left(\frac{L}{P+1}\right)^S.$$

If N_n is large enough, there is

$$\sum_i^{N_n}(L_i)_{\max} = \sum_{L=0}^{P} N_n p(L) L = P N_n \left[1 - \frac{1}{P}\sum_{L=1}^{P}(\frac{L}{P+1})^S\right], \tag{6.3}$$

In the absence of contrarians, the substitution of Eq. (6.3) into Eq. (6.1) leads to

$$\frac{\langle N_1\rangle}{N_n} = 1 - \frac{1}{P}\sum_{L=1}^{P}\left(\frac{L}{P+1}\right)^S = \left(\frac{M_1}{M_1+M_2}\right)_t \equiv m_n, \tag{6.4}$$

where m_n represents the transition point for the system with only normal agents.

6.5.2.2 With contrarians

Since normal agents still use their strategy with $(L_i)_{\max}$ at the transition point after adding contrarians into the resource-allocation system, therefore, for them we have

$$\frac{\langle N_{n1}\rangle}{N_n} = 1 - \frac{1}{P}\sum_{L=1}^{P}\left(\frac{L}{P+1}\right)^S = \left(\frac{M_1}{M_1+M_2}\right)_t \equiv m_n.$$

When contrarian c chooses k normal agents as his/her group, the probability to get a normal agent who chooses Room 1 can be expressed approximately as $\frac{\langle N_{n1}\rangle}{N_n} = \left(\frac{M_1}{M_1+M_2}\right)_t \equiv m_n$. Then, the probability for $x_c = 1$ (or 0) is

$$\sum_{q=0}^{y} C_k^q \left[\left(\frac{M_1}{M_1+M_2}\right)_t\right]^q \left[\left(\frac{M_2}{M_1+M_2}\right)_t\right]^{k-q} \equiv m_c \ \ (\text{or}\ \ 1-m_c),$$

where $\left(\frac{M_2}{M_1+M_2}\right)_t = 1 - m_n$, $y = \frac{k-1}{2}$, and k is odd. Thus, we have the average of x_c, $\langle x_c\rangle$, as

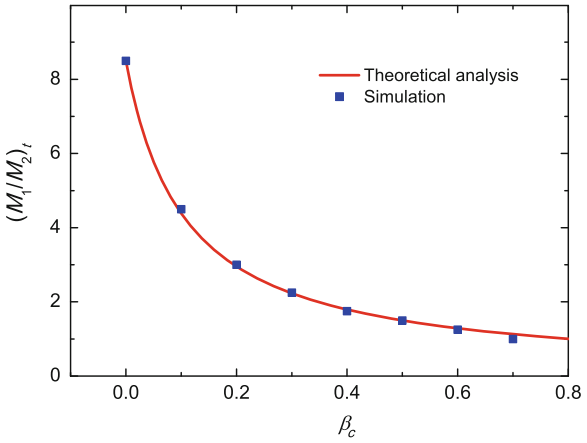

Fig. 6.6 Transition point $(M_1/M_2)_t$ versus β_c , as a result of theoretical analysis (curve obtained according to Eq. (6.6)) and simulation (data extracted from Fig. 6.5a). Parameters: $S = 8$ and $P = 64$. Adapted from Ref. [9]

$$\langle x_c \rangle = m_c = \sum_{q=0}^{y} C_k^q (m_n)^q (1 - m_n)^{k-q}. \tag{6.5}$$

Plugging Eq. (6.5) into Eq. (6.2) yields

$$\frac{\langle N_1 \rangle}{N} = \frac{PN_n m_n + PN_c m_c}{(1 + \beta_c) PN_n} = \left(\frac{M_1}{M_1 + M_2} \right)_{t'},$$

and then we have

$$\frac{\langle N_1 \rangle}{N} = \frac{m_n + \beta_c m_c}{1 + \beta_c} = \left(\frac{M_1}{M_1 + M_2} \right)_{t'}. \tag{6.6}$$

Clearly, by adjusting β_c, we can change the transition point of the resource-allocation system. Figure 6.6 shows the monotonically decreasing trend of $\left(\frac{M_1}{M_2} \right)_t$ for increasing β_c, which displays an excellent agreement between theoretical and simulation results.

In both experiments and computer simulations, we have found that when the system is in the balance state $[M_1/M_2 < (M_1/M_2)_t]$, the fluctuations in the system decrease after introducing a small number of contrarians. Because in both experiments and simulations the behavior of contrarians is set to follow the same rule, it is necessary to further analyze the influence of this behavior on the stability of the whole system. Equation (6.5) describes the probability of contrarians choosing to enter Room 1 when the system reaches balance. It is known that at this balance state, the number of subjects in the experiments (or normal agents in the simulations) choosing to enter each room still varies at every time step due to fluctuations. Hence we replace m_n in Eq. (6.5) with N_{n1}/N_n and get $\langle x_c \rangle = \sum_{q=0}^{y} C_k^q (N_{n1}/N_n)^q (1 - N_{n1}/N_n)^{k-q}$,

where N_{n1} is the number of subjects or normal agents who choose to enter Room 1, and the average of x_c, $\langle x_c \rangle$, represents the expected probability of contrarians choosing Room 1. Note that $\langle x_c \rangle$ is a random variable due to the fluctuations of N_{n1}. Then, according to Eq. (6.6), we obtain

$$\frac{N_1}{N} = \frac{N_{n1}/N_n + \beta_c \langle x_c \rangle}{1 + \beta_c}. \tag{6.7}$$

By drawing N_1/N versus N_{n1}/N_n, we achieve Fig. 6.7, which shows the influence of the deviations of N_{n1}/N_n on N_1/N under different values of β_c. For $M_1/M_2 = 1$, it is shown that the balance point of the system lies on A_0 (0.5,0.5) when $\beta_c = 0$, 0.1, 0.3, and 0.5. And the deviations of N_{n1}/N_n can cause the system to vibrate around A_0 along a certain line in Fig. 6.7 which is determined by β_c. Then, Fig. 6.7 shows that, under the same range of deviations of N_{n1}/N_n, by increasing β_c, we can bring down the vibration of N_1/N around $N_1/N = 0.5$. In addition, we can see from Fig. 6.7 that, when β_c becomes too large, such as $\beta_c = 1$ or 2, A_0 is no longer a stable point. The state of the system tends to move to the right end of the associated line because now more subjects or normal agents choosing to enter Room 1 will make Room 1 easier to win. That is, when β_c is too large, adding more contrarians will lead the system to a more unstable state. For a biased distribution of resources, say, $M_1/M_2 = 3$, Fig. 6.7 shows that the balance point of the system lies on different points for different values of β_c, i. e., B_0 (0.75, 0.75), B_1 (0.82, 0.75), and B_2 (0.97, 0.75) for β_c =0, 0.1, and 0.3. It can be shown that adding a small number of contrarians makes the system with a biased distribution of resources more stable due to the following two reasons: (1) under the same deviations of N_{n1}/N_n, the vibration of N_1/N (say, around B_0, B_1, or B_2 for $M_1/M_2 = 3$) decreases slightly when adding more contrarians; (2) when adding more contrarians, the values of N_{n1}/N_n at the balance points (e. g., B_0, B_1, and B_2 for $M_1/M_2 = 3$) increase; in this case, subjects or normal agents will be more certain to choose Room 1, which reduces the deviation range of N_{n1}/N_n, thus decreasing the vibration of N_1/N.

6.6 Conclusions

In summary, using the three tools, we have investigated the role of contrarian behavior in a resource-allocation system. In contrast to the common belief that contrarian behavior always plays a positive role in resource allocation (say, stabilizes resource allocation by shrinking the redundancy or the lack of resources), the transition points have helped us to reveal that the role of contrarian behavior in resource-allocation systems can be either positive (to stabilize the system, to improve the system efficiency, and to make the system unpredictable) or negative (to unstabilize the system, to reduce the system efficiency, and to make the system predictable) under different conditions. Further, the transition points identified herein have also helped us to

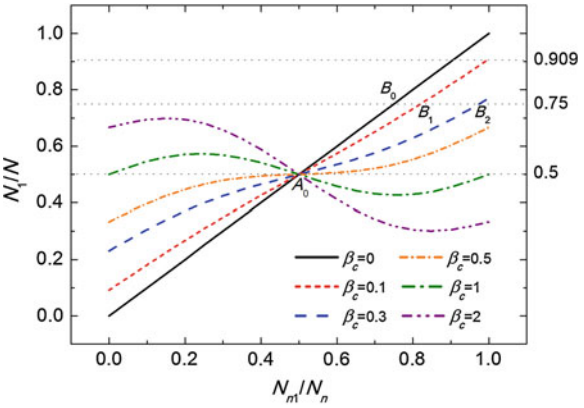

Fig. 6.7 N_1/N versus N_{n1}/N_n according to Eq. (6.7). The three horizontal gray dot lines are given by $N_1/N = 0.5$, 0.75, and 0.909, which are respectively related to the balance state of three resource ratios, $M_1/M_2 = 1$, 3, and 10. Adapted from Ref. [9]

Fig. 6.8 The control panel for the organizer to adjust parameters. Adapted from Ref. [9]

show that resource allocation can be optimized by including an appropriate size of contrarians.

This chapter is also expected to be of value to some other fields. In management and social science, administrators should not only conduct contrarianism when finding the formation of herd, but also need to consider system environment and timing to see whether contrarianism is globally positive or negative. In ecology and evolution, it is not only necessary to study the mechanism of contrarian formation, but also to pay more attention to the effect of contrarianism on the whole ecological system and evolution groups.

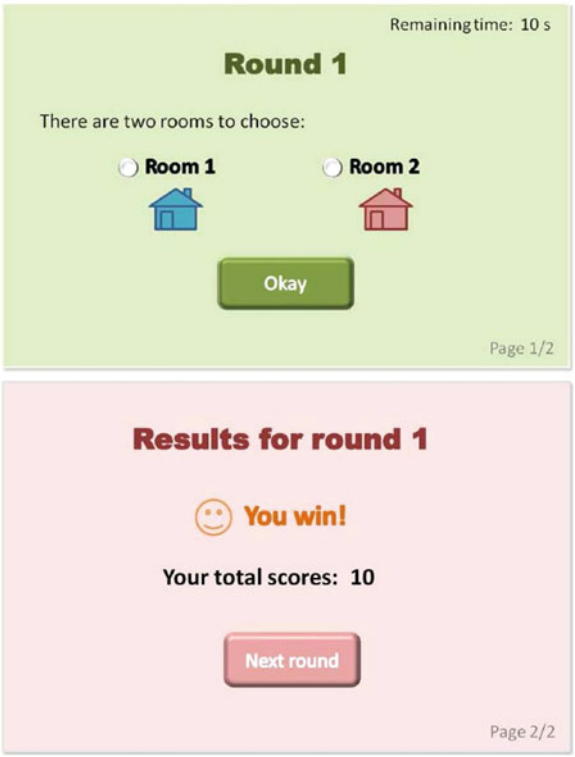

Fig. 6.9 The two panels for subjects in the experiments. Adapted from Ref. [9]

6.7 Supplementary Materials

6.7.1 About the Experiment

The existence of contrarians is not informed to the subjects in the experiment. The contrarians generated by the computer program play the online game together with the subjects. The parameters, M_1/M_2 and β_c, are controlled by the organizer via the control panel (Fig. 6.8) and every parameter set (i.e., each pair of M_1/M_2 and β_c) lasts for 30 rounds. The values of the parameter set are not informed to the subjects either. The organizer only lets every subject know whether he/she wins or loses after each experimental round (Fig. 6.9). Details can be found in the following leaflet which was explained to the subjects who participated in the computer-aided online human experiment.

6.7.2 Leaflet to the Experiment

Thank you for participating in this experiment! Please read the instructions of the experiment carefully before starting to play. If you have any questions, please feel free to ask. No communication is allowed once the experiment starts.

Everyone will be allocated with an anonymous account in the experiment. You will use the account throughout the experiment. After logging in, you will see page 1/2 (in Fig. 6.9) with two options: Room 1 and Room 2. Each room will own an amount of resources, labeled as M_1 and M_2. You can choose to enter either Room 1 or Room 2, and then click "Okay" and wait. The page will automatically turn to page 2/2 after all the subjects have finished. The result of this round and the current score will be shown in page 2/2. You will have 15 seconds to check the results. After that, the page will automatically change to page 1/2 again and the next round starts.

The total number of subjects entering Room 1 is N_1, and N_2 for Room 2. After all subjects finish, the computer program will choose the winners according to the resource per capita determined by $\frac{M_1}{N_1} > \frac{M_2}{N_2}$ or $\frac{M_1}{N_1} < \frac{M_2}{N_2}$.

If $\frac{M_1}{N_1} > \frac{M_2}{N_2}$, those who choose Room 1 win.

if $\frac{M_1}{N_1} < \frac{M_2}{N_2}$, those who choose Room 2 win.

Example:

Suppose the resources in Room 1 and Room 2 are both 100 units. If 30 subjects choose to enter Room 1 and 70 subjects choose to enter Room 2, each subject in Room 1 will have more resources per capital, and he/she wins. Suppose the resources in Room 1 and Room 2 are 100 units and 200 units, respectively. If 50 subjects choose to enter Room 1 and 50 subjects choose to enter Room 2, then each subject in Room 2 will have more resources per capital, and he/she wins.

Notice:

The resources in Room 1 and Room 2 (M_1 and M_2) and the number of subjects entering Room 1 and Room 2 (N_1 and N_2) will not be announced. You cannot see the other subjects' options. Only your results will be shown on your computer screen after every round. You ca use this information to decide which room to enter in the next round. Every account's original score is set to zero. 10 scores will be added in every round if you win and zero added if you lose. We will pay you cash with the exchange rate, 10 scores = 1 Chinese Yuan, after the experiment finishes. Besides, we pay every subject 30 Chinese Yuan as attendance fee, and reward the top 10 subjects (with the highest scores after all the experiment is completed), each with extra 100 Chinese Yuan.

Chapter 7
Hedge Behavior: Statistical Equivalence of Different Systems

Abstract In Chaps. 5 and 6, we have identified a class of phase transitions in the market-directed resource-allocation game, and found that there exists a critical point at which the phase transitions occur. The critical point is given by a certain resource ratio. Here, by performing computer simulations and theoretical analysis, we report that the critical point is robust against various kinds of human hedge behavior where the numbers of herds and contrarians can be varied widely. This means that the critical point can be independent of the total number of participants composed of normal agents, herds, and contrarians, under some conditions. This finding means that the critical points we identified in this complex adaptive system (with adaptive agents) is also an intensive quantity, similar to those revealed in traditional physical systems (with non-adaptive units).

Keywords Resource-allocation system · Hedge behavior · Critical point · Phase transition · Fluctuation

7.1 Opening Remarks

After introducing both Chaps. 5 and 6, one may ask: what if the system has both herd behavior and contrarian behavior? The combination of both of them is just hedge behavior, which is to be discussed in this chapter.

In Chaps. 5 and 6, we have identified a class of phase transitions in the market-directed resource-allocation game (MDRAG), and found that there exists a critical point at which the phase transitions occur. The critical point, which is given by a certain resource ratio, corresponds to the most stable state (with the minimum fluctuation) where the resources are the most effectively allocated and the total utilities of the system are maximal [7]. By previous researches, we have known that herd behavior or contrarian behavior always changes the location of the critical point.

Hedge behavior is also a kind of self-organization in complex adaptive systems (CASs). Here, we introduce hedge behavior into the MDRAG to analyze the effects

J.-P. Huang, *Experimental Econophysics*, New Economic Windows,
DOI 10.1007/978-3-662-44234-0_7

of hedge behavior on the whole system's fluctuations. By performing controlled experiments, agent-based simulations, and theoretical analysis, we report that the critical point can be robust against various kinds of human hedge behavior where the number of herds and contrarians is varied widely. The critical point also helps to reveal the robustness of the most stable state (corresponding to the minimal fluctuation) of the CAS when hedge behavior exists or disappears. This finding means that the critical points we identified in this CAS with adaptive agents may also be an intensive quantity, similar to those revealed in traditional physical systems with nonadaptive units. In other words, two systems with different numbers of agents may have the same critical point; this is what I mean "statistical equivalence of different systems" in the title of this chapter.

7.2 Controlled Experiments

Our experiment includes three types of participants, namely subjects, imitators, and contrarians. Subjects consist of students and teachers recruited from various departments of Fudan University, and they would independently make decisions to mimic the normal behavior of free competitions. An imitator (or contrarian) would make decisions by following the majority (or minority) of a reference group made of subjects, so as to model the herd (or contrarian) behavior. In our experiment, all the imitators and contrarians were robots generated by computer program because their strategies for making decisions were simple. The 68 subjects were requested to participate in the whole experiment (Systems A–D). The participants' structures of the four resource-allocation systems are given as follows:

- System A: 68 subjects;
- System B: 68 subjects + 55 imitators;
- System C: 68 subjects + 11 contrarians;
- System D: 68 subjects + 55 imitators + 11 contrarians.

Clearly, System D focuses on a kind of hedge behavior.

The human experiment was conducted in the computer laboratory of Fudan University. Before the experiment started, we gave leaflets (as shown in Supplementary Materials at the end of this chapter) to the subjects that interpreted how the experiment would be conducted. The experiment contains an online game that has two rooms, Room 1 and Room 2, denoted by two buttons in the working panel on each subject's computer screen. Each room owns an amount of virtual money marked as M_1 or M_2. Each subject could play the game with all the other subjects through the working panel, which shows not only the above-mentioned two buttons, but also the cumulative score the subject had obtained. No communication among subjects was allowed once the experiment started. Subjects were only told their own results by the working panel after each round, and they made decisions on choosing to enter which room for the next round according to their own results. It is worth noting that during the experiment, no information on imitators and/or contrarians was announced to the

subjects. Also, the subjects do not know the exact amount or ratio of resources (M_1 or M_2) in the two rooms in any round of the experiment. Human subjects choose to enter Room 1 or 2 independently in every round. In System A, after one round of the option, we remark the total number of the subjects in Room 1 and Room 2 as N_1 and N_2. If $M_1/N_1 > M_2/N_2$, then subjects in Room 1 win, and vice versa.

In System B, we secretly add imitators which subjects do not know. Imitators will follow human subjects' option to enter one of the two rooms. In every round, each imitator will randomly choose a reference group (five subjects) from the 68 subjects. Then, it will choose to enter the room which the majority of the five subjects in its group choose to enter. If most of the subjects in its group choose to enter Room 1, then it will choose to enter Room 1, and vice versa. After one round of the option, we remark the total number of the participants including subjects and imitators in Room 1 and Room 2 as N_1 and N_2. If $M_1/N_1 > M_2/N_2$, then the subjects (and imitators) in Room 1 win, and vice versa.

In System C, we secretly add contrarians. The behavior of contrarians is contrary to that of imitators. Namely, a contrarian chooses to enter the room which the minority of the five subjects in its group choose to enter. That is, if most of the human subjects in its group choose to enter Room 1, then it will choose to enter Room 2, and vice versa. After one round of the option, we remark the total number of the participants including subjects and contrarians in Room 1 and Room 2 as N_1 and N_2. If $M_1/N_1 > M_2/N_2$, then subjects (and contrarians) in Room 1 win, and vice versa.

In System D, imitators and contrarians are both secretly added. We remark the total number of the participants including subjects, imitators, and contrarians in Room 1 and Room 2 as N_1 and N_2. If $M_1/N_1 > M_2/N_2$, then human subjects (together with imitators and contrarians) in Room 1 win, and vice versa.

Total 30 rounds of experiment will be repeated for each of the four systems. In each round of the experiment, winners will be granted scores, and the final reward will be paid to each subject according to the scores they get in the experiment. Details can be found in the Leaflet shown in Supplementary Materials.

Throughout this chapter, for each system, the data of the first round is used for equilibration, and only the remaining 29 rounds are adopted for analysis (see Table 7.1).

To proceed, let us recall the number of human subjects as N_n, number of imitators as N_h, and number of contrarians as N_c. Also, we define $\beta_1 = N_h/N_n$ and $\beta_2 = N_c/N_n$. The total number of all the participants is $N = N_n + N_h + N_c = N_1 + N_2$. We conducted the experiment under two resource ratios: $M_1/M_2 = 1$ and $M_1/M_2 = 3$. The former (or the latter) corresponds to an unbiased (or a biased) distribution of resources. The most important parameter of the system is N_i ($i = 1$ or 2) because all the macroscopic properties of this system can only be analyzed on the basis of this parameter. Because N_i is directly proportional to the total number of participants in the system, it is naturally an extensive quantity. We are now in a position to investigate the fluctuations of N_i.

In statistical physics, a macroscopic quantity describing a system is the average of the relevant microscopic quantity, A, over all possible microstates, $\langle A \rangle$, under given macroscopic conditions. Namely, this average $\langle A \rangle$ is given by

Table 7.1 N_1 and N_2 from the 2nd to 30th experimental round under $M_1/M_2 = 1$ and 3 for Systems A, B, C and D

Round	$M_1/M_2 = 1$								$M_1/M_2 = 3$							
	A		B		C		D		A		B		C		D	
	N_1	N_2	N_1	N_2	N_1	N_2	N_1	N_2	N_1	N_2	N_1	N_2	N_1	N_2	N_1	N_2
2	42	26	71	52	36	43	69	65	32	36	80	43	52	27	105	29
3	33	35	73	50	38	41	61	73	38	30	87	36	57	22	92	42
4	36	32	41	82	39	40	63	71	44	24	101	22	51	28	73	61
5	39	29	66	57	45	34	71	63	42	26	92	31	49	30	92	42
6	37	31	70	53	35	44	78	56	48	20	89	34	50	29	104	30
7	33	35	51	72	43	36	56	78	47	21	87	36	58	21	95	39
8	38	30	45	78	38	41	80	54	52	16	95	28	57	22	107	27
9	33	35	55	68	42	37	78	56	43	25	97	26	59	20	107	27
10	20	48	60	63	49	30	48	86	49	19	98	25	59	20	96	38
11	30	38	65	58	46	33	64	70	52	16	94	29	65	14	96	38
12	30	38	60	63	39	40	72	62	50	18	66	57	47	32	97	37
13	38	30	72	51	40	39	73	61	57	11	105	18	58	21	89	45
14	27	41	79	44	37	42	81	53	55	13	77	46	60	19	90	44
15	35	33	62	61	41	38	83	51	41	27	92	31	57	22	103	31
16	37	31	48	75	41	38	66	68	49	19	101	22	55	24	97	37
17	29	39	50	73	33	46	77	57	52	16	76	47	57	22	103	31
18	36	32	63	60	40	39	38	96	48	20	97	26	60	19	98	36
19	43	25	44	79	38	41	58	76	46	22	82	41	65	14	111	23
20	41	27	69	54	40	39	68	66	50	18	74	49	52	27	106	28
21	37	31	56	67	42	37	49	85	55	13	91	32	59	20	87	47
22	28	40	57	66	39	40	57	77	56	12	86	37	62	17	101	33
23	38	30	59	64	44	35	61	73	54	14	76	47	54	25	98	36
24	23	45	72	51	36	43	78	56	45	23	86	37	57	22	104	30
25	21	47	59	64	38	41	80	54	55	13	97	26	57	22	98	36
26	39	29	58	65	43	36	70	64	43	25	78	45	56	23	97	37
27	23	45	84	39	37	42	61	73	48	20	109	14	58	21	107	27
28	28	40	72	51	42	37	74	60	53	15	99	24	62	17	114	20
29	33	35	80	43	42	37	63	71	43	25	90	33	56	23	88	46
30	41	27	67	56	41	38	69	65	56	12	102	21	56	23	89	45

$$\langle A \rangle = \sum_s \rho_s A_s, \tag{7.1}$$

where ρ_s is the probability when the system lies in the s-th microstate, and A_s is the value of A at the s-th microstate. Then, the fluctuation, σ_0^2, of A is defined as

$$\sigma_0^2 = \langle (A_s - \langle A \rangle)^2 \rangle = \sum_s \rho_s (A_s - \langle A \rangle)^2. \tag{7.2}$$

Thus, to proceed, we define the fluctuation, σ^2, of N_i according to Eq. (7.2) as

$$\sigma^2 = \langle \left(N_1 - \tilde{N}_1 \right)^2 \rangle = \langle \left(N_2 - \tilde{N}_2 \right)^2 \rangle \equiv \frac{1}{2} \sum_{i=1}^{2} \langle \left(N_i - \tilde{N}_i \right)^2 \rangle, \tag{7.3}$$

where $\langle \cdots \rangle$ denotes the average of $\cdots$ over the 29 rounds of experiment. The second "=" in Eq. (7.3) holds due to the feature of the resource-allocation system. According to Eq. (7.3), we obtain the fluctuation per participant, $\frac{\sigma^2}{N}$, as

$$\frac{\sigma^2}{N} = \frac{1}{2N} \sum_{i=1}^{2} \langle \left(N_i - \tilde{N}_i \right)^2 \rangle. \tag{7.4}$$

Regarding $\tilde{N}_i$ in Eqs. (7.3) and (7.4), according to Eq. (7.1), it should be the average of N_i over the 29 rounds, namely $\tilde{N}_i = \langle N_i \rangle$. The calculated values of $\frac{\sigma^2}{N}$'s for the four systems are displayed in Fig. 7.1. Let us start by discussing System A that contains only 68 subjects ($\beta_1 = \beta_2 = 0$). As a result of free competitions for either $M_1/M_2 = 1$ or $M_1/M_2 = 3$, the nonzero fluctuations come to appear in System A, which is consistent with our intuition. Adding imitators causes a higher degree of fluctuations; see System B. Inversely, adding contrarians yields a lower degree of fluctuations; see System C. Interestingly, adding both imitators and contrarians always yields a value of $\frac{\sigma^2}{N}$ between those of System B and System C; see System D. Therefore, it can be concluded that there exists an appropriate ratio between the amounts of imitators and contrarians, which will cause the value of $\frac{\sigma^2}{N}$ for System D to equal that of System A. That is, $\frac{\sigma^2}{N}$ could be a nonzero constant for both System A and System D. On the other hand, it is worth noting that System D has not only subjects, but also imitators and contrarians. However, System A has subjects only. In other words, the number of participants, N, in System D is distinctly different from that in System A. Owing to such arguments, we can conclude that the fluctuations of the system with collective behaviors (say, System D in this chapter) can, in principle, be equal to that one without collective behaviors (say, System A in this chapter) as long as the amounts of imitators and contrarians are appropriately introduced. This conclusion implies a way to stabilize the resource-allocation system by adding imitators and contrarians appropriately.

Figure 7.1 shows the results of $\frac{\sigma^2}{N}$ where $\tilde{N}_i = \langle N_i \rangle$ due to Eq. (7.1). To take into account the feature of the present system, we are allowed to define $\tilde{N}_i$ in a different way. Based on our previous study [7, 8], the resource-allocation system could eventually achieve the balance state where

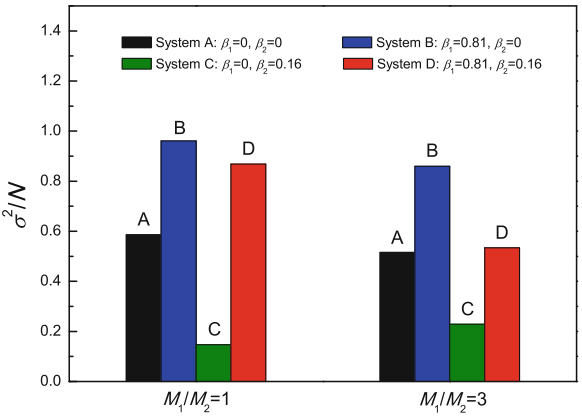

Fig. 7.1 $\frac{\sigma^2}{N}$ of Systems A, B, C, and D for $M_1/M_2 = 1$ and 3. $\tilde{N}_i$ was determined by Eq. (7.1). The experiment for each system lasts 30 rounds (the 2nd–30th rounds are used for statistics)

Table 7.2 $\langle N_1 \rangle$, $\langle N_2 \rangle$, and $\langle N_1 \rangle / \langle N_2 \rangle$ obtained under $M_1/M_2 = 1$ and $M_1/M_2 = 3$ for Systems A, B, C and D

System	Participant	M_1/M_2	$\langle N_1 \rangle$	$\langle N_2 \rangle$	$\langle N_1 \rangle / \langle N_2 \rangle$
A	$\beta_1 = 0, \beta_2 = 0$	1	33.38	34.62	0.964
B	$\beta_1 = 0.81, \beta_2 = 0$	1	62.35	60.65	1.028
C	$\beta_1 = 0, \beta_2 = 0.16$	1	40.14	38.86	1.033
D	$\beta_1 = 0.81, \beta_2 = 0.16$	1	67.1	66.9	1.003
A	$\beta_1 = 0, \beta_2 = 0$	3	48.38	19.62	2.466
B	$\beta_1 = 0.81, \beta_2 = 0$	3	89.79	33.21	2.704
C	$\beta_1 = 0, \beta_2 = 0.16$	3	56.72	22.28	2.546
D	$\beta_1 = 0.81, \beta_2 = 0.16$	3	98.07	35.93	2.729

The experiment for each system lasts 30 rounds (the 1st round is for equilibration, and the remaining 29 rounds are for statistics)

$$\frac{\langle N_1 \rangle}{\langle N_2 \rangle} = \frac{M_1}{M_2} \tag{7.5}$$

as long as the numbers of both rounds and participants are large enough. The balance state corresponds to the system where macroscopic arbitrage opportunities have been exhausted (or, the efficiency of resource allocation reaches the maximum) [7, 8]. For the present four systems, Table 7.2 displays the values of $\langle N_1 \rangle$, $\langle N_2 \rangle$, and $\langle N_1 \rangle / \langle N_2 \rangle$, and it clearly shows that Eq. (7.5) approximately holds in spite of the finite numbers of both rounds and participants. That is, the present four systems with various kinds of human behaviors have also a high efficiency of resource allocation. Thus, owing to Eq. (7.5), we may redefine $\tilde{N}_i$ as

$$\tilde{N}_i = \frac{M_i}{M_1 + M_2} N. \tag{7.6}$$

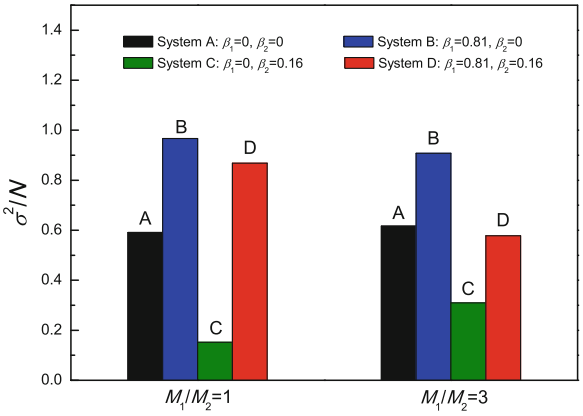

Fig. 7.2 Same as Fig. 7.1, but $\tilde{N}_i$ was determined by Eq. (7.6) instead

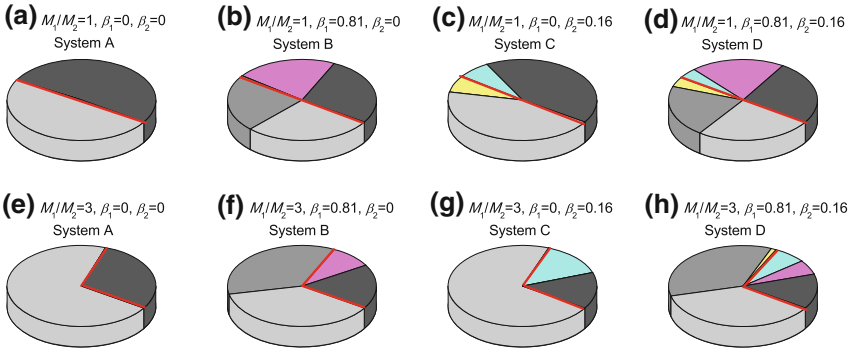

Preference	(a)	(b)	(c)	(d)	(e)	(f)	(g)	(h)
Subject: Room 1	49%	28%	44%	25.6%	71.1%	37.6%	71.6%	36.9%
Subject: Room 2	51%	27%	42.1%	25.2%	28.9%	17.7%	14.5%	13.9%
Imitator: Room 1	-	23%	-	20.6%	-	35.4%	-	35.3%
Imitator: Room 2	-	22%	-	20.4%	-	9.3%	-	5.8%
Contrarian: Room 1	-	-	6.8%	3.9%	-	-	0.2%	1.1%
Contrarian: Room 2	-	-	7.1%	4.3%	-	-	13.7%	7.2%

Fig. 7.3 The average preference of all kinds of participants for Systems **A**–**D** under two resource ratios: **a**–**d** $M_1/M_2 = 1$ and **e**–**h** $M_1/M_2 = 3$. The *red line* on each pie chart is used to divide the preference to Room 1 and Room 2. The experiment for each system lasts for 30 rounds (the 2nd–30th rounds are used for statistics)

The relevant result is shown in Fig. 7.2, which qualitatively agrees with Fig. 7.1. That is, adopting a different definition for $\tilde{N}_i$ (Eq. 7.6) does not affect the conclusions obtained from Fig. 7.1.

Figures 7.1 and 7.2 clearly show the possible equivalence of two different kinds of systems; that is, the different systems can, in principle, evolve with the same fluctua-

tion. Now, we are in a position to recover the underlying mechanism. This requires us to further observe the detailed participants' choice behaviors. One good way could be to analyze their preferences of choices in each experiment. As we all know, different individuals have different preferences on resources, which is reflected by the heterogeneity of preferences. This heterogeneity can have remarkable influence on achieving the balance of the system [7]. Here, the preference of each participant is defined as the average rate of entering into Room 1 or Room 2 in the 29 rounds of experiments. Figure 7.3 shows the statistical results of all the participants in the four systems under two resource ratios: $M_1/M_2 = 1$ and $M_1/M_2 = 3$. We note that in System A, the average preference of all human subjects varies with M_1/M_2, which can be clearly seen in Fig. 7.3a and e. In Systems B or C, the secret join of imitators or contrarians makes human subjects adjust their preferences. In System D, human subjects' preferences adjust accordingly under the combined actions of secretly added imitators and contrarians. Thus, we conclude that the equivalence mentioned above originates from the spontaneous changes in preferences of human subjects in different systems, which arises from human adaptability due to learning ability. In other words, this equivalence becomes true due to the spontaneous cooperation of imitators and contrarians arising from self-adaptive preference adjustment of subjects.

7.3 Agent-Based Simulations

The above experimental findings encourage us to do more researches, in order to generally reveal the influence of system's fluctuations caused by hedge behavior. So, we structured an agent-based model and carried out a series of computer simulations based on the MDRAG which is an extended version of the minority game [1]. This MDRAG can be described as followed. There will be two rooms: Room 1 and Room 2, each of which owns its resource marked as M_1 and M_2. Here, $M_1 \geqslant M_2$. Some agents see the two rooms, but do not know the amount and ratio of resources in two rooms. Everyone needs independently to choose to enter one of the two rooms. After all agents finish their choices, the resources in Room 1 are equally divided by who entered Room 1, while the resources in Room 2 are equally divided by the agents who entered Room 2. If the agents in Room 1 get more per capita resource than the agents in Room 2, we regard them (choosing Room 1) as winners, and vice versa. In this model, we label the number of agents in Room 1 and Room 2 N_1 and N_2, respectively. If $M_1/N_1 > M_2/N_2$, then agents in Room 1 win, and vice versa.

In the MDRAG, the system will reach a most stable state [7] at the critical point. Under the assumption that changing the behaviors of agents might change the system equilibrium, if we could observe how the introduction of different behaviors would change the resource allocation, the model will be optimal. Based on the previous researches [8, 9, 107, 111], we know that herd behavior and contrarian behavior in the MDRAG could respectively shift the critical point to opposite directions, accordingly affecting the fluctuation of the system. Hence, we introduced herd behavior and contrarian behavior as a kind of hedge behavior.

In our agent-based model, there are N_n normal agents, N_h imitators and N_c contrarians. We define $\beta_1 = N_h/N_n$ and $\beta_2 = N_c/N_n$. The total number of all agents is $N = N_n + N_h + N_c = N_1 + N_2$. Each of normal agents decides to enter one of the two rooms based on its strategy table. At the beginning, each normal agent has S strategy tables, each of which determined by a preference index L and has P potential situations [7]. L characterizes the heterogeneity of preferences of normal agents, where $L \in [0, P]$. At the end of a round, each normal agent will score the S strategy tables in its hand. Then, the best strategy table will be used for the next round. When the computer gives the current situation, P_i ($P_i \in [1, P]$), at every round, each normal agent enters the room according to its best strategy table. The table of a strategy's left column represents P potential situations and the right column is filled with 1 and 0, which represent entering Room 1 and Room 2, respectively. The probability of 1 or 0 is determined by a certain preference index of L. The rule of constructing the right column of the table is that for a probability of L/P the right column is filled with 1 and for probability of $(P - L)/P$ the right column is filled with 0.

Meanwhile, the system may secretly add some contrarians and imitators generated by the computer in certain rounds. Imitators and contrarians have no strategy tables, whose decisions at a certain round are based on the choices of normal agents. In every round, every imitator or contrarian will randomly choose several normal agents as its group from all normal agents. The logic is as follows: An imitator will choose to enter the room where majority of the normal agents in its group choose to enter. If most of the normal agents in its group choose to enter Room 1, then it will choose to enter Room 1, and vice versa. Contrarians choose to enter the room where minority of the normal agents in its group chooses to enter. If most of the normal agents in its group choose to enter Room 1, then it will choose to enter Room 2, and vice versa. After one round of the option, we remark the total number of agents in Room 1 and Room 2 including normal agents, contrarian and imitators, labeled as N_1 and N_2, respectively. If $M_1/N_1 > M_2/N_2$, then agents in Room 1 win, and vice versa.

Based on the mentioned model, computer simulations are carried out with 100 normal agents for simulation parameters, $S = 11$ and $P = 121$. In the process, we changed the parameters including the ratio of resource distribution between the two rooms and the ratio of contrarians and imitators. Total 400 time steps of simulation will be lasted under each parameter set. In order to scrutinize the effect of hedge behavior on the whole resource-allocation system, we calculated the fluctuation of the systems. The fluctuation of the systems can be defined as $\frac{\sigma^2}{N} = \frac{1}{2N}\sum_{i=1}^{2}\langle\left(N_i - \tilde{N}_i\right)^2\rangle$, the smaller the value is, the closer the system approaches to the equilibrium, because the optimal resource population is given by $\tilde{N}_i = M_i N/(M_1 + M_2)$. The previous studies indicated that the resource allocation system exhibits a phase transition as M_1/M_2 varies. In other words, at the critical point, $(M_1/M_2)_t$, $\frac{\sigma^2}{N}$ reaches the lowest value which means the system becomes the most stable. See Fig. 7.4. The systems reach the most stable state at $M_1/M_2 = 11$ without imitators and contrarians. At this moment, the critical point is $(M_1/M_2)_t = 11$. But the fluctuation of the system changes when herd behavior is

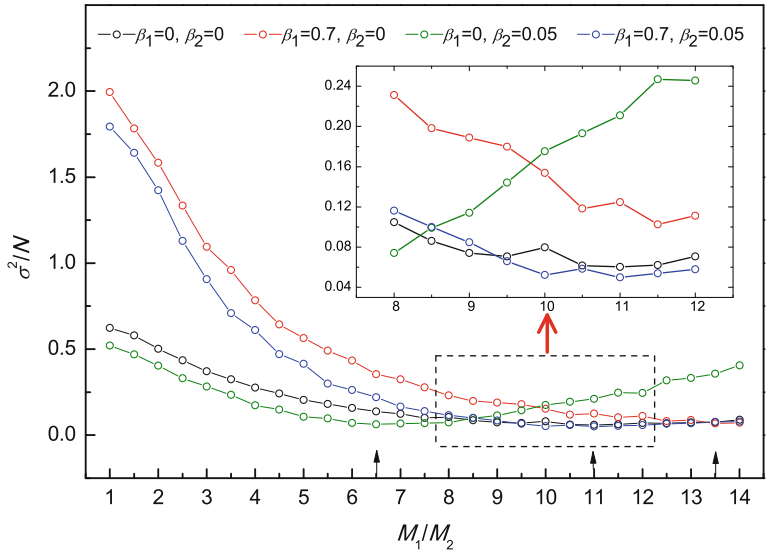

Fig. 7.4 Simulation results for fluctuation σ^2/N in different M_1/M_2 from 1 to 14 with normal agents (*black*), herd behavior (*red*), contrarian behavior (*green*), and hedge behavior (*blue*). The circles in *dashed frame* are magnified above the *red arrow* because the overlapped *circles* are hard to distinguish. Three *black* arrows on the horizontal axis indicate the four critical points of the most stable state of the four *curves*. The *arrow* at $M_1/M_2 = 6.5$ indicates the most stable state of *green curve* while the *arrow* at $M_1/M_2 = 13.5$ indicates the most stable state of *red curve* and the *arrow* at $M_1/M_2 = 11$ indicates the most stable state of *black* and *blue* curves. Note, the two critical points of the most stable state of *black* and *blue curves* are well overlapped, and thus denoted by one *arrow* only, which clearly shows that suitable hedge behavior could let the system (with hedge behavior) have the same most stable state as the original system (without hedge behavior). For each parameter set, simulations are run 100 times, each over 400 time steps (the last 200 time steps for statistics). Adapted from Ref. [116]

introduced. Likewise, contrarian behavior can also affect the system's fluctuations. However, if we introduce herd and contrarian behaviors simultaneously, we found the proper hedge proportion that makes the critical point unchanged by adjusting simultaneously the strength of the two different behaviors.

As we all know, the adaptive agents are the most remarkable feature of CASs. In order to analyze the robustness of critical points under hedge behavior, we need to scrutinize the microscopic behaviors of the system, i.e., the performance of each agent. Here, we observe their performance by normal agents' preference. We define the preference of each normal agent as the average rate of entering Room 1 or Room 2 in last 200 statistical time steps of simulations. We select three resource ratios to observe: $M_1/M_2 = 1$ that represents a uniform (or unbiased) distribution, $M_1/M_2 = 3$ that stands for a small bias, and $M_1/M_2 = 14$ that indicates an extreme bias. Figures 7.5 and 7.6 show the statistical results of simulations under different resource ratios and numbers of imitators and contrarians. We note that the average preference of all normal agents varied with M_1/M_2, which can be clearly seen in Fig. 7.5. This

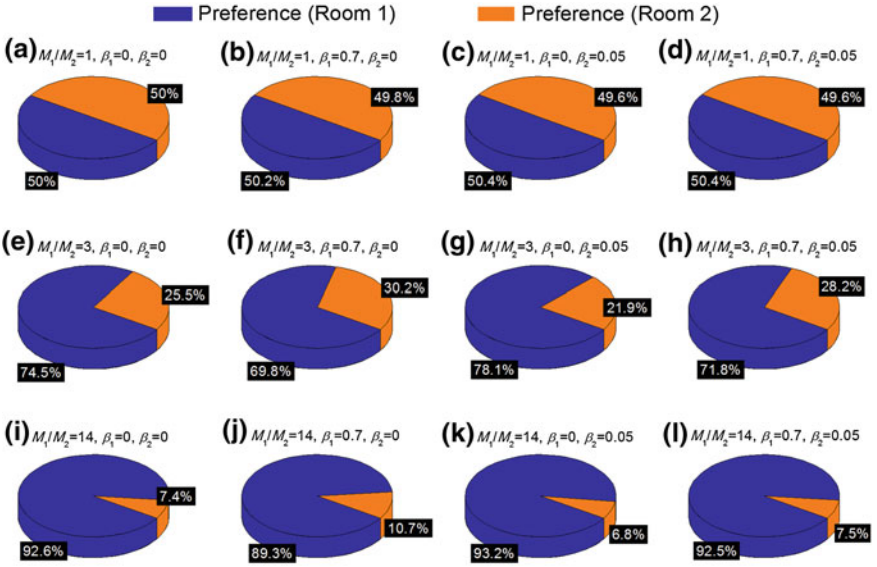

Fig. 7.5 The average preference of all normal agents for the 12 parameter sets: $M_1/M_2 = 1$ (**a**–**d**), 3 (**e**–**h**), and 14 (**i**–**l**) with $\beta_1 = 0$ and $\beta_2 = 0$ (**a**, **e**, **i**), $\beta_1 = 0.7$ and $\beta_2 = 0$ (**b**, **f**, **j**), $\beta_1 = 0$ and $\beta_2 = 0.05$ (**c**, **g**, **k**), and $\beta_1 = 0.7$ and $\beta_2 = 0.05$ (**d**, **h**, **l**). For each parameter set, simulations are run for 400 time steps (the first 200 time steps for equilibration and the last 200 rounds for statistics). Adapted from Ref. [116]

shows the global environmental adaptability of normal agents. It is noted that in the case with hedge behavior, the proportions of normal agents' preferences to two rooms are mainly same. It indicates that adaptability of normal agents results in consistent microscopic performances of systems in both cases, which further brings the robustness of critical points under the existence of hedge behavior. In Fig. 7.6 we can see that the preferences of each normal agent are different no matter in which environment of resources or behaviors. In this system, normal agents show heterogeneity of preferences, which has a remarkable influence on achieving the balance of CASs. It implies that even if individuals are different, they can still emerge consistency as a whole.

From Fig. 7.4, we infer that for any strength of one behavior, a proper hedge proportion exists to make critical points of the system robust. Also, by adjusting the hedge proportion, the resource allocation system could reach the most stable state in any satisfied resource ratio. Thus, it is very helpful for optimizing resources allocations under any resource distributions. Therefore, we carried out more comprehensive simulations. The simulation results are shown in Fig. 7.7.

In Fig. 7.7 each color represents the most stable equilibrium state (i.e., with the critical point, $(M_1/M_2)_t$, that corresponds to the minimum value of $\frac{\sigma^2}{N}$) in a certain combination of β_1 and β_2. We can see that, for the case without imitators and contrarians, system can reach equilibrium at the critical point, $(M_1/M_2)_t = 11$. Herd

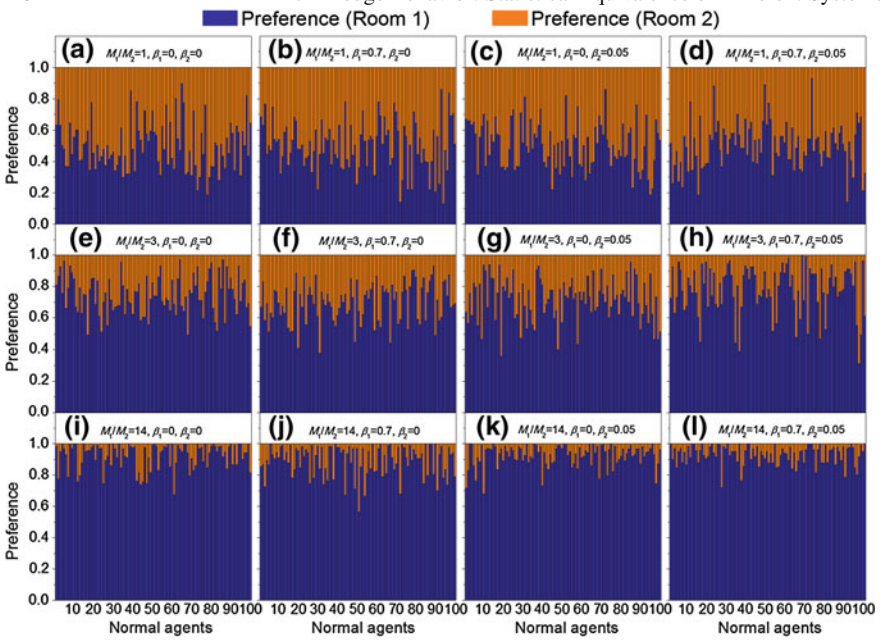

Fig. 7.6 The preference of each normal agent for the 12 parameter sets: $M_1/M_2 = 1$ (**a**–**d**), 3 (**e**–**h**), and 14 (**i**–**l**) with $\beta_1 = 0$ and $\beta_2 = 0$ (**a**, **e**, **i**), $\beta_1 = 0.7$ and $\beta_2 = 0$ (**b**, **f**, **j**), $\beta_1 = 0$ and $\beta_2 = 0.05$ (**c**, **g**, **k**), and $\beta_1 = 0.7$ and $\beta_2 = 0.05$ (**d**, **h**, **l**). For each parameter set, simulations are run 400 time steps (the first 200 time steps for equilibration and the last 200 rounds for statistics). Adapted from Ref. [116]

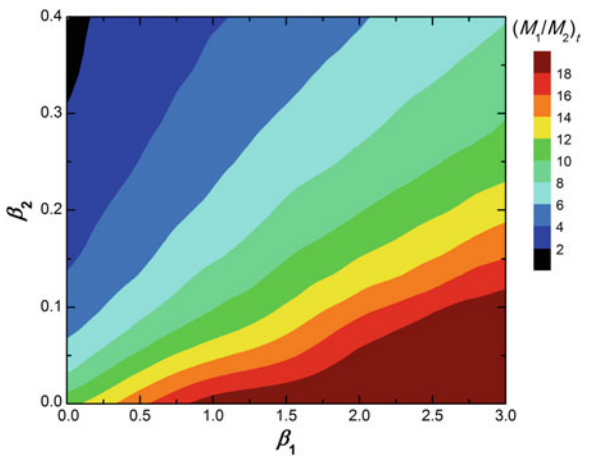

Fig. 7.7 Critical point, $(M_1/M_2)_t$, as functions of β_1 and β_2 as a result of the computer simulations with 100 normal agents. For each parameter set, simulations are run 100 times, each over 400 time steps (the last 200 time steps for statistics). Adapted from Ref. [116]

behavior makes the critical point shift to a larger M_1/M_2, while contrarian behavior makes the critical point shift to a smaller M_1/M_2, which means either herd behavior or contrarian behavior always changes the system's fluctuation. However, if we adjust the two behaviors simultaneously, then this kind of hedge behavior can make critical points robust no matter how many agents exist. Besides, the system can achieve the optimal state at any resource ratio by adjusting the values of β_1 and β_2 appropriately.

Such adjustment of hedge behavior can surely give references to CASs. We found that the critical point of the system is robust and independent of the total number of agents composed of normal agents, imitators and contrarians, under some conditions. Also, the resource allocation system could be controlled to reach the most stable state (corresponding to a certain critical point) in any resource bias through adjusting the proportion of two kinds of agents, β_1 and β_2.

7.4 Theoretical Analysis

The further understanding of critical point $(M_1/M_2)_t$ versus β_1 and β_2 is necessary for understanding the microscopic mechanism in the system. For this purpose, we conduct theoretical analysis.

For the fixed values of S and P, the system could reach the most stable state only at the critical point (i.e., specifically ratio of resource ratio, $(M_1/M_2)_t$) under the situation without contrarians and imitators. In order for resource allocation systems to reach the optimal states at any ratio of resource distribution, we have to adjust the values of β_1 and β_2, thus changing critical points, $(M_1/M_2)_t$, accordingly.

7.4.1 The Properties of Critical Points

7.4.1.1 MDRAG

All normal agents use the strategy $(L_i)_{\max}$ with the largest preference in their hand. Meanwhile, the ratio of numbers of agents in two rooms is equal to the ratio of resource distribution. Then, we have

$$N_1 = \sum x_i \ ,$$

where the choice of agent i is denoted as x_i=1 (Room 1) or 0 (Room 2). Next, we obtain

$$\frac{\langle N_1 \rangle}{N_n} = \frac{\sum \langle x_i \rangle}{N_n} = \frac{\sum_i^{N_n} (L_i)_{\max}}{P N_n} = \left(\frac{M_1}{M_1 + M_2} \right)_t , \tag{7.7}$$

where $\langle \cdots \rangle$ denotes the averaged value of $\cdots$.

7.4.1.2 MDRAG + Imitators + Contrarians

All normal agents use $(L_i)_{\max}$. An imitator follows the majority of its group to choose x_h, while every contrarian follows the minority in his group to choose x_c. Thus we obtain

$$\begin{aligned}\frac{\langle N_1\rangle}{N} &= \frac{\sum_i^{N_n}(L_i)_{\max} + P\sum_h^{N_h}\langle x_h\rangle + P\sum_c^{N_c}\langle x_c\rangle}{(1+\beta_1+\beta_2)PN_n} \\ &= \left(\frac{M_1}{M_1+M_2}\right)_{t'}, \end{aligned} \tag{7.8}$$

where $\beta_1 = \frac{N_h}{N_n}$ and $\beta_2 = \frac{N_c}{N_n}$.

7.4.2 Solve $\sum_i^{N_n}(L_i)_{\max}$, $\sum_h^{N_h}\langle x_h\rangle$ and $\sum_c^{N_c}\langle x_c\rangle$

(a) For normal agent i with S strategies, the probability of L_i taking 0 to P is $\frac{1}{P+1}$. Then, the probability of $(L_i)_{\max}$ being a certain value of L is

$$p(L) = \left(\frac{L+1}{P+1}\right)^S - \left(\frac{L}{P+1}\right)^S.$$

If N_n is large enough, there is

$$\begin{aligned}\sum_i^{N_n}(L_i)_{\max} &= \sum_{L=0}^{P} N_n p(L) L \\ &= PN_n\left[1 - \frac{1}{P}\sum_{L=1}^{P}\left(\frac{L}{P+1}\right)^S\right], \end{aligned} \tag{7.9}$$

Plugging Eq. (7.9) into Eq. (7.7), under the situation without contrarians and imitators, there is

$$\frac{\langle N_1\rangle}{N_n} = 1 - \frac{1}{P}\sum_{L=1}^{P}\left(\frac{L}{P+1}\right)^S = \left(\frac{M_1}{M_1+M_2}\right)_t \equiv m_n\,. \tag{7.10}$$

According to Eq. (7.10), it is known that if P and S are fixed, we can solve the critical point denoted by $(M_1/M_2)_t$ without contrarians and imitators.

(b) We know that normal agents still use their strategies with $(L_i)_{\max}$ at critical points after introducing contrarians and imitators into the system. Therefore, for

Table 7.3 Probability of x_c

x_c	Probability
1	$\sum_{q=0}^{y} C_k^q \left[\left(\frac{M_1}{M_1+M_2}\right)_t\right]^q \left[\left(\frac{M_2}{M_1+M_2}\right)_t\right]^{k-q} \equiv m_c$
0	$1 - m_c$

normal agents, there is

$$\frac{\langle N_{n1}\rangle}{N_n} = 1 - \frac{1}{P}\sum_{L=1}^{P}\left(\frac{L}{P+1}\right)^S = \left(\frac{M_1}{M_1+M_2}\right)_t \equiv m_n.$$

Approximately, when imitator h and contrarian c respectively choose k normal agents, the probability that they got the normal agents who came into Room 1 is denoted as $\frac{\langle N_{n1}\rangle}{N_n} = \left(\frac{M_1}{M_1+M_2}\right)_t \equiv m_n$. Then, the probability that x_c equals to 1 or 0 is shown in Table 7.3. Here $y = \frac{k-1}{2}$, and k is odd. Then we have

$$\langle x_c\rangle = m_c = \sum_{q=0}^{y} C_k^q (m_n)^q (1-m_n)^{k-q}. \tag{7.11}$$

So, $\langle x_h\rangle = 1 - m_c$.

(c) Plugging Eq. (7.11) into Eq. (7.8) yields

$$\begin{aligned}\frac{\langle N_1\rangle}{N} &= \frac{PN_n m_n + PN_h(1-m_c) + PN_c m_c}{(1+\beta_1+\beta_2)PN_n} \\ &= \left(\frac{M_1}{M_1+M_2}\right)_{t'}.\end{aligned}$$

Then, $\frac{\langle N_1\rangle}{N} = \frac{m_n+\beta_1(1-m_c)+\beta_2 m_c}{1+\beta_1+\beta_2} = \left(\frac{M_1}{M_1+M_2}\right)_{t'}$.

By adjusting β_1 and β_2 appropriately, we could get a robust critical point of the system. Besides, the system could reach the most stable state under any resource ratio M_1/M_2. Figure 7.8 shows $(M_1/M_2)_t$ versus β_1 and β_2 as a result of the theoretical analysis with the same parameters as those adopted in the previous simulations, which echoes with the simulation results shown in Fig. 7.7.

7.5 Conclusions

In summary, using controlled experiments, agent-based simulations and theoretical analysis, we have investigated the role of hedge behavior in a resource-allocation system. The critical point identified here helps to reveal the robustness of the most stable state of the system (at which the fluctuation becomes minimal) whether hedge behavior exists or not.

7.6 Supplementary Materials

7.6.1 Leaflet to the experiment

Everyone completes this experiment via a computer in front of you. You will use an allocated anonymous account throughout the experiment. After logging in, you will see two virtual rooms on the screen: Room 1 and Room 2. Each room owns a certain amount of virtual money, but you are not told the amount and ratio. You can choose to enter one of the two rooms by clicking the relevant button in the working panel on the computer screen, and then wait. The subjects chose in the same room will share equally the virtual money inside the room. After all the subjects finished, the system will calculate per capita money of the two rooms, respectively. The room in which subjects get higher per capita money is regarded as the winning room and the subjects who had entered the winning room as winners in this round. You will see your own result (win or lose) of this round and the current score on the computer screen. After that, next round starts. Throughout the experiment, the total number of human subjects was kept to be 68, but the number of subjects entering Room 1 and Room 2 in every round will not be told. Each subject cannot see the other subjects' options. Only your result (win or lose) will be told after every round. You can only use this information to judge which room to enter in the next round. After the experiment starts, any kinds of communication are not allowed. The experiment contains four systems, each will be conducted for 30 rounds.

Each account has an original score with zero point. Total 10 points will be added in every round if you win and zero point will be added if you lose. At the end of the whole experiment, we will pay you cash with the exchange rate: 10 points = 1 Renminbi. Besides, we will reward the top 3 plays, each with additional 100 Renminbi.

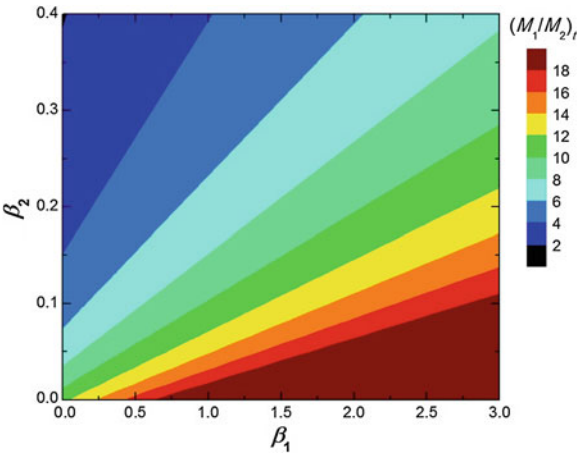

Fig. 7.8 Critical point, $(M_1/M_2)_t$, as functions of β_1 and β_2 as a result of theoretical analysis. Adapted from Ref. [116]

Chapter 8
Cooperation: Spontaneous Emergence of the Invisible Hand

Abstract There has been a belief that with the directing power of the market, the efficient state of a resource-allocation system can eventually be reached even in a case where the resource is distributed in a biased way. To mimic the realistic huge system for the resource allocation, we design and conduct a series of controlled experiments. From the experiments we find that efficient allocation can be spontaneously realized despite a lack of communications among the participants or any instructions to them. To explain the underlying mechanism, we construct an agent-based model by introducing heterogeneous preferences into the strategy-building procedures. The model produces results in good agreement with the experiments. We investigate the influence of agents' decision-making capacity on the system behavior and the phase structure of the model as well. A number of phase transitions are identified in the system. In the critical region, we find that the overall system will spontaneously display an efficient, stable, and unpredictable mode in which the market's invisible hand can fully play its role.

Keywords Resource-allocation system · The invisible hand · Balanced state · Phase transition

8.1 Opening Remarks

The statistical equivalence of different systems discussed in the preceding chapter implies a kind of spontaneous cooperation in different systems. In this chapter, we are prepared to investigate a single system to see the possibility of a different kind of spontaneous cooperation, namely the invisible hand [28].

As mentioned in the preceding chapters, most social, economic, and biological systems involving a large number of interacting agents can be regarded as complex adaptive systems (CAS) [105], because they are characterized by a high degree of adaptive capacities to the changing environment. The interesting dynamics and phase behaviors of these systems have attracted the interest of physical scientists.

J.-P. Huang, *Experimental Econophysics*, New Economic Windows,
DOI 10.1007/978-3-662-44234-0_8

A number of microscopic CAS models have been proposed [100, 117–120], among which the minority game (MG) [1, 31, 87] is a representative model. Along with the progress in the research on econophysics [14], MG has been mostly applied to simulate one kind of CAS, namely the stock market [32, 33]. Alternatively, MG can also be interpreted as a multiagent system competing for a limited resource [34, 35] which distributes equally in two rooms. However, agents in the real world often have to face competition in the limited resource, which distributes in different places in a biased manner. Examples for such phenomena include companies competing among markets of different sizes [121], drivers selecting different traffic routes [122], people betting on horse racing with the odds of winning a prize, and making decisions on which night to go to which bar [123].

From a global point of view, the ideal evolution of a resource allocating system would be the following: Although each agent would compete against others only with a self-serving purpose, the system as a whole could eventually reach a harmonic balanced state where the allocation of resource is efficient, stable, and arbitrage-free (which means that no one can benefit from the "misdistribution" of the resource). Note that during the process of evolution to this state, agents could neither have been told about the actual amount of the resources in a specific place, nor could they have any direct and full communications, just as if there were an "invisible hand" [28] directing them to cooperate with each other. Then, does this invisible hand always work? In practice, there is plenty of evidence that the invisible hand does have very strong directing power in places such like financial markets, though sometimes it fails to work. Such temporary ineffectiveness implies that there must be some basic conditions required for the invisible hand to exert its full power. Through an experimental and numerical study with a market-directed resource allocation game (MDRAG, which is an extended version of the MG model), we found that agents equipped with heterogeneous preferences, as well as a decision-making capacity which matches the environmental complexity, are sufficient for the spontaneous realization of such a harmonic balanced state.

Table 8.1 Results of GAME-I [7]

Session	Group	Round	M_1	M_2	M_3	$\langle N_1 \rangle$	$\langle N_2 \rangle$	$\langle N_3 \rangle$
1	A ($N = 12$)	1–10	3	2	1	5.3	4.6	2.1
2	A ($N = 12$)	1–10	3	2	1	5.5	3.8	2.7
3	B ($N = 12$)	1–10	3	2	1	5.5	4	2.5
4	C ($N = 24$)	1–20	3	2	1	12.2	7.4	4.4
5	D ($N = 10$)	1–10	5	3	–	6.1	3.9	–
6	D ($N = 10$)	1–10	3	1	–	7.4	2.6	–

Table 8.2 Results of GAME-II [7]

Session	Group	Round	M_1	M_2	$\langle N_1 \rangle$	$\langle N_2 \rangle$
1	D ($N = 10$)	1–10	2	1	6.2	3.8
2	E ($N = 10$)	1–10	1	3	3.3	6.7
3	F ($N = 11$)	1–10	3	1	7.2	3.8
3	F ($N = 11$)	11–20	3	1	8.3	2.7
4	C ($N = 24$)	1–15	7	1	17.8	6.2
4	C ($N = 24$)	16–30	7	1	21.1	2.9

8.2 Controlled Experiments

To illustrate the system behavior, we designed and conducted a series of economic experiments, collaborating with university students. In the experiments, 89 students from different (mainly physics, mathematics, and economics) departments of Fudan University were recruited and randomly divided into seven groups (Group A–G, see Tables 8.1, 8.2, 8.3, and 8.4). The number of students in each group was set for convenience and denoted by N in Tables 8.1, 8.2, 8.3, and 8.4. In the games played in the experiments, students were told that they have to make a choice among a number of rooms, in each round of a session, for sharing the different amounts of virtual money in different rooms. Students who get more than the global average, namely those belonging to the relative minority, would win the payoff. At the beginning of a session, subjects were told the number of rooms (2 or 3), and in some cases the different but fixed amount of virtual money in each room. In the following, M_i is used to denote the amount of virtual money in room i. A piece of global information, about the payoff in the preceding round in all rooms, is announced before a new round starts. In each round, the students must make their own choices without any kind of communication. The payoff per round for a student in room i is 2 points if $M_i/N_i > \sum M_i/N$, and -1 point otherwise. Here N_i is the number of the students choosing room i. The total payoff of a student is the sum of payoffs of all rounds which will be converted to money payoffs in RMB with a fixed exchange rate. Since the organizational and statistic procedures were done by humans, one session of 10 rounds took roughly 20 minutes. More details can be found in the leaflet to the experiment with nine items:

1. A group of subjects are taking part in this experiment. The game situation is the same for each subject. In the experiments, no kind of communication is allowed.
2. At the beginning of the game, all of you will be told the kind of game (GAME-I, GAME-II or GAME-III), as well as the total number of subjects (N), rooms (2 or 3) and play rounds, respectively.
3. In each round of the game, you have to choose and enter one of the rooms. The amount of virtual money in each room is different but fixed, represented by M_i ($i = 1, 2, \ldots$).
4. You will be told each M_i (only in GAME-I).

Table 8.3 Track of 11 subjects in group F ($N = 11$) converging to $M_1/M_2 = 3$ [7]

Round	N_1	N_2	Round	N_1	N_2
1	5	6	11	8	3
2	9	2	12	10	1
3	4	7	13	9	2
4	6	5	14	7	4
5	6	5	15	9	2
6	7	4	16	7	4
7	7	4	17	7	4
8	8	3	18	9	2
9	10	1	19	8	3
10	10	1	20	9	2

5. In each round, you can choose a room to share the virtual money in it and get your quota, M_i/N_i, if you select room i. Here N_i denotes the total number of subjects in room i.
6. You may make a new room choice in every round.
7. Your payoff per round: After the statistics of each round is done, you will receive a payoff which depends on the relation between your quota and the global average:

$$\text{payoff per round} = \begin{cases} 2\,\text{points}, & \text{if } M_i/N_i > \sum M_i/N \\ -1\,\text{point}, & \text{otherwise} \end{cases}.$$

8. Your information per round:

   - The current round number;
   - N_i of each room in the preceding round (only in GAME-I, announced by the game organizer);
   - Payoff (2 or -1) of each room in the preceding round (announced by the game organizer);
   - Your rooms chosen and payoffs got in the preceding game rounds (recorded by yourself);
   - Your cumulated payoffs (calculated by yourself).

9. The initial capital of each subject is 0 point. The exchange rate is 1 RMB per (positive) point.

Three kinds of games, GAME-I, GAME-II, and GAME-III, have been investigated. GAME-II differed from GAME-I in the global information being announced. In GAME-I, both the resource distribution M_i and the current population N_i in room i were announced, while only payoffs (2 or -1) in each room of the current round were conveyed to subjects in GAME-II. Note that the environmental complexity was increased in GAME-II, since in order to win the game, subjects

Table 8.4 Results of GAME-III [7]

Session	Group	Round	M_1	M_2	$\langle N_1 \rangle$	$\langle N_2 \rangle$
1	G ($N = 10$)	1–5	3	1	5.4	4.6
1	G ($N = 10$)	6–10	3	1	8.2	1.8
1	G ($N = 10$)	11–15	3	1	7	3
1	G ($N = 10$)	16–20	3	1	7	3
1	G ($N = 10$)	21–25	1	3	7.8	2.2
1	($N = 10$)	26–30	1	3	4.2	5.8
1	G ($N = 10$)	31–35	1	3	2.8	7.2
1	G ($N = 10$)	36–40	1	3	2.6	7.4
1	G ($N = 10$)	41–45	1	3	2.4	7.6

would have to predict other subjects' decisions, in the meantime, infer the actual amount of virtual money in different rooms. In GAME-III, the global information is the same as that of GAME-II, except an abrupt change of amount of virtual money is introduced during the play of the game without an announcement. (On the contrary, all the subjects have already been told that each M_i is unchanged.) No further information was given to the subjects.

Results of six sessions of GAME-I, four of GAME-II, and one of GAME-III are given in Tables 8.1, 8.2, 8.3, and 8.4. In Table 8.1, the results of GAME-I are listed, where the time average of the subject number in room i is represented as $\langle N_i \rangle$. As the data shows, a kind of cooperation seems to emerge in the game within 10 rounds. In particular, ratios of $\langle N_i \rangle$ converge to the ratios of M_i, implying that the system becomes efficient in delivering the resource even if it was distributed in a biased way. To the subjects, no room is better or worse in the long run, there is also no evidence that any of them could systematically beat the resource allocation "market." One might naively think that the system could evolve to this state only because the subjects knew the resource distribution prior to the play of the games, and the population in each room during the play. However, results of GAME-II show that this explanation could not be correct. As shown in Table 8.2, although subjects who know neither the resource distribution nor the current populations in different rooms, seem not to be able to adapt to the unknown environment during the first 10 or 15 rounds, eventually the relation $\langle N_1 \rangle / \langle N_2 \rangle \approx M_1/M_2$ is achieved again in groups C and F. For instance, Table 8.3 shows the track through which group F gradually found the balanced state under the environmental complexity $M_1/M_2 = 3$. Furthermore, the results of GAME-III support the conclusion of GAME-II, in which the system can reach this state even with an abrupt change of the unknown resource distribution during the play of the game, see the results of 21–45 rounds played by the G group in Table 8.4. It is surprising that subjects can "cooperate" even without direct communications as well as the information of the resource distribution. We can define the source of a force which drives the subjects to get their quota evenly as the "invisible hand" of the resource allocation market. In the sequel, however, we

Table 8.5 A typical strategy table [7]

Economic situations	Choices
1	0
2	1
3	1
...	...
$P-1$	0
P	1

shall show that the effectiveness of this invisible hand relates to the heterogeneous preference and the adequate decision-making capacity of the subjects of the game.

8.3 Agent-Based Modeling

To find the mechanism behind this adaptive system of resource distribution, two multiagent models are used and their results are compared with each other. The first model is the traditional MG, while the second one is an extended MG called as Market-Directed Resource Allocation Game (MDRAG). MG and MDRAG have a common framework: There are N agents who repeatedly join a resource allocation market. The amounts of resource in two rooms are M_1 and M_2, respectively. Before the game starts, each agent will choose S strategies to help him/her make decision in each round of play. The strategy used in MG and MDRAG is typically a choice table which consists of two columns, as shown in Table 8.5. The left column is for the P possible economic situations, and the right side is filled with the corresponding room number, namely room 0 or room 1. Thus, if the current situation is known, an agent should immediately choose to enter the corresponding room. With a given P, there are totally 2^P different strategies. At each time step, based on a randomly given exogenous[1] economic state [124], each agent chooses between the two rooms with the help of the prediction of his/her best scored strategy. After everyone has made a decision, agents in the same room will share the resource in it. Agents who earn more than the global average $(M_1 + M_2)/N$ become the winners, and the room which they entered is denoted as the winning room. To a strategy in the game, a unit of score would be added if it had given a prediction of the winning room, whether it was actually used or not.

On the other hand, MDRAG differs from MG in the strategy-building procedures. In traditional MG, agents "randomly" choose S strategies from the strategy pool of 2^p size. Here "randomly" means that each element of the right column of a strategy table is filled in with 0 or 1 equiprobably. Using this method, strategies of different preferences will have a binomial distribution. Here the preference of a strategy is defined as the tendency or probability with which a specific room will be chosen when

[1] The alternative is the use of endogenous binary history of the game results as the economic situations. We have confirmed that there would be no change in the simulation results.

the strategy is activated. For a large P, the number of 0 and the number of 1 in the right column are nearly equal. Hence, globally there would be no preference difference among agents who uniformly pick up these strategies. In MDRAG, however, we use a new method to fill the strategy table to introduce heterogeneous preferences to the agents. First, $K(0 \leq K \leq P)$ denoting the number of 0 in the right column is randomly selected from the $P + 1$ integers. In other words, strategies with different preferences (different values of K) are chosen equiprobably from the strategy pool. Second, each element of the strategy's right column should be filled in by 0 with the probability K/P, and by 1 with the probability $(P - K)/P$. It is clear that a strategy with an all-zero right column can be picked up with the probability $1/(P + 1)$ in MDRAG, while this could happen only with a probability of $1/2^p$ in the traditional MG and practically could never be chosen by any MG agent if $NS \ll 2^p$.

To make descriptions easier to understand, explanations of the model parameters are provided. The ratio M_1/M_2 represents the environmental complexity of the games. Note that if $M_1/M_2 = 1$, agents need only to worry about other people's decision. Assuming that room 1 always contains more resource, the trivial case will be $M_1/M_2 > N - 1$, since all the agents can easily find out that going to room 1 would be the right choice under this situation. On the other hand, when the ratio is set $1 < M_1/M_2 \leq N - 1$, the larger this ratio is, the more difficult it would be for the market to direct the system to the ideal state. Other parameters concern with the decision-making capacity, which can be generalized into three elements (http://plato.stanford.edu/entries/decision-capacity/), namely (i) the possession of a set of values and goals necessary for evaluating different options; (ii) the ability to communicate and understand information; (iii) the ability to reason and to deliberate about one's choices. The first element has already been built in both the models as the evaluation of the strategies with the minority-favorable payoff function. The second element relates to the model parameter P. Since the total number of possible situations is dependent on the completeness of the perception of the world, we relate it to the cognition ability. Finally, more strategies could be helpful if one needs to deliberate his/her choices of decisions, hence the strategy number S is related to the third element of the decision-making capacity, the ability of choice deliberation.

8.4 Results

Results of the economic experiments are compared with the simulation results of the traditional MG and MDRAG in Fig. 8.1. For each parameter set, we performed the simulation 200 times. In each of these simulations, the code was run over 400 time steps. The first half of the time evolution is for the equilibration of the system, while the remaining half is for the statistics. With a certain set of parameters ($S = 8$ and $P = 16$), MDRAG's results perfectly agree with the experimental data under a higher environmental complexity. In other words, agents in both experiments and MDRAG can be directed by the market to cooperate with each other, so that an efficient allocation of the biasedly distributed resource can be realized even without giving the agents full information or instructions. On the other hand, the traditional

Table 8.6 Performances of MDRAG and MG in 3-room cases [7]

Resource			MDRAG			MG		
M_1	M_2	M_3	$\langle N_1\rangle$	$\langle N_2\rangle$	$\langle N_3\rangle$	$\langle N_1\rangle$	$\langle N_2\rangle$	$\langle N_3\rangle$
1	1	1	39.9	40.3	39.8	39.2	41.5	39.3
1	2	3	19.7	40.1	60.2	25.1	40.7	54.2
1	4	7	9.6	40	70.4	24.8	40.4	54.8
1	2	9	9.8	19.6	90.6	29.3	33.8	56.9

MG fails to reproduce the experimental results unless the distribution of resource is biased very weakly up to $M_1/M_2 = 3$. Note that MDRAG differs from MG solely in the introduction of heterogeneous preferences in the strategies; hence one may infer that the heterogeneity of agents' preferences is a significant factor to have the "invisible hands" to be effective. This argument is further supported by numerical experiments in the 3-room cases (with parameters $P = 24$, $N = 120$ and $S = 10$). Again, here MDRAG is superior to MG in bringing out the directing power of the market. Shown in Table 8.6, the ratio of $\langle N_1\rangle : \langle N_2\rangle : \langle N_3\rangle$ converges to $M_1 : M_2 : M_3$ only in the equilibrium states of MDRAG.

Figure 8.1 also shows that the decision-making capacity, in particular the deliberation of choices (the parameter S), would be another factor having influence on the effectiveness of the invisible hand. Typically, as the environmental complexity (M_1/M_2) increases, both MG and MDRAG will deviate from the experimental results. Nevertheless, the problem of MG is much severe. As shown in the figure, even MG with extremely large S ($S = 48$, a situation which is inconsistent with the real system and will drastically increase the computational cost) can just work at a very low level of environmental complexity. At the same time, the result of MDRAG provides a perfect fit with the experimental data when S is large enough, but not too

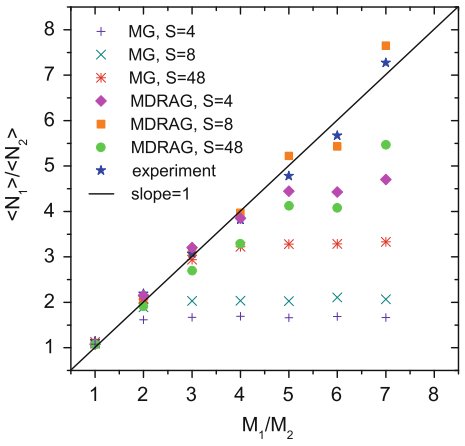

Fig. 8.1 $\langle N_1\rangle/\langle N_2\rangle$ as functions of M_1/M_2, $P = 16$ in MG and MDRAG, and $N = 24$ for all the simulations and the experiment. Simulations are run 200 times, each over 400 time steps (first half for equilibration, the remaining half for statistics). The line with slope $= 1$ indicates the efficient states: $\langle N_1\rangle/\langle N_2\rangle = M_1/M_2$. Adapted from Ref. [7]

large for a given P value (the reason will be explained in the following discussion). In other words, MG does not provide a good fit even for large S, while MDRAG can fit the data with less demanding condition in terms of computational cost.

8.5 Discussion and Conclusions

Through a large number of numerical simulations, we have found the dependence of equilibrium states of the system on the model parameters, together with a number of phase transitions in the models. To explore in detail, three parameters are defined which describe system behaviors in three aspects, namely efficiency, stability, and predictability. First, the efficiency of resource allocation can be described as $e = |\langle N_1\rangle/\langle N_2\rangle - M_1/M_2|/(M_1/M_2)$. Note that $0 \leq e < 1$ and a smaller e means a higher efficiency in the allocation of the resource. The stability of a system can be described by $\sigma^2/N \equiv \frac{1}{2N}\sum_{i=1}^{2}\langle(N_i - \tilde{N}_i)^2\rangle$, which denotes the population fluctuation away from the optimal state.[2] Here $\tilde{N}_i = M_i N/\sum M_i$, and $\langle A\rangle$ is the average of time series A_t. The predictability is related to $H \equiv \frac{1}{2NP}\sum_{\mu=1}^{P}\sum_{i=1}^{2}\langle N_i - \tilde{N}_i|\mu\rangle^2$, in which $\langle A|\mu\rangle$ is the conditional average of A_t given that $\mu_t = \mu$, one of the P possible economic situations. If $\sigma^2/N \neq H$, it means that agents may take different actions at different times for the same economic situation (namely the market behavior is unpredictable). For clarity, we describe the predictability of system by defining $J = 1 - HN/\sigma^2$. It is obvious that $0 \leq J < 1$ and a smaller J means higher predictability.

The variation of system behavior along with the change in environmental complexity M_1/M_2 is shown in Fig. 8.2. As shown in Fig. 8.2a, the system changes from an efficient state into an inefficient state at some critical value $(M_1/M_2)_c \sim S$. For other values of P, the system behavior keeps the same as long as P is larger than M_1/M_2. In Fig. 8.2b, around the same critical value of M_1/M_2, σ^2/N changes from a decreasing function to an increasing function, giving the smallest fluctuation in the population distribution at the critical point. Meanwhile, the order parameter J also falls to zero at $(M_1/M_2)_c$, suggesting that a phase transition, called the "M_1/M_2 phase transition," occurs at this critical point. To be more illustrative, when the environmental complexity is smaller than the critical value, the system could reside in an efficient, unpredictable, but relatively unstable state. Getting closer to the phase transition point, the stability of system will be improved until the most stable state is reached. Then after crossing the critical point, the decision-making capability of the whole system is exhausted and it will fall into an inefficient, predictable, and unstable state. At the vicinity of the critical point, as if participants of the game are worried about being eliminated from the competition, the market inspires all of its guiding potential and leads the system to the ideal state for resource allocation, a state that is both efficient and stable and where no unfair arbitrage chance can exist.

[2] Large fluctuations in populations can cause a higher dissipation in the system. Hence an efficient and stable state means an optimal state with a low waste in the resource allocation.

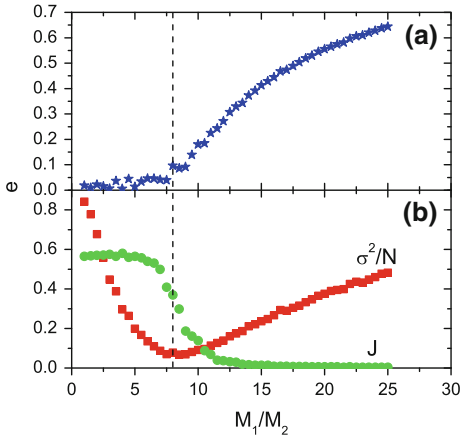

Fig. 8.2 The "M_1/M_2 phase transition" in MDRAG, for $N = 100$, $P = 64$, and $S = 8$. Simulations are run 300 times, each over 400 time steps (first half for equilibration, the remaining half for statistics). The *dashed line* denotes $M_1/M_2 = 8$. **a** e as a function of M_1/M_2. **b** σ^2/N and J versus M_1/M_2, respectively. Adapted from Ref. [7]

It is important to know that MDRAG and MG have totally different phase structures, which could be analyzed by comparing the $S - P$ contours of the descriptive parameters for the two models, see Fig. 8.3. From the analysis, we could also know how the decision-making capacity influences the overall performance of the resource allocation system, in case the environmental complexity is fixed ($M_1/M_2 = 4$). Features of the contour maps (Fig. 8.3) are summarized as the following (different M_1/M_2's do not change the conclusions):

(i) Comparing with the traditional MG as a whole, MDRAG has a much wider range of parameters for the availability of efficient, stable, and unpredictable states. In particular, there is almost no eligible region in Fig. 8.3a if we take the criterion of efficiency as $e < 0.08$. Also, the predictable region ($J < 0.02$) in Fig. 8.3f is smaller than the MG's results in Fig. 8.3c. These facts indicate that MDRAG has a better performance than MG as a resource allocating system.

(ii) Patterns of the contour maps suggest that MG and MDRAG have totally different dependencies on parameters. Figure 8.3a–c indicates that P and S are not independent in the traditional MG model, which confirms the previous findings [20]. On the other hand, in MDRAG, there is always a region where the system behavior is almost controlled by the parameter S. In Fig. 8.3d, for large enough P, the system can reach the efficient state if S exceeds a critical value S_p, where S_p will converge to the limit value M_1/M_2 with increasing P. For $S < S_p$, the system can never reach the efficient state no matter how P changes. For a very large P and $S < M_1/M_2$, it can be proved that the probability for agents to enter the richer room is $S/(S + 1)$, so that the system stays in the inefficient states ($\langle N_1\rangle/\langle N_2\rangle < M_1/M_2$).

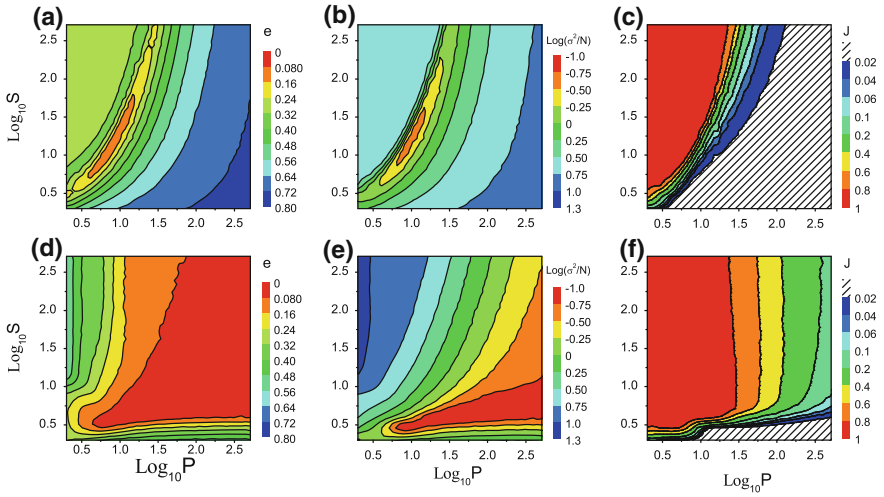

Fig. 8.3 $S - P$ contour maps for different parameters on log–log scales with $N = 80$ and $M_1/M_2 = 4$. For each data point, simulations are run 50 times, each over 400 time steps (first half for equilibration, the remaining half for statistics). **a–c** are e, σ^2/N, and J as functions of S and P in MG, respectively. **d–f** are e, σ^2/N, and J as functions of S and P in MDRAG, respectively. Regions filled with slash shadow denote the predictable states. Adapted from Ref. [7]

(iii) Observing Fig. 8.3d, f, one may find both an "S phase transition" and a "P phase transition." As mentioned above, for large enough P, the increase in S can abruptly bring the system from the inefficient/predictable phase to the efficient/unpredictable phase, which is called "S phase transition." On the other hand, in the narrow region where $S < M_1/M_2$, the increase in P can also produce a drastic change from the unpredictable to the predictable phase, which is called "P phase transition." The existence of the "S phase transition" can be explained by the fact that the number of available choices in decision-making is a key factor for agents to find the right choice from strategies with an adequate heterogeneity of preferences. But for $S \gg P$, it will also cause a slight decrease in the efficiency because of the conflicts in the different predictions from the equally good strategies with the same preference. This explains why "MDRAG, $S = 48$" performs worse than "MDRAG, $S = 8$" when $P = 16$ in Fig. 8.1. The "P phase transition" reflects that for some incompetent ability of choice deliberation, a critical value of the cognition ability can enhance the decision-making capacity to match the environmental complexity.

(iv) It is also noteworthy that the parameter $\alpha = 2^p/N$, which is the main control parameter in the MG model [1, 87], no longer controls the behavior of the MDRAG system. Varying N while keeping M_1/M_2 as a constant, the basic feature, especially the critical position of the contour maps, will remain unchanged.

In aspects of the competition for resources, the feed of global information and the inductive optimization of strategies, both MG and MDRAG may be regarded as eligible models for the economic experiments. However, MG fails to reproduce experimental results in most cases. By simply accommodating a broader preference distribution of the strategies, MDRAG fits the experimental results without any coordinating capability of the agents. This enables us to comment on the possible mechanism of the "invisible hand," and conditions under which the complex adaptive systems will spontaneously converge to the efficient states. The most important thing for the "invisible hand" to work is that different subjects of the economic games should have different preferences, just like the agents in the MDRAG model who have heterogeneous preferences in their strategies. Next, the subjects should also own an adequate capacity of decision-making which matches the complexity of the environment. From the M_1/M_2 phase transition in the MDRAG simulations, we could infer that there would be a failure in achieving the balanced efficient state if the game of experiment were designed too complicated, e.g., too many rooms or too biased distribution of the virtual money. Nevertheless, for the MDRAG model itself, since the model parameters can be tuned freely, we believe that the market directing power can always be brought out completely in this paradigm as long as the computational power is enough. To put it further, when the experiment happens to be set at the critical range of subjects' decision-making capacity, just like a finely tuned MDRAG where parameters are set to be critical values of the phase transitions mentioned above, an idealized state of the resource allocating system can be realized, namely the system is efficient, stable, and unpredictable. For example, see the overlapped regions for small e, small σ^2/N and finite J in Fig. 8.3d–f.

Finally, although these intriguing conclusions are supported by the results of MDRAG simulations, there are still some important effects in the real world not included in the model, such as the difference in the decision-making capacities among the agents and the agents' responses to changes of the environment. One challenging task is to consider a suitable relation between agents' behavior and the distribution of resources (M_1/M_2) which may have an influence on the dynamic behavior of the whole system.

Chapter 9
Business Cycles: Competition Between Suppliers and Consumers

Abstract Drastic fluctuations of economic indices (stock market indices, gross domestic product, inflation rates, etc.) are a common phenomenon from country to country. Such economic fluctuations often contain the periodicity of boom and bust, thus forming business cycles. Then searching for the origins of business cycles has received extensive attention in the literature. Although controlled human experiments in the laboratory offer a direct way to reveal causalities, researchers have seldom been able to use such experiments to directly study business cycles because of the complexity of human systems. Here we propose a free-competition market, which consists of two types of alternative products to trade with, and then recruit human subjects into the market to do a series of controlled experiments. Strikingly, business cycles emerge in this market, which is due to the endogenous competitions among the subjects (acting as suppliers and consumers) with heterogeneous preferences and a decision-making capacity that matches with environmental complexity. The accompanying agent-based simulations also confirm the emergence of business cycles, thus generalizing our experimental results beyond specific experimental conditions. Moreover, we reveal that by changing the adaptability level of agents, the business cycles undergo a new phase transition from a nonstationary fractional Brownian motion to a stationary fractional Gaussian noise. This chapter should be of value to different disciplines, such as physics, economics/finance, complexity science, and sociology.

Keywords Free competition market · Business cycle · Economic fluctuation · Phase transition

9.1 Opening Remarks

The preceding chapter helped to reveal a kind of cooperation, the invisible hand, in a single system. The mechanism lies in free competitions between subjects for sharing fixed amount of resources. But, what happens if the amount of resources is no longer

J.-P. Huang, *Experimental Econophysics*, New Economic Windows,
DOI 10.1007/978-3-662-44234-0_9

fixed? This is the topic of this chapter. We shall show the emergence of business cycles.

It is common sense that economic indices like gross domestic products, inflation rates, and stock market indices always evolve with fluctuations [59, 125, 126]. The fluctuations can be classified as noises and drastic fluctuations [48]. Noises are inevitable, which come from a large number of stochastic processes in human society; drastic fluctuations are caused by fundamental changes in a country's economy, which can lead to either a huge craze or a deep depression in the populations. Through a long historical view, one can see that drastic economic fluctuations usually form so-called business cycles with a periodicity of boom and bust [127, 128] (e.g., the bust may be closely related to the 1997 Asian financial crisis, the bursting of dot-com bubbles in 2001, or the recent subprime mortgage crisis which triggered the global recession of 2008). Clearly, to study the microscopic dynamics of business cycles is of particular importance [129]. First, it may uncover the general basic mechanisms under the evolutions of economic indices in different countries. Second, it may help to predict the emergence or the burst of bubbles so as to prevent economic crises. However, by reviewing the literature on business cycles, we find that most research has only studied some factors empirically that may affect the properties of business cycles [130, 131], or have put particular emphasis on technical methods of analyzing the time series of business cycles [50, 132]. Understanding the dynamics of business cycles is still far from satisfactory [129].

In the research on complex adaptive systems like human society, one can see that bottom-up modeling is usually an efficient method to study the microscopic dynamics under the macroscopic phenomena appearing in the systems [115, 133, 134]. Generally, microscopic entities in bottom-up modeling can either be real human subjects or virtual agents with artificial intelligence. The former participate in controlled human experiments [7, 9, 11], while the latter compose agent-based models [119, 135]. Due to the following reasons, we believe that the bottom-up approach is a reasonable choice to study business cycles as well. (1) For most products or financial assets, there are a large number of suppliers and consumers in the associated market. (2) The interactions among the suppliers and consumers are usually complex and cannot be easily described by simple stochastic processes. (3) Intuitively, business cycles are caused by fundamental changes in a country's economy. However, tracing back to the very beginning, it is the transformation of behaviors of the suppliers and consumers that leads to the overall changes in the economic indices.

Therefore, in this chapter, we design a free-competition artificial market with two types of alternative products to trade. The participants in the market are divided into two groups, namely suppliers and consumers. Every supplier chooses which type of products to produce, while every consumer has to decide on which to buy, in order to maximize his/her own utility. As mentioned above, the participants can be real human subjects or virtual agents. So, we recruit students from Fudan University and conduct a series of controlled experiments in this market. Then we also construct an associated agent-based model. In both the human experiments and the agent-based model, it is found that business cycles can be generated naturally through interactions among the

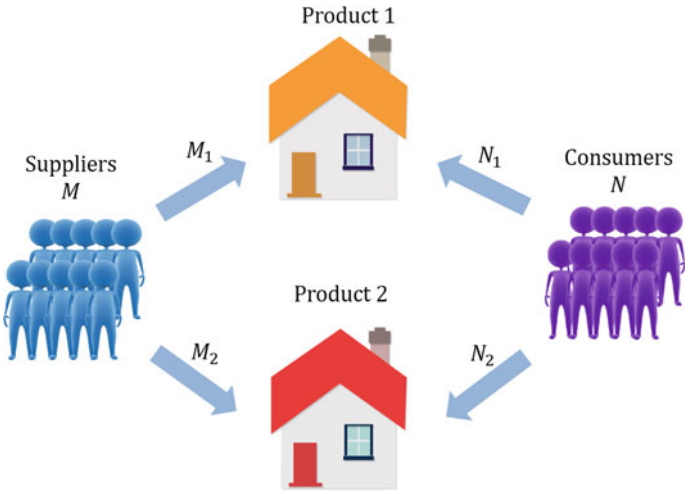

Fig. 9.1 A sketch showing the design of our artificial market. There are two types of products trading freely in the market, Product 1 and Product 2. Participants are divided into two groups, suppliers and consumers. Every supplier should choose which type of products to produce, while every consumer has to decide which to buy. Obviously, to maximize their own utilities, suppliers prefer to produce those products that sell at a higher price, while consumers like to buy those that come cheaper. Adapted from Ref. [136]

participants. Thanks to the flexibility of the agent-based modeling method, we also investigate the influence of agents' adaptability on the generation of business cycles in the simulations. Interestingly, by changing the adaptability level of agents, it is shown that business cycles undergo a phase transition from a nonstationary fractional Brownian motion to a stationary fractional Gaussian noise. This may help us to better understand the microscopic dynamics of business cycles in human society.

9.2 The Design of an Artificial Market

Figure 9.1 shows a sketch of our market design. To order to wipe off unrelated factors in the study of business cycles, we built a simple free-competition artificial market described as follows.

1. The market is an isolated system without interference from outside. Hence, if the phenomenon of business cycles emerges in this system, it can only be attributed to the interactions among the market subjects.
2. There are two types of alternative products in the market, Product 1 and Product 2, which can be traded freely. The word "alternative" here means that the general functions of the two types of products can be seen as nondistinctive, for example,

umbrella and raincoat, desktop computer and laptop computer, similar stocks in the same stock sector, etc.

3. The subjects in the market are divided into two groups, suppliers and consumers. The total number of suppliers is denoted as M, while N is the total number of consumers. The suppliers can choose the type of products to produce, while the consumers can decide which to buy. The number of suppliers for Product 1 or Product 2 is denoted as M_1 or M_2 respectively with $M = M_1 + M_2$. Similarly, the number of consumers for Product 1 or Product 2 is N_1 or N_2 with $N = N_1 + N_2$.
4. We assume that one supplier produces one unit of the type of products he/she chooses, and one consumer only purchases one unit of the associated type of products. Hence, M_1 (or N_1) denotes the amount of supply (or demand) for Product 1, while M_2 (or N_2) represents the amount of supply (or demand) for Product 2.
5. Since the two types of products are alternatives, it is obvious that $M_1/N_1 = M_2/N_2$ is the balanced state for the market. If $M_1/N_1 > M_2/N_2$, Product 1 is cheaper than Product 2. Hence, in this situation, suppliers producing Product 2 and consumers buying Product 1 make the right choices. In contrast, for $M_1/N_1 < M_2/N_2$, suppliers for Product 1 and consumers for Product 2 are the winners because now Product 2 is cheaper. For the two types of products, it is clear that, to maximize their own utilities, suppliers prefer to produce that which sells at a higher price, while consumers like to buy that which is cheaper.
6. The time in the market is discretized. One time step may represent 1 week, 1 month, etc. Every consumer has to decide the type of products to purchase at each time step. However, suppliers cannot alter their product lines so frequently, thus they will make a choice at a longer timescale. This setting is specified later in the description of our human experiments and agent-based simulations.
7. To eliminate herd effects in the market, we rule that at each time step subjects should make decisions independently, which means no kind of communication is allowed.

9.3 Human Experiments and Results Analyses

9.3.1 Scenario of Human Experiments

Here we describe the specific settings of our controlled human experiments. In the experiments, about 50 students from Fudan University were recruited to trade in our market via a local area network (the number of subjects has small fluctuations because a few students joined in the middle of the experimental process, which in fact does not affect the final statistical results). The students were randomly assigned to two groups, suppliers and consumers, before the experiment started. As mentioned above, consumers make a choice at every time step. For suppliers, the experiment is

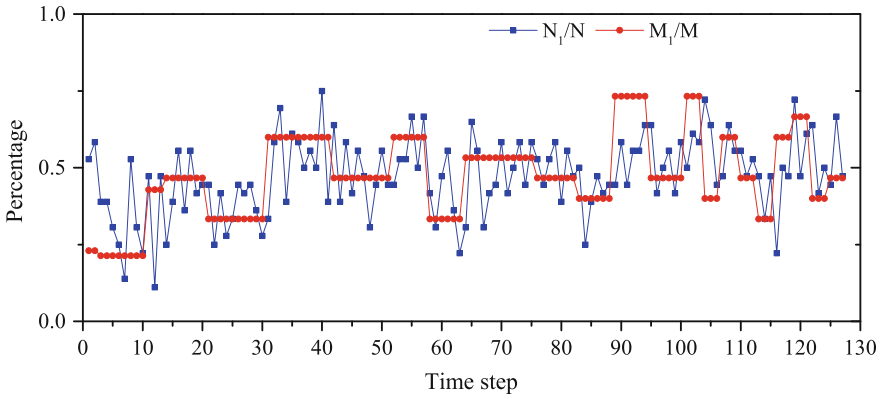

Fig. 9.2 The results of the controlled human experiments. *Blue* points stand for the percentage of consumers who decide to buy Product 1 (i.e., N_1/N), while *red* for that of suppliers to produce Product 1 (i.e., M_1/M). In the experiment, ΔT is set as 10, 6, and 3 accordingly for the three successive stages. There are several errors caused by students who attend in the middle of the experiments. Due to technical problems, from Round 31 there should be one round of 10 time steps followed, but in fact the round was conducted by actually 11 time steps; similarly, from Round 76, there should be one round of 6 time steps but actually the round had 7 time steps. However, it should be noted that these errors did not affect the statistical results of the experiments. Adapted from Ref. [136]

divided into three stages, each of which lasts about 40–50 time steps. In each stage, we define one round as ΔT time steps. The suppliers can choose the type of products to produce at the beginning of one round and then they should produce one unit of the products at one time step until the round ends. The values of ΔT for the three stages in a series are set as 10, 6, and 3 accordingly, in the experiments. At every time step, the suppliers choosing to produce the type of products that sell at a higher price, or the consumers buying the other type of products that come cheaper, get one point each. To give the subjects incentives for better performance, we announced before the experiments that the students could exchange their total points into cash and the top 3 subjects could also win an additional cash reward after finishing all the experiments. After several warm-up steps for the students to get familiar with the market rules, our experiments were finally conducted for 127 time steps.

Figure 9.2 shows the evolution of the percentage of consumers to buy Product 1 (i.e., N_1/N) as well as the percentage of suppliers to produce Product 1 (i.e., M_1/M) during the 127 experimental time steps. It can be seen that N_1/N fluctuates around M_1/M regardless of how M_1/M changes after each round. One can also see that a rise in the value of M_1/M in one round is usually followed by a drop in its value in the next round. To make the patterns of N_1/N and M_1/M clearer, more data processing is carried out in the next two subsections.

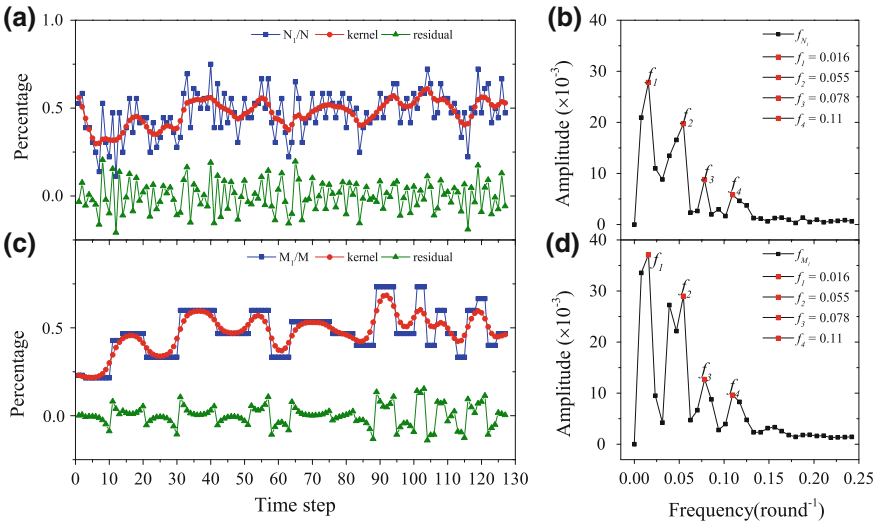

Fig. 9.3 The smoothing regression and the frequency spectrum analysis on the experimental data. **a** and **c** show the local linear kernel regression results for the two experimental time series, N_1/N and M_1/M (shown in *blue*), respectively. The smooth kernel part $f(t)$ (shown in *red*) and the noisy residual part ε_t (shown in *green*) are separated from the two original series accordingly. **b** and **d** show the spectral analysis results for the two series. The prominent peaks, f_2, f_3 and f_4, are trivial because they are related to the round length ΔT set manually in the experiments. However, the smallest frequency f_1 is intrinsic which emerges only from the interactions among the human subjects. Adapted from Ref. [136]

9.3.2 Smoothing Regression

As mentioned above, fluctuations can be classified as noises and drastic fluctuations. To check whether business cycle phenomenon exists in the experimental time series of N_1/N and M_1/M, it is obvious that noises should be eliminated at first from the two series accordingly. Therefore, here we adopt the linear kernel smoothing method, which is commonly used in image processing to obtain the regression results for the two time series as shown in Fig. 9.3 (details of the linear kernel smoothing method can be found in Part I of Supplementary Materials at the end of this chapter). In Fig. 9.3a and c, the "residual" part separated by the smoothing method shows the noises and the extracted "kernel" part gives the nontrivial information about the drastic fluctuations for the two series respectively. Next, we analyze the "kernel" parts of the two time series to find business cycles.

9.3.3 Frequency Spectrum

Spectral analysis is adopted here to find whether business cycles emerge in the two experimental time series of N_1/N and M_1/M. By using the discrete Fourier transform (see Part II of Supplementary Materials) on the extracted kernel parts, we finally obtain the frequency spectrums for the two series as shown in Fig. 9.3b and d. The prominent peaks are labeled by the corresponding frequency values in the two subfigures. It should be noted that f_2, f_3, and f_4 in the two subfigures are trivial because these frequencies are related to the round length ΔT which is set previously as 10, 6, and 3 successively, with an approximate relation of $f_i = \frac{1}{2\Delta T}$, for $i = 2, 3, 4$. However, the smallest frequency $f_1 = 0.016$ (round^{-1}) in the two subfigures refers to an intrinsic periodicity under the two kernel series respectively. Hence, we call this frequency the intrinsic frequency, which emerges only from the interactions among the human subjects.

Although business cycle phenomenon shows clearly in our controlled human experiments, it should be noted the experiments inevitably have some shortages. First, the number of human subjects and the time steps conducted in the experiments are limited. Second, the round length ΔT is set manually by the directors of the experiments, but a better way should be that suppliers can decide ΔT on their own. To overcome these shortages, we further build an agent-based model accordingly on the market which is discussed in the following section.

9.4 Agent-Based Modeling and Results Analyses

9.4.1 Agents' Decision-Making Process

The decision-making process for the agents in our model is modified based on that in the market-directed resource allocation game [1, 7, 11]. Before trading in the market, every agent should create S strategies first. A particular strategy is shown in Table 9.1. The left column represents the P situations and the right offers the associated choice, one for Product 1, and zero for Product 2. For each agent's S strategies, he/she will first draw a random integer L from the range [0, P], and then fill 1 in the "Choice" column with a probability of L/P and hence zero with $(P - L)/P$. At a time step, a situation P_i is drawn randomly from the range [1, P] to represent the current situation. If an agent's strategy gives the right choice under the situation at this time step (namely, for suppliers, the strategy suggests to sell the type of products with a higher price, or for consumers, to buy the other type that comes cheaper), the performance of the strategy will be added one point accordingly whether it is used or not. Every supplier or consumer will use his/her highest-scored strategy when he/she has to make decisions in the market. And if there is more than one strategy that ties for the best performance, the agent will randomly choose one from them.

Table 9.1 A particular strategy

Situation	Choice
1	0
2	1
3	0
.	.
.	.
.	.
$P-1$	1
P	1

Similar to the human experiments, consumers in the agent-based model should choose which type of products to buy at each time step. However, artificial suppliers will have the ability to determine the round length ΔT on their own. It is easy to understand that if the market is generally in the balanced state, namely $M_1/N_1 = M_2/N_2$, no supplier can gain any excess profits any longer, so now the suppliers will prefer to make a change. Therefore, we define an arbitrage index (AI) [137, 138] for the suppliers, which is derived from the Shannon entropy (Sect. 2.5), as $AI = 1 + \sum_{i=1}^{2} p_i \log_2 p_i$, where $p_i = \frac{\langle M_i/N_i \rangle}{\langle M_1/N_1 \rangle + \langle M_2/N_2 \rangle}$ and $\langle \ldots \rangle$ stands for the average of $\ldots$ from the last time step denoted as t_r when the suppliers are able to make new choices to the current time step t. Clearly, $AI \in [0, 1]$ and a lower value of AI means that the market is closer to the balanced state. In the model, we suppose that suppliers will make new choices from the two types of products once the value of AI drops below a warning value.

The numbers of suppliers and consumers are set equally in all the simulations, namely $M = N = 100$. For the same parameter settings (i.e., the values of S and P, and the warning value of AI) of the model, a simulation with 5,000 time steps will be repeated 20 times to do the statistical analyses. Figure 9.4 shows segments of N_1/N and M_1/M series from time step 3,000 to 4,000 with $S = P = 32$ with the warning value of AI being 0.2. The patterns are similar to what we have seen for the experimental results in Fig. 9.2. By applying the linear kernel smoothing method on the simulated N_1/N and M_1/M series, we obtain Fig. 9.5a and c. The "kernel" parts also show a degree of periodicity in the two series. In order to show the periodicity clearly in the frequency domain, we again use the discrete Fourier transform on the "kernel parts" of the two series. Several prominent peaks are shown in Fig. 9.5b and d which indicate that business cycle phenomenon can also occur in our agent-based model. We can see that the smallest peak frequency (i.e., f_1 in the Fig. 9.5b and d) is much lower than the ones in the experimental results (as shown in Fig. 9.3b and d), which is due to the different adaptability levels of the human subjects and virtual agents. Besides, the warning value of AI can also affect the simulated business cycles, which will be discussed in the analyses followed.

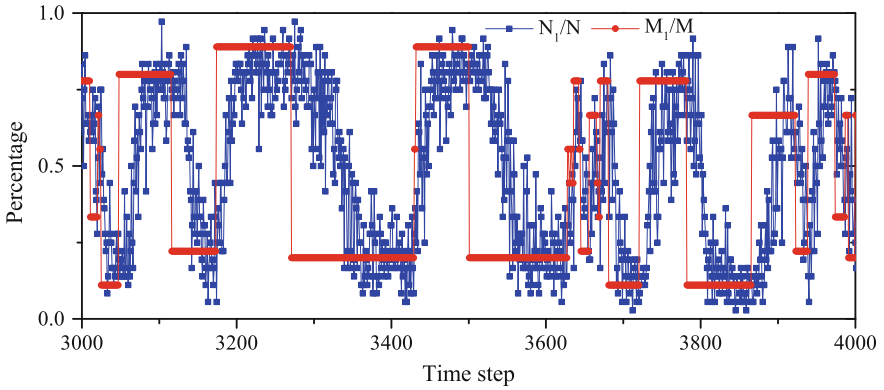

Fig. 9.4 The N_1/N and M_1/M series generated by our agent-based model with $S = 32$, $P = 32$ and the warning value of AI being 0.2. The simulation results are only shown from time step 3,000 to 4,000 here. Adapted from Ref. [136]

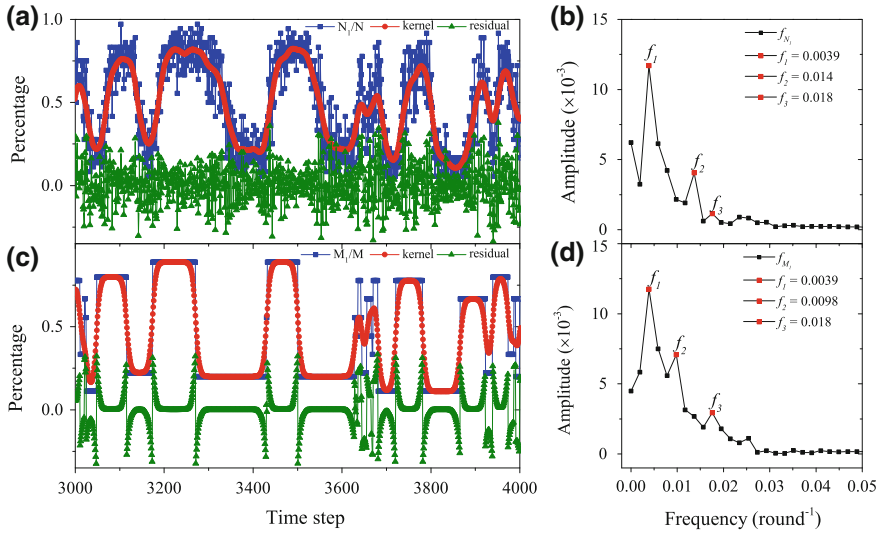

Fig. 9.5 The smoothing regression and frequency spectrum analysis on the simulated data. **a** and **c** show the local linear kernel regression results for N_1/N and M_1/M series respectively (shown in *blue*). The smoothed kernel parts are shown in *red* and the noisy residual parts are in *green*. **b** and **d** show the spectral analysis results for the two series. Each prominent peak is also labeled in the two subfigures. Adapted from Ref. [136]

9.4.2 Stationarity Analysis

Because we are able to obtain data with much longer time steps in the simulations than in the human experiments, more analyses can be done on the simulated series of

N_1/N and M_1/M. Besides the previous adopted discrete Fourier transform method, we also employ Periodogram method (see Part III of Supplementary Materials) to analyze the "kernel" parts of the two series.

We know that a power-law noise, such as the pseudo-random process following the fractional Brownian motion (fBm) or the fractional Gaussian noise (fGn), has a power spectrum density that satisfies $A(f) \sim 1/f^{\beta}$ [139, 140]. For a process of fBm, the exponent β is greater than one, which means that the process is nonstationary with strong persistence. In contrast, for a process of fGn, there is $\beta < 1$, which has a property of stationarity. Therefore, $\beta = 1$ becomes the boundary between the two types of processes with different natures.

Figure 9.6a and c show the simulated N_1/N series for two sets of S and P. We then calculate the values of the exponent β for the two series using the Periodogram method, and it can be seen in Fig. 9.6b and d that the model with $S = 60$ and $P = 180$ is of the fGn process and the other model with $S = 180$ and $P = 60$ belongs to the fBm process. Clearly, the business cycle phenomenon is more apparent in the fBm process than in the fGn. Note that the parameters S and P represent the number of strategies that an agent holds and that of possible situations he/she could face, respectively. Obviously, a larger value of S alongside a smaller value of P stands for a higher adaptability level of the agents compared to the environments around them. Therefore, we can conclude that the adaptability level of the agents can affect the stationarity and cyclicity of the system.

9.4.3 Phase Transitions

As we mentioned above, the warning value of AI can affect the properties of business cycles. So here we first try to check how the warning value influences the exponent β. As shown in Fig. 9.7, by increasing the warning value of AI, β abruptly drops from the upper part with values greater than one to the lower part smaller than one. This means a phase transition occurs from the fBm state to the other fGn state. The difference between the models with the two different parameter settings is that the model in which agents have higher adaptability level reaches the transition point at a bigger warning value of AI.

To further investigate the effect of the adaptability level of the agents on the properties of business cycles, we draw a contour map to show the relation between β and various S and P values as in Fig. 9.8. The warning value of AI is set as 0.2 for all the simulations. Transitions between the fBm and fGn phases for our agent-based simulations are clearly shown at the two sides of the critical line $\beta = 1.00$. Compared to the agents in the fGn phase, agents in the fBm phase generally have a higher value of S alongside a lower value of P, which represents a higher adaptability level.

Therefore, we conclude that the model consisting of agents with higher adaptability level (i.e., larger S values alongside with small P values) can generate more apparent business cycle phenomenon with nonstationary fBm process (shown in

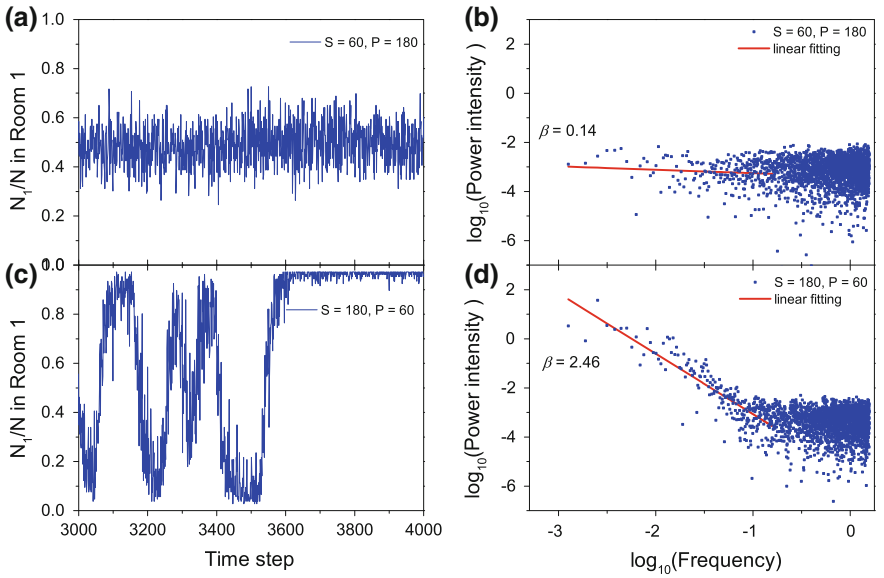

Fig. 9.6 Effect of the values of S and P on the business cycle properties for the simulated time series. The parameters used in (**a**) are: $S = 60$, $P = 180$. And the ones used in (**c**) are: $S = 180$, $P = 60$. The warning value of AI is set as 0.2 in both simulations. Each figure depicts one of 20 simulations with corresponding parameters. Only the time steps from 3,000 to 4,000 are displayed. Clearly, series in (**a**) and (**c**) are of different natures. The former is fGn and the latter is fBm, given the values of β shown in (**b**) and (**d**) using the Periodogram method. Since the tail part in (**b**) or (**d**), roughly accounted for 90 % of the total points, is meaningless for our statistics, we neglect this tail part when we do the linear fitting to get the value of β accordingly [141]. For 20 times simulations with parameters $S = 60$ and $P = 180$, averaged $\beta = 0.14 \pm 0.09$, and for that with $S = 180$ and $P = 60$, averaged $\beta = 2.45 \pm 0.08$. Adapted from Ref. [136]

Figs. 9.6 and 9.8), and the associated business cycles are more robust to the changes in the warning value of AI for the suppliers in the model.

9.5 Conclusions

In this chapter, an artificial market with two types of alternative products has been designed to study the microscopic dynamics under the business cycle phenomenon. First, we have conducted a series of controlled human experiments and found that the business cycles can be generated only through interactions among human subjects.

To overcome the shortages in the human experiment method, we have then designed an agent-based model on the market accordingly. In the simulations, it has been confirmed again that business cycles can emerge only from the agents' interactions. By raising the adaptability level of the agents, phase transitions have been found from the stationary fGn (fractional Gaussian noise) state to the nonsta-

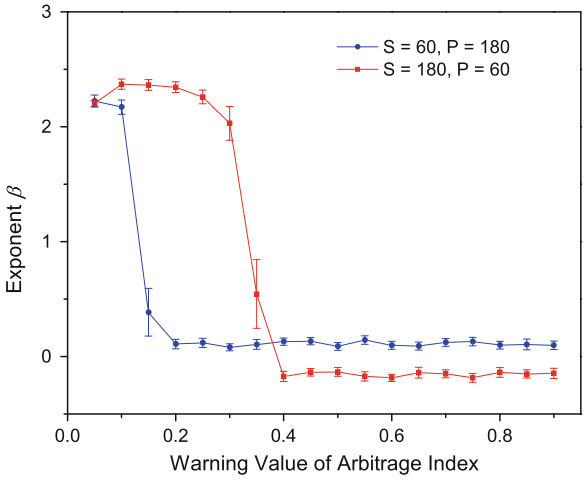

Fig. 9.7 The relation between the warning value of AI and the exponent β for the corresponding simulated series. The *blue points* show the results for the model with $S = 60$ and $P = 180$, and the red for the model with $S = 180$ and $P = 60$. It is clearly shown that when increasing the warning value, the phases of both the models transfer from the process of fBm to fGn, although with different transition points. Error bars indicate standard errors in 95 % confidence level. Adapted from Ref. [136]

tionary fBm (fractional Brownian motion) state. Compared with the fGn state, the business cycle phenomenon in the fBm state is more apparent and also more robust with respect to the changes in the warning value of AI (Arbitrage Index).

In further research, an information generator can be added into the market to broadcast good or bad news related to the products, for the purpose of investigating the effect of the exogenous market information on the business cycles. Besides, the herd effect on business cycles can also be studied in the framework of our market. The market can also be modified to contain more types of products for participants to trade with. Obviously, these modifications can be easy to carry out thanks to the flexibility in the nature of the bottom-up approach.

Finally, this chapter is of value to a range of different disciplines such as economics, social science, complexity science, and physics. Through this chapter, one can see that the combination of controlled human experiments and agent-based models have the potential to become a rigorous method to study the underlying dynamics in complex human systems.

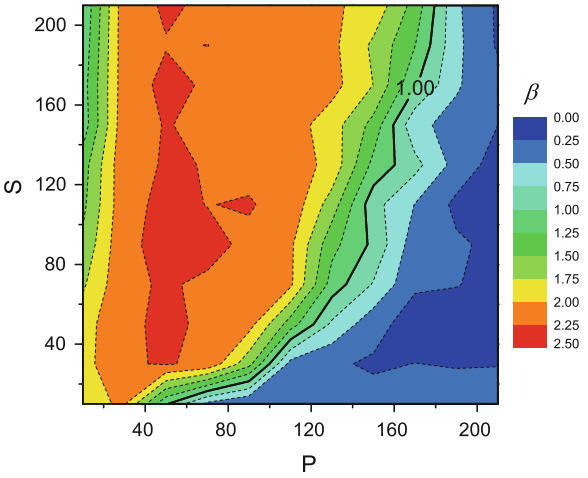

Fig. 9.8 The contour map for the relation between the exponent β and the model parameters S and P. The warning value of AI is set as 0.2 for all the simulations. The critical line of $\beta = 1.00$ is shown in the map which separates the two different phases (*black solid line*). The area above the critical line is the fBm phase with mostly $S > P$, which indicates the associated agents have a high level of adaptability. And the area under the critical line is the fGn phase with mostly $S < P$, and the agents here are inclined to make choices randomly because of their low adaptability. Adapted from Ref. [136]

9.6 Supplementary Materials

9.6.1 Part I: Local Linear Kernel Regression

This regression works the same as the Hodrick-Prescott filter (Sect. 2.6). Its details are as follows.

The most popular smoothing method is the moving average method. From the idea of moving average, centered moving average has been developed. Similarly, a kernel used to distribute weights has also been developed for smoothing regression. Thus, the local linear kernel regression is also called the kernel smoothing regression derived from k-nearest-neighbors (kNN) algorithm [142].

For our human experimental series with T time steps, denoted as y_t, $t = 0, \ldots, T-1$, this regression can be represented as $y_t = f(t) + \varepsilon_t$, where $f(t)$ is an estimate for the nonparametric regression of y_t and ε_t stands for noise fluctuations [143]. Different from the kNN algorithm using the moving average value of the k nearest neighbors for the corresponding data y_0 at each time t_0, the local linear kernel regression fits these data with an optimum linear function, $\hat{f}(t_0) = \hat{\alpha}(t_0) + \hat{\beta}(t_0) \cdot t_0$, and a specific kernel function, $K_h(\frac{t_j - t_0}{h})$, $j = 1, \ldots, k$. The h in the kernel function denotes the bandwidth, standing for the distance between the core data and its furthest neighbor. Usually, a kernel function for estimating or regression, which is

nonnegative, continuous, symmetric, real-valued, and integrates to one, determines the weight distribution of the core data's neighbors. In addition, given that logistic distribution is commonly used for modeling discrete choices [144] and it has heavier tails and more distinct robustness [145], we use $K_h(u) = (e^u + 2 + e^{-u})^{-1}$ as the kernel function instead of normal distribution. Eventually, the local linear regression process can be interpreted by solving a minimizing problem,

$$\min_{\alpha(t_0),\beta(t_0)} \sum_{j=1}^{k} K_h(\frac{t_j - t_0}{h})(y_j - \alpha(t_0) - \beta(t_0) \cdot t_j).$$

Hence, the solved regression function $\hat{f}$ differs with respect to the bandwidth h. In fact, if it lacks smoothness, $\hat{f}$ has bigger variance and lower bias. Otherwise, if it smoothes too much, $\hat{f}$ has smaller variance but higher bias instead. To balance the tradeoff, it is required to minimize the mean squared error, namely

$$\text{MSE}(\hat{f}) = \text{Bias}^2(\hat{f}) + \text{Variance}(\hat{f}).$$

Using the estimating method from Bowman and Azzalini [143], the optimal h_{opt} can be calculated by, $h_{\text{opt}} = \sqrt{h_y \cdot h_t}$, where the h_y and h_t satisfy the following formula:

$$h_m = \left(\frac{4}{3T}\right)^{\frac{1}{5}} \frac{\text{median}(|m - \text{median}(m)|)}{0.6745},$$

where m denotes the y or t series. After obtaining the optimal bandwidth substitute it into the former minimizing problem to get the associated smoothed series. Compared with Gaussian kernel function, the logistic kernel can make the extracted series smoother with the assurance of the minimum of MSE.

9.6.2 Part II: Discrete Fourier Transform

Since the 1960s, mathematicians, statisticians, and economists have published enormous articles to discuss the application of the spectral analysis in economics [125]. The fundamental idea of the spectral analysis is that, the economic time series are believed to be the composition of a large number of sine waves with different frequencies. The discrete Fourier transform is one of these spectral analysis methods. The discrete Fourier transform converts a time series from the time domain into the frequency domain with the aim to analyze the frequency components in that series.

For our human experimental series with T time steps, i.e., $y_t, t = 0, \ldots, T-1$, the transformed series $f(k), k = 0, \ldots, T-1$, can be obtained by the discrete Fourier transform below, and the inverse transform expression is also shown as follows:

$$f(k) = \sum_{t=0}^{T-1} y_t e^{\frac{2\pi}{T} itk}, 0 \leq k \leq T-1,$$

$$y_t = \frac{1}{T} \sum_{k=0}^{T-1} f(k) e^{-\frac{2\pi}{T} ikt}, 0 \leq t \leq T-1.$$

9.6.3 Part III: Periodogram Method

The periodogram method also converts a series from the time domain into the frequency domain like the discrete Fourier transform. Actually, it shows the power spectrum density of the signal series. In signal processing, for a power-law noise such as fractional Brownian motion (fBm) and fractional Gaussian noise (fGn), its power spectrum density is proportional to $1/f^{\beta}$. β stands for the color of a signal as an exclusive exponent. It can be calculated as

$$A(f) = \frac{1}{2\pi T} \left| \sum_{t=0}^{T-1} y_t e^{itf} \right|^2.$$

It gives the frequencies density distribution, where f stands for frequency and $A(f)$ for its amplitude. Actually, $A(f)$ is proportional to $f^{-\beta}$, indicating a power law, so a linear fitting for a log–log periodogram can be used to get the coefficient β.

Chapter 10
Partial Information: Equivalent to Complete Information

Abstract It is a common belief in economics and social science that if there is more information available for agents to gather in a human system, the system can become more efficient. The belief can be easily understood according to the well-known efficient market hypothesis. In this work, we attempt to challenge this belief by investigating a complex adaptive system, which is modeled by a market-directed resource-allocation game with a directed random network. We conduct a series of controlled human experiments in the laboratory to show the reliability of the model design. As a result, we find that even under partial information, the system can still almost reach the optimal (balanced) state, which was demonstrated as a result of complete information in Chap. 8. Furthermore, the ensemble average of the system's fluctuation level goes through a continuous phase transition. This behavior means that in the second phase if too much information is shared among agents, the system's stability will be harmed instead, which differs from the belief mentioned above. Also, at the transition point, the ensemble fluctuations of the fluctuation level remain at a low value. This phenomenon is in contrast to the textbook knowledge of continuous phase transitions in traditional physical systems, namely fluctuations will rise abnormally around a transition point since the correlation length becomes infinite. Thus, this work is of potential value to a variety of fields, such as physics, economics, complexity science, and artificial intelligence.

Keywords Resource-allocation system · Partial information · Complete information · Balanced state · Continuous phase transition

10.1 Opening Remarks

In Chaps. 5–9, each subject always knows the overall competition results of all the other subjects, which is defined as complete information herein. In reality however, one often makes decisions according to the result of a part of a crowd (which is defined as partial information in this chapter), rather than on the complete information. So,

J.-P. Huang, *Experimental Econophysics*, New Economic Windows,
DOI 10.1007/978-3-662-44234-0_10

it becomes interesting to know the different effect of partial information. This is the topic of the present chapter.

It is well known in statistical physics that there exist a lot of phase transition phenomena, e.g., the melting of ice (classified as first-order phase transition) and the superfluid transition (classified as second-order phase transition); both second-order and higher order phase transitions are also called continuous phase transitions [38]. In complex adaptive systems, phase transition phenomena can be seen as well [7, 87, 146–148].

In economics and social science, it is a common belief that if more information is distributed to agents, the associated system will be more efficient (here "more efficient" means that the system is easier to lie in the optimal state and also the fluctuation level of the system is lower). For example, the famous Efficient Market Hypothesis [149] implies that market efficiency will be higher if more information is available to investors, i.e., efficiency upgrading from the weak form to the strong form [149, 150]. In this chapter, we recheck this information effect in a complex adaptive system related to resource-allocation problems [1, 7–10, 151] as these problems are of particular importance. For instance, some believe governments should get involved to guarantee that resources are distributed to places where they are needed the most, while others think markets can use the invisible hand [28] to ensure the efficiency of resource allocation [28, 152]. Both agent-based simulations and controlled human experiments have been adopted to discuss these problems. In the associated artificial system, the invisible hand phenomenon emerges as well [7]. In previous research [7], all subjects could get access to global information to evaluate their strategies. However, in many real problems, global information is either difficult to collect or is confidential. For example, when a company hesitates whether or not to step into an emerging market, it is hard to know all the other competitive companies' reactions and, also, it would take a long time to learn about the real return on investment. Therefore, the company can only draw up its own strategies under the currently obtained partial information. This leads to the question: when market participants obtain only partial information, can the invisible hand still work in the market?

To model this question, agents in our system are connected via a directed random network and everyone evaluates his/her own performance through partial information gathered from his/her first-order neighborhood. It is obvious that a higher connection rate can make the system more information-concentrated. Our agent-based model is designed on the basis of the market-directed resource allocation game [7], which can be used to simulate the biased or unbiased resource distribution problems. We also conduct a series of controlled human experiments to show the reliability of the model design. We find that the system can reach the optimal (balanced) state even under a small information concentration. Furthermore, when the information concentration increases, the ensemble average of the fluctuation level goes through continuous phase transition, which means that in the second phase, agents getting too much information will harm the system's stability (a higher fluctuation level means a lower stability of the system). This is contrary to the belief mentioned above (namely, it will be better for market efficiency when more information is shared). At the transition point, the ensemble fluctuations of the fluctuation level remain low. We

also show that when the system becomes infinitely large, this fluctuation transition phenomenon remains. Our finding is in contrast to the textbook knowledge about continuous phase transitions, which states fluctuations will rise abnormally around a transition point since the correlation length becomes infinite. Thus, we call this continuous phase transition *anomalous continuous phase transition*.

10.2 Agent-Based Modeling

To proceed, let us first introduce the abstract resource allocation system of interest. The system contains a repeated game. In the game, there are N agents facing two rooms labeled Room 1 and Room 2. Each room has a certain amount of resources, denoted as M_1 and M_2 accordingly, and let $M = M_1 + M_2$. Both M_1 and M_2 are fixed during the repeated game. It can be seen that our system is more general than the famous minority game [1]; in the minority game [1], values of M_1 and M_2 are the same, which is only the case of unbiased resource distribution. Agents decide at each time step on which room to enter and then divide the resources in it evenly. Here, the number of agents entering Room 1 or Room 2 at a time step is marked as N_1 or N_2 respectively ($N = N_1 + N_2$). Obviously, the goal for every agent is the same, namely to choose the room from where they can obtain more resources. The values of M_1 and M_2 are unknown to all the agents. They cannot know the global values of M_1/N_1 and M_2/N_2 at each time step in the game either, which is the amount of resources actually distributed to one agent in each room. So an agent can only evaluate his/her performance by viewing information from his/her acquaintances. In the model, every agent has a probability of k to make another agent into his/her group (for convenience of description, the agent himself/herself is also included in the group). Hence, the agents form a directed random network that is fixed during the game. At each time step, suppose in Agent i's group, there is $M_1/N_1^i \geq M_2/N_2^i$, where N_1^i or N_2^i is the number of agents in his/her group that enter Room 1 or Room 2. As a result, for Agent i, Room 1 is the winning room. However, in other agents' eyes, Room 2 may be the winning room according to the information from their own groups. It is obvious that if $k = 1$, all the agents can obtain global information. As k decreases, the information an agent can get becomes less and less, compared to the global information. Particularly, $k = 0$ means Agent i's group has only himself/herself inside. So now Agent i obtains no information from the other agents. Therefore, we may say that the value of k represents the system's information concentration, $0 \leq k \leq 1$. Note that our system's framework is closer to reality than that of [153]. In [153], market states are not affected by agents' production or exchange behaviors so that an agent can even get the exact information about what state the market will be in before his/her decision is made.

As regards our agent-based model, what is left is the design of agents' decision-making process. In order to test our system under a variety of M_1/M values, we adopt the design from the market-directed resource allocation game [7], which models biased or unbiased resource distribution problems satisfactorily. In the model, every

Table 10.1 A particular strategy. Adapted from Ref. [154]

Exogenous situation	Choice
1	0
2	1
3	1
.	.
.	.
.	.
P − 1	0
P	1

agent will create S strategies before the game starts. Every strategy has two columns and one is shown in Table 10.1. The left column is P exogenous situations (here exogenous situations mean a combination of endogenous situations, i.e., history tracks of the winning room one agent observes, and the other situations that affect one agent's decisions. It was shown in [124] that statistical properties are almost the same for models that use either exogenous or endogenous situation strategies). For every situation, the right column offers a choice, respectively, and here number 1 is for the choice of Room 1 and 0 for the choice of Room 2. When an agent creates a strategy, he/she will first randomly choose a number L from 0 to P and then fill the number 1 in the right column of the strategy with a probability of L/P, and so 0 with a $(P - L)/P$ probability (here we can see the difference in strategy creation process between the market-directed resource allocation game [7] and the minority game [1]. In the minority game, the right column of a strategy is filled in by 1 or 0 with equal probabilities, i.e., both with a probability of 0.5). The strategies are fixed once they are created before the game start. At each time step, a particular exogenous situation will be picked randomly from 1 to P. Every agent will use his/her highest-scored strategy to choose rooms under the current situation. After each time step, every agent will then assess the performance of his/her strategies based on the partial information obtained from his/her group. For example, to Agent i, if Room 1 is winning, all his/her strategies that offer the right choice at the given situation will be added one point. In the simulations, we set $S = 8$ and $P = 16$. Based on the former theoretical analysis [8], it can be calculated that now $(\langle N_1\rangle/N)_{\max} = 1 - \frac{1}{P}\sum\_\tilde{L} = 1^P\left[\left(\frac{\tilde{L}}{P+1}\right)^S\right] = 0.911$. And for $M_1/M \leq (\langle N_1\rangle/N)_{\max}$, namely $M_1/M \leq 0.911$, the system in which agents all get access to global information (i.e., $k = 1$) can reach the optimal (balanced) state where $\langle N_1\rangle/N = M_1/M$. Here $\langle\cdots\rangle$ denotes the time average of $\cdots$. Hence, we vary the value of M_1/M from 0.667 to 0.9 in the simulations.

At the beginning of a repeated game, every agent randomly creates his/her S strategies and a directed network is also linked stochastically. Then this micro-structure is fixed during the game. Therefore, in our simulations, the concept of ensemble is used to analyze the average properties of the systems that have the same parameter settings but with different micro-structures.

10.3 Controlled Experiments

It is well known that for a targeted system, there can be many different designs in the agent-based modeling method. Thus, how to validate a model is crucial. One way is to compare simulated results with field data [83, 155–159]; the other is to do controlled experiments in laboratory systems [7, 8–10, 160]. In this research we prefer the latter, and recruited 25 students from the Department of Physics at Fudan University as the human subjects. The game settings are the same as our agent-based model except that artificial agents are now replaced by human subjects. Two kinds of money rewards are provided to give the subjects incentives: (A) Each subject will be given one virtual point if he/she chooses the right room at each time step, and after the experiments, the accumulative virtual points a subject wins will be exchanged for cash in the ratio: 1 point = 1 Chinese Yuan; (B) Bonuses of 150, 100, and 50 Chinese Yuan are also offered to the three best-performed subjects, respectively. The rules and rewards are made clear to the students before the experiments [30]. A round of repeated pre-games with 15 time steps is also offered to the students to let them become familiar with the rules. Each set of parameters (i.e., k and M_1/M) is then carried out to the students for one round with 15 time steps. Note that each set of k's and M_1/M's values is selected randomly before each round of repeated game so that the students can hardly figure out whether his/her experience gained in the last game can be used in the next one.

10.4 Results

The blue stars in Fig. 10.1 show the ensemble average of $\langle N_1\rangle/N$ versus M_1/M under four different values of k for 50 simulated systems. The error bars represent standard deviation (denoted as SD_m) among the 50 systems' $\langle N_1\rangle/N$ values. The experimental results are given in Tables 10.2, 10.3, 10.4 and 10.5. For each set of k and M_1/M, $\langle N_1\rangle/N$ (represented as red circles in Fig. 10.1) is calculated on the last five experimental time steps to avoid relaxation time. In both simulations and experiments, $N = 25$. Deviations between the simulated and experimental results in each sub-figure (denoted as Dev) are defined as the average of $|(\langle N_1\rangle/N)_e - (\langle N_1\rangle/N)_m|/SD_m$ over all the points (here $|\cdots|$ denotes the absolute value of $\cdots$; the subscript m stands for the simulations and e for the experiments). For the four sub-figures, the values of Dev are (a) 2.33, (b) 1.56, (c) 1.81, and (d) 2.71, respectively. Suppose in the simulated ensemble, $\langle N_1\rangle/N$ follows a Gaussian distribution, then the experimental values of $\langle N_1\rangle/N$ fall in (a) 98 %, (b) 88.2 %, (c) 93 %, and (d) 99.4 % confidence interval accordingly. In the experiments, there always exist some uncontrolled factors such as mood swings of the students during the games. So for Fig. 10.1, it can be said that our agent-based model is a good mimic of the human system. Thanks to the flexibility of the agent-based modeling method, we further extend the number of agents to $N = 1{,}001$ and the ensemble size to 500. The

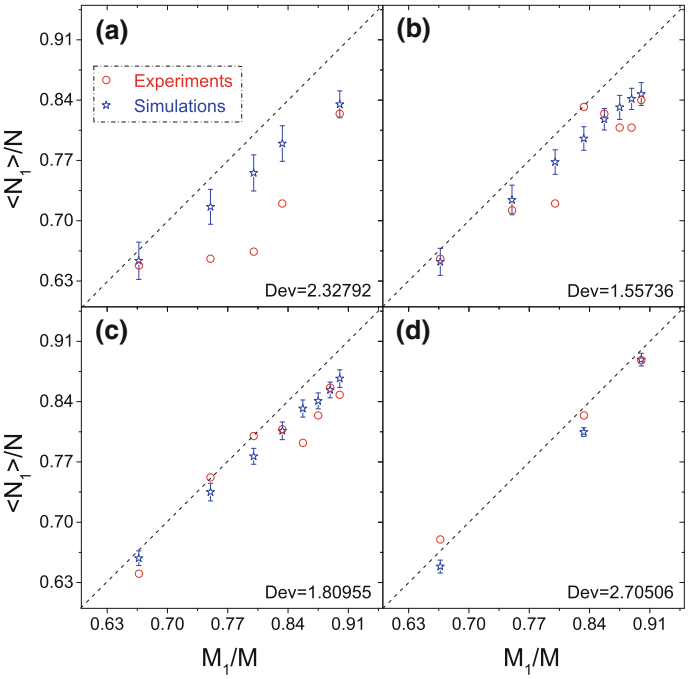

Fig. 10.1 $\langle N_1\rangle/N$ versus M_1/M for $k =$ **a** 0.2, **b** 0.52, **c** 0.76, and **d** 1. The simulated ensemble contains 50 systems, each of which has the same parameters: $N = 25$, $S = 8$, and $P = 16$. Each system evolves for 600 time steps (the first half for stabilization which is enough for system relaxation and the second half for statistics). The *blue stars* show the ensemble average of $\langle N_1\rangle/N$ and error bars are added. The *red circles* show the experimental results and for each data point, one system with the associated parameters is conducted for 15 time steps and $\langle N_1\rangle/N$ is calculated on the last 5 time steps shown in Tables 10.2, 10.3, 10.4 and 10.5 to avoid the relaxation time steps. The number of human subjects recruited in the laboratory system is the same as the simulations, i.e., $N = 25$. The *diagonal dash line* with slope = 1 indicates the optimal (balanced) state: $\langle N_1\rangle/N = M_1/M$. Adapted from Ref. [154]

simulated $\langle N_1\rangle/N$ versus k is shown in Fig. 10.2. It can be seen that even for a small value of information concentration, e.g., $k = 0.2$, the system can still reach the optimal (balanced) state where $\langle N_1\rangle/N = M_1/M$. This means that the invisible hand can still influence the system when only a small part of information is distributed to every agent.

For the system discussed in Fig. 10.2, the other important property is the fluctuation level which is given as

$$\text{Var} = \frac{1}{2N}\sum_{i=1}^{2}\langle(N_i - \langle N_i\rangle)^2\rangle \equiv \frac{1}{N}\langle(N_1 - \langle N_1\rangle)^2\rangle. \tag{10.1}$$

Table 10.2 Experimental data of N_1/N's under different values of M_1/M for $k = 0.2$ within the 15 time steps

Time step	$M_1/M = 0.667$	$= 0.75$	$= 0.8$	$= 0.833$	$= 0.9$
1	0.6	0.56	0.56	0.72	0.8
2	0.6	0.68	0.68	0.76	0.8
3	0.64	0.72	0.64	0.68	0.8
4	0.56	0.6	0.76	0.64	0.72
5	0.68	0.76	0.76	0.76	0.84
6	0.64	0.6	0.76	0.76	0.76
7	0.52	0.76	0.72	0.76	0.84
8	0.6	0.68	0.72	0.72	0.76
9	0.6	0.48	0.64	0.76	0.84
10	0.56	0.68	0.72	0.68	0.8
11	0.64	0.64	0.84	0.76	0.76
12	0.68	0.56	0.64	0.68	0.84
13	0.56	0.72	0.64	0.72	0.88
14	0.68	0.72	0.56	0.76	0.84
15	0.68	0.64	0.64	0.68	0.8
Average	0.648	0.656	0.664	0.72	0.824

The last 5 time steps are taken to calculate the time average value of N_1/N (denoted as "Average" in the table), i.e., $\langle N_1 \rangle / N$ shown in Fig. 10.1. Adapted from Ref. [154]

Table 10.3 Experimental data of N_1/N's under different values of M_1/M for $k = 0.52$ within the 15 time steps

Time step	$M_1/M = 0.667$	$= 0.75$	$= 0.8$	$= 0.833$	$= 0.857$	$= 0.875$	$= 0.889$	$= 0.9$
1	0.64	0.64	0.56	0.8	0.76	0.8	0.76	0.88
2	0.6	0.68	0.72	0.48	0.76	0.64	0.76	0.6
3	0.6	0.6	0.68	0.72	0.88	0.76	0.76	0.72
4	0.68	0.68	0.8	0.76	0.68	0.84	0.84	0.88
5	0.52	0.64	0.72	0.84	0.84	0.8	0.76	0.72
6	0.72	0.84	0.72	0.52	0.72	0.64	0.84	0.84
7	0.64	0.68	0.72	0.68	0.8	0.76	0.76	0.68
8	0.44	0.88	0.72	0.84	0.84	0.84	0.76	0.8
9	0.56	0.6	0.72	0.68	0.6	0.8	0.8	0.84
10	0.68	0.8	0.72	0.76	0.72	0.76	0.76	0.76
11	0.68	0.68	0.68	0.88	0.76	0.68	0.72	0.72
12	0.56	0.68	0.72	0.84	0.8	0.76	0.84	0.84
13	0.64	0.8	0.64	0.8	0.84	0.88	0.8	0.84
14	0.68	0.76	0.76	0.84	0.88	0.84	0.84	0.92
15	0.72	0.64	0.8	0.8	0.84	0.88	0.84	0.88
Average	0.656	0.712	0.72	0.832	0.824	0.808	0.808	0.84

The last 5 time steps are taken to calculate the time average value of N_1/N, i.e., $\langle N_1 \rangle / N$ shown in Fig. 10.1. Adapted from Ref. [154]

Table 10.4 Experimental data of N_1/N's under different values of M_1/M for $k = 0.76$ within the 15 time steps

Time step	$M_1/M = 0.667$	$= 0.75$	$= 0.8$	$= 0.833$	$= 0.857$	$= 0.875$	$= 0.889$	$= 0.9$
1	0.52	0.8	0.8	0.76	0.84	0.64	0.84	0.68
2	0.88	0.44	0.64	0.84	0.6	0.84	0.64	0.8
3	0.6	0.64	0.8	0.76	0.88	0.76	0.8	0.8
4	0.56	0.76	0.68	0.72	0.68	0.8	0.8	0.88
5	0.76	0.64	0.64	0.88	0.72	0.8	0.8	0.76
6	0.68	0.76	0.76	0.72	0.84	0.88	0.8	0.84
7	0.6	0.68	0.68	0.8	0.8	0.72	0.92	0.88
8	0.56	0.68	0.84	0.76	0.68	0.84	0.8	0.8
9	0.72	0.68	0.68	0.8	0.88	0.76	0.84	0.88
10	0.52	0.6	0.76	0.72	0.8	0.72	0.76	0.84
11	0.6	0.76	0.8	0.76	0.92	0.68	0.8	0.76
12	0.68	0.76	0.76	0.88	0.92	0.84	0.84	0.88
13	0.64	0.76	0.76	0.8	0.64	0.88	0.8	0.96
14	0.68	0.68	0.84	0.84	0.64	0.88	0.92	0.8
15	0.6	0.8	0.84	0.76	0.84	0.84	0.92	0.84
Average	0.64	0.752	0.8	0.808	0.792	0.824	0.856	0.848

The last 5 time steps are taken to calculate the time average value of N_1/N, i.e., $\langle N_1 \rangle / N$ shown in Fig. 10.1. Adapted from Ref. [154]

Table 10.5 Experimental data of N_1/N's under different values of M_1/M for $k = 1$ within the 15 time steps

Time step	$M_1/M = 0.667$	$= 0.833$	$= 0.9$
1	0.6	0.8	0.8
2	0.88	0.76	0.88
3	0.8	0.76	0.8
4	0.6	0.8	0.84
5	0.68	0.72	0.72
6	0.6	0.76	0.92
7	0.64	0.88	0.84
8	0.68	0.8	0.84
9	0.64	0.64	0.6
10	0.64	0.72	0.76
11	0.68	0.8	0.8
12	0.68	0.84	0.92
13	0.64	0.84	0.92
14	0.68	0.8	0.88
15	0.72	0.84	0.92
Average	0.68	0.824	0.888

The last 5 time steps are taken to calculate the time average value of N_1/N, i.e., $\langle N_1 \rangle / N$ shown in Fig. 10.1. Adapted from Ref. [154]

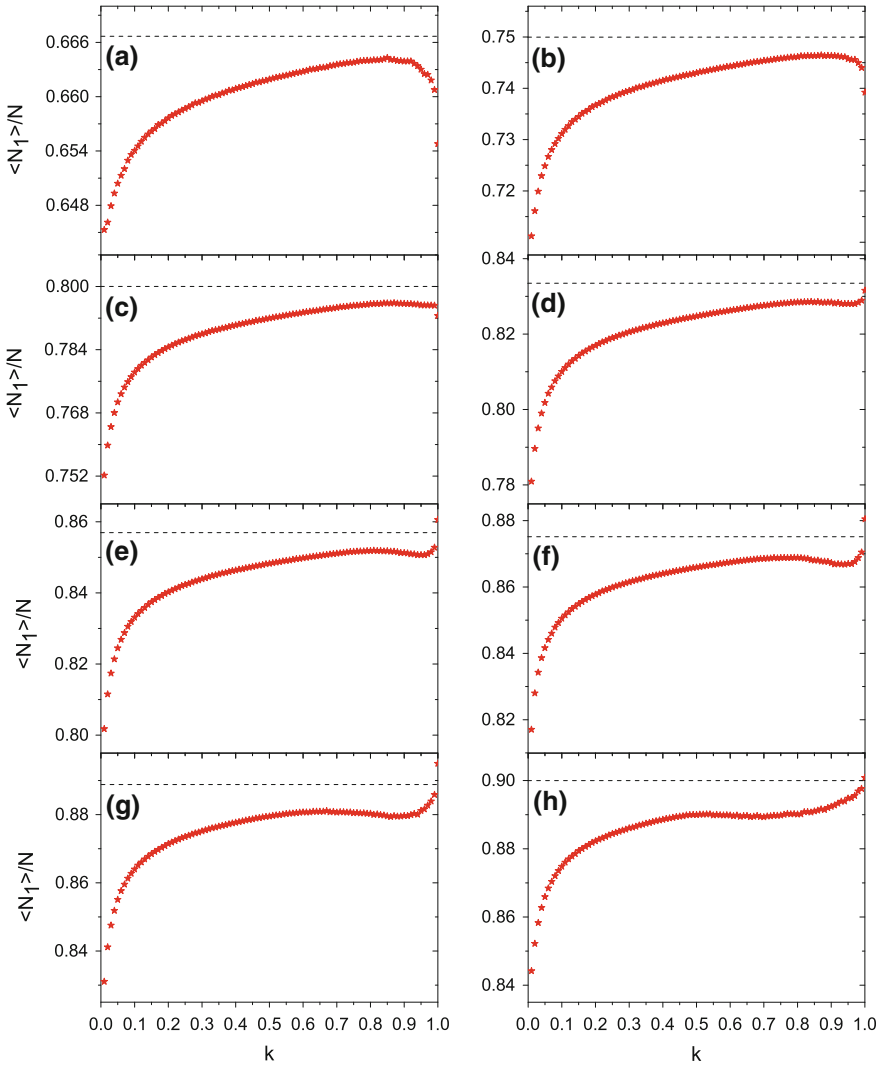

Fig. 10.2 Simulated results of $\langle N_1\rangle/N$ versus k for different values of M_1/M. The values of $\langle N_2\rangle/N$ are not shown here because of $\langle N_2\rangle/N = 1 - \langle N_1\rangle/N$. The ensemble contains 500 systems each of which has the same parameters: $N = 1{,}001$, $S = 8$, and $P = 16$. Each system evolves for 600 time steps (the first half for stabilization which is enough for system relaxation and the second half for statistics). The *horizontal dash line* shows the value of $\langle N_1\rangle/N$ for the optimal (balanced) state: $\langle N_1\rangle/N = M_1/M$. Adapted from Ref. [154]

The ensemble average of the simulated system's fluctuation level, denoted as Mean(Var), is shown in Fig. 10.3. It can be seen that Mean(Var) declines slightly when information concentration k increases from zero. This is normal due to the following reason: as k increases, Agent i's group becomes larger, and then the infor-

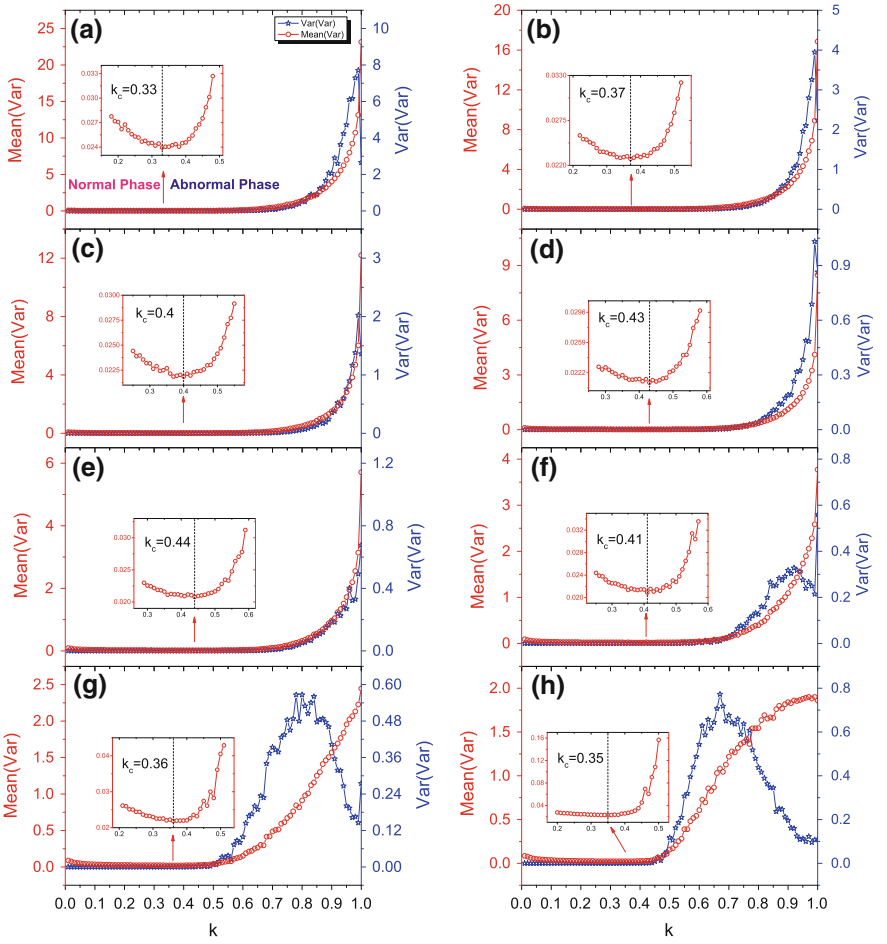

Fig. 10.3 Fluctuations in the simulated system. For the eight M_1/M values, the ensemble averages of the fluctuation level (denoted as Mean(Var)) under different k values are represented by *red circles*, while *blue stars* are for the ensemble fluctuations of the fluctuation level (denoted as Var(Var)). Mean(Var) goes through a continuous phase transition from a normal phase to an abnormal phase as k increases. The insets give detailed information around the transition point (k_c stands for the critical value of k) accordingly. The ensemble contains 500 systems, each of which has the same parameters: $N = 1{,}001$, $S = 8$, and $P = 16$. Each system evolves for 600 time steps (the first half for stabilization which is enough for system relaxation and the second half for statistics). Adapted from Ref. [154]

mation he/she obtains at every time step will be more stable, which makes Agent i more certain about his/her choices. Hence, we interpret it as a normal phase. But after that, Mean(Var) climbs up abnormally, which means that now agents getting more information will be more harmful to the system's stability (a higher fluctuation level means a lower stability of the system); this is in contrast to the belief that more infor-

mation is better, so we interpret this as an abnormal phase. This phenomenon can be explained by the following feedback process. For $k = 1$, because of the full network connection, uncertainties in Agent i's choice can be transferred to all the other agents and increase their own uncertainties, and then the other agents' uncertainties will be again transferred back to Agent i and further increase his/her choice fluctuations. However, when k decreases from 1, owing to the presence of the directed network, for one acquaintance in Agent i's group, he/she may not have Agent i in his/her own group. This means the uncertainties of Agent i cannot be fully transferred to his/her group members now, so the overall fluctuation level will decrease. Hence, here a continuous phase transition between a normal phase and an abnormal phase comes to appear as k increases from 0 to 1. The lowest Mean(Var) point is labeled as the transition point and the associated critical value of k is denoted as k_c. Detailed information around the transition point is shown in the insets of Fig. 10.3.

In the traditional continuous phase transition theory [38], it is stated that around a transition point, fluctuations will increase heavily since the correlation length becomes infinite. On the contrary, in Fig. 10.3, it can be seen that at the transition point, the ensemble fluctuations of the fluctuation level, denoted as Var(Var), remain at a low value, which is only of magnitude 10^{-5} versus Mean(Var) being 10^{-2}. However, at the abnormal phase where k is large, Var(Var) has a great rise as k increases, and for $M_1/M \geq 0.875$, Var(Var) even begins to decline obviously when k increases further.

The above phase transition phenomenon comes to appear in our system that contains a limited number of agents. So we attempt to analyze the relation between k_c and N. Because the critical information concentration k_c shows no relation to M_1/M in Fig. 10.3, we average it over different values of M_1/M and obtain $\overline{k}_c$. Figure 10.4 displays a power-law relation between $\overline{k}_c$ and N in the tail (i.e., for $N \geq 401$) as $\overline{k}_c = 50 * N^{-0.71}$. Hence, when the system becomes infinitely large, i.e., $N \to +\infty$, there still exists this anomalous phase transition at $\overline{k}_c \to 0^+$.

10.5 Discussion and Conclusions

In this chapter, we have designed an agent-based model with partial information for biased resource-allocation problems. A series of controlled human experiments have been conducted to show the reliability of the model design. We have found that even for a small information concentration, the system can still reach the optimal (balanced) state. Furthermore, we have found that the ensemble average of the simulated system's fluctuation level has a continuous phase transition. This means that in the abnormal phase, too much information can hurt the system's stability. Hence, back to the question raised at the beginning, we can say that markets are able to use the invisible hand most efficiently only at the transition point where partial information is obtained by agents.

On the other hand, at the transition point, the ensemble fluctuations of the fluctuation level remain low. When increasing the number of agents, the critical value of in-

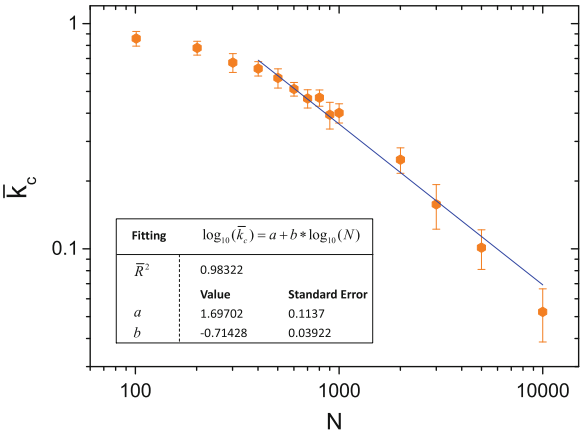

Fig. 10.4 A log–log plot showing $\bar{k}_c$ versus N. Here, $\bar{k}_c$ is the average of k_c's under different values of M_1/M. For each value of N, the ensemble contains 50 systems each of which has the same parameters: $S = 8$ and $P = 16$. Each system evolves for 600 time steps (the first half for stabilization which is enough for system relaxation and the second half for statistics). The *blue line* fits the tail of the data (i.e., from $N = 401$ to $N = 10{,}001$) according to $\log_{10}(\bar{k}_c) = a + b * \log_{10}(N)$; details are given in the inset where the regression coefficient, $\bar{R}^2 = 0.98322$, indicates well fitting of the tail since $\bar{R}^2 = 1.0$ means a perfect fit [161]. Error bars are added as well. Adapted from Ref. [154]

formation concentration obeys a power-law decay in the tail. This behavior confirms that when the system becomes infinitely large, there still exist this kind of fluctuation transition phenomena. This finding is in contrast to the textbook knowledge of continuous phase transitions also addressed at the beginning, namely fluctuations will rise abnormally around a transition point since the correlation length becomes infinite. This may pave the way for investigating the role of human adaptability in further developing traditional physics.

Therefore, this chapter is expected to be of value to various fields ranging from physics, economics, complexity science to artificial intelligence.

Chapter 11
Risk Management: Unusual Risk-Return Relationship

Abstract For survival and development, autonomous agents in complex adaptive systems involving the human society must compete against or collaborate with others for sharing limited resources or wealth, by using different methods. One method is to invest, in order to obtain payoffs with risk. It is a common belief that investments with a positive risk-return relationship (namely high risk high return and vice versa) are dominant over those with a negative risk-return relationship (i.e., high risk low return and vice versa) in the human society; the belief has a notable impact on the daily investing activities of investors. Here we investigate the risk-return relationship in a model complex adaptive system, in order to study the effect of both market efficiency and closeness that exist in the human society and play an important role in helping to establish traditional finance/economics theories. We conduct a series of computer-aided human experiments, and also perform agent-based simulations and theoretical analysis to confirm the experimental observations and reveal the underlying mechanism. We report that investments with a negative risk-return relationship have dominance over those with a positive risk-return relationship instead in such complex adaptive systems. We formulate the dynamical process for the system's evolution, which helps to discover the different role of identical and heterogeneous preferences. This work might be valuable not only to complexity science, but also to finance and economics, to management and social science, and to physics.

Keywords Resource-allocation system · Risk-return relationship · Preference · Dynamic process

11.1 Opening Remarks

Subjects in all kinds of laboratory markets, introduced in Chaps. 3–10, are always facing risks. In this chapter, we shall show the relationship between risk and return by studying a laboratory market.

J.-P. Huang, *Experimental Econophysics*, New Economic Windows,
DOI 10.1007/978-3-662-44234-0_11

For survival and development, agents in various kinds of complex adaptive systems (CASs) involving human society must compete against or collaborate with each other for sharing limited resources or wealth, by utilizing different methods. One of the methods is to invest, in order to obtain payoffs with risk. Accordingly, understanding the risk-return relationship (RRR) is of both academic value and practical importance. So far this relationship has a two-fold character. On one hand, investments are considered as high risk high return and vice versa; the RRR is positive (risk-return tradeoff) [162, 163]. This is also an outcome of the traditional financial theory under the efficient market hypothesis. On the other hand, some investments are found high risk low return and vice versa; the RRR is negative (Bowman's paradox) [164, 165]. However, almost all investment products take "high risk high return" as a bright spot to attract investors, and neglect the possible existence of "high risk low return". This actually results from a received belief that investments with a positive RRR are dominant over those with a negative RRR in the human society; the belief directs investors to operate investing activities including gambling [166]. Here we investigate the RRR by designing and investigating a model CAS which includes the following two crucial factors:

- *Market efficiency.* The present system exhibits market efficiency at which it reaches a statistical equilibrium [8, 7]. We shall address more relevant details at the end of the next section.
- *Closeness.* The system involves two conservations: one is the population of investors (Conservation I), the other is wealth (Conservation II). Regarding Conservation I/II, we fix the total number/amount of the subjects/wealth in the system. Clearly the two factors have real traces in human society. Accordingly they have played an important role in helping to establish traditional finance/economics theories. The present designing system just allows us to investigate the joint effect of the two factors on the RRR.

11.2 Controlled Experiments

On the basis of the CAS, we conducted a series of computer-aided human experiments. Details are as follows. There are two virtual rooms, Room 1 and Room 2 (represented by two buttons on the computer screen of the subjects), for subjects to invest in. The two rooms have volumes M_1 and M_2, which may represent the arbitrage space for a certain investment in the real world. For the experiments, we recruited 24 students from Fudan University as subjects. These subjects acted as fund managers, who were responsible for implementing investing strategy of the fund and managing its trading activities. We told the subjects the requirement of total 30 rounds for every single M_1/M_2, and offered every subject 1,000 points (the amount of virtual money constructs the fund managed by the subject) as his/her initial wealth for each M_1/M_2. In an attempt to make the subjects maximize their pursuit of self-interest, we promised to pay the subjects Chinese Yuan according to a

fixed exchange rate, 100:1 (namely, one hundred points equal to one Chinese Yuan), at the end of the experiments, and to offer every subject 30 Chinese Yuan as a bonus of attendance. Extra 50 Chinese Yuan would be given to the subject who gets the highest score for a single M_1/M_2. At the beginning of the 1st round of each M_1/M_2, we told the 24 subjects the value of M_1/M_2, and asked each subject to decide his/her investing weight [signed as $x(i)$ for Subject i]. Note the investing weight, $x(i)$, is the percentage of his/her investing wealth (investment capital) with respect to his/her total wealth, and it will keep fixed within the 30 rounds for a certain M_1/M_2. In each round, each subject can only invest in one of the two rooms independently. After all the subjects made their decisions, with the help of the computer program, we immediately knew the total investments in each room (signed as W_1 and W_2 for Room 1 and Room 2, respectively) in this round. While keeping the total wealth conserved, we redistributed the total investment $W_1 + W_2$ according to the following two rules:

(1) We divided the total investment, $W_1 + W_2$, by the ratio of M_1 and M_2, yielding $(W_1 + W_2)\frac{M_1}{M_1+M_2}$ and $(W_1 + W_2)\frac{M_2}{M_1+M_2}$ as the payoff for Room 1 and Room 2, respectively.
(2) We redistributed the payoff of Room k ($k = 1\,or\,2$) by the investment of the subjects. Namely, for each round, the payoff for Subject i choosing Room k to invest in, $w_{\text{payoff}}(i)$, is determined by $w_{\text{payoff}}(i) = (W_1 + W_2)\frac{M_k}{M_1+M_2} \times \frac{w_{in}(i)}{W_k}$, where $w_{in}(i)$ is the investing wealth of Subject i, $w_{in}(i) = x(i)w(i)$. Here $w(i)$ is the total wealth possessed by Subject i at the end of the previous round.

Before the experiments, we told the subjects the above two rules for wealth reallocation. After each round, every subject knows his/her payoff, $w_{\text{payoff}}(i)$. If there is $w_{\text{payoff}}(i) > w_{in}(i)$, that is, Subject i gets more than the amount he/she has invested, we consider Subject i as a winner at this round. Equivalently, if $\frac{W_1}{M_1} < \frac{W_2}{M_2}$, the subjects choosing Room 1 to invest in win. Clearly, when $\frac{W_1}{W_2} = \frac{M_1}{M_2}$, every subject obtains the payoff which equals to his/her investing wealth. Namely, the arbitrage opportunity has been used up. Accordingly, we define the $\frac{W_1}{W_2} = \frac{M_1}{M_2}$ state as an equilibrium (or balanced) state [1]. This state may have some practical significance because global arbitrage opportunities for investing in the human society always tend to shrink or even disappear once known and used by more and more investors. As shown in Fig. 11.1 (as well as Table 11.1), our experimental system can indeed achieve $\langle W_1/W_2\rangle \approx M_1/M_2$ at which the system automatically produces the balanced allocation of investing wealth; this system thus reaches a statistical equilibrium. In other words, the "Invisible Hand" plays a full role [7], or alternatively the system exhibits market efficiency. That is, all subjects are pursuing self-interest and we run the present system under three conditions: with sufficient information (namely, the wealth change for each round reflects the possible information), with free competition (i.e., no subjects dominate the system and there are zero transaction costs), and without externalities (the wealth change of a subject reflects the influence of his/her behavior on the others).

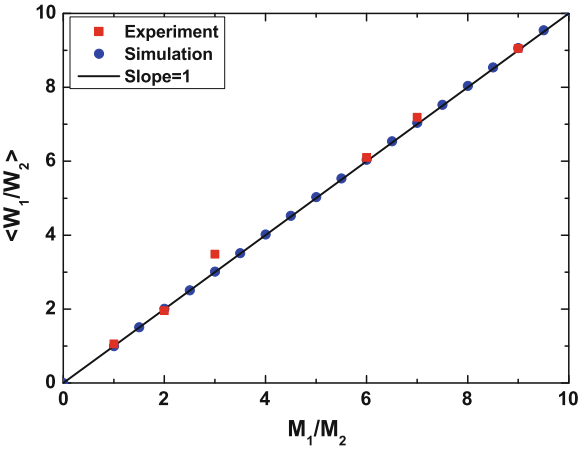

Fig. 11.1 Averaged ratio, $\langle \mathbf{W_1}/\mathbf{W_2} \rangle$, versus $\mathbf{M_1}/\mathbf{M_2}$ for the human experiments with 24 subjects (*red squares*) and agent-based computer simulations with 1,000 agents (*blue dots*). Here "$\langle \cdots \rangle$" denotes the average over the total 30 experimental rounds (experimental data of W_1/W_2 for each round are shown in Table 11.1) or over the 800 simulation rounds (the additional 200 rounds were performed at the beginning of the simulation for each $M1/M2$; during the 200 rounds, we train all of the strategies by scoring them whereas the wealth of each agent remains unchanged). All the experimental and simulation points lie on or beside the diagonal line ("slope $= 1$"), which is indicative of $\langle W_1/W_2 \rangle \approx M_1/M_2$. Parameters for the simulations: $S = 4$ and $P = 16$. Adapted from Ref. [10]

If a subject chooses a large investing weight, he/she will invest more virtual money in a room. According to the rules of our experiment, the room he/she chooses will then be more likely to be the losing one. Besides, the initial wealth is the same for every subject and he/she knows nothing about the others. From this point of view, the larger investing weight he/she chooses, the higher risk (or uncertainty) he/she will take for the fund (i.e., the initial 1,000 points). Therefore, throughout this chapter, we simply set the investing weight, $x(i)$, to equal the risk he/she is willing to take. Here we should remark that the present definition of risk appears to be different from that in financial theory. For the latter, one often defines risk according to variance. Nevertheless, these two "risk"s are essentially the same because they both describe the uncertainty of funds and have a positive association with each other. On the other hand, we should mention that the risk for each subject does not change with the evolution of time. This is a simplification which makes it possible to discuss the pure effect of a fixed value of "risk". Nevertheless, if we choose to let the "risk" change with the time, for the same purpose, we may take an average of the "risk" over the full range of time. Figure 11.2a–f displays the risk-return relationship for the investments in the designing CAS. From statistical point of view, we find that investments with a negative RRR are dominant over those with a positive RRR in the whole system.

Table 11.1 Experimental data of W_1/W_2's for six M_1/M_2's within 30 rounds. Adapted from Ref. [10]

Round	$M_1/M_2 = 1$	$M_1/M_2 = 2$	$M_1/M_2 = 3$	$M_1/M_2 = 6$	$M_1/M_2 = 7$	$M_1/M_2 = 9$
1	1.247723	1.143654	5.267782	2.98977	24.41429	2.146853
2	0.582237	0.702725	1.717598	11.02642	6.827457	4.860541
3	0.759914	1.897306	2.43237	10.32266	11.25343	11.30546
4	1.903253	1.240914	2.699907	2.97036	5.688661	9.681926
5	1.940527	1.564242	3.999681	3.977399	6.546176	5.249869
6	1.4852	4.711605	2.815152	6.900399	5.13295	6.16301
7	0.71966	2.087147	8.280381	2.991117	9.27272	7.25918
8	0.675138	1.692307	4.590899	3.35285	7.12301	8.996662
9	1.029128	2.73341	1.833477	4.363129	4.329496	7.133701
10	0.867554	2.095702	3.063358	7.273544	8.198398	14.26918
11	1.50125	1.305197	3.862686	18.23372	5.927536	5.500789
12	0.846259	2.292878	3.826587	8.50234	4.673143	5.141253
13	0.629585	1.992493	5.31337	4.613084	13.47519	34.4646
14	0.784858	2.462247	4.687499	19.73941	4.867279	3.889573
15	1.484235	1.807911	2.991726	3.40541	9.820732	7.442826
16	2.309969	1.544355	3.301258	4.864645	19.63957	15.74645
17	1.01251	2.078769	1.009523	8.219743	4.389477	11.55617
18	0.987891	2.624829	1.531467	2.935522	6.684373	8.712361
19	1.319123	2.25104	2.29988	3.813827	6.655679	6.623739
20	0.872338	2.045779	3.140856	5.690231	9.253236	7.973963
21	1.166773	2.006077	5.282071	5.889009	5.021116	5.825073
22	0.896165	1.419159	3.53215	6.137386	7.409623	8.32772
23	0.872224	2.141954	2.629218	11.09127	7.033376	15.57089
24	1.275063	1.990766	4.722947	5.989491	7.216511	10.87512
25	0.695696	2.151347	3.410795	7.790409	8.787551	4.759215
26	1.149307	2.150258	3.400615	8.213546	6.472158	13.14246
27	1.379602	1.621164	5.898509	5.078065	6.915495	7.992252
28	0.809361	1.62651	2.421057	3.698009	5.514453	11.76899
29	0.772988	1.670855	3.576442	7.848631	7.483899	16.27463
30	0.367173	2.010509	2.90843	11.10609	8.9996	4.854004

11.3 Agent-Based Modelling

Obviously the human experiments have some unavoidable limitations: specific time, specific avenue (a computer room of Fudan University), specific subjects (students from Fudan University), and the limited number of subjects. Now we are obliged to extend the experimental results (Fig. 11.2a–f) beyond such limitations. For this purpose, we resort to an agent-based model [1, 4, 115].

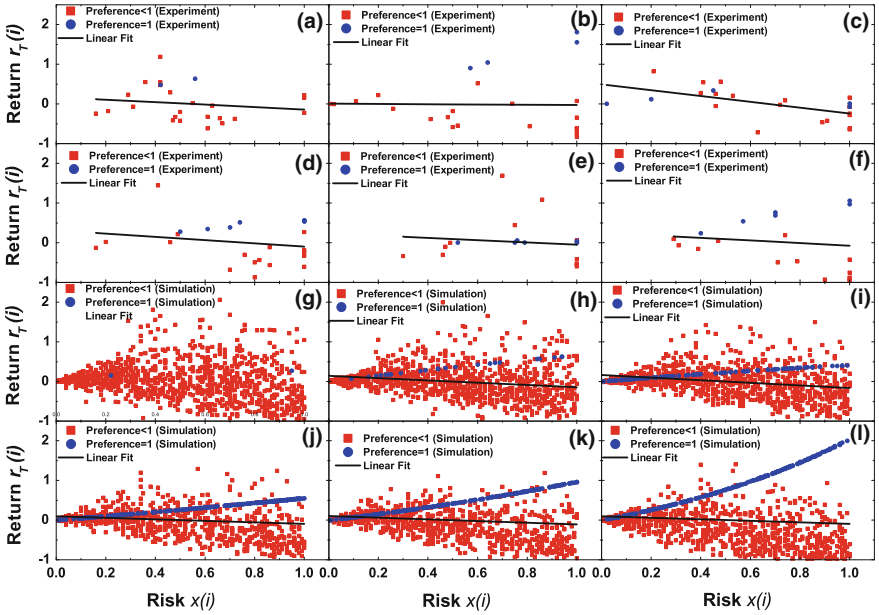

Fig. 11.2 Relationship between the risk, $\mathbf{x(i)}$, and the return, $\mathbf{r_T(i) = [w_T(i) - w_0(i)]/w_0(i)}$, for **a**–**f** 24 subjects and **g**–**l** 1,000 agents at various $\mathbf{M_1/M_2}$'s. **a**–**f** Data of the human experiments (total 30 rounds for each M_1/M_2); **g**–**l** Data of the agent-based computer simulations (total 800 rounds for each M_1/M_2, with additional 200 rounds performed at the beginning of the simulations; during the 200 rounds, we train all of the strategies by scoring them whereas the wealth of each agent remains unchanged). Here $w_T(i)$ is Agent i's wealth at the end of T rounds (the total number of rounds, T, is $T = 30$ and 800 for the experiments and simulations, respectively), and $w_0(i)$ is Agent i's initial wealth. All of the subjects or agents are divided into two groups with preference <1 (*red squares*) and preference $= 1$ (*blue dots*). Here, the "preference" is given by C_1/T, where C_1 is the number of times for subjects or agents to choose Room 1 within the total T rounds. The values or distribution of the preferences of the subjects or agents can be found in Figs. 11.4 and 11.5. Here, "Linear Fit" denotes the straight line fitting of the data in each panel using the least square method, which serves as a guide for the eye. (The fitting functions are listed in Table 11.2.) All of the lines are downward, which indicate a statistically negative relationship between risk and return. The present negative relationship just reflects the dominance of investments with a negative RRR in the whole system, in spite of a relatively small number of investments with a positive RRR. Other parameters: **g**–**l** $S = 4$ and $P = 16$. Adapted from Ref. [10]. **a** M1/M2 = 1 **b** M1/M2 = 2 **c** M1/M2 = 3 **d** M1/M2 = 6 **e** M1/M2 = 7 **f** M1/M2 = 9 **g** M1/M2 = 1 **h** M1/M2 = 2 **i** M1/M2 = 3 **j** M1/M2 = 6 **k** M1/M2 = 7 **l** M1/M2 = 9

Similar to the above experiments, we set two virtual rooms, Room 1 and Room 2 (with volume M_1 and M_2, respectively), for N agents (fund managers) to invest in. Then, for each M_1/M_2, assign every agent 1,000 points as his/her initial wealth and an investing weight, $x(i)$, which is randomly picked up between 0 and 1 with a step size of 0.001. In order to avoid the crowding or overlapping of strategies of different

Table 11.2 Linear fitting functions for Fig. 11.2a–l. Adapted from Ref. [10]

M_1/M_2	For the experimental data	For the simulation data
1	$r_T(i) = 0.17 - 0.31x(i)$ (Fig. 11.2a)	$r_T(i) = 0.40 - 0.82x(i)$ (Fig. 11.2g)
2	$r_T(i) = 0.0073 - 0.036x(i)$ (Fig. 11.2b)	$r_T(i) = 0.53 - 1.08x(i)$ (Fig. 11.2h)
3	$r_T(i) = 0.49 - 0.74x(i)$ (Fig. 11.2c)	$r_T(i) = 0.37 - 0.76x(i)$ (Fig. 11.2i)
6	$r_T(i) = 0.31 - 0.41x(i)$ (Fig. 11.2d)	$r_T(i) = 0.44 - 0.89x(i)$ (Fig. 11.2j)
7	$r_T(i) = 0.24 - 0.29x(i)$ (Fig. 11.2e)	$r_T(i) = 0.35 - 0.68x(i)$ (Fig. 11.2k)
9	$r_T(i) = 0.26 - 0.33x(i)$ (Fig. 11.2f)	$r_T(i) = 0.20 - 0.38x(i)$ (Fig. 11.2l)

agents [87, 167, 168], we design the decision-making process for each agent with four steps.

Step 1 set a positive integer, P, to represent the various situations for investing [7, 8].

Step 2 assign each agent S strategies according to S integers between 0 and P, respectively. For example, if one of the S integers is L, then the corresponding strategy of the agent is given by the ratio L/P ($0 \leq L/P \leq 1$), which represents the probability for the agent to choose Room 1 to invest in [8].

Step 3 for an agent, each strategy has its own score with an initial score, 0, and is added one score (or zero score) if the strategy predicts (or does not predict) the winning room correctly after each round.

Step 4 every agent chooses either Room 1 or Room 2 to invest in according to the prediction made by the strategy with the highest score.
In addition, both the payoff function and the rules for re-distributing investing wealth in Room 1 and Room 2 are set to be the same as those already mentioned in Sect. 11.2.

11.4 Comparison Between Experimental and Simulation Results

As shown by Fig. 11.1, our agent-based computer simulations also give $\langle W_1/W_2 \rangle \approx M_1/M_2$, that is, the system under simulation also exhibits market efficiency. Furthermore, according to the simulations, we achieve the same qualitative conclusion: investments with a negative RRR are statistically dominant over those with a positive RRR in the whole system; see Fig. 11.2g–l. Nevertheless, when we scrutinize Fig. 11.2j–l, we find that some particular data seem to be located on a smooth upward line. We plot these data in blue, and further find that they just correspond to all the agents with "preference = 1". Encouraging by this finding, we blue all the data of "preference = 1" in the other 9 panels of Fig. 11.2, and observe that a similar upward

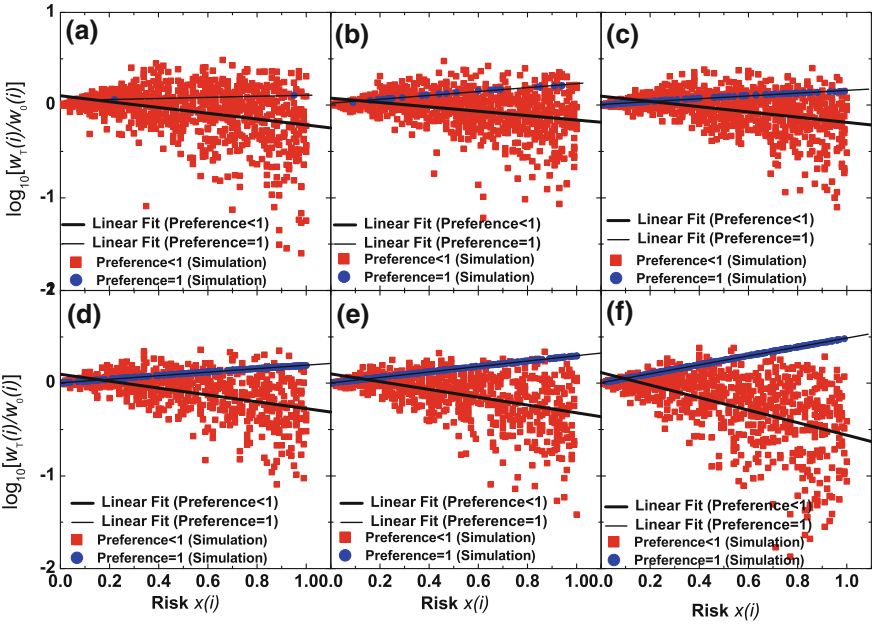

Fig. 11.3 Same as Fig. 11.2g–l, but showing the relationship between the risk, $\mathbf{x(i)}$, and the relative wealth, $\mathbf{w_T(i)/w_0(i)}$, on a logarithmic scale. "Linear Fit" corresponds to the line fitting the data of preference <1 or preference $=1$ using the least square method, which serves as a guide for the eye. (The fitting functions are listed in Table 11.3.) Adapted from Ref. [10]. **a** M1/M2 = 1 **b** M1/M2 = 2 **c** M1/M2 = 3 **d** M1/M2 = 6 **e** M1/M2 = 7 **f** M1/M2 = 9

line also appears in the experimental results [see the blue dots in Fig. 11.2a–f; note the blue dots in Fig. 11.2c, e are also, on average, in an upward line even though they appear to be not so evident].

For the upward lines themselves, they are clearly indicative of investments with a positive RRR. Hence, to distinctly understand our main conclusion about the dominance of investments with a negative RRR in the whole system, we have to overcome the puzzle, namely, the strange appearance of these upward lines (constructed by the blue dots in Fig. 11.2). For convenience, we just need to answer Question 1: why do all the "preference $=1$" data dots of Fig. 11.2g–l exist in an upward line? To this end, the answer to Question 1 will also help to reveal the mechanism underlying the above main conclusion.

11.5 Comparison among Experimental, Simulation, and Theoretical Results

To answer Question 1, we attempt to study the relationship between risk and wealth; see Fig. 11.3. In Fig. 11.3, the "preference $=1$" data dots appear to be arranged in an

Table 11.3 Linear fitting functions for Fig. 11.3a–l. Adapted from Ref. [10]

$\frac{M_1}{M_2}$	For "preference < 1"	For "preference $= 1$"
1	$\log_{10}\frac{w_T(i)}{w_0(i)} = 0.10 - 0.31x(i)$ (Fig. 11.3a)	$\log_{10}\frac{w_T(i)}{w_0(i)} = 0.05 + 0.058x(i)$ (Fig. 11.3a)
2	$\log_{10}\frac{w_T(i)}{w_0(i)} = 0.07 - 0.23x(i)$ (Fig. 11.3b)	$\log_{10}\frac{w_T(i)}{w_0(i)} = 0.02 + 0.24x(i)$ (Fig. 11.3b)
3	$\log_{10}\frac{w_T(i)}{w_0(i)} = 0.09 - 0.28x(i)$ (Fig. 11.3c)	$\log_{10}\frac{w_T(i)}{w_0(i)} = 0.01 + 0.05x(i)$ (Fig. 11.3c)
6	$\log_{10}\frac{w_T(i)}{w_0(i)} = 0.09 - 0.37x(i)$ (Fig. 11.3d)	$\log_{10}\frac{w_T(i)}{w_0(i)} = 0.01 + 0.19x(i)$ (Fig. 11.3d)
7	$\log_{10}\frac{w_T(i)}{w_0(i)} = 0.10 - 0.42x(i)$ (Fig. 11.3e)	$\log_{10}\frac{w_T(i)}{w_0(i)} = 0.003 + 0.29x(i)$ (Fig. 11.3e)
9	$\log_{10}\frac{w_T(i)}{w_0(i)} = 0.11 - 0.68x(i)$ (Fig. 11.3f)	$\log_{10}\frac{w_T(i)}{w_0(i)} = 0.004 + 0.48x(i)$ (Fig. 11.3f)

upward straight line, and the straight line exactly corresponds to the upward line constructed by the blue dots in Fig. 11.2g–l due to the relationship between the wealth and return. So, Question 1 equivalently becomes Question 2: why do all the "preference $=$ 1" data dots of Fig. 11.3 exist in an upward straight line? To answer it, we start by considering Agent i with investment weight, $x(i)$. His/her return and wealth after t rounds are, respectively, $r'_t(i)$ and $w_t(i)$. Here, the subscript $t \epsilon [0, T]$. (Note T stands for the total number of simulation rounds, $T = 800$.) Clearly, when $t = 0$, $w_t(i) = w_0(i)$, which just denotes the initial wealth of Agent i. Then, we obtain the expression for $r'_t(i) = [w_t(i) - w_{t-1}(i)]/[w_{t-1}(i)x(i)]$. Accordingly, we have $w_1(i) = w_0(i)[1 + r'_1(i)x(i)]$ and $w_2(i) = w_1(i)[1 + r'_2(i)x(i)] = w_0(i)[1 + r'_1(i)x(i)][1 + r'_2(i)x(i)]$, thus yielding $w_T(i) = w_0(i)[1 + r'_1(i)x(i)] \ldots [1 + r'_T(i)x(i)] = w_0(i) \prod_{t=1}^{T}[1 + r'_t(i)x(i)]$. As a result, we obtain $\log_{10}\frac{w_T(i)}{w_0(i)} = \log_{10}\{\prod_{t=1}^{T}[1 + r'_t(i)x(i)]\} = \sum_{t=1}^{T}\log_{10}[1 + r'_t(i)x(i)] = \left[\sum_{t=1}^{T} r'_t(i)\right]x(i) = T\langle r'_t(i)\rangle x(i)$. Here the third "$=$" holds due to $r'_T(i)x(i) \to 0$ for the T simulation rounds of our interest. In this equation, $\langle r'_T(i)\rangle$ denotes the average return, namely, the value obtained by averaging $r'_T(i)$ over the T rounds, and $\frac{w_T(i)}{w_0(i)}$ represents the relative wealth. Thus, the relationship between $\log_{10}\frac{w_T(i)}{w_0(i)}$ and $x(i)$ should be linear; the sign of the slope of the straight lines is only dependent on the average return, $\langle r'_T(i)\rangle$. Because the agents with preference $= 1$ always enter Room 1 with $M_1 (> M_2)$, the average return, $\langle r'_T(i)\rangle$, for them is not only positive but also the same. This is why all the blue points in Fig. 11.3 lie on an upward straight line. However, for the other agents with preference < 1 (Fig. 11.3), they will change rooms from time to time, so their average return, $\langle r'_T(i)\rangle$, is different from one another. This is the reason why the red points do not form a straight line as the blue points do. From this point of view, the downward straight line we draw from the red points in Fig. 11.3 is just a statistical analysis showing a trend. So, the answer to Question 2 can simply be "because for the small number of agents with preference $= 1$, their average return, $\langle r'_T(i)\rangle$, is not only positive but also the same".

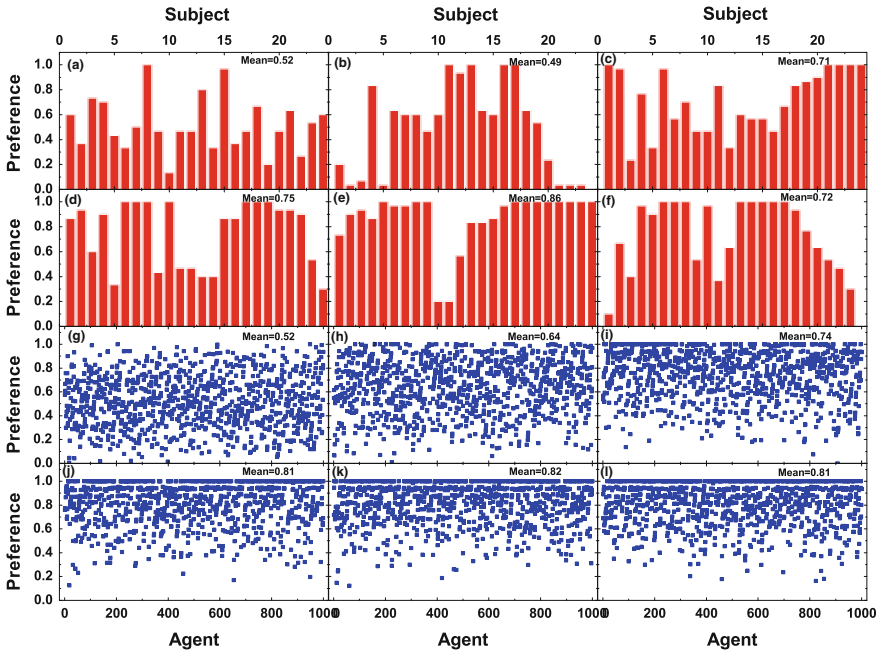

Fig. 11.4 Preferences of **a**–**f** the 24 subjects in the human experiments (plotted in the *bar graph*) or **g**–**l** the 1,000 agents in the agent-based computer simulations, for various M_1/M_2's. Here, "Mean" denotes the preference value averaged for **a**–**f** the 24 subjects or **g**–**l** 1,000 agents. In **a**–**f**, the present 24 subjects are ranked by their risk (namely, their investing weight) from low to high, within the range **a** [0.16, 1], **b** [0.01, 1], **c** [0.02, 1], **d** [0.16, 1], **e** [0.31, 1], and **f** [0.29, 1]; see Table 11.4 for details. Similarly, in **g**–**l**, the 1,000 agents are ranked by their risk from low to high, within the range (0, 1] assigned according to the code "(double)rand()%1, 001/1, 000" in the C programming language. In **a**–**f**, the ratio between the numbers of subjects with "preference = 1" and "preference < 1" are, respectively, **a** 2/22, **b** 4/20, **c** 5/19, **d** 7/17, **e** 11/13, and **f** 8/16. In **g**–**l**, the ratio between the numbers of agents with "preference = 1" and "preference < 1" are, respectively, **g** 2/998, **h** 23/977, **i** 94/906, **j** 233/767, **k** 200/800, and **l** 220/780. Adapted from Ref. [10]. **a** M1/M2=1 **b** M1/M2 = 2 **c** M1/M2 = 3 **d** M1/M2 = 6 **e** M1/M2 = 7 **f** M1/M2 = 9 **g** M1/M2 = 1 **h** M1/M2 = 2 **i** M1/M2 = 3 **j** M1/M2 = 6 **k** M1/M2 = 7 **l** M1/M2 = 9

According to the above theoretical analysis, we can now understand that the statistical dominance of investments with a negative RRR in the whole system results from the distribution of subjects'/agents' preferences: the heterogeneous preferences (<1) owned by a large number of subjects/agents together with the identical preferences (=1) possessed by a small number of subjects/agents. Details about the actual values for the preferences can be found in Figs. 11.4 and 11.5. Figures 11.4 and 11.5 also show the environmental adaptability of subjects or agents.

Table 11.4 Values for the risk (namely, investing weight) of the 24 subjects for six M_1/M_2's in the human experiments. We ranked the 24 subjects by their risk from low to high, as already used in Fig. 11.4a–f. Adapted from Ref. [10]

Subject	$\frac{M_1}{M_2} = 1$ [(a)]	$\frac{M_1}{M_2} = 2$ [(b)]	$\frac{M_1}{M_2} = 3$ [(c)]	$\frac{M_1}{M_2} = 6$ [(d)]	$\frac{M_1}{M_2} = 7$ [(e)]	$\frac{M_1}{M_2} = 9$ [(f)]
1	0.16	0.01	0.02	0.16	0.31	0.29
2	0.21	0.02	0.2	0.2	0.46	0.31
3	0.29	0.11	0.21	0.41	0.47	0.39
4	0.31	0.2	0.4	0.46	0.49	0.4
5	0.36	0.26	0.41	0.49	0.52	0.47
6	0.42	0.41	0.45	0.5	0.7	0.57
7	0.42	0.48	0.46	0.61	0.75	0.7
8	0.42	0.5	0.46	0.7	0.75	0.7
9	0.46	0.5	0.48	0.7	0.79	0.71
10	0.47	0.52	0.5	0.74	0.86	0.74
11	0.48	0.57	0.63	0.76	1	0.79
12	0.5	0.6	0.72	0.8	1	0.9
13	0.5	0.64	0.74	0.8	1	1
14	0.55	0.74	0.89	0.82	1	1
15	0.56	0.81	0.91	0.86	1	1
16	0.61	1	1	0.86	1	1
17	0.61	1	1	1	1	1
18	0.63	1	1	1	1	1
19	0.66	1	1	1	1	1
20	0.67	1	1	1	1	1
21	0.72	1	1	1	1	1
22	1	1	1	1	1	1
23	1	1	1	1	1	1
24	1	1	1	1	1	1

11.6 Discussion and Conclusions

On the basis of the designed CAS (complex adaptive system), we have revisited the relationship between risk and return under the influence of market efficiency and closeness by conducting human experiments, agent-based simulations, and theoretical analysis. We have reported that investments with a negative RRR (risk-return relationship) have dominance over those with a positive RRR in this CAS. We have also revealed the underlying mechanism related to the distribution of preferences. Our results obtained for the overall system do not depend on the evolutionary time, T, as long as T is large enough. On the other hand, the experimental data for each T have been listed in Table 11.1. Clearly, the results for each T can change accordingly.

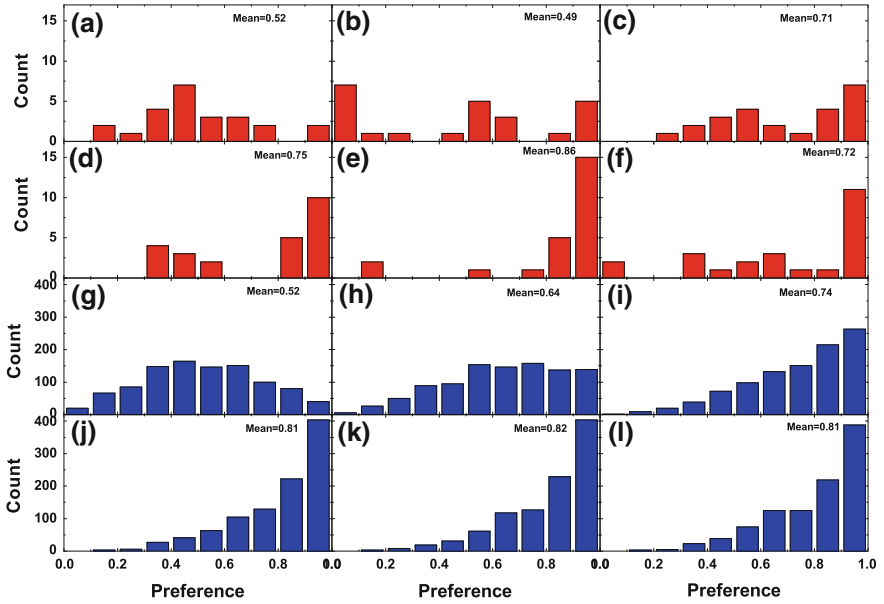

Fig. 11.5 Same as Fig. 11.4, but showing the distribution of preferences. Adapted from Ref. [10]. **a** M1/M2 = 1 (Experiment) **b** M/M2 = 2 (Experiment) **c** M1/M2 = 3 (Experiment) **d** M1/M2 = 6 (Experiment) **e** M1/M2 = 7(Experiment) **f** M1/M2 = 9 (Experiment) **g** M1/M2 = 1 (Simulation) **h** M1/M2 = 2 (Simulation) **i** M1/M2 = 3 (Simulation) **j** M1/M2 = 6 (Simulation) **k** M1/M2 = 7 (Simulation) **l** M1/M2 = 9 (Simulation)

In fact, such changes echo with those fluctuations or volatilities yielding arbitrage opportunities for investors in the real human society.

This chapter should be valuable not only to complexity science, but also to finance and economics, to management and social science, and to physics. In finance and economics, it may remind investors about their investing activities. In management and social science, our results are valuable to clarify the relationship between risk and return under some conditions. In physics, the present chapter helps to reveal a new macroscopic equilibrium state in such a CAS.

Chapter 12
Prediction: Pure Technical Analysis Might not Work Satisfactorily

Abstract The prediction of market trends is crucial for both investors and researchers. Based on various kinds of historical market information, many theories of technical analysis have been established. Here, by using controlled human experiments, we would like to figure out whether the pure technical analysis improves investors' prediction on the price movement indeed. We discover that the average predictive accuracy of experienced subjects is similar to that of unexperienced subjects under different conditions, such as the emerging or mature market, markets with either noisy fluctuations or clear trends, and markets with different information of technical indicators. Further, we study the wealth distribution of subjects and report that the Gini coefficient always increases as the experiment continues, indicating the Matthew effect in our experiment. Our findings question the validity of pure technical analysis, and pave a way for further investigation.

Keywords Predictive accuracy · Technical analysis · Sharpe ratio · Wealth distribution · Gini coefficient

12.1 Opening Remarks

The aim of econophysics research could be at least twofold: first, to explain existing economic or financial phenomena and second, to predict or forecast the trend of markets. In Chaps. 3–11, we mainly paid attention to the former. In this chapter, we intend to focus on the latter. As an initial task, here we want to ask whether pure technical analysis holds for predicting.

Technical analysis is a study of how to forecast future price trends through past market actions, primarily prices and volumes [169]. In 1882, C.H. Dow (November 6, 1851–December 4, 1902), E.D. Jones (October 7, 1856–February 16, 1920), and C.M. Bergstresser (June 25, 1858–September 20, 1923) founded Dow Jones and Company. Dow wrote a series of articles for Wall Street Journal expressing his ideas. Later, S. A. Nelson compiled Dow's articles in his book named *The ABC of Stock*

J.-P. Huang, *Experimental Econophysics*, New Economic Windows,
DOI 10.1007/978-3-662-44234-0_12

Speculation [170, 171]. Most technicians regard Dow's Theory as the foundation for technical analysis [169, 172].

Technical analysis is based on three premises [169, 173–175]. First, market action discounts everything. That is, factors determining market prices are all included in the price changes, such as macroeconomy, government's interference, and investor psychology. Second, prices move in trends. The purpose of technical analysis is to find the beginning of a trend in the early stage. Then, technicians will follow it until the trend is reaching an end. Third, history repeats itself. Through the study of past market data, technicians identify and categorize different chart patterns, which indicate certain market trends. Since they occurred in history several times, they are assumed to repeat in the future.

Why is technical analysis useful? Some people believe that it is due to the inefficiency of markets. There is a time interval before any influential factors thoroughly reflect the price change. Thus, it is the residual information that generates the trend. Nevertheless, some think that it is based on the investor psychology [169, 176]. Technical analysis is a practical and widely used method for stock investors. There are many well-known and influential theories such as Elliott wave theory, Fibonacci numbers, reversal patterns, support and resistance, time cycle, Japanese candlesticks, moving averages, and so on [174, 177–179]. In the turning point of the market or the initial stage of a market trend, technicians can always discover such crucial timing at an early time point with technical indicators and theories.

Nowadays, methods of technical analysis expand from traditional chart patterns to new areas such as quantitative and statistical analysis [180, 181]. With the development of computer science, technicians develop mechanical trading systems or trading models, which enable computers to automatically detect signals to buy or sell [182, 183]. Actually, today almost all well-known funds and investment banks employ technicians to study market trends in technical analysis particularly. For example, Renaissance Technologies and Medallion Fund became one of the most profitable funds in the world merely based on technical analysis. Therefore, the importance and influence of technical analysis is self-evident.

However, there are often some criticisms to the technical approach. The controversy between fundamental analysis and technical analysis has been existing for long. When tracing the trends, technicians do not need to consider the potential causes of price changes as they are all included in the market, while the cause for price changes is the key point for these fundamental analysts [169, 174]. Apart from this controversy, some believe that technical analysis is a self-fulfilling prophecy [184, 185]. History repeats itself because most traders act according to the theory. Thus, investors create so-called patterns such as the wave theory. Self-fulfilling prophecy is a great challenge to the foundation of technical analysis. Another question is whether or not past data can be used to forecast the future. After all, past data only indicates what has happened [186]. Moreover, the randomness of analysis indicators sometimes leads to contradictory predictions. Randomness also means that the technical indicator guiding investors' operation is somewhat subjective [187]. Further, the basic concepts of technical analysis violate economical theories such as the efficient

market hypothesis [149] and the random walk hypothesis [188]. The bankrupcy of some well-known technical analysis companies also casts a shadow on this theory.

12.2 Controlled Experiments

12.2.1 Experiment Design

To study whether the stock market is predictable and what factors affect the accuracy of such predictability, we designed a computer-aided human experiment. The purpose of this experiment is to study whether human subjects can predict price trends based on technical analysis and beat the markets. If it does happen, then what technical indicators are useful in the prediction and when are these indicators effective? Therefore in the experimental design stage, we need to consider the following aspects:

1. Valuation criteria: predictability. This experiment is based on real market data. As there is so much historical data in the world, subjects do not have enough time to use all of them. Thus, we have to select representative data according to their predictability.

2. Controllable indicators:

    a. *Different markets.* If the price is predictable, then there are arbitrage opportunities. Comparing a mature market and an emerging market, theoretically it is harder to predict the price trends in a mature market. Therefore, we choose two typical markets to study. We adopt NASDAQ Index in the United States, representing the mature market, and the CSI 300 Index in China, representing the emerging market, as the object of study in our experiment. We also reshuffle these data to make a comparison.

    b. *Different trends.* Even for the same index, its levels of predictability are not always the same. For example, investors always adjust their operations according to the current markets trends. Investors certainly have different market prediction when in a strong bull market or in a market with large fluctuations. Therefore, we choose trends as another indicator. But, is there a quantitative method to evaluate trends? Yes, of course. For instance, the Sharpe ratio [189] and predictability [190] in minority game are able to provide us with such methods. In our experiment, we prefer to use the Sharpe ratio as our indicator. Actually, we found the results of predictability to be similar regardless of which indicator we chose.

c. *Different scale.* Markets show different characteristics in different timescales, such as minutes, hours, days, and weeks. Thus, timescale might be another indicator that affects the market predictability. However, our data are limited in daily price, and thus, timescale is not included in our experiment.

d. *Technical indicators.* As some subjects might use technical approaches in the experiment to make predictions, we offer different technical indicators, namely two kinds of information: one including only daily closing price and the other including candlestick as well as moving average of 5 and 20 days. There are of course many other technical indicators such as volumes. As an initial task, we do not choose all of them due to limitation of time. We study whether the subjects perform better when they are given more information.

e. *Subjects.* Do subjects' features affect their performance in this experiment? Will a well-experienced investor make more accurate predictions than a novice? Will the knowledge of technical theories be beneficial in the experiment? Furthermore, will subjects with different genders and educational background perform differently? Accordingly, in our experiment, we distinguish subjects according to their investment experience, educational background, and gender.

Finally, based on the previous discussion we choose seven groups of daily data from the CSI Index and NASDAQ Index. Each group is composed of 140 daily prices, the first 120 of which are for reference and the last 20 are for subjects to predict. Moreover, we add four groups of reshuffled data to make a comparison. We also design a questionnaire for the subjects.

12.2.2 Experimental Process

The experiment was performed in the computer room of Fudan University; each subject's computer was connected to the server through a local area network. The 46 subjects were all students of Fudan University, who chose the course of *Econophysics*. Their performance would determine 15 % of their final academic scores in this course. Specific details are as follows (which were announced to the subjects before the experiment). The performance of each student accounted for 15 % academic score of this course. Every student who attended the experiments would get a basic academic score of 5 %. The other 10 % academic score was based on the trading performances of the students. In detail, we summed the rankings of students for 11 rounds of experiments. The top 10 % of students would get all the remaining 10 % academic score, while the next 10 % would get 9 %, and so on. Accordingly, the worst 10 % would get only 1 % academic score.

Fig. 12.1 Experimental interface. Subjects were requested to make choices in the left column with the information provided in the right column. This experiment provided candlesticks and moving average of 5 (red curve) and 20 (dark blue curve) days. Adapted from Ref. [191]

a. Pre-experiment training. Before the experiment, the organizers distributed questionnaires to collect subjects' information. Subjects were informed about the background and the basic process of the experiment, such as moving average, candlestick, and method of scoring. The organizers offered a group of experiment as warm-up. Subjects were required to sign an *Agreement of participance in the experiment* after they fully understood the experiment.
b. Experiment process. Every subject logged in the website with previously provided username and password. After log-in, subjects entered an interface with two columns, as shown in Fig. 12.1.

The right column displays the past data. Data in the yellow frame are the previous 120 daily prices. Subjects needed to predict the price changes in the white frame, and they did not know which real market index and which specific time we chose for the experiment. This setting was used to prevent subjects from figuring out the price trends before predictions. In case subjects recognized the data, we processed the market index and unified them over 10,000. Subjects were requested to make choices in the left column. For each round, subjects had six kinds of investment ratios, indicating subjects' different levels of prediction to the price change in the next round. For example, if subjects chose "100 % sell out," they firmly believed the next round's price would drop. While if they chose "100 % buy in," they were fully confident of the rise in price. After subjects made a choice, they clicked the NEXT button and waited for the (experimental) score for this round.To prevent some subjects from choosing faster and releasing the next round's data to other subjects, the server revealed the score of this round only after all subjects made their choices. The score was calculated as follows: Round score = investment ratio × index revenue. Index revenue = difference between the closing price of two adjacent rounds ÷ closing price of last round. Therefore, the score of each subject was based merely on his/her own performance, having no connection with other subjects.

Table 12.1 The order and information of 11 groups of experiment

Order	Market	Sharpe ratio	Price chart	Reshuffle
1	CSI	0.01	Candlestick + moving average	
2	CSI	0.03	Closing price	
3	CSI	0.01	Candlestick + moving average	Yes
4	NASDAQ	5.83	Closing price	
5	NASDAQ	0.03	Candlestick + moving average	
6	NASDAQ	0.02	Closing price	Yes
7	NASDAQ	5.55	Candlestick + moving average	
8	NASDAQ	0.02	Closing price	
9	CSI	3.57	Candlestick + moving average	
10	NASDAQ	5.5	Candlestick + moving average	Yes
11	CSI	3.57	Candlestick + moving average	Yes

CSI is the abbreviation of the CSI 300 Index and NASDAQ the NASDAQ index. The price chart column has two levels of information provided to subjects. Here, "Candlestick + moving average" denotes that candlesticks and moving averages of prices are provided; "Closing price" means that only closing prices are provided to the subjects, see for e.g., Fig. 12.2. Reshuffle column shows the real market data that are reshuffled. Adapted from Ref. [191]

When subjects got to know their score, they started the next prediction. There were 20 rounds of prediction for each group; we performed 11 groups in total (Table 12.1). Particularly, when subjects made choices at each round, they were supposed to give one unit of capital to make investment. Previous gains or losses could not be invested in the next round. Thus, earnings in every round were independent. The subjects' final score was the summation of scores in 20 rounds. During the experiment, subjects could see their rankings in the computer screen in order to stimulate subjects and add some fun. As subjects were independent, they were permitted to discuss and exchange ideas during the experiment. The order of 11 groups is shown in Table 12.1. As there were three kinds of controlled indicators, we separated the order of similar experiments.

After 11 groups of experiments, subjects handed in the questionnaire and left the lab.

12.3 Experimental Results

12.3.1 Winning Percentage

We calculate the winning percentage of different markets. If the subject's score of a round is larger than zero, the subject's prediction and the market trends are in the same direction. That is to say, the subject wins in this round. In this method, we can get the winning percentage of each group of experiment. The results are shown in Table 12.2. From Table 12.2, we can see that in general, the winning percentage is

Fig. 12.2 Experiment only with the closing price. Sometimes subjects were provided with this kind of price chart to make predictions. Adapted from Ref. [191]

Table 12.2 The average winning percentage of the 46 subjects in each group of experiment

Experiment	Average winning percentage (%)
CSI-0.01 (CMA)	49.78
CSI-0.01-reshuffle (CMA)	41.63
CSI-0.03	40.11
CSI-3.57 (CMA)	59.67
CSI-3.57-reshuffle	54.35
NASDAQ-0.02	51.41
NASDAQ-0.02-reshuffle	46.52
NASDAQ-0.03 (CMA)	44.13
NASDAQ-5.55 (CMA)	55.33
NASDAQ-5.55-reshuffle (CMA)	57.93
NASDAQ-5.83	50.87

Details of each subject are shown in Fig. 12.3. Here, the digit following either "CSI-" or "NASDAQ-" is the Sharpe ratio of the experiment; "CMA" in parentheses means that the price chart includes both candlesticks and moving averages, whereas other experiments without "(CMA)" mean they only show closing prices to the subjects. Adapted from Ref. [191]

around 0.5. Here the discussion of the absolute number of the Sharpe ratio is of little significance. We separate it into categories by their magnitude: 10^{-2} and 10^{0}.

In the above, we have considered several controlled indicators affecting the accuracy of predictability, including the markets, trends, technical analysis, and reshuffle. Now we are in a position to discuss these indicators in detail.

First, for the CSI 300 Index, when the market has noisy fluctuations (namely with small Sharpe ratios), subjects tend to predict less successfully. The winning percent-

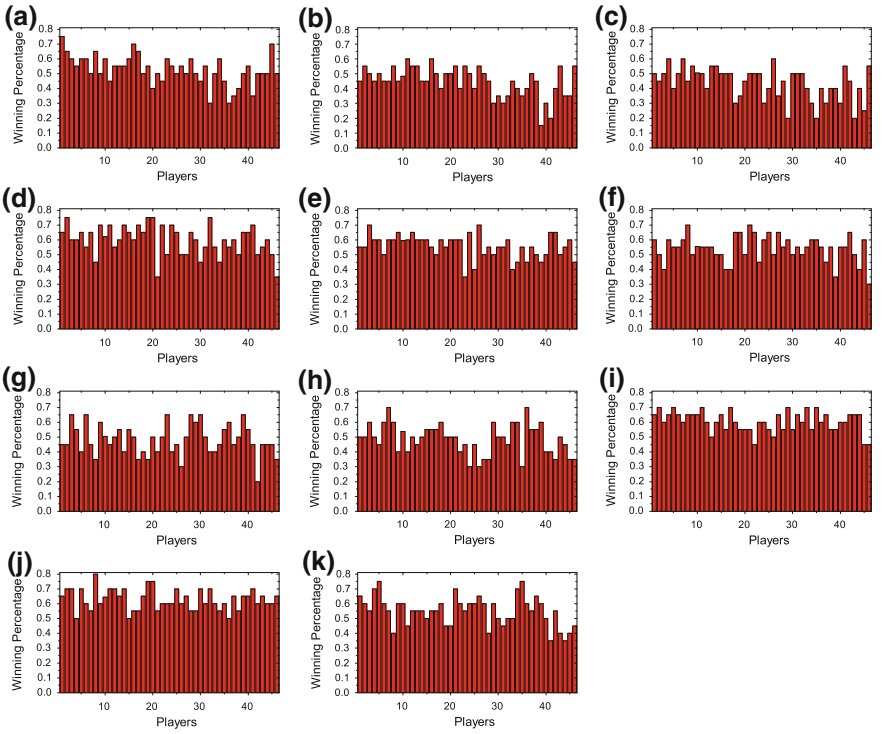

Fig. 12.3 The winning percentage of subjects (players) for the 11 groups of experiment. **a–k** corresponds to the experiment order in Table 12.2: **a** CSI-0.01 (CMA); **b** CSI-0.01-reshuffle (CMA); **c** CSI-0.03; **d** CSI-3.57 (CMA); **e** CSI-3.57-reshuffle; **f** NASDAQ-0.02; **g** NASDAQ-0.02-reshuffle; **h** NASDAQ-0.03 (CMA); **i** NASDAQ-5.55 (CMA); **j** NASDAQ-5.55-reshuffle (CMA); **k** NASDAQ-5.83. The *horizontal axis* corresponds to the 46 subjects and the *vertical axis* their winning percentages. Adapted from Ref. [191]

ages of experiments with the Sharpe ratio of 0.01 and 0.03 are obviously smaller than 3.57. However, it is not always the same for the NASDAQ Index. Specifically, the winning percentages of experiment with the Sharpe ratio of 0.02 are slightly larger than 5.83. Second, we study the effects of different market information on predictability. For experiments with similar trends in the CSI 300 Index, such as the first and third lines of Table 12.2, subjects given more information tend to make more accurate predictions. But for experiments of NASDAQ index, such as the sixth and eighth lines in Table 12.2, subjects' forecast based merely on closing prices is more accurate than that based on more information. The technical indicators do not have significant impacts on the results of our experiment. Third, we move on to the reshuffled data where the autocorrelation of stock prices is removed. For the experiment and its reshuffle data, such as the first two lines in Table 12.2, the winning percentage is lower after reshuffle. While for the experiments such as the ninth and tenth lines in Table 12.2, the winning percentage rises. Some reason might be used to explain this phenomenon. We suppose that when confronted with complicated

time series (small Sharpe ratios), people tend to care more about the correlation of details, which helps them grasp some regulations. Thus after the reshuffle, subjects' performance turns worse. However, when there is a strong and clear price trend (large Sharpe ratios), people choose to buy and hold. Their strategy lacks elasticity when the market changes. Reshuffled data average the fluctuations in the real market and avoid successive losses. Thus, subjects tend to win more often.

12.3.2 Statistics of Subjects

We analyze the questionnaire to further discuss subjects' performance in the experiment, and study whether gender, educational background, experience, and technical analysis really affect the predictions. Our statistical result is shown in Table 12.3. We average subjects' winning percentage according to four factors.

According to Table 12.4, we can see that subjects' predictions show little difference considering these four factors. To our surprise, the subject with years of investment experiences does not perform best in our experiment. Some real market investors even rank near the bottom in our experiment. Thus based on the results in our experiment, investment experience is not a crucial factor in predictions. Well-experienced investors do not distinguish from novices by candlesticks and moving averages. Subjects using technical analysis here do not have obvious advantages.

12.3.3 Wealth Distribution

In our experiment, subject's score = investment ratio $\times$ index revenue. The sign of scores determines whether they win or lose, while the absolute number of scores represents subject's investment earnings. In fact, during the experiment, every subject is supposed to make investments based on their judgment of price changes. If we understand the subjects' operations in this way, we can study the wealth distribution based on subjects' scores.

First let us look at, for example, the experiment with data from the CSI 300 Index with the Sharpe ratio of 0.01, shown in Fig. 12.4. Before the first round, subjects have nothing in their hands and everyone's wealth is equal. After that, subjects receive one unit of capital every round. As the experiment continues, the wealth difference of 46 subjects widens. Finally, there is a relatively broad distribution of wealth.

The process of widening wealth gap is called the Matthew effect in economics. This effect represents the phenomenon of "the rich get richer" [192]. Our experiment shows the similar phenomena. We can use the Gini coefficient to illustrate the gap between the amounts of wealth. The Gini coefficient describes the inequality of wealth or income. The zero value of Gini coefficient means perfect equality, and the Gini coefficient close to 1 means an extreme inequality [193]. The Gini coefficient of each group is shown in Fig. 12.5.

Table 12.3 Statistical results of the questionnaire

Username	Gender	Grade	Experience	Background	Winning percentage (%)
13110190069	1	3	3	3	57.3
12110190071	1	3	3	3	55.5
13110190051	1	3	3	3	54.1
13110190085	1	3	3	3	52.7
09110190005	1	3	3	3	52.3
13110190028	1	3	3	3	52.3
13110190056	1	3	3	3	52.3
13110190074	1	3	3	3	50.0
13110190080	1	3	3	3	45.0
13110190063	2	3	3	3	51.8
13210190001	1	2	3	3	56.8
13110190011	1	2	3	3	54.1
13110190041	1	2	3	3	53.2
13110190040	1	2	3	3	51.4
10300190001	1	1	3	3	58.2
10300190024	1	1	3	3	57.3
11307110036	1	1	3	3	55.5
11307110076	1	1	3	3	55.5
11307110034	1	1	3	3	54.1
11307110201	1	1	3	3	53.6
11307110197	1	1	3	3	52.3
11307110018	1	1	3	3	51.4
11307110207	1	1	3	3	50.9
10300190059	1	1	3	3	50.0
11307110168	1	1	3	3	48.2
10301020077	1	1	3	3	47.7
11300200007	2	1	3	3	56.4
11307110322	2	1	3	3	51.4
11307110308	2	1	3	3	50.5
13110190073	2	3	1	3	52.7
11300300032	1	1	1	3	50.5
13250190001	1	2	3	2	58.2
13110190060	1	2	3	2	49.5
12210720009	2	2	3	2	55.5

(countinued)

For all the 11 groups of experiments, at first the Gini coefficient equals zero. As the experiment continues, the Gini coefficient becomes larger. However, the final Gini coefficient is quite different. We suppose the controllable indicators might contribute

Table 12.3 (countinued)

Username	Gender	Grade	Experience	Background	Winning percentage (%)
11307110028	1	1	3	2	55.0
11307110348	1	1	3	2	55.0
11307110233	1	1	3	2	52.3
10300190038	1	1	3	2	51.4
11307110256	2	1	3	2	54.1
11307110318	2	1	3	2	51.4
11307110333	2	1	3	2	50.9
11307110035	1	1	2	2	56.4
10300190005	1	1	2	2	51.8
12110190036	1	3	1	1	58.2
12110190005	1	3	1	1	56.8
13110190014	1	2	1	1	45.0

The second column is the gender (1-male and 2-female); the third column is the educational background (1-undergraduate and 2/3-graduate); the fourth column is the subject's investment experience (1/2-yes and 3-no); the fifth column is the subjects' background of technical analysis (1/2-yes and 3-no). Adapted from Ref. [191]

Table 12.4 Average winning percentage of subjects with different features

Gender	Male	53.00 %
	Female	52.70 %
Grade	Undergraduate	53.10 %
	Graduate	52.90 %
Investment experience	Yes	53.10 %
	No	52.90 %
Tech analysis background	Yes	53.40 %
	No	52.70 %

Adapted from Ref. [191]

to the different Gini coefficient. Thus, we distinguish the experimental results and average their Gini coefficients. The results are shown in Fig. 12.6. Figure 12.6d shows that the Gini coefficient of real markets is larger than that of the reshuffled data. Apart from that, results in Fig. 12.6a–c do not have an obvious difference.

12.4 Discussion and Conclusions

The prediction of market prices might be the most important job for investors. Traditional technical analysis tries to discover market trends based on historical market data, and many theories have been established. In order to study the predictability of technical analysis in real markets, we have designed the computer-aided human

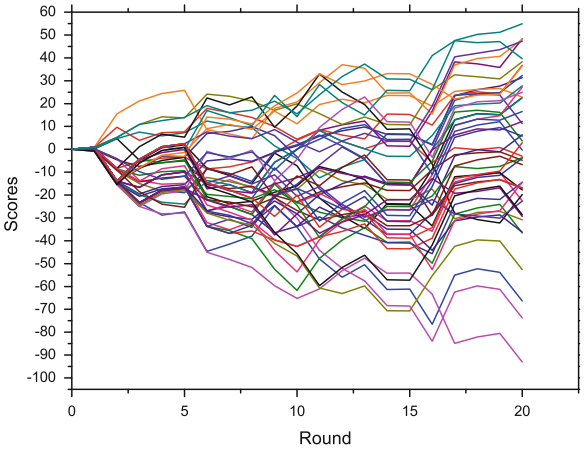

Fig. 12.4 An example of subjects' scores changing with round. For the experiment with data from the CSI 300 Index and the Sharpe ratio of 0.01, the wealth difference of 46 subjects widens during the experiment. Adapted from Ref. [191]

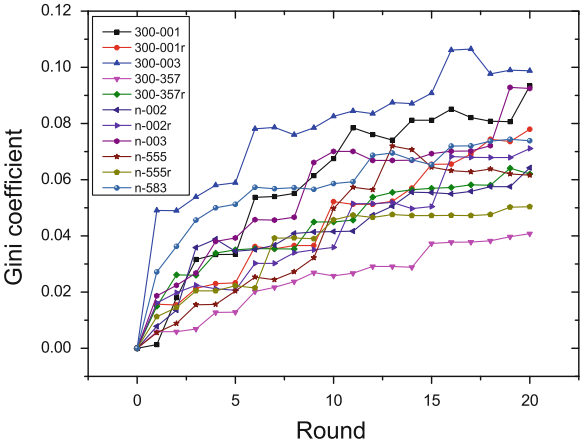

Fig. 12.5 Gini coefficient. All the Gini coefficients for the 11 groups of experiment increase from zero, representing the widening gap of subjects' wealth. The final value of the Gini coefficient is different for each group of experiment. Adapted from Ref. [191]

experiment. In our experiment, we first discuss the predictability under different controllable variables. Our experimental results have shown that there is no evident difference in predictability between mature and emerging markets, between noisy fluctuations and (relatively) clear trends, or between different information-levels of technical indicators. This means that in our experiments technical analysis can hardly be useful for forecasting future trends. The different degrees of predictability revealed

in our experiment might result from others factors, which remains to be studied in the future.

We have also investigated factors affecting subjects' performance. In our experimental results, we found that gender, educational background, and investment experience have little impact on the subjects' performance. Actually, some well-experienced subjects are even worse than the novices. Then which factor contributes to the subjects' predictability results? Will subjects predict more accurately due to their higher ability or just due to their better luck? We have found that some subjects always rank higher in the 11 groups of experiments. We believe pure luck cannot illustrate this phenomenon.

Finally, we calculated the wealth distribution of subjects and found the Matthew effect in the experiments. For each experiment, the Gini coefficient always increases as the experiment continues. The wealth distribution appears to be quite different in the 11 groups of experiment. Due to limited experimental conditions, we only had

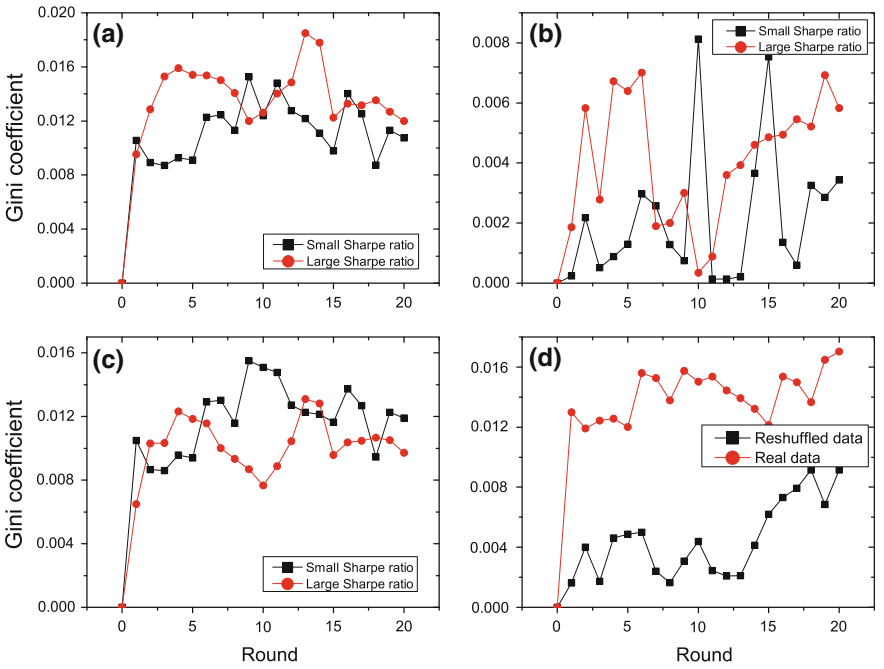

Fig. 12.6 Average of the Gini coefficients with different controllable indicators. **a** Data with the small Sharpe ratios (experiment 1 with Sharpe ratio of 0.01, experiment 2 with 0.03, experiment 5 with 0.03, and experiment 8 with 0.02) versus data with the large Sharpe ratios (experiment 4 with Sharpe ratio of 5.83, experiment 7 with 5.55, and experiment 9 with 3.57). Reshuffled data are not included. **b** Reshuffled data with small Sharpe ratios (experiment 3 with Sharpe ratio of 0.01 and experiment 6 with 0.02) versus reshuffled data with large Sharpe ratios (experiment 10 with Sharpe ratio of 5.55 and experiment 11 with 3.57). **c** Combination of (**a**) and (**b**). **d** Reshuffled data versus real market data. The experiment order is from Table 12.1. Adapted from Ref. [191]

46 subjects and 11 groups of experiment in total. These are not enough to draw a solid conclusion. The experimental results can only provide a qualitative judgment. We hope further study will be conducted, and hopefully more hiding connections may be revealed eventually.

Chapter 13
Summary and Outlook

Abstract I first summarize all the content introduced in Chaps. 1-12. Then, I give my personal outlook on experimental econophysics.

Keywords Experimental econophysics · Empirical analysis · Controlled experiment · Theoretical analysis

This book describes the field of experimental econophysics with focus on the following topics related to economics or finance: stylized facts, fluctuation phenomena, herd behavior, contrarian behavior, hedge behavior, cooperation, business cycles, partial information, risk management, and stock prediction. The book covers the basic concepts, methods, and latest progress in the field of experimental econophysics.

The combination of empirical analysis, controlled experiments, and theoretical analysis is the fundamental method in the field of experimental econophysics (Chap. 1). Clearly, controlled experiments are the most important part within this combination. Thus, how to develop experimental econophysics mainly relies on how to design and perform controlled experiments convincingly. The laboratory markets presented in this book offer an approximation of real markets, which are made of diverse traders. The results of our controlled experiments lend support to the Hayek hypothesis [27, 29] which asserted that markets can work correctly even though the participants have very limited knowledge of their environment or other participants (see Sect. 2.1). In fact, traders have different talents, interests, and abilities, and they may interpret data differently or be swayed by fads. Nevertheless, there is still room for markets to operate efficiently. These comments on the Hayek hypothesis might also be used to explain why our laboratory markets could be a reasonable approximation of real markets.

Regarding the further development of controlled experiments in the field of experimental econophysics, below I point out the following three directions [194].

(1) It is necessary to develop controlled experiments to study and predict the movement of real financial/economic markets that are often out-of-equilibrium [195],

J.-P. Huang, *Experimental Econophysics*, New Economic Windows,
DOI 10.1007/978-3-662-44234-0_13

which should be helpful for making suggestions for policy makers. For this purpose, it is necessary to take into account the development of complex networks [196–202] that can be used to describe the relations among humans, thus yielding emergent features originating from the interplay between the structure and the corresponding function of markets.

(2) With the deep development of economic and financial systems in global scope, economic/financial crises have more catastrophic influences than ever. However, mathematical statistics is unable to dig the essential mechanism underlying the crises. This points to a truth: it is urgently needed a more efficient method to model the social human systems. Controlled experiments, combined with empirical analysis and theoretical analysis, might be a promising candidate. As a result, statistical physics might play a more important role in the prediction of crises.

(3) Extending controlled experiments from humans to other animals like ants [203] or fish [204] could be of value in studying statistical physics of other kinds of adaptive agents beyond human beings. By doing so, people can understand these animals more by using concepts or tools originating from the traditional statistical physics.

So far, I have listed only three directions of controlled experiments. The readers are definitely smarter than me, and they might be able to dig out more instructive directions. Certainly, with the development of controlled experiments, accompanying empirical analysis and theoretical analysis should also be developed accordingly, to make the experimental results more useful and universal. In the mean time, econophysicists should also try to get a lot of nutrients from other successful disciplines like experimental (or behavioral) economics [30] and social psychology [205], so that experimental econophysics could flourish and prosper as soon as possible.

Appendix A

A.1 A Model Ethics Statement

Physicists (working on traditional physics) are not familiar with ethics statements because physical experiments under their study are always related to non-intelligent samples like Au/SiO_2 composites. When physicists perform controlled human experiments in the field of econophysics, they need to prepare ethics statements. This is because such experiments are performed to study human beings and human rights must be respected. As a result, every controlled experiment described in this book needs to be conducted under the requirement of ethics. Here, let me take the controlled experiment presented in Chap. 10 as an example, and provide the relevant ethics statement (with updates) as follows.

Applicant Name: J. P. Huang
Email address: jphuang@fudan.edu.cn
Experiment name: Resource allocation game
The number of human subjects needed: 25–30
Brief experiment plan:

We plan to recruit 25–30 students from the Department of Physics, Fudan University to do a series of resource allocation game. All the experiments are computer-aided and will be conducted for 2 h in Computer Room 121, Physics Building, Fudan University.

In the game, the subjects are connected by virtual directed random networks. A player's first-order neighborhood becomes his/her group members. The subjects are faced with two virtual rooms with different amount of resource. At each time step, every subject should decide on which room to choose to enter on the basis of the partial information obtained from his/her own group. After the experiments, all the subjects are offered a certain amount of money as reward according to their own performances. The average cash reward is 100 Chinese Yuan per capita.

J.-P. Huang, *Experimental Econophysics*, New Economic Windows,
DOI 10.1007/978-3-662-44234-0

All the experimental data are collected anonymously and used only for research purpose.

Applicant's Signature:

Date:

Statement of the Ethics Committee of Department of Physics, Fudan University

(a) On April 29, 2013

The application for the human experiments submitted by Prof. J. P. Huang has been approved by the committee.

(b) On May 7, 2013

The process of the experiments was supervised by the committee. The committee confirms that the human experiments were carried out under the requirement of ethics.

Signature of the Committee Director:

Date:

A.2 Announcement of Free Experimental Data Sharing

The book describes a number of controlled human experiments conducted in the laboratory. These experiments have offered us a large amount of experimental data. We are willing to freely share these data with any researchers, who have interest in developing controlled experiments in the field of experimental econophysics. In order to get the relevant original experimental data, email me at jphuang@fudan.edu.cn.

Bibliography

1. Challet, D., Zhang, Y.C.: Emergence of cooperation and organization in an evolutionary game. Phys. A: Stat. Mech. Appl. **246**, 407–418 (1997)
2. Platkowski, T., Ramsza, M.: Playing minority game. Phys. A: Stat. Mech. Appl. **323**, 726–734 (2003)
3. Bottazzi, G., Devetag, G.: A laboratory experiment on the minority game. Phys. A: Stat. Mech. Appl. **324**(1), 124 (2003)
4. Laureti, P., Ruch, P., Wakeling, J., Zhang, Y.C.: The interactive minority game: a web-based investigation of human market interactions. Phys. A: Stat. Mech. Appl. **331**, 651–659 (2004)
5. Wang, S.C., Yu, C.Y., Liu, K.P., Li, S.P.: A web-based political exchange for election outcome predictions. In: Proceedings of the IEEE/WIC/ACM international conference on web intelligence (WI' 04), pp. 173–178 (2004).
6. Wang, S.C., Tseng, J.J., Tai, C.C., Lai, K.H., Wu, W.S., Chen, S.H., Li, S.P.: Network topology of an experimental futures exchange. Eur. Phys. J. B **62**, 105–111 (2008)
7. Wang, W., Chen, Y., Huang, J.P.: Heterogeneous preferences, decisionmaking capacity, and phase transitions in a complex adaptive system. Proc. Natl. Acad. Sci. U. S. A **106**, 8423–8428 (2009)
8. Zhao, L., Yang, G., Wang, W., Chen, Y., Huang, J.P., Ohashi, H., Stanley, H.E.: Herd behavior in a complex adaptive system. Proc. Natl. Acad. Sci. U. S. A **108**, 15058–15063 (2011)
9. Liang, Y., An, K.N., Yang, G., Huang, J.P.: Contrarian behavior in a complex adaptive system. Phys. Rev. E **87**, 012809 (2013)
10. Song, K.Y., An, K.N., Yang, G., Huang, J.P.: Risk-return relationship in a complex adaptive system. PLoS ONE **7**, e33588 (2012)
11. An, K.N., Li, X.H., Yang, G., Huang, J.P.: A controllable laboratory stock market for modeling real stock markets. Eur. Phys. J. B **86**, 436 (2013)
12. Lux, T., Westerhoff, F.: Economics crisis. Nat. Phys. **5**, 2–3 (2009)
13. Stanley, H.E., Afanasyev, V., Amaral, L.A.N., Buldyrev, S.V., Goldberger, A.L., Havlin, S., Leschhorn, H., Maass, P., Mantegna, R.N., Peng, C.-K., Prince, P.A., Salinger, M.A., Stanley, M.H.R., Viswanathan, G.M.: Anomalous fluctuations in the dynamics of complex systems: from DNA and physiology to econophysics. Phys. A: Stat. Mech. Appl. **224**, 302–321 (1996)
14. Mantegna, R., Stanley, H.E.: An Introduction to Econophysics: Correlations and Complexity in Finance. Cambridge University Press, Cambridge (2000)
15. Rapaport, D.C.: The Art of Molecular Dynamics Simulation, 2nd edn. Cambridge University Press, Cambridge (2004)
16. Binder, K., Heermann, D.: Monte Carlo Simulation in Statistical Physics: An Introduction, 5th edn. Springer, New York (2010)

J.-P. Huang, *Experimental Econophysics*, New Economic Windows,
DOI 10.1007/978-3-662-44234-0

17. Hughes, T.J.R.: The Finite Element Method: Linear Static and Dynamic Finite Element Analysis. Dover Publications, New york (2000)
18. Gao, Y., Huang, J.P., Liu, Y.M., Gao, L., Yu, K.W., Zhang, X.: Optical negative refraction in ferrofluids with magneto-controllability. Phys. Rev. Lett. **104**, 034501 (2010)
19. Huang, J.P.: Experimental econophysics: complexity, self-organization, and emergent properties (submitted) (2014).
20. Johnson, N.F., Jefferies, P., Hui, P.M.: Financial Market Complexity. Oxford University Press, Oxford (2003)
21. Challet, D., Marsili, M., Zhang, Y.C.: Minority Games: Interacting Agents in Financial Markets. Oxford University Press, Oxford (2005)
22. Voit, J.: The Statistical Mechanics of Financial Markets. Springer, Berlin (2005)
23. Chakraborti, A., Toke, I.M., Patriarca, M., Abergel, F.: Econophysics: empirical facts and agent-based models. Quant. Finance **11**, 991–1041 (2011)
24. Sornette, D.: Physics and financial economics (1776–2014): Puzzles, ising and agent-based models. Rep. Prog. Phys. **77**, 062001 (2014)
25. Zhou, W.X.: An Introduction to Financial Physics (in Chinese). Shanghai University of Finance and Economics Press, Shanghai (2007)
26. Huang, J.P.: Econophysics: Using the Methods and Ideas of Physics to Discuss some Economic or Financial Problems (in Chinese). Higher Education Press, Beijing (2013)
27. Hayek, F.A.: The use of knowledge in society. Am. Econ. Rev. **35**, 519–530 (1945)
28. Smith, A.: An Inquiry into the Nature and Causes of the Wealth of Nations. A. and C. Black, Edinburgh (1863)
29. Smith, V.L.: Markets as economizers of information: experimental examination of the "hayek hypothesis". Econ. Inq. **20**(2), 165–179 (1982)
30. Kagel, J.H., Roth, A.E. (eds.): The Handbook of Experimental Economics. Princeton University Press, Princeton (1995)
31. Arthur, W.B.: Inductive reasoning and bounded rationality. Am. Econ. Rev. **84**, 406–411 (1994)
32. Jefferies, P., Hart, M.L., Hui, P.M., Johnson, N.F.: From market games to real-world markets. Eur. Phys. J. B **20**, 493–501 (2001)
33. Challet, D., Marsili, M., Zhang, Y.C.: Stylized facts of financial markets and market crashes in minority games. Phys. A: Stat. Mech. Appl. **294**, 514–524 (2001)
34. Martino, A.D., Marsili, A., Mulet, R.: Adaptive drivers in a model of urban traffic. Europhys. Lett. **65**, 283–289 (2004)
35. Yip, K.F., Hui, P.M., Lo, T.S., Johnson, N.F.: Efficient resource distribution in a minority game with a biased pool of strategies. Phys. A: Stat. Mech. Appl. **321**, 318–324 (2003)
36. Chmura, T., Pitz, T.: Successful strategies in repeated minority games. Phys. A: Stat. Mech. Appl. **363**(2), 477 (2006)
37. Gilbert, N.: Agent-Based Models. SAGE Publications Inc, New York (2007)
38. Pathria, R.K.: Statistical Mechanics, 2nd edn. Butterworth-Heinemann, Oxford (1996)
39. Krawiecki, A., Holyst, J.A., Helbing, D.: Volatility clustering and scaling for financial time series due to attractor bubbling. Phys. Rev. Lett. **89**, 158701 (2002)
40. Harras, G., Tessone, C.J., Sornette, D.: Noise-induced volatility of collective dynamics. Phys. Rev. E **85**, 011150 (2012)
41. Shannon, C.E.: A mathematical theory of communication. Bell Syst. Tech. J vol. 27, pp. 379–423, 623–656 (1948).
42. Carter, A.H.: Classical and Statistical Thermodynamics. Pearson Education Inc, Upper Saddle River (2001)
43. Jaynes, E.T.: Information theory and statistical mechanics. Phys. Rev. **106**, 620–630 (1957)
44. Landauer, R.: Irreversibility and heat generation in the computing process. IBM J. Res. Dev. **5**, 183–191 (1961)
45. Bennett, C.H.: Notes on landauer's principle, reversible computation, and maxwell's demon. Stud. Hist. Philos. Sci. Part B: Stud. Hist. Philos. Modern Phys. 34, 501–510 (2003).

46. Bennett, C.H.: The thermodynamics of computation-a review. Int. J. Theor. Phys. **21**, 905–940 (1982)
47. Mandal, D., Quan, H.T., Jarzynski, C.: Maxwell's refrigerator: an exactly solvable model. Phys. Rev. Lett. **111**, 030602 (2013)
48. Hodrick, R.J., Prescott, E.C.: Postwar U.S. business cycles: an empirical investigation. J. Money Credit Banking **29**(1), 1–16 (1997)
49. Cogley, T., Nason, J.M.: Effects of the hodrick-prescott filter on trend and difference stationary time series implications for business cycle research. J. Econ. Dyn. Control **19**(1), 253–278 (1995)
50. Baxter, M., King, R.G.: Measuring business cycles: Approximate band-pass filters for economic time series. Rev. Econ. Stat. **81**(4), 575–593 (1999)
51. Murray, C.J.: Cyclical properties of baxter-king filtered time series. Rev. Econ. Stat. **85**(2), 472–476 (2003)
52. Christiano, L.J., Fitzgerald, T.J.: The band pass filter. Int. Econ. Rev. **44**(2), 435–465 (2003)
53. Wälti, S.: The myth of decoupling. Appl. Econ. **44**(26), 3407–3419 (2012)
54. Butterworth, S.: On the theory of filter amplifiers. Wirel. Eng. **7**, 536–541 (1930)
55. Gómez, V.: The use of butterworth filters for trend and cycle estimation in economic time series. J. Bus. Econ. Stat. **19**(3), 365–373 (2001)
56. Ravn, M.O., Uhlig, H.: On adjusting the hodrick-prescott filter for the frequency of observations. Rev. Econ. Stat. **84**(2), 371–376 (2002)
57. Mantegna, R.N., Stanley, H.E.: Scaling behaviour in the dynamics of an economic index. Nature **376**, 46–49 (1995)
58. Plerou, V., Gopikrishnan, P., Amaral, L.A.N., Meyer, M., Stanley, H.E.: Scaling of the distribution of price fluctuations of individual companies. Phys. Rev. E **60**, 6519–6529 (1999)
59. Gopikrishnan, P., Plerou, V., Amaral, L.A.N., Meyer, M., Stanley, H.E.: Scaling of the distribution of fluctuations of financial market indices. Phys. Rev. E **60**, 5305–5316 (1999)
60. Plerou, V., Gopikrishnan, P., Rosenow, B., Amaral, L.A.N., Stanley, H.E.: Universal and nonuniversal properties of cross correlations in financial time series. Phys. Rev. Lett. **83**, 1471–1474 (1999)
61. Gabaix, X., Gopikrishnan, P., Plerou, V., Stanley, H.E.: A theory of power-law distributions in financial market fluctuations. Nature **423**, 267–270 (2003)
62. Zhou, W.C., Xu, H.C., Cai, Z.Y., Wei, J.R., Zhu, X.Y., Wang, W., Zhao, L., Huang, J.P.: Peculiar statistical properties of chinese stock indices in bull and bear market phases. Phys. A: Stat. Mech. Appl. **388**, 891–899 (2009)
63. Kantar, E., Deviren, B., Keskin, M.: Investigation of major international and turkish companies via hierarchical methods and bootstrap approach. Eur. Phys. J. B **84**, 339–350 (2011)
64. Liu, L., Wei, J.R., Zhang, H.S., Xin, J.H., Huang, J.P.: A statistical physics view of pitch fluctuations in the classical music from bach to chopin: evidence for scaling. PLoS ONE **8**, e58710 (2013)
65. Smith, V.L.: Economics in the laboratory. J. Econ. Perspectives **8**, 113–131 (1994)
66. Friedman, D.: How trading institutions affect financial market performance: some laboratory evidence. Econ. Inq. **31**, 410–435 (1993)
67. Porter, D.P., Smith, V.L.: Stock market bubbles in the laboratory. J. Behavioral Finance **4**, 7–20 (2003)
68. Hirota, S., Sunder, S.: Price bubbles sans dividend anchors: Evidence from laboratory stock markets. J. Econ. Dyn. Control **31**, 1875–1909 (2007)
69. Yang, J.: The efficiency of an artificial double auction stock market with neural learning agents. Stud. Fuzziness Soft Comput. **100**, 85–105 (2002)
70. Bouchaud, J.-P., Potters, M.: Theory of Financial Risk and Derivative Pricing: From Statistical Physics to Risk Management. Cambridge University Press, Cambridge (2003)
71. Oliveira, J.G., Barabási, A.-L.: Human dynamics: Darwin and Einstein correspondence patterns. Nature **437**, 1251 (2005)
72. Barabási, A.-L.: The origin of bursts and heavy tails in human dynamics. Nature **435**, 207–211 (2005)

73. Grabowski, A., Kruszewska, N., Kosiński, R.A.: Properties of on-line social systems. Eur. Phys. J. B **66**, 107–113 (2008)
74. Zhou, T., Kiet, H.A.T., Kim, B.J., Wang, B.H., Holme, P.: Role of activity in human dynamics. Europhys. Lett. **82**, 28002 (2008)
75. Feldman, T.: Leverage regulation: an agent-based simulation. J. Econ. Bus. **63**, 431–440 (2011)
76. Hamel, G., Prahalad, C.K.: Strategy as stretch and leverage. Harvard Bus. Rev. **71**, 75–84 (1993)
77. Lang, L., Ofek, E., Stulz, R.M.: Leverage, investment, and firm growth. J. Financial Econ. **40**, 3–29 (1996)
78. Adrian, T., Shin, H.S.: Liquidity and leverage. J. Financial Intermed. **19**, 418–437 (2010)
79. Thurner, S., Farmer, J.D., Geanakoplos, J.: Leverage causes fat tails and clustered volatility. Quant. Finance **12**, 695–707 (2012)
80. Carmassi, J., Gros, D., Micossi, S.: The global financial crisis: causes and cures. J. Common Mark. Stud. **47**, 977–996 (2009)
81. Baxter, N.D.: Leverage, risk of ruin and the cost of capital. J. Finance **22**, 395–403 (2012)
82. Jin, H., Zhou, X.Y.: Greed, leverage, and potential losses: a prospect theory perspective. Math. Finance **23**, 122–142 (2013)
83. Cont, R., Bouchaud, J.-P.: Herd behavior and aggregate fluctuations in financial markets. Macroecon. Dyna. **4**, 170–196 (2000)
84. Farmer, J.D.: Market force, ecology and evolution. Ind. Corp. Chang. **11**, 895–953 (2002)
85. Yeung, C.H., Wong, K.Y.M., Zhang, Y.-C.: Models of financial markets with extensive participation incentives. Phys. Rev. E **77**, 026107 (2008)
86. Yang, G., Zhu, C.G., An, K.N., Huang, J.P.: Fluctuation phenomena in a laboratory stock market with leveraged trading (submitted) (2014).
87. Savit, R., Manuca, R., Riolo, R.: Adaptive competition, market efficiency, and phase transitions. Phys. Rev. Lett. **82**, 2203–2206 (1999)
88. Christie, A.A.: The stochastic behavior of common stock variances: value, leverage and interest rate effects. J. Financial Econ. **10**, 407–432 (1982)
89. Geanakoplos, J.: The leverage cycle. NBER Macroecon. Annu. **24**, 1–65 (2010)
90. Zhu, C.G., Yang, G., An, K.N., Huang, J.P.: The leverage effect on wealth distribution in a controllable laboratory stock market. PLoS ONE **9**, e100681 (2014)
91. Halloy, J., Sempo, G., Caprari, G., Rivault, C., Asadpour, M., Tache, F., Said, I., Durier, V., Canonge, S., Ame, J.M., Detrain, C., Correll, N., Martinoli, A., Mondada, F., Siegwart, R., Deneubourg, J.L.: Social integration of robots into groups of cockroaches to control self-organized choices. Science **318**, 1155–1158 (2007)
92. Ballerini, M., Cabibbo, N., Candelier, R., Cavagna, A., Cisbani, E., Giardina, I., Lecomte, V., Orlandi, A., Parisi, G., Procaccini, A., Viale, M., Zdravkovic, V.: Interaction ruling animal collective behavior depends on topological rather than metric distance: evidence from a field study. Proc. Natl. Acad. Sci. U. S. A **105**, 1232–1237 (2008)
93. Cavagna, A.: Scale-free correlations in starling flocks. Proc. Natl. Acad. Sci. U. S. A **107**, 11865–11870 (2010)
94. Hamilton, W.D.: Geometry for the selfish herd. J. Theor. Biol. **31**, 295–311 (1971)
95. Arch, S.: Social Psychology. Prentice-Hall, Upper Saddle River (1952)
96. Deutsch, M., Gerard, H.B.: A study of normative and informational social influences upon individual judgment. J. Abnorm. Psychol. **51**, 629–636 (1955)
97. Bikhchandani, S., Hirshleifer, D., Welch, I.: Learning from the behavior of others: conformity, fads, and informational cascades. J. Econ. Perspectives **12**(3), 151–170 (1998)
98. Morris, S.: Contagion. Rev. Econ. Stud. **67**, 57–78 (2000)
99. Banerjee, A.V.: A simple model of herd behavior. Q. J. Econ. **107**, 797–817 (1992)
100. Fu, D., Pammolli, F., Buldyrev, S.V., Riccaboni, M., Matia, K., Yamasaki, K., Stanley, H.E.: The growth of business firms: theoretical framework and empirical evidence. Proc. Natl. Acad. Sci. U. S. A **102**, 18801–18806 (2005)

101. Gourley, S., Choe, S.C., Hui, P.M., Johnson, N.F.: Effects of local connectivity in a competitive population with limited resources. Europhys. Lett. **67**, 867 (2004)
102. Lo, T.S., Chan, H.Y., Hui, P.M., Johnson, N.F.: Theory of networked minority game based on strategy pattern dynamics. Phys. Rev. E **70**, 056102 (2004)
103. Shannon, C.E.: Prediction and entropy of printed english. Bell Syst. Tech. J. **30**, 50–64 (1951)
104. Dreman, D.: Contrarian Investment Strategies. Random House, New York (1979)
105. Holland, J.H.: Adaptation in Natural and Artificial Systems. MIT Press, Cambridge (1992)
106. Park, A., Sabourian, H.: Herding and contrarian behavior in financial markets. Econometrica **79**, 973–1026 (2011)
107. Zhong, L.X., Zheng, D.F., Zheng, B., Hui, P.M.: Effects of contrarians in the minority game. Phys. Rev. E **72**, 026134 (2005)
108. Galam, S.: Contrarian deterministic effects on opinion dynamics: "the hung elections scenario". Phys. A: Stat. Mech. Appl. **333**, 453–460 (2004)
109. Galam, S.: From 2000 Bush-Gore to 2006 italian elections: voting at fifty-fifty and the contrarian effect. Qual. Quant. J. **41**(2007), 579–589 (2000)
110. Borghesi, C., Galam, S.: Chaotic, staggered, and polarized dynamics in opinion forming: the contrarian effect. Phys. Rev. E **73**, 066118 (2006)
111. Li, Q., Braunstein, L.A., Havlin, S., Stanley, H.E.: Strategy of competition between two groups based on an inflexible contrarian opinion model. Phys. Rev. E **84**, 066101 (2011)
112. Plerou, V., Gopikrishnan, P., Stanley, H.E.: Econophysics: two-phase behaviour of financial markets. Nature **421**, 130 (2003)
113. Lillo, F., Farmer, J.D., Mantegna, R.N.: Econophysics: master curve for price-impact function. Nature **421**, 129–130 (2003)
114. Podobnik, B., Stanley, H.E.: Detrended cross-correlation analysis: a new method for analyzing two nonstationary time series. Phys. Rev. Lett. **100**, 084102 (2008)
115. Farmer, J.D., Foley, D.: The economy needs agent-based modelling. Nature **460**, 685–686 (2009)
116. Liang, Y., Huang, J.P.: Robustness of critical points in a complex adaptive system: effects of hedge behavior. Frontiers Phys. **8**, 461–466 (2013)
117. Grimm, V., Revilla, E., Berger, U., Jeltsch, F., Mooij, W.M., Railsback, S.F., Thulke, H.-H., Weiner, J., Wiegand, T., DeAngelis, D.L.: Pattern-oriented modeling of agent-based complex systems: lessons from ecology. Science **310**, 987–991 (2005)
118. Janssen, M.A., Walker, B.H., Langridge, J., Abel, N.: An adaptive agent model for analysing co-evolution of management and policies in a complex rangeland system. Ecol. Model. **131**, 249–268 (2000)
119. Tesfatsion, L.: Agent-based computational economics: modeling economies as complex adaptive systems. Inf. Sci. **149**, 263–269 (2003)
120. Liljeros, F., Edling, C.R., Amaral, L.A.N., Stanley, H.E., Åberg, Y.: The web of human sexual contacts. Nature **411**, 907–908 (2001)
121. Cody, M.L., Diamond, J.M.: Ecology and Evolution of Communities. Belknap Press, Cambridge (1975).
122. Helbing, D., Schoenhof, M., Kern, D.: Volatile decision dynamics: experiments, stochastic description, intermittency control and traffic optimization. New J. Phys. **4**, 33 (2002)
123. Chakrabarti, B.K.: Kolkata restaurant problem as a generalised el farol bar problem. In: Econophysics of Markets and Business Networks, pp. 239–246. Springer (2007).
124. Cavagna, A.: Irrelevance of memory in the minority game. Phys. Rev. E **59**, R3783–R3786 (1999)
125. Korotayev, A.V., Tsirel, S.V.: A spectral analysis of world gdp dynamics: kondratieff waves, kuznets swings, juglar and kitchin cycles in global economic development, and the 2008–2009 economic crisis. Struct. Dyn. **4**, 1 (2010)
126. Ciccarelli, M., Mojon, B.: Global inflation. Rev. Econ. Stat. **92**, 524–535 (2010)
127. Preis, T., Schneider, J.J., Stanley, H.E.: Switching processes in financial markets. Proc. Natl. Acad. Sci. U. S. A **108**, 7674–7678 (2011)

128. Stock, J.H., Watson, M.W.: Business cycle fluctuations in U.S. macroeconomic time series. Handb. Macroecon. **1**, 3–64 (1999)
129. Polak, J.J., Tinbergen, J.: Dynamics of Business Cycles. Routledge, London (2012)
130. Fidrmuc, J., Korhonen, I.: The impact of the global financial crisis on business cycles in asian emerging economies. J. Asian Econ. **21**, 293–303 (2010)
131. Mandelman, F.S., Rabanal, P., Rubio-Ramirez, J.F., Vilan, D.: Investment-specific technology shocks and international business cycles: an empirical assessment. Rev. Econ. Dyn. **14**, 136–155 (2011)
132. Kim, C.J., Nelson, C.R.: Has the U.S. economy become more stable? A bayesian approach based on a markov-switching model of the business cycle. Rev. Econ. Stat. **81**, 608–616 (1999)
133. Grimm, V., Berger, U., Bastiansen, F., Eliassen, S., Ginot, V., Giske, J., Goss-Custard, J., Grand, T., Heinz, S.K., Use, G., Huth, A., Jepsen, J.U.: Jørgensen, C., Mooij, W.M., Mueller, B., Peer, G., Piou, C., Railsback, S.F., Robbins, A.M., Robbins, M.M.: A standard protocol for describing individual-based and agent-based models. Ecol. Model. **198**, 115–126 (2006)
134. Bonabeau, E.: Agent-based modeling: methods and techniques for simulating human systems. Proc. Natl. Acad. Sci. U. S. A **99**, 7280–7287 (2002)
135. Raberto, M., Teglio, A., Cincotti, S.: Debt, deleveraging and business cycles: an agent-based perspective. Economics (The Open-Access, Open-Assessment E-Journal) 6, 1–49 (2012).
136. Li, X.H., Yang, G., An, K.N., Huang, J.P.: Fluctuation, stationarity and phase transition in a laboratory market undergoing business cycles (submitted) (2014).
137. Zheng, W.Z., Liang, Y., Huang, J.P.: Equilibrium state and non-equilibrium steady state in an isolated human system. Frontiers Phys. **9**, 128–135 (2014)
138. Liang, Y., An, K.N., Yang, G., Huang, J.P.: A possible human counterpart of the principle of increasing entropy. Phys. Lett. A **378**, 488–493 (2014)
139. Mandelbrot, B.B., Ness, J.W.V.: Fractional brownian motions, fractional noises and applications. SIAM Rev. **10**, 422–437 (1968)
140. Bak, P., Tang, C., Wiesenfeld, K.: Self-organized criticality: an explanation of 1/f noise. Phys. Rev. Lett. **59**, 381–384 (1987)
141. Taqqu, M.S., Teverovsky, V., Willinger, W.: Estimators for long-range dependence: an empirical study. Fractals **3**, 785–798 (1995)
142. Altman, N.S.: An introduction to kernel and nearest-neighbor nonparametric regression. Am. Stat. **46**(3), 175–185 (1992)
143. Bowman, A.W., Azzalini, A.: Applied Smoothing Techniques for Data Analysis. Oxford University Press, Oxford (1997)
144. Stukel, T.A.: Generalized logistic models. J. Am. Stat. Assoc. **83**(402), 426–431 (1988)
145. Azzalini, A.: A class of distributions which includes the normal ones. Scand. J. Stat. **12**, 171–178 (1985)
146. Biswas, S., Ghosh, A., Chatterjee, A., Naskar, T., Chakrabarti, B.K.: Continuous transition of social efficiencies in the stochastic-strategy minority game. Phys. Rev. E **85**, 031104 (2012)
147. Parshani, R., Buldyrev, S.V., Havlin, S.: Interdependent networks: reducing the coupling strength leads to a change from a first to second order percolation transition. Phys. Rev. Lett. **105**, 048701 (2010)
148. Fujie, R., Odagaki, T.: Self-organization of social hierarchy on interaction networks. J. Stat. Mech.: Theory Exp. 2011, P06011 (2011).
149. Fama, E.F.: Effcient capital markets: A review of theory and empirical work. J. Finance **25**, 383–417 (1970)
150. Bodie, Z., Kane, A., Marcus, A.J.: Investments, 8th edn. McGraw-Hill Education, New York (2009)
151. Mello, B.A., Souza, V.M.C.S., Cajueiro, D.O., Andrade, R.F.S.: Network evolution based on minority game with herding behavior. Eur. Phys. J. B **76**, 147–156 (2010)
152. Keynes, J.M.: The General Theory of Employment. Interest and Money. Atlantic Books & Dist, London (2006)
153. Hirshleifer, J.: The private and social value of information and the reward to inventive activity. Am. Econ. Rev. **61**, 561–574 (1971)

154. Yang, G., Zheng, W.Z., Huang, J.P.: Partial information, market efficiency, and anomalous continuous phase transition. J. Stat. Mech.: Theory Exp. P04017 (2014).
155. Johnson, N.F., Xu, C., Zhao, Z., Ducheneaut, N., Yee, N., Tita, G., Hui, P.M.: Human group formation in online guilds and offline gangs driven by a common team dynamic. Phys. Rev. E **79**, 066117 (2009)
156. Starnini, M., Baronchelli, A., Pastor-Satorras, R.: Modeling human dynamics of face-to-face interaction networks. Phys. Rev. Lett. **110**, 168701 (2013)
157. Parisi, D.R., Sornette, D., Helbing, D.: Financial price dynamics and pedestrian counterflows: a comparison of statistical stylized facts. Phys. Rev. E **87**, 012804 (2013)
158. Bartolozzi, M.: A multi agent model for the limit order book dynamics. Eur. Phys. J. B **78**, 265–273 (2010)
159. Galla, T., Zhang, Y.-C.: Minority games, evolving capitals and replicator dynamics. J. Stat. Mech.: Theory Exp. 2009, P11012 (2009).
160. Jia, T., Jiang, B., Carling, K., Bolin, M., Ban, Y.F.: An empirical study on human mobility and its agent-based modeling. J. Stat. Mech.: Theory Exp. 2012, P11024 (2012).
161. Clauset, A., Shalizi, C.R., Newman, M.E.J.: Power-law distributions in empirical data. SIAM Rev. **51**, 661–703 (2009)
162. Sharpe, W.F.: Capital asset prices: a theory of market equilibrium under conditions of risk. . J. Finance **19**, 425–442 (1964)
163. Fama, E.F., MacBeth, J.D.: Risk, return, and equilibrium: empirical tests. J. Political Econ. **81**, 607–636 (1973)
164. Ruefli, T.W.: Mean-variance approaches to risk-return relationships in strategy: paradox lost. Manag. Sci. **36**, 368–380 (1990)
165. Bowman, E.H.: A risk/return paradox for strategic management. Sloan Manag. Rev. **21**, 17–31 (1980)
166. Takano, Y., Takahashi, N., Tanaka, D., Hironaka, N.: Big losses lead to irrational decision-making in gambling situations: relationship between deliberation and impulsivity. PLoS ONE **5**, e9368 (2010)
167. Hart, M., Jefferies, P., Johnson, N.F., Hui, P.M.: Crowd-anticrowd theory of the minority game. Phys. A: Stat. Mech. Appl. **298**, 537–544 (2001)
168. Johnson, N.F., Choe, S.C., Gourley, S., Jarrett, T., Hui, P.M.: Crowd effects in competitive, multi-agent populations and networks. In: Lux, T., Reitz, S., Samanidou, E. (eds.) Nonlinear Dynamics and Heterogeneous Interacting Agents, pp. 55–70. Springer, Heidelberg (2005)
169. Murphy, J.J.: Technical analysis of the financial markets: A comprehensive guide to trading methods and applications. Penguin, New York (1999)
170. Nelson, S.A.: The ABC of Stock Speculation. Doubleday, Page & Company, New York (1912)
171. Browning, E. : Reading market tea leaves. The Wall Street Journal Europe pp. 17–18 (2007).
172. Achelis, S.B.: Technical Analysis from A to Z. McGraw Hill, New York (2001)
173. Colby, R.W.: The Encyclopedia of Technical Market Indicators. McGraw-Hill, New York (2002)
174. Edwards, R.D., Magee, J., Bassetti, W.: Technical Analysis of Stock Trends. CRC Press, Boca Raton (2012)
175. Bauer, R.J., Dahlquist, J.R.: Technical Markets Indicators: Analysis & Performance. Wiley, New York (1999)
176. Baiynd, A.M.: The Trading Book: A Complete Solution to Mastering Technical Systems and Trading Psychology. McGraw-Hill, New York (2011)
177. Nison, S.: Japanese Candlestick Charting Techniques: A Contemporary Guide to the Ancient Investment Techniques of the Far East. Penguin, New York (2001)
178. Dewey, E.R., Mandino, O.: Cycles: The Mysterious Forces That Trigger Events. Manor Books, New York (1973)
179. Frost, A.J., Prechter, R.R.: Elliott Wave Principle: Key to Market Behavior. Elliott Wave International (2005).
180. Lo, A.W., Mamaysky, H., Wang, J.: Foundations of technical analysis: computational algorithms, statistical inference, and empirical implementation. J. Finance **55**, 1705–1770 (2000)

181. Mandelbrot, B.B.: A multifractal walk down wall street. Sci. Am. **280**, 70–73 (1999)
182. Brock, W., Lakonishok, J., LeBaron, B.: Simple technical trading rules and the stochastic properties of stock returns. J. Finance **47**, 1731–1764 (1992)
183. Brabazon, A., ONeill, M.: Biologically Inspired Algorithms for Financial Modelling. Springer, Heidelberg (2006).
184. Sant, R., Zaman, M.A.: Market reaction to business week inside wall street column: a self-fulfilling prophecy. J. Banking Finance **20**, 617–643 (1996)
185. Ferraro, F., Pfeffer, J., Sutton, R.I.: Economics language and assumptions: how theories can become self-fulfilling. Acad. Manag. Rev. **30**, 8–24 (2005)
186. Fama, E.F.: The behavior of stock-market prices. J. Bus. **38**, 34–105 (1965)
187. Park, C.H., Irwin, S.H.: What do we know about the profitability of technical analysis? J. Econ. Surv. **21**, 786–826 (2007)
188. Fama, E.F.: Random walks in stock market prices. Financial Analy. J. **21**, 55–59 (1965)
189. Sharpe, W.F.: The sharpe ratio. In: Bernstein, P.L., Fabozzi, F.J. (eds.) Streetwise: The Best of the Journal of Portfolio Management, pp. 169–185. Princeton University Press, Princeton (1998)
190. Wawrzyniak, K.: On phenomenology, dynamics and some applications of the minority game, Ph.D. thesis, Institute of Computer Science, Polish Academy of Sciences (2011).
191. Liu, L., Huang, J.P.: Prediction: Pure technical analysis might not work satisfactorily (2014).
192. Merton, R.K.: The matthew effect in science. Science **159**, 56–63 (1968)
193. Yitzhaki, S.: Relative deprivation and the gini coefficient. Q. J. Econ. **93**, 321–324 (1979)
194. Liang, Y., Huang, J.P.: Statistical physics of human beings in games: controlled experiments. Chin. Phys. B **23**, 078902 (2014)
195. Arthur, W.B.: Out-of-equilibrium economics and agent-based modeling. Handb. Comput. Econ. **2**, 1551 (2006)
196. Watts, D.J., Strogatz, S.H.: Collective dynamics of 'small-world' networks. Nature **393**, 440–442 (1998)
197. Albert, R., Barabási, A.-L.: Statistical mechanics of complex networks. Rev. Modern Phys. **74**, 47–97 (2002)
198. Boccaletti, S., Latora, V., Moreno, Y., Chavez, M., Hwang, D.-U.: Complex networks: structure and dynamics. Phys. Rep. **424**, 175–308 (2006)
199. Arenas, A., Díaz-Guilera, A., Kurths, J., Moreno, Y., Zhou, C.: Synchronization in complex networks. Phys. Rep. **469**, 93–153 (2008)
200. West, B.J., Geneston, E.L., Grigolini, P.: Maximizing information exchange between complex networks. Phys. Rep. **468**, 1–99 (2008)
201. Centola, D.: The spread of behavior in an online social network experiment. Science **329**, 1194–1197 (2010)
202. Fiedor, P.: Networks in financial markets based on the mutual information rate. Phys. Rev. E **89**, 052801 (2014)
203. Altshuler, E., Ramos, O., Núñez, Y., Fernández, J., Batista-Leyva, A.J., Noda, C.: Symmetry breaking in escaping ants. Am. Nat. **166**, 643–649 (2005)
204. Liu, R.T., Chung, F.F., Liaw, S.S.: Fish play minority game as humans do. Europhys. Lett. **97**, 20004 (2012)
205. Myers, D.G.: Social Psychology, 11th edn. McGraw-Hill, New York (2012)